The Embryonic Development of *Elminius modestus* Darwin, 1854

(Thecostraca: Cirripedia)

D i s s e r t a t i o n

zur Erlangung des akademischen Grades

d o c t o r r e r u m n a t u r a l i u m

(Dr. rer. nat.)

im Fach Biologie

eingereicht an der

Mathematisch-Naturwissenschaftlichen Fakultät I
der Humboldt-Universität zu Berlin

von

M.Sc. Biol. Ekaterina Alexandrovna Ponomarenko

Präsident der Humboldt-Universität zu Berlin
Prof. Dr. Jan-Hendrik Olbertz

Dekan der Mathematisch-Naturwissenschaftlichen Fakultät I
Prof. Dr. Stefan Hecht

Gutachter/innen: 1. Prof. Dr. Gerhard Scholtz

2. Assoc. Prof. Jens Høeg

3. PD Dr. Carsten Lüter

Tag der mündlichen Prüfung: 04.04.2014

Посвящаю моему дедушке
To my grandpa

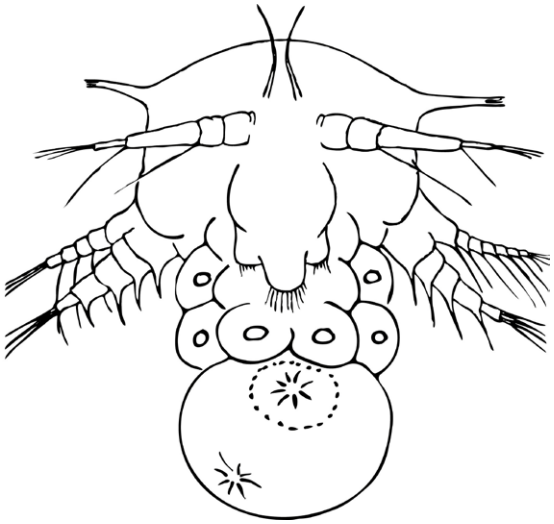

“We're not here because we're free;
we're here because we're not free.
There's no escaping reason,
no denying purpose,
for as we both know,
without purpose we would not exist.”
AS, 2003

TABLE OF CONTENT

1. INTRODUCTION

Cirripedes, more commonly known as barnacles, represent an absolutely amazing group of animals. Indeed, one can find among them unbelievable creatures, like nearly headless beings living upside down or guys losing their charater just to castrate a distant relative.

Clearly, the mystery of barnacles was driving and motivating dozens of scientists including Charles Darwin himself (1854). More than a hundred years ago Bigelow (1902) wrote: "The history of the development of our knowledge of the Cirripedia has been so often written...". What can a scientist write now? The list of cirripedologists over the last century has grown gradually and became numerous. It seems that by now everything should be observed and analysed about these little creatures. It is certainly true that a lot of things are known, but still not all. Even when you look in the works of the old with their gorgeous preciseness and unbelievably beautiful descriptions, you can find a lot of blank gaps. So, this is the answer: scientists nowadays try to look at those blank gaps.

The early development of cirripedes might be considered as one of those gaps. Even with a number of studies addressing this subject on different levels of detailedness, including three highly conscientious works (Bigelow, 1902; Delsman, 1917; Anderson, 1969), it still remains one of the most controversially described parts of the barnacle's life cycle. The available studies do not seem to agree on very crucial developmental points like cleavage asynchrony, cell lineage, blastopore organisation, germ layer origin, or major outlines of limb development.

However, it was not just curiosity for a mystery and blank spots, which motivated and initiated this study. The development of cirripedes was described in the times of an older phylogenetic system of Protostomia. According to it, the groups of Arthropoda and Annelida were suggested to form a monophyletic clade, the Articulata, which was regarded to be the sister group of Mollusca and to have a common polychaete-like ancestor (Anderson, 1979; Dogiel, 1981; Nielsen, 1995). The development of both molluscs and annelids passes through a special way of development. This developmental mode was often referred as spiral due to the highly organized arrangement of the blastomeres during the cleavage stages (Selenka, 1881; Lang, 1884). One has to add, that since the time of its first description the definition of spiral development comprised not only the cleavage pattern, but a whole set of characteristics including specific and highly conserved cell lineages of trochoblasts, nervous system, endoderm, and mesoderm (Zilch, 1978; Dohle, 1989; Nielsen, 1995). The former position of Arthropoda led scientists, who investigated crustacean development, to search for such traits of spiral development. Many of them failed and had to conclude, that there are none (Kühn, 1912; Zilch, 1978; 1979; Dohle, 1979; Weygoldt, 1960; Hertzler and Clark, 1992; Scholtz, 1997; Wolff and Scholtz, 2002; Alwes and Scholtz, 2004). Nevertheless, there were also those, who have seen some resemblance to the spiral pattern and interpreted the developmental mode of crustaceans as such (Taube, 1909; Delsman, 1917;

Anderson, 1969; Costello and Henley, 1976). By chance or by providence the crustaceans, in which the similarities to spiral cleavage were found, were no others but barnacles!

With the revision of the system of Protostomia (Aguinaldo et al., 1997) and the allying of Arthropoda with Cycloneuralia to form the new clade Ecdysozoa, the barnacle development had to be reinterpreted (Valentine, 1997; Scholtz, 1997). Nowadays, nobody would expect the cirripedes or the crustaceans in general to have spiral cleavage. But what if the once described similarities between the barnacle development and that of the classic spiralians are still there? And what if these similarities are not just a result of convergent evolution? Their meaning might be of another value now.

Therefore one major goal of the current work was to reinvestigate the embryonic development of a barnacle as detailed as currently possible and find out whether the "shared" features between Cirripedia and Spiralia observed long ago were really just an artefact of perception. In particular, the study includes the analysis of the cleavage pattern and the establishment of the cell lineage up to the 16-cell stage.

In general, studies on the arthropod development represent different interest. By now the clade of Ecdysozoa seems to be a stable outcome in most molecular analyses (e.g. Dunn et al., 2008; Edgecombe et al., 2011), although the morphological and especially developmental support is still very poor (Alwes, 2008; Ungerer and Scholtz, 2009; Scholtz and Wolff, 2013). Therefore an additional goal of the present study was to gather data on the cleavage and cell lineage of a representative of the crustaceans in order to contribute to a common search for possible apomorphies of Ecdysozoa.

Special emphasis in this work will be given to the development and the specification of the mesoderm. One has to say, that the subject of mesoderm formation is absolutely amazing (possibly as amazing as the cirripedes). Main questions in this research field are related to the origin of the mesoderm, the differentiation of the mesodermal cells, the homology of the two existing types of mesoderm (ectomesoderm, the line of which is connected to the ectoderm, and endomesoderm, which is connected to the endoderm in its origin), the polarity of the mesoderm specification in the area of the blastopore, and the induction of the ectomesoderm (Tannreuther, 1915; Siewing, 1977; Jellies, 1990; Bate, 1990; Henry et al., 2000; Rodaway and Patient, 2001; Lartillot et al., 2002; Technau, 2001; Martindale, 2004). Out of this list in particular the last two points will be addressed in the discussion.

The research of the distribution of mesoderm precursors in the blastopore area of crustaceans has a long history (e.g. Baldass, 1941; Manton, 1949; Anderson, 1979). Most of these studies seem to agree that a posterior placement of the mesendoblast in relation to the endoblast is a common state for many crustaceans as well as protostomians. The difference in the placement of the mesectoblasts between different animals, on the other hand, was very seldomly addressed in a phylogenetic context. With the contribution of modern molecular data the idea was developed that a

radial placement of the mesodermal precursors in relation to the endoblast is ancestral for the bilaterians. The split into anterior and posterior precursors in the area of the blastopore led to the formation of the two types of the mesoderm (Lartillot et al., 2002a; Technau and Scholz, 2003). As in trochozoan spiralians the anterior position is taken in many cases by mesectoblasts, the ectomesoderm of these animals was homologized with the anterior mesoderm of others (Lartillot et al., 2002a; Nederbragt et al., 2002). The presence of ectomesoderm was reported for many crustaceans as well (e.g. Kühn, 1912; Cannon, 1921; Hertzler, 2002). However, the position of the mesectoblasts during the gastrulation process was never addressed. That is rather unfortunate though, as these data might contribute to both the discussion on the evolution in mesodermal specification and the phylogeny of Ecdysozoa.

Another interesting point to deal with is the induction of the ectomesoderm. There are two types of cell fate specification: autonomous (via intracellular determinants) and conditional (via extracellular signals, coming from adjacent cells or from a region of the embryo) (Freeman and Lundelius, 1992). By now all studies show that the secondary mesoderm (or ectomesoderm in protostomians) is specified conditionally (e.g. Rodaway and Patient, 2001; Priess, 2005). And in this specification either endomesoblast (Schnabel, 1991) or endoblast (Nishida, 2005; Rodaway and Patient, 2001) play a key role. However, the studies were mostly performed either on deuterostomes or on nematodes within protostomes. In crustaceans only two studies slightly deal with the mesoderm specification. A study on *Parhyale hawaiensis* provides information on the stage of cleavage, at which the mesoblast is specified, however gives no data on the possible mechanisms responsible for the specification (Price et al., 2010). Another experimental study, which was performed on *Sicyonia ingentis*, suggests that it is the mesendoblastic cells, which initiate the oriented division of the mesectoblasts and, thus, lead to the internalization of the ectomesoderm (Wang et al., 2008). In the current study the established cell lineages of the gastrulating cells are used to draw conclusions on cell interactions, which possibly cause the ectomesoderm specification in the analysed barnacle. This data may serve as starting point for further experimental and molecular investigations on this topic.

To address the mentioned questions a single barnacle species was taken: *Elminius modestus*. The research work was subdivided into three main steps: the investigation of the cleavage, the identification of the cell fates, and the tracing of the differential steps of the mesoderm. Each step involved the application of different methods, like 4D microscopy, *in vivo* labelling, fluorescent histochemistry, confocal laser scanning microscopy, and 3D reconstructions. The description of the results is organized according to the steps of the investigation. Additional chapters, like staging and anatomical descriptions of the nervous and muscle systems, are added to facilitate the description of the main results and are not addressed in the discussion.

2. MATERIALS AND METHODS

2.1. Material

2.1.1. Animal collection

The barnacles taken for the current work were representatives of the species *Elminius modestus* (Thecostraca: Cirripedia: Thoracica: Balanidae) (Fig. 2.1.1.A). The species was chosen due to several reasons. First of all, these animals have short breeding cycles and are easy to be initiated to spawn. Secondly, both the adults and the embryos of *E. modestus* are quite comfortable with the laboratory conditions. The negative point about the animals of this species is that their em-

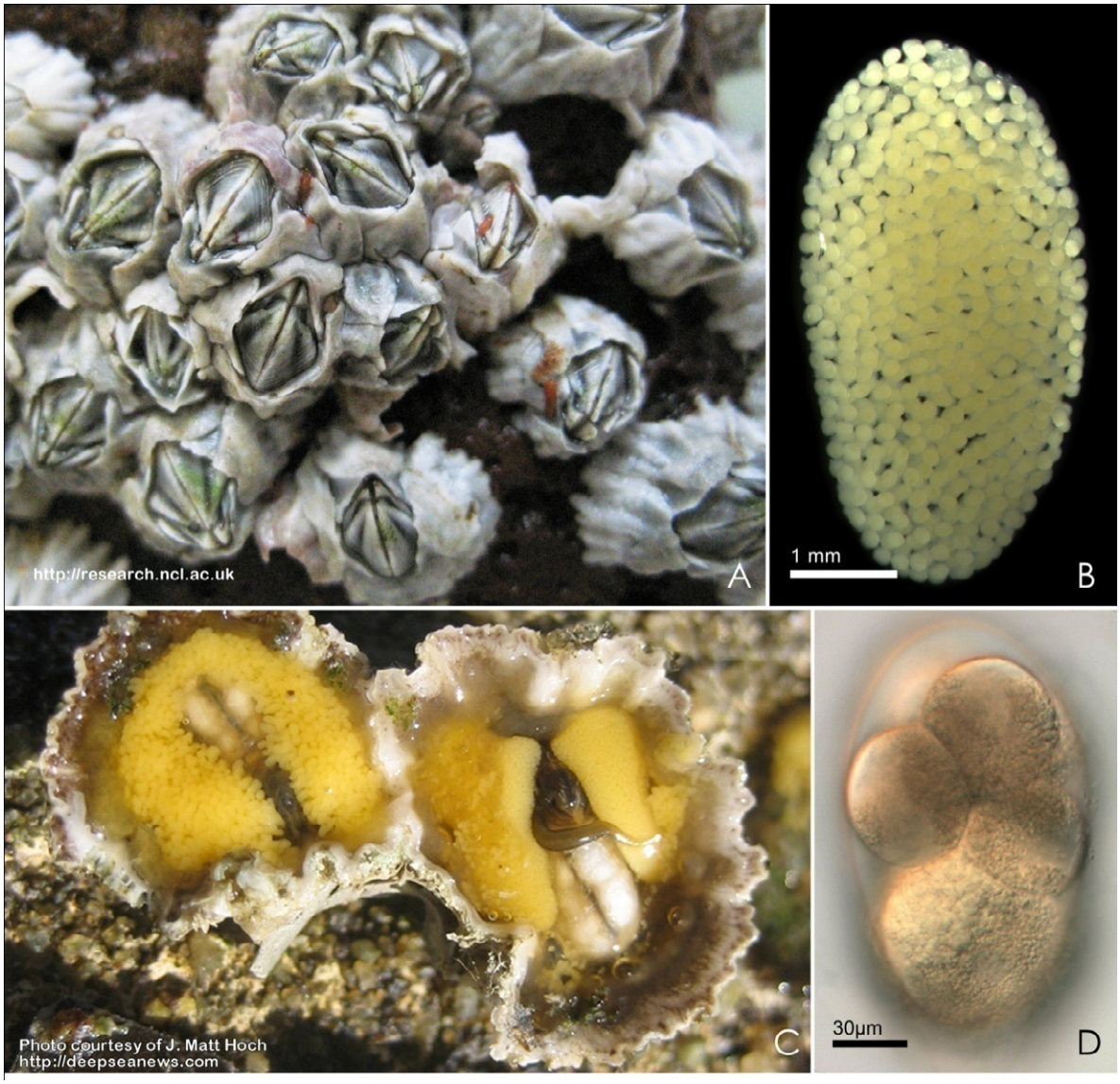

Fig. 2.1.1. Different faces of the barnacle *E. modestus.*
A – The adult barnacle attached to a substrate in nature; **B** – The brood of freshly fertilized eggs (before Zygote formation), note that the eggs are not yet tightly packed like on the later stages of the development; **C** – Two adult specimens detached from a substrate and viewed from "under" the house, the left one has the matured ovaries, the right one has two fertilized broods of eggs; **D** – Alive embryo at the 8-cell stage.

bryos are relatively small (90/170 mkm in average, Fig. 2.1.1.D). This restricts certain methods (e.g. *in vivo* labelling during the late cleavage, alive observation in stereo binoscope (Zeiss Stereo Lumar.V12, etc). However, exactly this characteristic of the embryos allows the mounting of several specimens for 4D recordings (up to 3) and for *in vivo* injections (up to 30). Logically, it brings more outcome in a shorter time.

The specimens of *Elminius modestus* had been collected during low tides in the littoral zones in Wilhelmshaven (Northern Sea, Niedersachsen, Deutschland). Alive animals attached to different substrates such as shells of the marine bivalves, little stones, and to the wooden sticks were brought to the aquarium of the Department of Comparative Biology (Institute of Biology, HU, Philippstr. 13, house 2).

2.1.2. Animal culture

The specimens were kept under the temperature 15ºC and fed with freshly hatched larvae of *Artemia salina*.

Each well fed and happy barnacle produced a pair of egg broods (Fig. 2.1.1.B,C) every two-three weeks during a certain period of the year (which for the species chosen for the study is from April till November). The broods are normally placed on the very bottom of the barnacle house (Fig. 2.1.1. C). It would naturally imply that in order to obtain embryos adults had to be brutally detached from a substrate, what caused their death. After this procedure broods with embryos were put into a clean dish with artificial sea water (ASW, 32 g/l) for further development and observation.

The further temperature of cultivation varied (see below) depending on the experiments. Most of the broods were dissected and embryos were laying freely in ASW. One has to mention that barnacle embryos appeared to be quite tough guys and survived all “inconveniences” of the laboratory conditions without obvious suffering. “Inconviences” included abnormally long exposure to light, drastic drops and rises of the temperature, lowered (compared to natural conditions) oxygen etc.

2.2. Methods

2.2.1. 4D microscopy

Mounting

The specimens taken for this method were normally on the very early stages of development: from fertilization till four-cell stage. They were mounted on the slide in a relatively small drop of ASW and covered with a cover glass with plasticin stubs (Fig. 2.2.1.A,B). To prevent evapora-

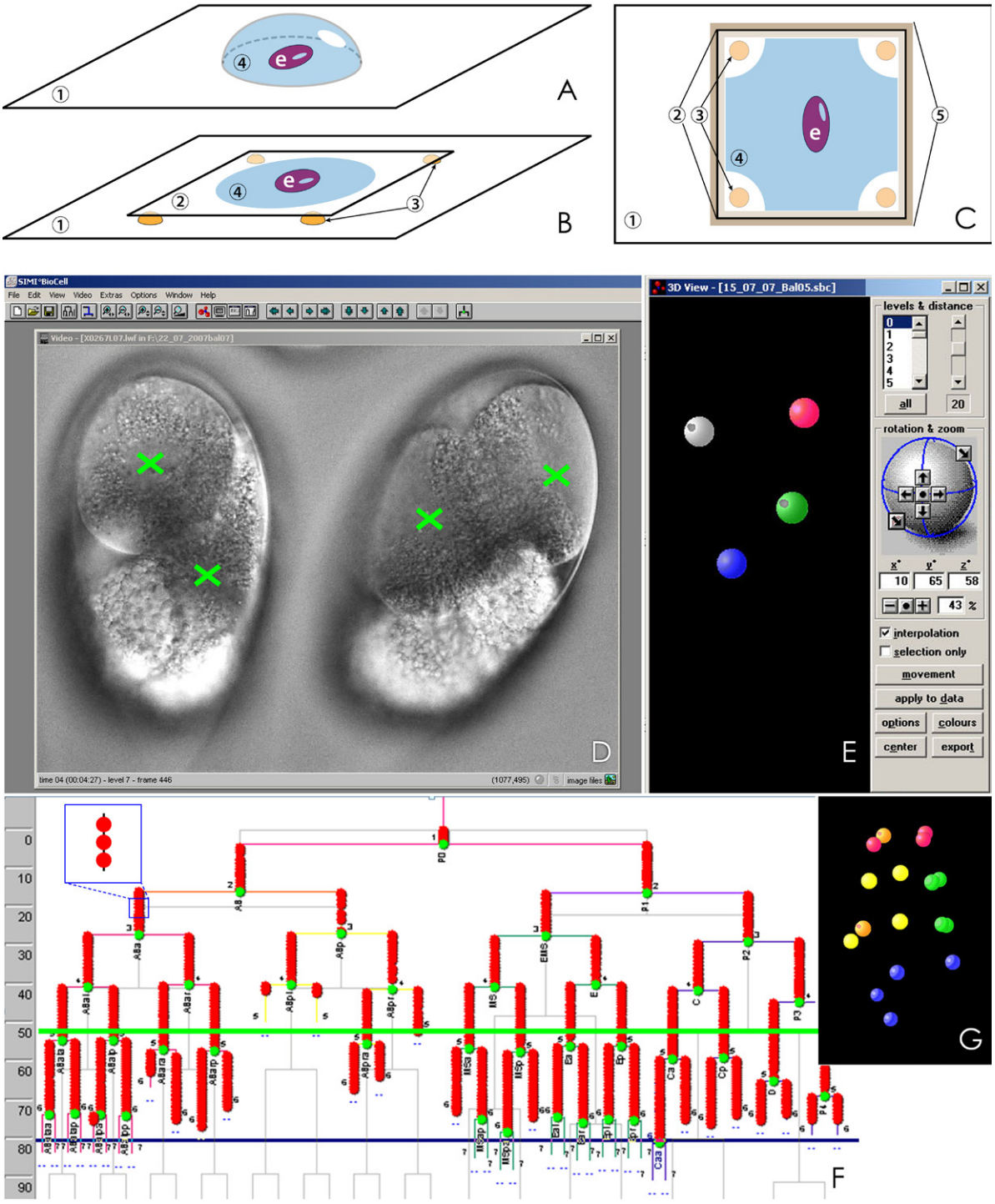

Fig. 2.2.1. Some stages of 4D miscroscopy.

A – The slide (1) with a drop of ASW (4) and an embryo (e); **B** – The same from A, but covered with a cover slide (2) on the plasticin stubs (3); **C** – The same as on B surrounded by a Vaseline rand (5); **D**-**G** – Interface of Simi°BioCell software, **D** – The window with recorded optical section of the two barnacle embryos, in this part of the program it is possible to mark the positions of necessary structures of the embryo in different points in time, green crosses label the positions of the nuclei in this case (only those nuclei are labelled which are visible for a viewer); **E** – An "easy" 3D model of one of the specimens in D (the perspective is not the same), coloured spheres correspond to the positions of the nuclei; **F** – Summarized cell lineage of an analyzed specimen, where the bold red lines are formed by the red circles (**Insertion**), each of the red circles correspond to a single mark in D; **G** - An "easy" 3D model of the embryo corresponding to the point of time marked by a green line in F, each colour corresponds to the progeny of each quadrant (never mind the orange, it was never meant to be there).

tion of the water the cover glass was surrounded by vazeline (Fig. 2.2.1.C:5), so the reservoir was hermetically sealed. In the corners of obtained incubator there was some air containing space left to avoid extremely low levels of oxygen in the water.

The temperature was attempted to be kept around 18 degrees by means of the cooling system adjusted to the microscope (described in detail in Alwes, 2008).

Recording

Mounted embryos were put under a motorised microscope (Zeiss Axiophot: Axioplan II Imaging) devised with a digital camera (PCO pixelfly). Every 60-90 seconds camera made a number of pictures from the different focal planes of the developing embryo, thus performing a short scan. The software controlling the camera settings and assisting with the recording was C++ program (developed by Schulz and Schnabel). Obtained during this process images gave an overview of entire developmental process (Movie 3.1.1.). The outcoming format of the pictures was LWF (lura wave format).

The total recording took about 5-7 days until the embryo was formed. The data were transferred afterwards into the 4D analysing software Simi Bio Cell.

Analysis

The analysis of the obtained scans was carried out in the program called SIMIºBioCell. The software allows to mark the positions of nuclei (or cells) on every short scan and to reconstruct an easy 3D model of the embryo at a certain moment of development (Fig. 2.2.1.D,E,G). Combination of these models in time gave us an overview of the spatial arrangement of the cells during cleavage. The most important of the 4D analysis is that the detailed marking of the cell nuclei during the cleavage and early gastrulation stage facilitate the cell lineaging. As a result it is possible to visualize both the precise cell genealogy and the relative times of all the divisions (Fig. 2.2.1.F,G). The lineage reconstruction is restricted by limited transparency of the embryos and in present work never proceeded beyond 64 cell stage.

The principles of 4D recording as well as of the following analysis are in detail described in Schnabel et al. (1997) and Alwes (2008)

2.2.2. In vivo labelling

For this technique the embryos of the 4-, 8-, and 16-cell-stages had been picked. To slow down the process of development the specimens were put in the isothermal box containing ice with internal temperature of 8-10ºC.

Mounting

The specimens were put on the cover glass in a drop of ASW and covered with another cover glass of a smaller size with vazeline stubs. The second cover glass was placed so, that the em-

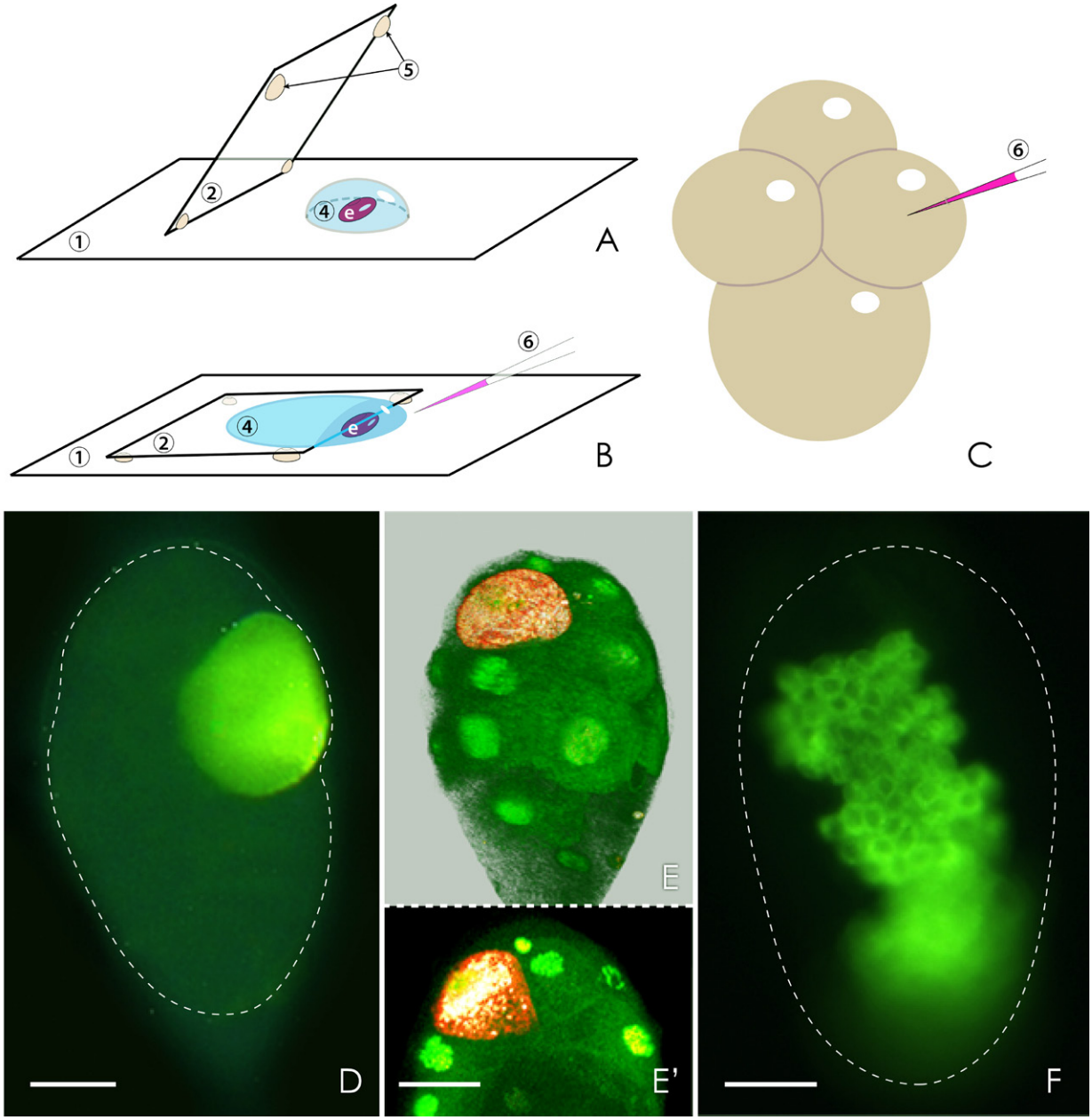

Fig. 2.2.2. Some stages of *in vivo* labelling.

A - The slide (1) with a drop of ASW (4), an embryo (e), and a cover slide (2) with Vaseline stubs (5) ready to be mounted. Note the size of the stubs is different: those stubs on the line with embryo are bigger than the ones on the opposite edge. The final oblique position of the cover glass prevents the water from fast spreading, which might "suck" the small embryos of the barnacle deep under the cover glass; **B** – The same as in A, but with mounted cover glass, the embryo is right under the edge of the cover glass and is slightly pressed to prevent movement; **C** – A schematic example of the singular blastomere labelled at the 4-cell stage embryo, the needle is filled with DiI; **D** – A resulting product of the labelling performed in C; **E**-**E**' – A fixed embryo right after the labelling at 16-cell stage, Imaris Surpass view, blend mode (**E**) and Imaris Extended section view, MIP(max) mode (**E'**), the dye fills entire cell and marks all the intracellular membranes; **F** – Alive specimen observed in epifluorescent microscope 3 days after the labelling at the 4-cell stage, one sees the extended clone of cells, each of which bears the fluorescent dye inside. Scalebars: 20 µm.

bryos were localized under its edge and a half of the water drop remained outside (Fig. 2.2.2.A,B). In this way the embryo is easy accessible for the injections and it is still totally covered by the water to prevent drying out. Additionally, the specimens were fixed in this position by putting slight pressure over the cover glass.

The number of mounted on every slide embryos varied from 10 to 30. The slides with the prepared embryos proceeded under the inverted microscope (Leica DM IRB) mounted with the microinjector (Eppendorf FemtoJet).

Labelling

The single cells (blastomeres) of the chosen specimens were marked with fluorescent dye (DiI, solution in oil) by means of micro-needle (Fig. 2.2.2.C) The needles were prepared in a special way with help of KOPF Vertical Pipette Puller (Model 720) and Narishige Microgrinder (angles 14-18 grad) (see Wolff, 2002 and Caspari, 2010 for details). Many embryos died at this stage or right after, suffering from remounting and changes of salinity (see Chapter 3.4.1.). Those embryos, which survived the procedure were carefully placed into a watch glass with ASW for the further observation.

In most of the cases only certain cell was targeted in the embryos placed on the same slide. However, to filter out the mistakes if any happened, the embryos were checked soon after the injection under fluorescent stereo binoscope (Zeiss Stereo Lumar.V12).

During the next days the development of the clones from the labelled cells was thoroughly observed and some stages were documented by means of the digital camera (AxioCam 12HRc) mounted on the epifluorescence microscope (Zeiss Axioskop 2) (Fig. 2.2.2.D). Unfortunately, fluorescence after these procedures was somewhat bleached out. Therefore, it was impossible to do it repeatedly for the same embryo.

Healthy looking and developing specimens were fixed daily in 4% solution of paraformaldehyde (PFA) in phosphate buffer (PBS) for the forthcoming documentation and analysis. The time of fixation was minimum 30 min.

2.2.3. Fluorescent histochemistry

For all the stainings performed in this work the specimens were sonicated (Elma Transsonic 310) by 3 pulses per 3-4 sec each. The times of fixation for each staining varied (see Table 2.2.1.). For the list of full names and the solution proportions of the chemicals used in this work see Table 2.2.2.

Nuclear staining

The range of the nuclear dyes had been used in the work pursuing different purposes. In the early developmental stages (cleavages and gastrulation) mainly Sytox was applied. This stain is specific for all the nucleic acids, which allows to visualize not only nuclear DNA, but also cytoplasmic RNA. Therefore it is possible to use Sytox-stained embryos in 3D analysis to reconstruct the size and the shape of the cleaving or migrating cells.

In the later stages, beside of Sytox, additional set of dyes, including Hoechst, DAPI, and Draq5, was used. All of them perform counterstaining to embryos marked with other fluorescent dyes. Main advantage of these dyes in relation to Sytox Green was the range of their emission. It is located closer to the marginal zones of the visual spectrum (with peaks for Hoechst in 450-460 nm, DAPI at around 500 nm, and Draq5 in 670 nm). This prevented overlapping of the signals in the specimens carrying additional marking of DiI or Phallacidin.

The best for the cirripede embryos of the three mentioned dyes happened to be DAPI, due to both its easy penetration ability and its slow bleaching speed.

Nervous system staining

To visualize the structure of the nervous system both in the embryos and naupliua antibodies against α-tubulin (raised in mouse) were used. The secondary antibodies (raised in goat) were conjugated with fluorochrome Cy-3. The standard protocol of the staining was a bit modified. The usual step with washing in PBT (BSA, TritonX-100, DMSO in 1xPBS) was skipped. Instead, material had been washed in PT (1xPBS, 1% TritonX-100 (Roth)) for up to 2h. Following solutions of NGS and antibodies were made also on the base of PT. Besides, incubation in primary antibodies was elongated and the best results were obtained after 36h of incubation time under room temperature.

Musculature staining

For the observation of the muscle structure in the barnacles we used phallacidin, which is specific for microfilaments. Phallacidin dye belongs to the family of phallotoxins together with another famous actin marker – Phalloidin. Phallacidin demonstrated clear advantage though. Unlike Phalloidin, it was successful while staining embryonic stages of the muscle development. This was necessary not only for the reconstruction of the developing muscles, but also as an additional dye to DiI. The latter tended to gradually degenerate during the development of the animal, and on the stage of late muscle or nerve formation the remaining DiI was hardly enough to recognize the structure it localized in.

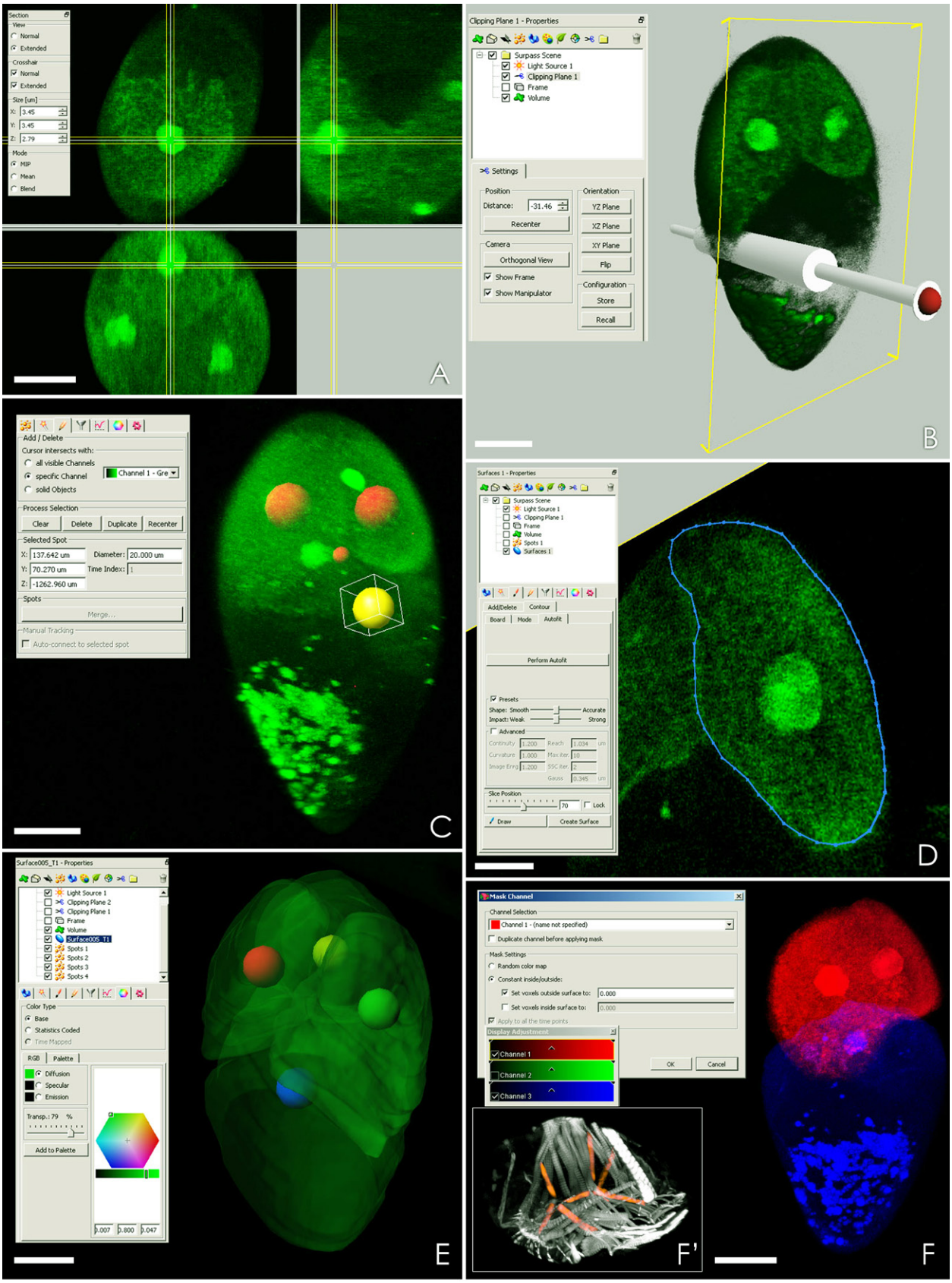

Fig. 2.2.3. Tools of Imaris.

A – Extended section view, MIP(max) mode, allows to view the object in three different planes, yellow running guidelines assist with the positioning of the view; **B** – Surpass view (blend mode), Clipping plane allows to cut the object in any possible plane; **C** – Surpass view (MIP(max) mode), the scene Spots allows

However, Phallacidin itself appeared to be very unstable (or associated with it fluorochrome was), and bleaching occurred very fast. To be able to proceed with CLSM some specimens had never been taken out of the dye solution and mounted in it right on the slide.

2.2.4. Confocal Laser Scanning Microscopy

The specimens successfully stained with fluorescent dyes were processed under the confocal laser scanning microscope (Leica TCS SP2 AOBS). For this they were mounted on the slides under cover glasses in the anti-bleaching medium of DABCO-glycerol.

A very detailed description of the confocal microscope as well as physical laws behind its mechanism was provided by Caspari (2011). In general the method of CLSM allows to obtain

Table 2.2.1. A summary on different protocols of the staining used in the work (simplified).

** applicable only to antibody staining*
*** depends on the main staining*
**** additional to sonication*
***** if applied as a counter stain to DiI, Triton can not be used*
nn – not necessary

Step	Sytox		DAPI/Hoechst		Draq5		Phallacidin		α-Tubulin
	single	counter-	single	counter-	single	counter-	single	counter-	
Fixation	1h and >	**	15min and >	**	15min and >	**	1h	**	20 30 min
Washing	1h and >								
Permeabilization***	nn	****	nn	****	15-30 min in 0,5% Triton	****	1h in 0,5-1% Triton	****	2h in 1% Triton
Blocking*									2h in NGS-PT
Incubation 1	30 min and >	5-10 min	10-15 min		15-20 min		2h and >		24-36h
Washing*									3h
Blocking*									2h in NGS-PT
Incubation 2*									12h
Washing	1h and >	**	1h and >	**	1h and >	**	30-40 min		2h
Mounting	DABCO Glycerol								

to locate spheres in the places of interest, in this case the spheres are placed in the positions of the nuclei; **D** – The first step to creating a Contour Surface scene, one can outline manually a zone of interest on every plane through the object. In the figure the borders of a blastomere are outlined with a blue line; **E** - Contour Surface and Spots scenes combined, the Surfaces for each blastomere were calculated on the base of singular outlines shown in D; **F** – Another possible application of a Contour Surface scene. The original channel is masked by the created surface. One can either single out a content of the surface to a separate channel or to cut it off out of the main one, or combine both steps together. In the provided example different blastomeres are transferred to their own channels. **Insertion** demonstrates a highlighted supporting musculature of the late embryo, which is taken out of the main channel and assigned a specific colour.

Table 2.2.2. List of the chemical substances applied for the present work.

** All the solutions are made on the base of PBS unless specified otherwise.*

Common name	Substance	Manufacturer	Used solution*
PBS	Phosphate Buffered Saline (pH 7,4) NaH_2PO_4 Na_2HPO_4 NaCl	ROTH	1x
PFA	Paraformaldehyde	ROTH	4%
Sytox	SYTOX Green Dye	Invitrogen	1:1500
Dapi	4',6-diamidine-2-phenyl indole (D1306)	Invitrogen	1:1000
Hoechst	Hoechst 33342 trihydrochloride, trihydrate, Fluoro Pure™ grade (H21492)	Invitrogen	1:1000
Draq5	DRAQ5™ 1,5-Bis[[2-(dimethylamino)ethyl]amino]-4,8-dihydroxyanthracene-9,10-dione	Biostatus Ltd	1:500
Phallacidin	BODIPY(R) FL Phallacidin 300U	Invitrogen	1:200
α-Tubulin	acetylated α-Tubulin (IgG 2b Isotype, clone 6-11B-1)	Sigma	1:100-150 in NGS-PT
Cy3	Cy™3-conjugated AffiniPure goat anti-mouse IgG (H+L)	Dianova	1:500 in NGS-PT
DiI	DiI D-282 (1,1'-dioctadecyl-3,3,3',3'-tetramethylindocarbocyanine perchlorate)	Molecular Probes	3mg/ml in oil
Triton	Triton X 100	ROTH	0,5/1:100
NGS	Normal Goat Serum	Southern Biotech	
DABCO-glycerol	DABCO (1.4- diazobicyclo[2.2.2]octane)	Sigma	2.5 mg/ml in 90% glycerol-PBS

extremely detailed results on the anatomy of any specific organ system or entire animal. The outcome of each scan is a stack of images taken from different planes of the specimen. This stack is used by a 3D reconstructing software to produce 3D models of the scanned organism.

2.2.5. 3D Reconstruction

For the purposes of the present work Imaris v7.4.2. (Bitplane AG, Zürich) was mainly used. Most of its modes and tools required in the work are shown and described on the Fig. 2.2.3.

2.3. Nomenclature

Blastomeres

In the early stages of development, starting from one cell on, organism passes through the successive divisions of the cells, known as cleavages. To recognize each particular cell, which is called a blastomere during the cleavage, scientists elaborated a special nomenclature. For each group of animals the name system, which is applied, is usually peculiar. The nomenclature adopted in this work for barnacles was developed by Blochman (1882) and Conklin (1897). This system was chosen due to two reasons. The first one is its simplicity. The second, the system was

already applied on the barnacles by the previous researcher Anderson (1969) and it appears to be convenient to use the same system in order to facilitate the comparisons.

The fact of choosing the nomenclature, which is known to be used mostly for spiralians, should not divert the reader's mind. It is not applied to show the homology of the blastomeres with the same names. The basic principle of assigning first four blastomeres (here often referred as quadrants) with four capital letters A, B, C, and D is the same though and it is based on the backward lineage. First cell to be named is D, and it is a blastomere, which offspring includes the mesendoblastic cell. Its sister quadrant is named C. The quadrant opposite to D is called B and its sister cell is called A. The daughter cells of each quadrant are called by a capital (the one closer to the vegetal pole) and a lower case (the one closer to the animal pole) letters, and an Arabic digit is being added in front. In the following divisions the digit changes only for the blastomeres on the vegetal pole and shows the number of the division for the quadrant. From the fourth division on those blastomeres, which are placed on the animal pole and named with a low case letters, are added an indexed letter. These letters distinguish the positions between two sister cells in relation to entire embryo. There were eight letters used:

a – anterior	**l** – left
p – posterior	**r** – right
v – ventral	**e** – external
d – dorsal	**i** – internal

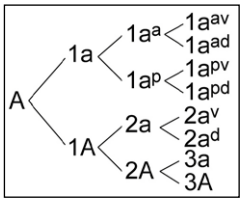

Fig. 2.2.4. Example of the names of the cells, descending from A quadrant.

After the sixth division the indexed letters are also applied for the blastomeres, which are named with the capital letters. At this stage it is impossible to distinguish their relation to the vegetal pole, as their daughter cells internalize. A sample of the names for the blastomeres within quadrant A is presented on the Fig. 2.2.4. A general overview of the names of all the blastomeres one can see on the Fig. 3.3.1.

Despite of the names, which show to what quadrant the cell belongs, all the early cells are often assigned the names depending on their fate. Not to mix certain terms we propose the following nomenclature of the cells:

ectoblast – the blastomere giving rise to the ectodermal structures.
endoblast – the blastomere producing endodermal structures.
mesoblast – the term is in general discouraged as it doesn't reflect its origin, although can be used.
mesectoblast – the blastomere giving rise to both ecto- and mesodermal structures, but not to the endoderm.
mesend(t)oblast[♣] – the blastomere producing both endo- and mesodermal structures, but not to the ectoderm (introduced by Wilson, 1898, the same meaning).

[♣] Traditionally the term "mesenToblast" is used, although the germ layer originating from is traditionally called enDoderm. In the present work the terms mesenDoblast and mesenDoderm are used.

ectomesoblast – the blastomere giving rise to the mesodermal structures, the sister cell to the ectoblast (introduced by Lillie, 1895, the meaning was the same, although by many scientists it is often used for mesectoblast).

endomesoblast – the blastomere producing mesodermal structures, sister cell to the endoblast.

ectomesoderm – the germ layer originating from ectomesoblast, sometimes referred as a secondary mesoderm. The latter, however, is not a total synonym to the ectomesoderm, as in deuterostomes the secondary (induced) mesoderm does not necessarily originates from ectoblasts (for review see Rodaway and Patient, 2001).

endomesoderm – the germ layer originating from endomesoblast.

Poles and axes

There were two types of axes considered during the description: the axes of the egg shell and the axes of the embryo. The axes of the egg are two, longitudinal and transversal, and are mainly used to assist with the orientation of the embryo during development.

Embryonic axes are three: anterior-prosterior (AP axis), dorso-ventral (DV axis), and left-right (LR axis). In *E. modestus* establishment of those happens at the four cell stage (see Chapter 3.3.2.). Additionally, there is another axis mentioned in the work, the animal-vegetal axis (AV axis). This axis passes between animal and vegetal poles. The animal pole is marked by a polar body, the vegetal pole by a blastopore. In the stages of cleavage the vegetal pole is referred as a place opposite to the animal pole.

In the barnacle embryos the AV axis does not strictly corresponds to AP axis as it does for many animals. During the cleavage the animal pole is "localized" on the border of A-, B-, and C-progenitors, whereas the anteriormost part of the embryo is found more or less in the middle of the descendants of B quadrant. Therefore during the description of the early stages these two axes are always mentioned.

3. RESULTS

3.1. Staging of the embryonic development

To make the description of results easier, it seems logical to introduce the staging of the embryonic development in *Elminius modestus*. The staging is generally based on that done by Groom (1894) and Crisp (1954). Some stages, which they distinguished in their studies, are here fused or subdivided. This staging is, however, not absolute and should be relied on with caution. The development in general is one constant and undividable process. The larval development of barnacles is usually artificially subdivided into stages marked by moults. In contrast to that, the embryo does not pass through moults during development. For that reason there cannot be clearly defined borders between the certain stages described below.

Fig. 3.1.1. Embryonic stages 0 – 3.

p17

A – Stage 0, segregation, alive specimen; **B**-**C** – Stage 1, 2-cell stage (**B**) and 8-cell stage (**C**), alive specimens; **D**-**F** – Stage 2, **D** – epiboly, the arrows show the direction of overgrowing blastoderm, alive specimen; **E** – Sytox-stained embryo at the stage of gastrula, several hours after closure of blastopore, fixed specimen; **F** – section through the Sytox-stained embryo, embryo is of the same age as the one in E, arrows show forming mesoblast, fixed specimen; **G**-**I** – Stage 3, G (alive specimen) and **H** (fixed specimen) – general view of the stage, mesoblast is now placed between blastoderm and endoderm; **I** – section through the embryo in H, arrows indicate nuclei from the three germ layers, fixed specimen. Scalebar 20 µm.

Fig. 3.1.2. Embryonic stages 4 – 6.

p18

A-**D** – Stage 4, **A**-**B** – alive specimen, arrowheads pointing the limb buds bulging out, in ventral (**A**) and left-lateral (**B**) view; **C** – fixed and Sytox stained embryo, forming limb buds are outlined, dorsal view; **D** – transversal section through a fixed and Sytox-stained embryo at the level of the antennary segment; **E**-**H** – Stage 5, **E**-**F** – right-lateral view of alive (**E**) and Sytox-stained (**F**) specimen, on F slightly invaginating gut is visible, the lateral ectodermal grooves separating limbs become diagonal; **G** – fixed and Sytox-stained embryo, the developing gut and slightly bulging labrum are outlined, ventral view; **H** – transversal section through fixed and stained embryo at the level of antennary segment, the dorsal groove of ectoderm cuts deeper into the embryo and splits the limb buds away from the forming nauplius body; **I**-**K** – Stage 6, **I** – right-lateral view of alive specimen; **J** – left-lateral view of fixed and Sytox-stained embryo, limbs are elongated and directed towards posterior, tips of *all* and *mb* show signs of bifurcation, which is better visible on the example of *mb* (**J**); **K** – transversal cut through the fixed and Sytox-stained embryo at the midlevel of the body, tube-like limbs and oesophagus are outlined. Scalebar 20 µm.

Fig. 3.1.3. Embryonic stages 7 – 9.

p19

A-**C** – Stage 7, **A** – right-lateral view of alive specimen, double arrowheads show cuticular excretion of epidermis, forming setae of limbs; **B** – right-lateral view of fixed and Sytox-stained embryo; **C** – dorsolateral view of the embryo on B, bifurcation of *all* and *mb* is more pronounced than in stage 6; **D**-**G** – stage 8, **D** – right lateral side of alive specimen, cuticular setae are well discernible; **G** – ventral view (slightly turned to the right side) of fixed and Sytox-stained embryo; **E**-**F** – early stage 9, alive specimens in right-lateral (**E**) and ventral view (**F**), arrows point at the lightly pigmented nauplius eye and the well formed and visible oesophagus; **H** – stage 9, fixed, taken out of the egg shell, and Sytox-stained embryo in ventral view. Scalebar 20 µm.

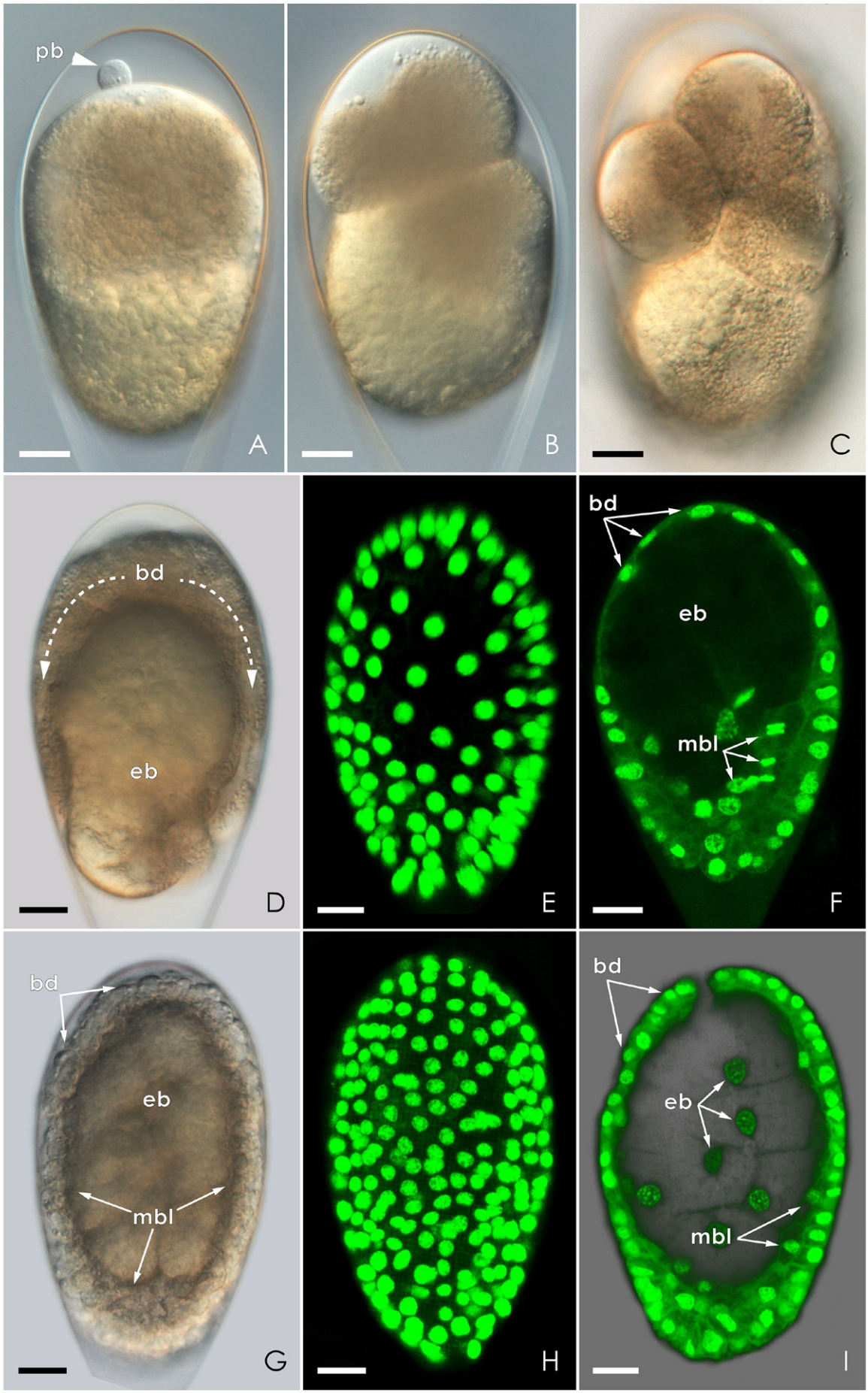

Fig. 3.1.1. Embryonic stages 0 – 3.

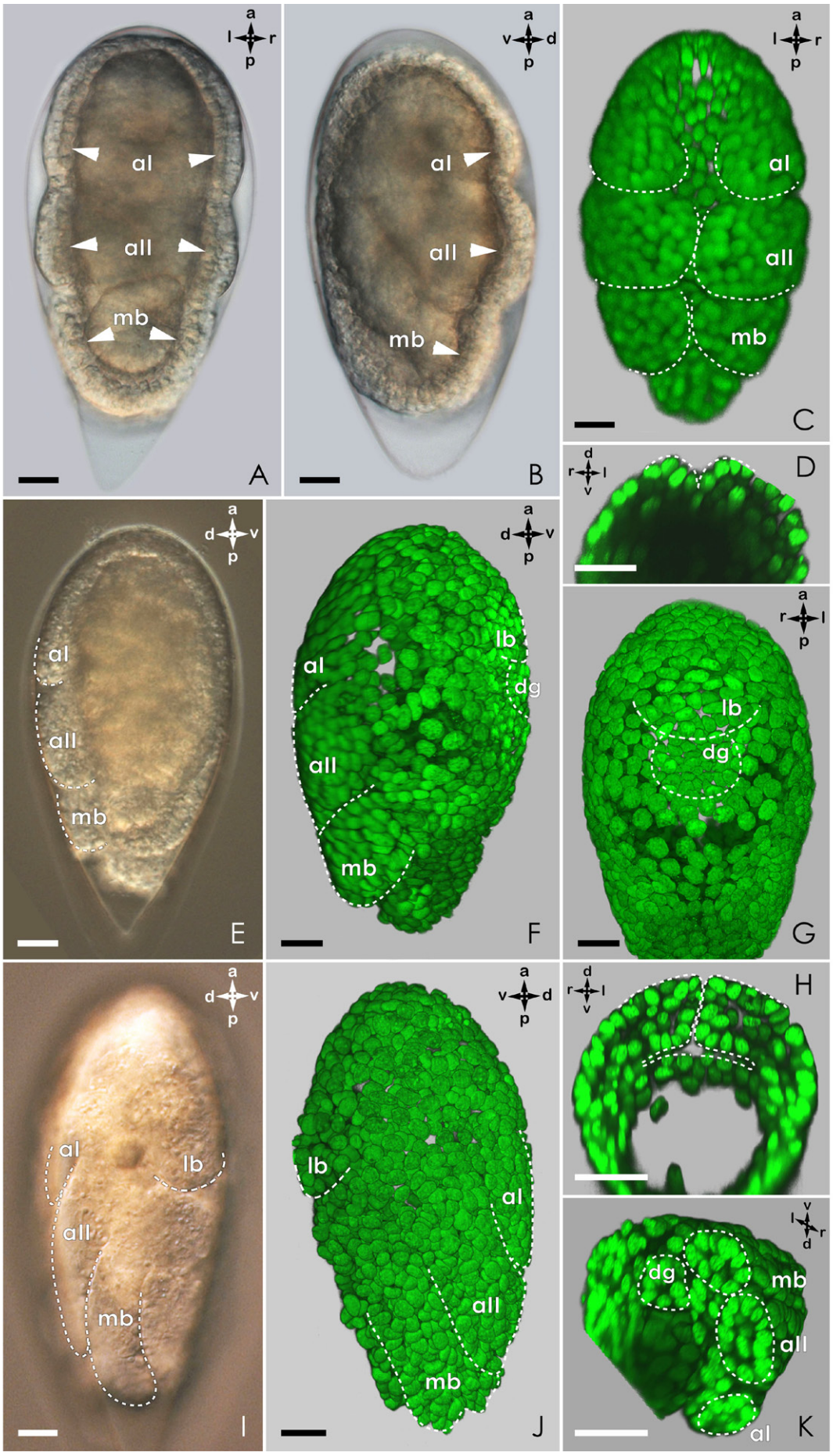

Fig. 3.1.2. Embryonic stages 4 – 6.

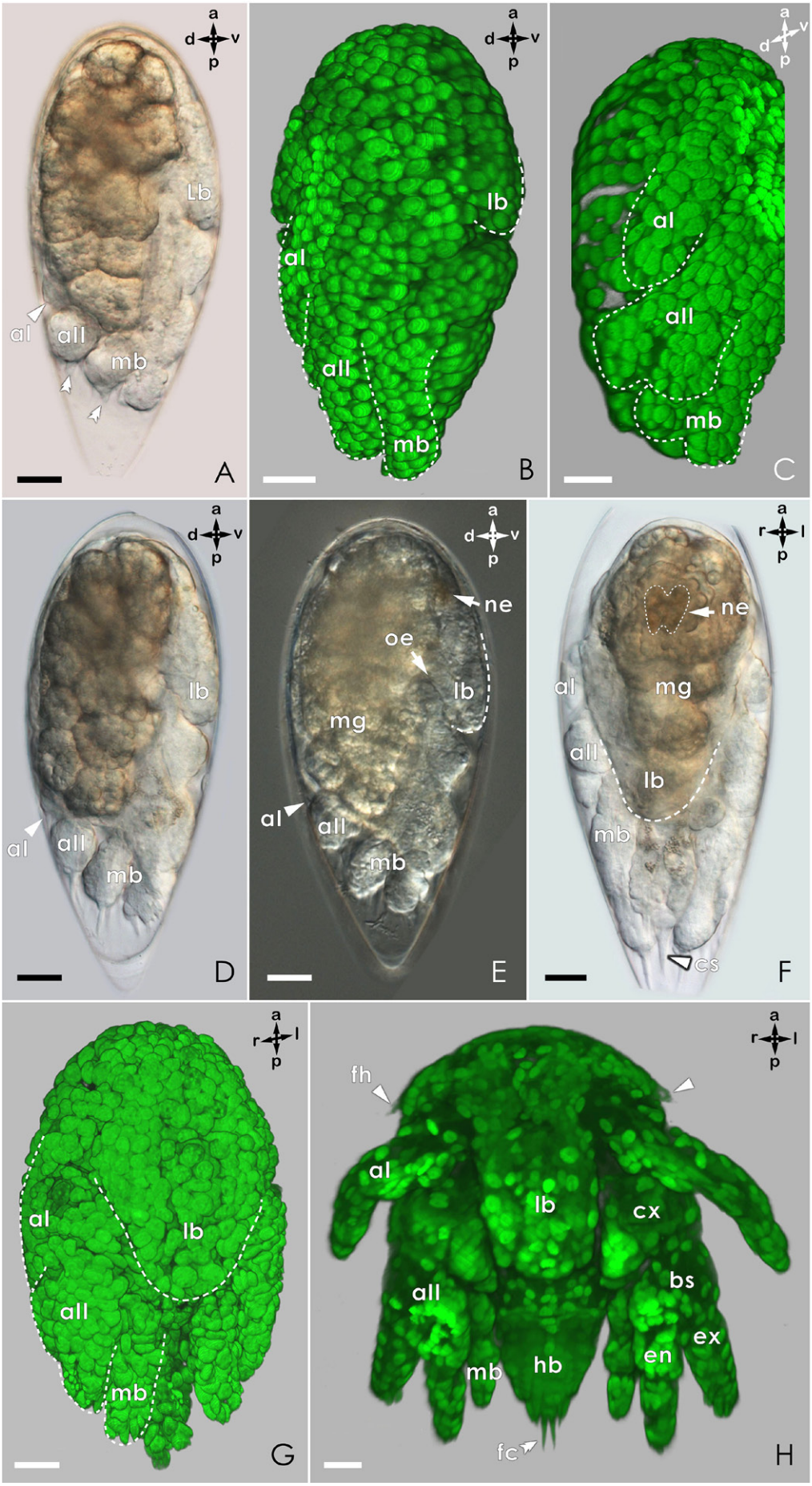

Fig. 3.1.3. Embryonic stages 7 – 9.

Table 3.1.1. Staging of the embryonic development of *Elminius modestus.*

Fig. 3.1.1-3. Movie 3.1.1.

Stage	Characteristics of the stage	Stage by Groom, 1894	Stage by Crisp, 1954
0	- From fusion of nuclei, which is marked by undulation of the cytoplasm, until segregation of the cytoplasm is completed. (Fig. 3.1.1. A)	A	1
1	- First – fourth cleavages (zygote – 16-cell stage). (Fig. 3.1.1. B,C)	A/B[♣]	2,3
2	- Epiboly, formation of a blastopore, first equal divisions of a yolky cell (16-30-cell stage). (Fig. 3.1.1. D-F)	B	3,4,5
3	- End of gastrulation and germ layer formation, 2-8 yolky cells The stage takes around 2-2.5 days. (Fig. 3.1.1. G-I)	C	6,7
4	- Formation of the limb anlagen on the dorsal side of the embryo. Grooves separating limb buds are transversal and, additionally, one longitudinal. (Fig. 3.1.2. A-D)	D,E	8
5	- Limb buds are elongated and separated by diagonal grooves now. Limb bud tips point dorso-posteriorly. - On the ventral side of the embryo at the level of antennal segment there is a slight invagination of a forming gut. (Fig. 3.1.2. E-H)	F	9
6	- Limb anlagen are of tube-like shape, placed diagonally, the tips of *aII* and *mb* show slight bifurcation. - Labrum outline become visible, further invagination of the ectodermal portions of the digestive tract. (Fig. 3.1.2. I-K)		
7	- Tips of appendages point more to the posterior compared to the stage before. Bifurcation of the second and third pair of limbs is well discernible. Ectodermal cells start to produce cuticle of the limb setae (at this stage the setae look like spikes). - Labrum anlage becomes prominent, now covering the developing oesophagus. (Fig. 3.1.3. A-C)	G	10
8[♣♣]	- The appendage setae elongate taking a seta shape. - Labrum occupies most of the ventral surface of the embryo. - Forming nauplius eye acquires red and light-brown pigmentation. (Fig. 3.1.3. D,G)		11
9	- Completely formed larva, shortly before hatching. - Limbs elongate significantly (Movie 3.1.) filling in the posterior space of the egg shell. - Pigmentation of the nauplius eye is dark brown. - Yolk-containing cells transform into a spacious midgut. - The whole body of the larva exhibits movements. (Fig. 3.1.3. E,F,H)	H	12, 13

[♣] Groom includes both zygote formation and first division in one stage.

[♣♣] The stage 8 and early stage 9 are almost impossible to distinguish from outward appearance. There are, however, many events happening internally especially concerning nervous and muscle system (see below).

3.2. Morphology and anatomy of nauplius larva

All of the data presented in this chapter refer to the nauplius stage I. One reason for this is that the gross morphology and anatomy of the nauplius larva is already established at this stage. Another reason: current research does not go beyond the nauplius I.

Morphologically nauplius of *Elminius modestus* represents a typical cirriped nauplius (which were investigated a lot, for general overview see Walker, 1992) (Fig. 3.1.3.H). Its headshield is of a drop-like shape, being broad on the anterior and narrowing to the posterior. The larva consists of three segments, each of which is equipped with a pair of limbs, and an elongated hindbody furnished on the posterior tip by a ventral furca and a dorsal caudal spine (Fig. 3.1.3.F,H). The three pairs of limbs appear as following: uniramous first antennae (*aI*), biramous second antennae (*aII*), and biramous mandible (mb). The two branches of both *aII* and *mb* are the dorsal exopodite and the ventral endopodite. Further details on limb structure (like the number of articles and setae, which are of value for systematic analyses) were not the goals of the current study and can be found, if desired, in Knight-Jones and Waugh (1949). The anterior region of the nauplius carries laterally a pair of tubular structures, the fronto-lateral horns, which are apomorphic for Cirripedia (Høeg, 1992). Anterio-ventrally there is a pair of slender processes, the outer part of the frontal-filament complex (which will be described below). At the ventral side the most prominent structure is the labrum, placed posteriorly to the frontal filaments and between the bases of *aII*. It covers the mouth and oesophagus.

The oesophagus, representing the foregut of the nauplius, leads to a midgut, occupying the most of the inner volume of the larva. At the nauplius stage I the midgut is not subdivided into different compartments, as it was reported for the later stages (Walley and Rees, 1969). Posteriorly the midgut is connected with the hindgut, or proctodaeum, which terminates in the anal opening placed between furcal rami and caudal spine.

3.2.1. Anatomy of the nervous system

The nervous system of the barnacle nauplius comprises four paired central ganglia connected to each other via connectives and a set of peripheral nerves running to different organs of the larva. The first three ganglia form a tri-partite brain arranged in a circumoesophageal ring (Fig. 3.2.2.A,B,C). The simplified scheme of the naupliar nervous system is presented on Fig. 3.2.1.

3.2.1.1. The brain

The preoesophageal part of the brain department includes a pair of protocerebral ganglia connected via a protocerebral commissure and a pair of deutocerebral ganglia (Fig. 3.2.2.C). Each *protocerebral ganglion* includes numerous somata, which are placed antero-dorsally and latero-

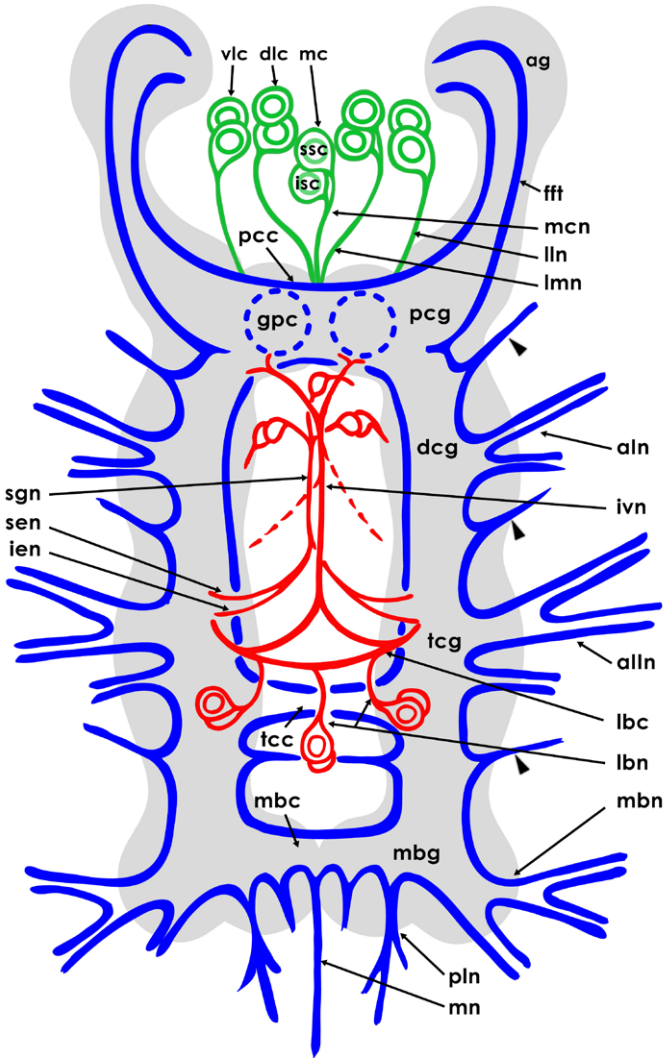

Fig. 3.2.1. Schematic overview of the nauplius nervous system.

Ventral view. Arrowheads point at the intersegmental nerves. Further description se in the text.

ventrally with respect to the neuropil and around the neuronal tract leading to the frontal filament complex (see below; Fig. 3.2.2.C,F,G). The protocerebral commissure has a characteristic architecture. Ventrally it can be subdivided into a prominent anterior portion consisting of numerous neurites and a slender posterior part consisting of several neuronal strands (Fig. 3.2.2.B,H). Dorsal to the anterior "bulgy" part there is a pair of globular neuropils with associated dorsal somata (Fig. 3.2.2.D,E,F). The main innervations of the protocerebral ganglia are going to the nauplius eye and the frontal filament complex (Fig. 3.2.2.B,I).

The *nauplius eye* consists of five distinct units arranged in three cups: two lateral cups comprising two units each (Fig. 3.2.2.I,J,N) and one median cup consisting of only one unit (Fig. 3.2.2.M). In between the three cups two pigment cells are placed (Fig. 3.2.2.K,L). Each unit includes a superior and an inferior sensory cell (Fig. 3.2.2.D,E,H). The neurites of these two cells are united in one nerve. The nerve of the single unit of the median cup projects into the dorso-medial region of the protocerebral commissure, between the globular neuropils (Fig. 3.2.2.H). The dorso-medial unit of each lateral cup sends its nerve to a medial area of the globular protocerebral neuropils (Fig. 3.2.2.E,I). The nerve of the ventro-lateral unit connects to a lateral area of the same (Fig. 3.2.2.I,J). With the methods used in this work it was impossible to identify other cells related to the nauplius eye.

The *frontal filament complex* is a paired structure, consisting of outer and inner parts (Fig. 3.2.2.O). The outer parts are two slender processes placed on the ventral side of the nauplius, anterior to the labrum and covered by cuticle (Fig. 3.1.3.K). The internal content of the latter

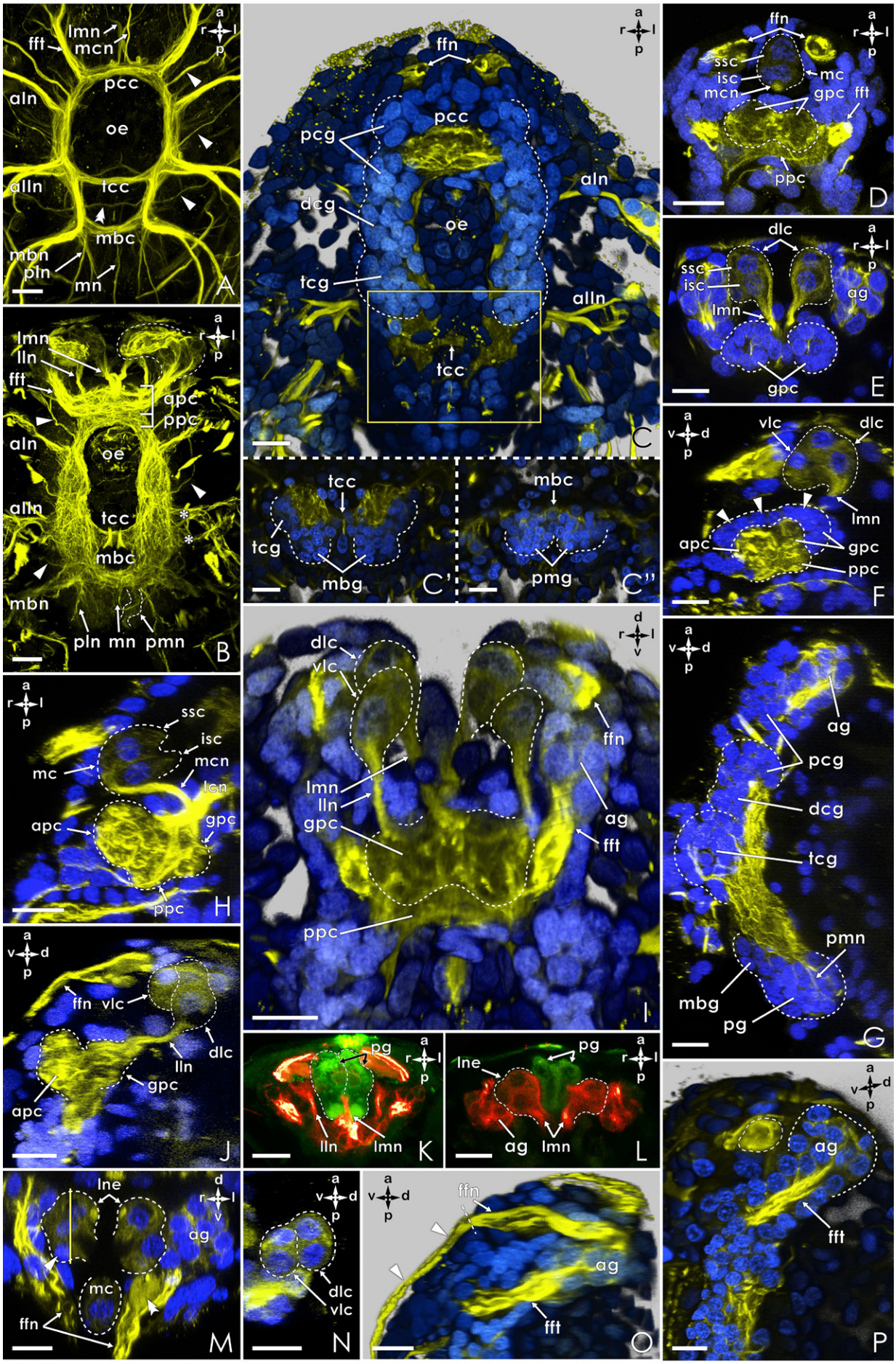
A
lmn
mcn
fft
pcc
aln
oe
alln
tcc
mbc
mbn
pln
mn
B
lmn
lln
fft
qpc
ppc
aln
oe
alln
tcc
mbc
mbn
pln
mn
pmn
C
ffn
pcc
pcg
aln
dcg
oe
tcg
alln
tcc
C'
tcc
tcg
mbg
C''
mbc
pmg
D
ffn
ssc
isc
mcn
mc
gpc
fft
ppc
E
dlc
ssc
isc
lmn
ag
gpc
F
vlc
dlc
lmn
apc
gpc
ppc
G
ag
pcg
dcg
tcg
pmn
mbg
pg
H
ssc
isc
mcn
mc
lcn
apc
gpc
ppc
I
dlc
vlc
ffn
lmn
lln
gpc
ag
fft
ppc
J
ffn
vlc
dlc
lln
gpc
apc
K
pg
lln
lmn
L
pg
lne
ag
lmn
M
lne
ag
mc
ffn
N
dlc
vlc
O
ffn
ag
fft
P
ag
fft

appears to be mostly tubulin fibres (no nuclei or fibrillar actin were revealed by corresponding stainings). Each process is connected to the inner parts represented by neuronal tracts of a "V"-shape (Fig. 3.2.2.B,O). The tip of the "V" is an agglomeration of somata placed dorsally and forming an anterior ganglion[♣] (Fig. 3.2.2.G,I,P). The arms of the "V" are directed ventrally, with one leading to an outer part (frontal filament nerve) and another to a lateral region of the proto-cerebral neuropil (frontal filament tract) (Fig. 3.2.2.O). At the base of the outer part there is a vesicular structure unspecifically stained with Sytox Green (Fig. 3.2.2.M, arrowhead, P, out-lined).

Fig. 3.2.2. Anatomy of the nervous system of the Nauplius I larva. Central ganglia and protocerebral region.

All images are obtained from Nauplius I (unless specified otherwise) in Imaris Extended Section view, MIP(max) mode, except for C,I,O, and P: Imaris Surpass view, Blend mode of Volume Scene, assisted with Clipping Plane.

Color code:

α-tubulin *Serotonin*
α-tubulin *DAPI or Sytox*

A-**G** – Central nervous system; **D**-**F**, **H**-**P** – innervations of protocerebral region;
A – general view of central nervous system, early Stage 9, ventral view, the stomatogastric nervous system is cut out, arrowheads indicate intersegmental nerves, double arrowhead indicates additional commissure; **B** – general view of central nervous system of Nauplius I, ventral view, the stomatogastric nervous system is cut out, arrowheads indicate intersegmental nerves, V-shaped inner part of frontal filament complex is outlined; **C** - general view of tripartite brain, outlined, ventral view; **C'** – deeper cut through the outlined region on C, soma cortex of mandibular ganglia; **C"** – deeper cut through the outlined region on C, somatic part of posterior mandibular ganglia, outlined; **D** – frontal section through protocerebral region at the level of dorsal part of protocerebral commissure; **E** – frontal section through protocerebral region at the level of soma cortex of dorsal protocerebral ganglia; **F** – sagittal section through protocerebral region, at the level of the left dorsal protocerebral ganglion, arrowheads indicate somata surrounding of protocerebral commissure; **G** – sagittal section through entire central nervous system at the level of the connectives, both frontal filament tract and tritocerebral/mandibular connective are bent dorsally, the general placement of somata in relation to neuropils is shown; **H** – median section through protocerebral region; dorsal globular part of the commissure is minimized in its median part; **I** – general view of the protocerebral innervations, antero-posteriorly tilted transverse cut at the level of dorso-posterior part of protocerebral commissure, median cup of the nauplius eye is not shown; **J** – sagittal section inclined in relation to left-right axis through the dorso-median component of the nauplius eye; **K**-**L** – frontal sections through different regions of pigment cells of nauplius eye; **M** – transverse section through nauplius eye at the level of superior sensory cells of nauplius eye, since the section being capable of showing all the five superior cells was too thick, one can also see the inferior cell of the ventro-lateral component of the lateral cup (arrowhead), double arrowhead indicates the vesicular portion of the inner part of the left frontal filament; **N** – longitudinal section through the lateral cup at the region shown by the yellow line on M; **O** – sagittal cut tilted in relation to left-right axis through the frontal filament complex, V-shaped inner part is clearly visible, the arrowheads point out the outer part of the frontal filament complex on the left, the dashed line indicates the border between the outer and inner parts; **P** – slightly deeper cut of the sample shown on O, the outlined by slender dashed line region represents a vesicular portion, a somatic part of the anterior ganglion is outlined by a dicker dashed line. Scalebar 15 µm.

[♣] It is named by other researchers as a lateral protocerebrum, here it is preferred to use the neutral term "anterior ganglion".

The *deutocerebral ganglia* have hardly distinguishable borders to the protocerebral ganglia (Fig. 3.2.2.C). Deutocerebral somata are placed ventral to the neuropil (Fig. 3.2.2.G). Due to the absence of a separate deutocerebral commissure the course of transversely crossing neurites between the two ganglia remains unresolved. Some in vivo data suggest, however, that they have linking neurites in both the protocerebral and tritocerebral commissures. From the deutocerebral ganglion one prominent nerve leads to antenna I (Fig. 3.2.2.A,B,*aI*n). In its proximal part it bifurcates, with one branch going dorsally and the other ventrally (Fig. 3.2.3.A,1). The ventral nerve branches within the limb and is placed centrally with regard to the intrinsic muscles of *aI*. Halfway along the length of a1 there is a small cluster of neuronal cell somata (Fig. 3.2.3.B).

The postoesophageal part of the brain comprises paired *tritocerebral ganglia* connected with the preoesophageal part via long and thick circumoesophageal connectives. The tritocerebral somata are placed ventral to the neuropil (Fig. 3.2.2.G). The tritocerebral commissure is composed of numerous neurites, but significantly thinner than that of the protocerebral ganglia (Fig. 3.2.2.A,B). Slightly posterior to it there is a slender commissure (Fig. 3.2.2.A, double arrowhead). The main projection of the tritocerebral ganglion goes to *aII*. In the early embryonic stage 9 it is one nerve splitting into two branches (Fig. 3.2.2.A, *aII*n). The anterior branch inserts ventrally to the protopodite of *aII*, bifurcates and sends innervations into the exo- and endopodites. The posterior branch turns dorsally (Fig. 3.2.3.A,2). Its further course was not followed in detail. In the nauplius larva it appears to consist of two nerves: anterior and posterior (Fig. 3.2.2.B, asterisks).

Apart from segmental innervations there are three pairs of intersegmental nerves running from the proto/deutocerebral, deuto/tritocerebral, and tritocerebral/mandibular connectives in a latero-dorsal direction (Fig. 3.2.3.A). The first pair of these nerves leads towards the fronto-lateral horns and via a set of somata interconnects with the short nerve running within each fronto-lateral horn. The second pair of intersegmental nerves extends towards the fronto-lateral horns as well, but after the fasciculation with the somata cluster it runs further dorsally (Fig. 3.2.3.A, dashed arrow). It seems to end in the area of the second pair of dorsal headshield setae. The third pair of the intersegmental nerves goes laterally and turns to the dorsal side. The further course of this nerve was impossible to follow.

3.2.1.2. Stomatogastric nervous system

The stomatogastric nervous system in the barnacle nauplius is composed of the nerves innervating the oesophagus with the covering labrum, the midgut, and the hindgut. The part associated with labrum and foregut is the most complicated. The most ventral component is the inferior ventricular nerve running outside of the circular muscles of the oesophagus (Fig. 3.2.3.D,E,F,H).

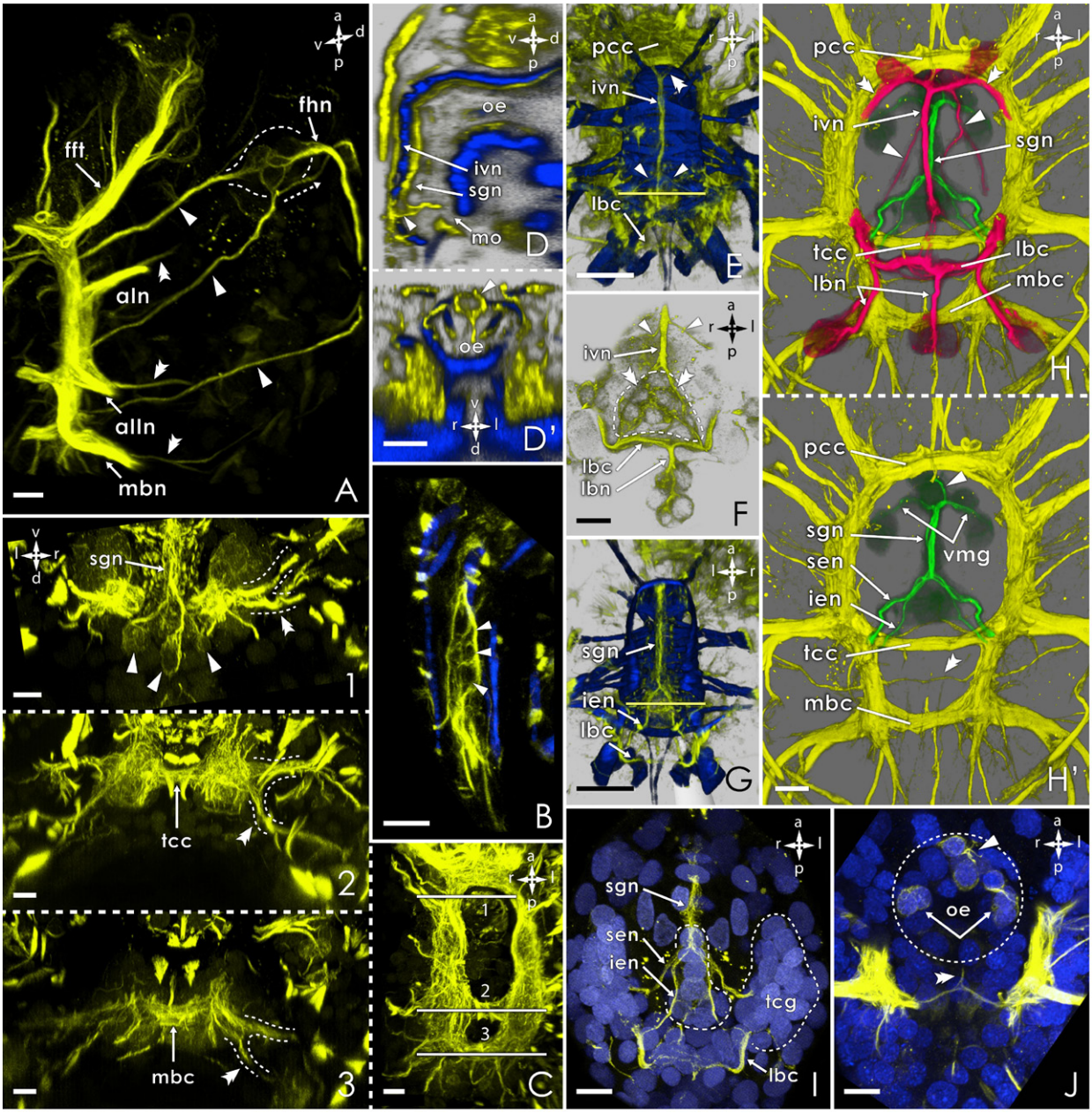

Fig. 3.2.3. Anatomy of the nervous system of Nauplius. Peripheral nervous system.

All the images are obtained from Nauplius I (unless specified otherwise) in Imaris Extended Section view, MIP(max) mode (D,F,4,5 – Blend Mode), except for A,E,G, and H: Imaris Surpass view, Blend mode of Volume Scene (A – MIP(max) mode), assisted with Clipping Plane.

Colour code:

α-tubulin - *B,D,E,G – Phallacidin*

- *I,J – Sytox*

A-**C** – segmental and intersegmental nerves; **D**-**J**, **M**-**O** – stomatogastric nervous system; **K**-**L** – innervations of the hindbody;

A – dorsal segmental (double arrowheads) and intersegmental nerves (arrowheads), Stage 9, ventro-lateral view, the ventral branches of the segmental nerves are cut away, the fasciculation of intersegmental nerves with the nerve of the fronto-lateral horns is outlined, the dashed arrow shows the continuation of the second intersegmental nerve; **B** – longitudinal section through the *aI*, arrowheads point at the α-tubulin-positive cellular structure; **C** – general view of central neuropils, the ventral branches of the segmental nerves are cut away on the right side, numbers correspond to the numbers of the pictures on the left, which represent transverse sections through different regions of the cns: 1 – section

It is connected to the posterior protocerebral commissure and possibly to the deutocerebral neuropil as well (Fig. 3.2.3.H, double arrowheads). Along its way it sends some delicate neurite bundles towards the posterior (Fig. 3.2.3.E,F,H, arrowheads). Halfway along the labrum it splits into two and connects to the labral commissure (Fig. 3.2.3.F). A group of α-tubulin-positive cells (the "outer" cluster) borders the bifurcation place (Fig. 3.2.3.F, outlined). The function of these cells and their relation to the stomatogastric innervations are not clear. The labral commissure is an arch-like neurite bundle arising from the tritocerebral ganglia and ventrally embracing the oesophagus/stomodaeum (Fig. 3.2.3.F,H,I). There are three nerves going from the labral commissure to the distal portion of the labrum (labral nerves, Fig. 3.2.3.H) and two pairs of nerves directed anteriorly (superior and inferior oesophageal nerves, Fig. 3.2.3.G,H',I). The oesophageal nerves unite medially into the stomatogastric nerve, which runs anteriorly and in parallel to the inferior ventricular nerve, but inside of the oesophageal muscle tube (Fig. 3.2.3.D,G,H,H'). Where the oesophageal nerves fuse, another group of α-tubulin-positive cells (the "inner" cluster) is located (Fig. 3.2.3.I, outlined by a slender dashed line). These cells seem to be connected to the cells of the more ventral "outer" cluster that lies just above (Fig. 3.2.3.D,D'). Additionally, these cells send short projections into the oesophageal lumen. There is one short suboesophageal nerve leading to the proximal part of the oesophagus and originating from lateral loci of the tritocerebral commissure (Fig. 3.2.3.H'). The stomatogastric nerve is leading into the midgut. On the entrance into it the nerve gives off two lateral branches (Fig. 3.2.3H',1; Fig. 3.2.4.D), which run along the ventral side of the midgut (ventral midgut nerves). Slightly more dorsal the stoma-

through deutocerebral region, segmental nerve is outlined, double arrowheads show its dorsal branch, arrowheads show the branching of the sgn; 2 – section through the tritocerebral region; 3 – section through the mandibular region; **D**-**D'** – median (**D**) and transversal (**D'**) sections through the labrum and oesophagus, arrowheads indicates the possible interconnection between the "outer" and "inner" cell clusters; **E** – ventral view of labral and oesophageal musculature and of the "ventral" part of the sns, the ivn extends on the ventral external surface of oesophageal circular muscles, the yellow line corresponds to the transverse section on D'; **F** – ventral view of the inferior ventricular nerve, "outer" cell cluster (outlined), and labral commissure, arrowheads mark the neurites branching out of the ivn, double arrowheads indicate the two end branches of the ivn; **G** – dorsal view of labral and oesophageal musculature, stomatogastric and oesophageal nerves, and labral commissure, the sgn extends along the dorsal internal surface of oesophageal circular muscles, view from the inside of the oesophagus, the yellow line corresponds to the transverse section on D'; **H**-**H'** – general view of the stomatogastric nervous system, early Stage 9, only masked channels are shown: yellow – general scaffold of nervous system, red – the outer (with respect to muscles) part of the sns, green – the internal part of the sns; **H** – arrowheads show the branches of the ivn leading towards the deutocerebral neuropil, double arrowheads show the lateral branches of ivn; **H'** – the arrowhead indicates the continuation of sgn towards the dorsal side of the midgut, double arrowhead indicates the additional commissural strand; **I** – ventral view of the "internal" part of the sns, the "inner" cell cluster is outlined by a slender dashed line; **J** – frontal section through the region right under the circumoesophageal ring, early Stage 9, arrows point at the somata of the first two branches stemming out of sgn, arrowhead indicates the somata of the sgn running along the midgut anterior-dorsally, double arrowhead points at short suboesophageal nerve. Scalebar 10 µm.

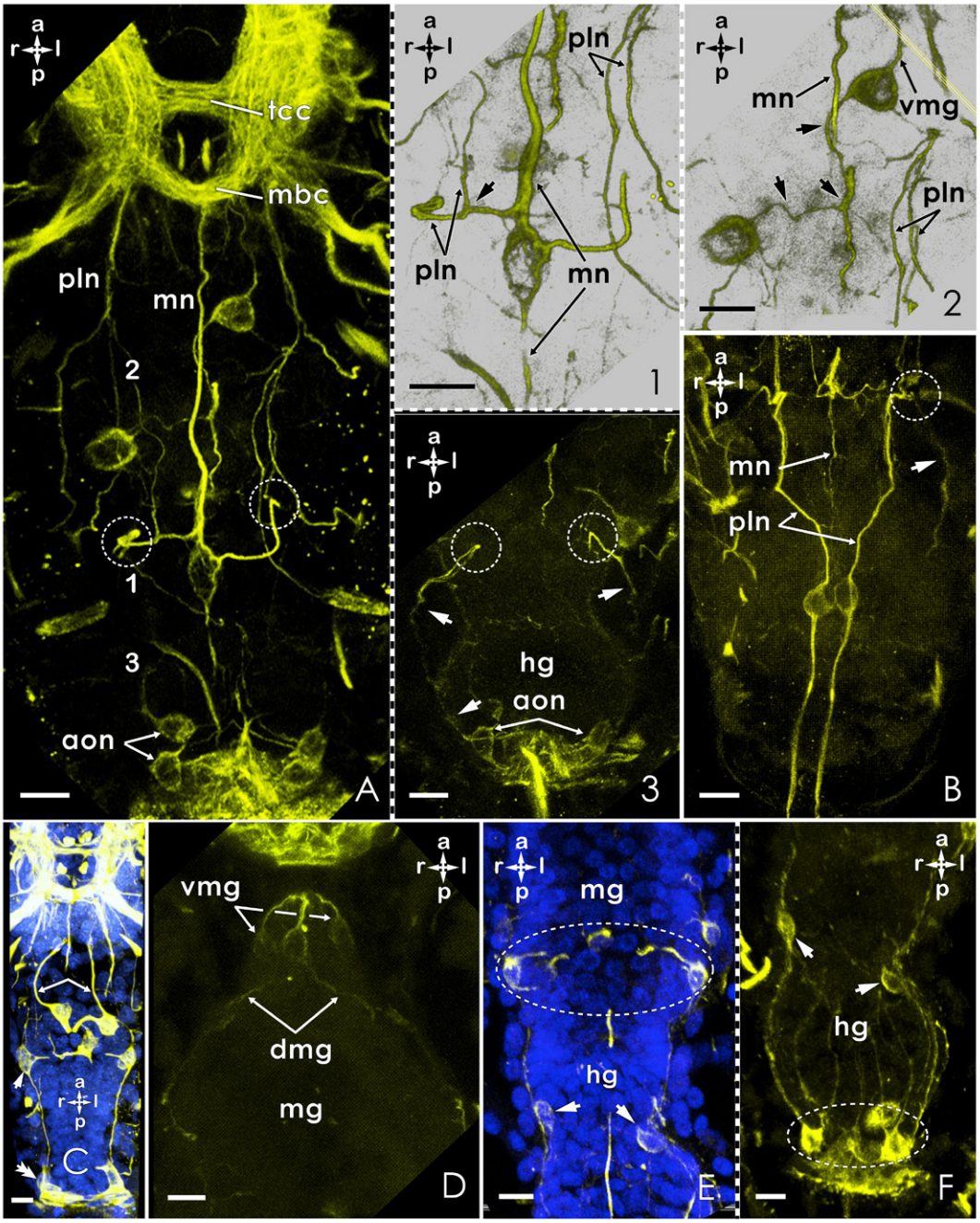

Fig. 3.2.4. Anatomy of the nervous system of Nauplius. Stomatogastric (continuation) and ventral nervous system.

All the images are obtained from Nauplius I in Imaris Extended Section view, MIP(max) mode (1,2 – Blend Mode).
Colour code:
α-tubulin *DAPI*

A-**B** – innervations of the hindbody; **C**-**F** – Midgut and hindgut innervations;
A – general view of the innervations of the hindbody, dashed circles outline the dorsal turns of the lateral branches of the mn, the numbers correspond to the numbers of the pictures on the right, which show sections through different regions and at different levels; **1** – view of the branching region of the mn, arrowhead indicates the fasciculation of one of the neurites of pln with the lateral neurite of mn; **2** – deeper section than the one shown in 1, region of somata anteriorly connected to vmg, arrowheads point at the transversal connection of the somata; **3** – continuation of the lateral branches of mn (arrowheads), the dashed circles correspond to those on A; **B** – ventral view of posterior portion of the

togastric nerve splits into two nerves that extend along the dorso-lateral sides of the midgut (Fig. 3.2.4.D). In the posterior portion of the midgut there is a ring of somata, the processes of which being directed into the lumen (Fig. 3.2.4.E, dashed ellipse). Some of these somata are anteriorly connected to the ventral and dorso-lateral midgut nerves and some send posterior projections into the hindgut (Fig. 3.2.4. 2,C,E). The innervation of the hindgut comprises these longitudinal neurites passing along the epithelium as well as another ring of somata placed around the anus (anal plexus) (Fig. 3.2.4.F, dashed ellipse). Additionally, midway along the hindgut there is a pair of lateral somata, being connected via their neurites to both the midgut and the hindgut rings of somata (Fig. 3.2.4.C,E,F, arrowheads).

3.2.1.3. Postcerebral nervous system

This part includes the paired mandibular ganglia and a ventral nervous system of the hindbody. The connectives spanning between the tritocerebral and *mandibular ganglia* are shorter than the circumoesophageal ones and bent dorsally (Fig. 3.2.2.A,B,G). The somata are placed ventral to the neuropil (Fig. 3.2.2.C',G). Dorso-posteriorly to the commissure there is another pair of ganglia (here referred to as posterior mandibular ganglia, Fig. 3.2.2.C",G).

From the mandibular commissure a set of neurites runs posteriorly and dorsally. The most prominent ones are an unpaired median nerve, a pair of postero-median nerves/tracts, and a pair of postero-lateral nerves (Fig. 3.2.2.A,B; Fig. 3.2.4.A). The median nerve extends posteriorly along the ventral midline of the hindbody. Halfway along its course there is a pair of somata sending their projections laterally and afterwards posteriorly along the lateral sides of the hindbody towards the anal plexus (Fig. 3.2.4.A,1,3, arrowheads, L, arrowhead). The postero-median nerve tracts are short and end in the posterior mandibular ganglia (Fig. 3.2.2.B,G). Each of the postero-lateral nerves starts on the ventral side of the hindbody, but then it intensively branches and only one of the median branches continues along the ventral surface into the furca (Fig. 3.2.4.B). Another median branch seems to fasciculate with transversal branches of the median nerve (Fig. 3.2.4. 1, arrowhead). The exact course of the other branches is unclear, but some appear to innervate the gut.

◁ hindbody, the ventral branches of pln lead to the furca, arrowhead shows the posterior way of the lateral branches of mn, dashed circle regionally correspond to those in A; **C** – ventral view of the posterior part of the sns, arrows point to the vmg, arrowhead shows the lateral somata of the hindgut, double arrowhead shows the anal plexus; **D** – dorsal view of the anterior portion of the midgut, stomatogastric nerve splits into two dorso-lateral branches; **E** – frontal section of the posterior portion of the midgut and the anterior part of the hindgut, dashed ellipse outlines the circle of midgut somata, arrowheads indicate the lateral somata of the hindgut; **F** – frontal section of thehindgut of the same sample shown on E, arrowheads correspond to those on E, dashed ellipse outlines the anal circle of somata. Scalebar 10 µm.

3.2.2. Anatomy of the muscle system

The musculature of the nauplius larva can be subdivided into several muscle groups. The most prominent one is the group of limb muscles presented by extrinsic dorsal, extrinsic ventral, and intrinsic muscles (Fig. 3.2.4B). Another group includes muscles associated with the digestive system: muscles of the digestive tract and the labral musculature (Fig. 3.2.5.C,D; Fig. 3.2.6.B,K). Relatively small is a group of dorso-ventral muscles and muscles of the endosternites (they are referred here as "supporting muscles", according to their function) (Fig. 3.2.6.A). Additionally, there is a pair of postero-lateral muscles (plm), which are difficult to be classified into any of the mentioned groups (Fig. 3.2.4.D). They attach inside to a dorsal part of the headshield and to a ventral region of the hindbody (Fig. 3.2.6.A,L). The muscles consist of multiple muscle fibres of different structure. These muscles are used to bend the hindbody and are, in fact, the biggest muscles of the early nauplius.

3.2.2.1. Limb musculature

The limb musculature, as it was said, can be subdivided into three main groups according to the muscle's position and its attachment sites.

The first group includes the dorsal extrinsic muscles (Fig. 3.2.5.G). They attach to the dorsal carapace and to the protopodites of the limbs. To antenna I four pairs of dorsal extrinsic muscles are attached (a1d1 – a1d4). They have three attachment sites on the dorsal side of the headshield (a1d3 and a1d4 share a common site) (Fig. 3.2.5.D,E-G; Fig.4.1.2.A). To the protopodites of antenna II ten pairs of muscles are attached. Among those six pairs are attached at the base of exopodite (a2d1-d4, a2d7, a2d8) and four at the base of endopodite (a2d5, a2d6, a2d9, a2d10) (Fig. 3.2.5.D,G). On the dorsal side of the carapace the muscles have in total eight attachment sites (Fig. 3.2.5.D,F; Fig.4.1.2.A). Each muscle has its own attachment site, except for a2d4-d6 sharing one site. Three pairs of dorsal muscle bundles lead to each mandible. Two of them are attached at the base of the exopodite and one at the base of the endopodite (Fig. 3.2.5.G). Dorsally every bundle has its own attachment site (Fig. 3.2.5.E,F; Fig.4.1.2.A). The precise number of muscles forming one bundle was not identified both during differential stage and in nauplius I (Fig. 3.2.5.E: Insertion). For this reason bundle names were taken in quotation marks "mbd1", "mbd2", and "mbd3".

Another group of limb muscles is represented by the ventral extrinsic muscles. They are attached to the endosternites and to the protopodites of the limbs. On the ventral endoskeleton there are in total five common attachment sites for the limb muscles of each side (Fig.4.1.2.E; Fig.4.1.3.A). Two of them are paired and placed laterally (1 and 2). Three of them are singular and placed on the ventral midline (3-5). To antenna I two ventral muscles are attached (Fig. 3.2.5.H). One of

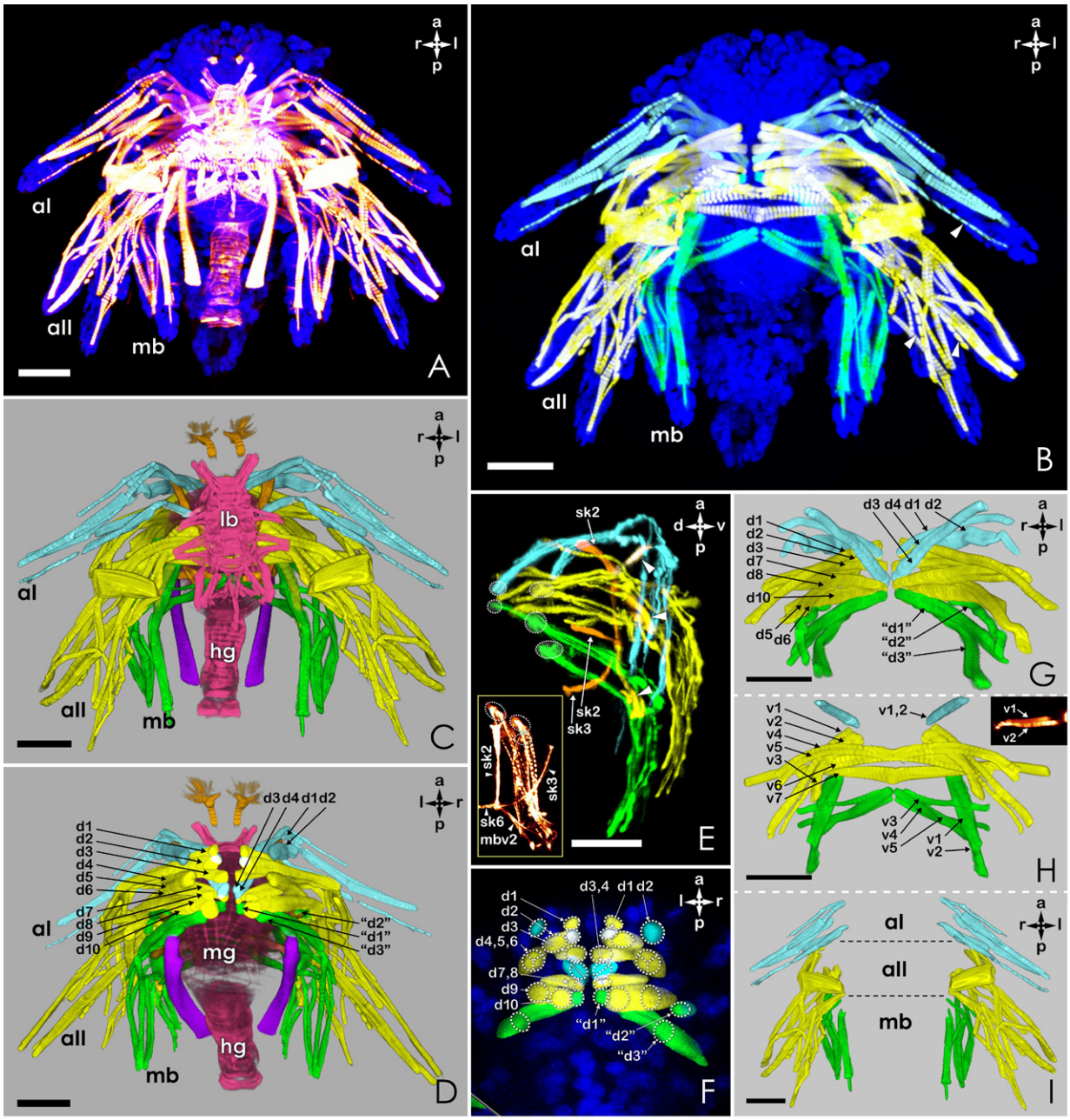

Fig. 3.2.5. Anatomy of the muscle system of the Nauplius: limb musculature.

All the images are obtained in Imaris Surpass view, Volume Scene, except for F: Imaris Extended Section view.

Colour code of masked channels:
muscles of antenna I (muscle name: a1**), muscles of antenna II (muscle name: a2**), muscles of mandible (muscle name: mb**), endoskeletal muscles, muscles of digestive system, postero-lateral muscles.

A – general view of the muscle system of the nauplius larva, ventral view, MIP(max) mode, original two channels: DAPI and Phallacidin; **B** – muscles of the limbs, MIP(max) mode, one original channel: DAPI and three masked channels, arrowheads point at muscle fibres built of long sarcomeres; **C** and **D** – general view of the muscle system, ventral (C) and dorsal (D) view, Blend mode, six masked channels, dorsal extrinsic muscles are labelled, use the colour code for the full limb names; **E** – limb and partly endoskeletal musculature of the right side of an embryo, stage 8, latero-dorsal view, circles outline dorsal attachment sites shared by several muscles, arrowheads point at "unidentified" muscles (for explanations see text), MIP(max) mode, four masked channels; **Insertion**: extrinsic muscles of the left mandible and partly of the endoskeleton (shown by arrowheads), embryo of the early stage 9, circles outline dor-

them (a1v2) has long sarcomeres (Fig. 3.2.5.H: Insertion). Both of these muscles are attached on the site 1 (Fig.4.1.2.E). Seven ventral muscles are attached to antenna II (Fig. 3.2.5.H). Three of them are attached on site 1 (a2v1-v3, a2v2 is built of long sarcomeres), three on the site 3 (a2v4-v6), and one on the site 4 (a2v7) (Fig.4.1.2.E). Five ventral muscles are attached o the protopodite of the mandible (Fig. 3.2.5.H). Two of these muscles are by the other ends attached to the site 2 (mbv1 and mbv2, the latter one is of long-sarcomeric structure), and three muscles are attached to the site 5 (mbv3-v5) (Fig.4.1.2.E).

The third group of limb muscles includes numerous intrinsic muscles. In the current work their number was not counted. On the Fig. 3.2.5.I they are grouped according to the limbs. Among these muscles both short-sarcomeric and long-sarcomeric muscles are found (Fig. 3.2.5B, arrowheads).

3.2.2.2. Supporting musculature

Muscles, which seem to fulfill supporting function are grouped and described here.

One group contains muscles attached on the endosternites (presumably, since the methods used in the current research do not allow to discern cuticular structures) (Fig. 3.2.6.A). Among these muscles three pairs (sk1 - sk3) are attached to the dorsal part of the headshield (Fig. 3.2.5.E; Fig. 3.2.6.H,J), four pairs (sk5 - sk8) are attached by both ends on the ventral endoskeleton (Fig. 3.2.6.A,H-J), and one single muscle (sk4) also has both attachment sites on the ventral endoskeleton just behind the oesophagus (Fig. 3.2.6.A,J). The precise arrangement of these muscles is shown on Fig.4.1.3.A.

Additionally, there are three pairs of muscles of long-sarcomeric structure, which attach to the protopodites of the limbs (a1v2, a2v2, and mbv2) (Fig. 3.2.4.E, arrowheads; Fig. 3.2.5.E). These muscles are already described in the part devoted to the limb musculature. It is, however, not clear whether their function is movement, or support, or both.

In the anterior part of the nauplius there is a pair of muscles of long-sarcomeric structure (dv), which are attached to the dorsal and ventral plates of the carapace (Fig. 3.2.6.A,J,K). Each muscle of the pair passes between the internal part of the frontal filament and the lateral cup of the nauplius eye.

◁ sal attachment sites of three mandibular bundles, it is hard to count a total number of fibres forming each bundle, MIP(max) mode, one original channel; **F** – dorsal attachment sites of the extrinsic muscles of the limbs, dorsal view, MIP(max) mode, one original (DAPI) and three masked channels, dashed outlines mark the attachment sites, subdivision within some dashed outlines show how many muscles attached to the site; **I** – limb musculature separated into dorsal extrinsic muscles (**G**), ventral extrinsic muscles (**H**), and intrinsic muscles (**I**), ventral view, Blend mode, three masked channels; **Insertion**: ventral extrinsic muscles of *aI*, MIP(max) mode, one original channel. Scalebar 30 µm.

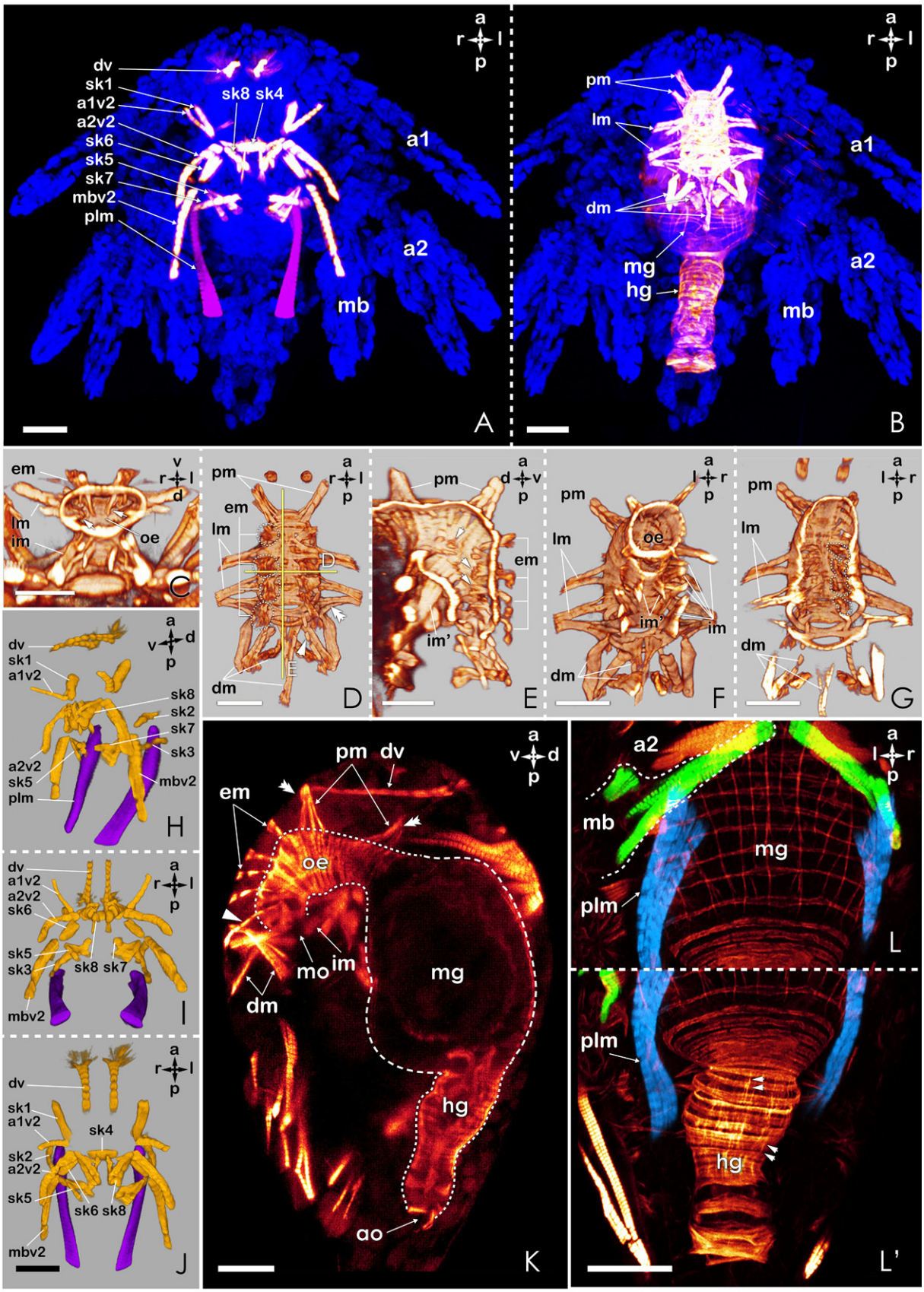

Fig. 3.2.6. Anatomy of the muscle system of the Nauplius: supporting muscles and muscles associated with digestive tract.

All the images are obtained in Imaris Surpass view, Volume Scene, except for K and L, which are obtained in Imaris Extended Section view.

3.2.2.3. Musculature of the digestive system

This group of muscles includes the labral musculature and muscles of the alimentary channel (Fig. 3.2.6.B-G,K-L'). The labral muscles are attached on the internal surface of the labrum and on the oesophagus. Most of the labral muscles are of pyramid shape (Fig. 3.2.6.D,K, double arrowhead; Fig. 3.2.7). They consist of several muscle fibres each. These fibres are piled together on the "top" of the pyramid and slightly spread at the "base" of it. By the "top" the muscles are attached to the surface of labrum and by the "base" to the oesophagus. All of the "pyramid" muscles seem to have a structure constructed of long-sarcomeres.

In total on the outer side of the oesophagus there are 17 pairs of muscles attached (Fig. 3.2.6.C-E; Fig. 3.2.7.A). They are subdivided into groups according to their location: 4 pairs of proximal muscles (pm, attached on the anterior side of the oesophagus, all are of pyramid structure), 4 pairs of lateral muscles (lm, attached on the lateral sides of the oesophagus and labrum, all of pyramid-like shape), 4 pairs of external muscles (em, attached along the ventral side of the oesophagus, all are of regular shape), 5 pairs of distal muscles (dm, attached around the mouth opening and within the tip of the labrum, one is of pyramid structure and one is also of long-sarcomeric structure, but of regular shape) (Fig. 3.2.6.D,K, arowhead). To the inner (or dorsal) side of the oesophagus there are 6 pairs of muscles attached (Fig. 3.2.6.F,G; Fig. 3.2.7.B): 5 of them are attached laterally along the oesophagus and on the ventral endoskeletal attachment site 1 (all are of pyramid-like shape), 1 is attached centrally on the oesophagus and on the ventral attachment site 4 (of regular shape and long-sarcomeric structure).

The muscles of the alimentary channel itself can be subdivided in structure into two main groups. One group is formed by the massive circular muscles. They are found in the walls of the

Colour code of masked channels:
muscles of mandible, endoskeletal muscles, postero-lateral muscles, L,L' – postero-lateral muscles.

A – supporting and postero-lateral muscles, ventral view, MIP(max) mode, one original (DAPI) and two masked channels; **B** – musculature of labrum and of digestive tract, ventral view, MIP(max) mode, one original and one masked channel; **C**-**G** – labral and oesophageal muscles, Blend mode, Clipping plane scene, one original channel; **C** – transversal section through the region shown by yellow line in D, arrowheads show internal parts of labral muscles; **D** – ventral view, outer pairs of labral muscles, external muscles are outlined, arrowhead shows long-sarcomeric distal muscle, double arrowhead shows "pyramid" distal muscle; **E** – longitudinal section through the region shown by yellow line on C, arrowheads show internal parts of labral muscles; **F** – dorsal (internal) view, internal labral muscles are shown; **G** – frontal section through F, internal view of the ventral side of oesophagus, internal parts of the labral muscles are outlined ; **H**-**J** – supporting and postero-lateral muscles, ventro-lateral (**H**), ventro-posterior (**I**), and ventro-anterior (**J**) view, Blend mode, two masked channels; **K** –musculature of digestive tract, median section, MIP(max) mode, one original channel, arrowhead shows long-sarcomeric distal muscle, double arrowheads show "pyramid" distal muscle; **L** and **L'** – fine structure of the musculature of the digestive tract, dorsal view, MIP(max) mode, one original and two masked channels, **L** – grid-like structure of the muscles of the midgut; **L'** – circular muscles of the hindgut, arrowheads show the longitudinal muscle fibres; Scalebar 30 µm on A, B; 15 µm on C-L'.

oesophagus and proctodaeum (Fig. 3.2.6.B,K,L'). Another group includes gentle longitudinal and transversal muscle fibers. They are mostly found within the walls of the midgut (Fig. 3.2.6.B,L). The longitudinal gentle strands are also seen within the oesophageal and proctodaeal walls (Fig. 3.2.6.L', arrowheads). Neither massive circular muscles nor gentle muscle strands demonstrate a sarcomeric arrangement.

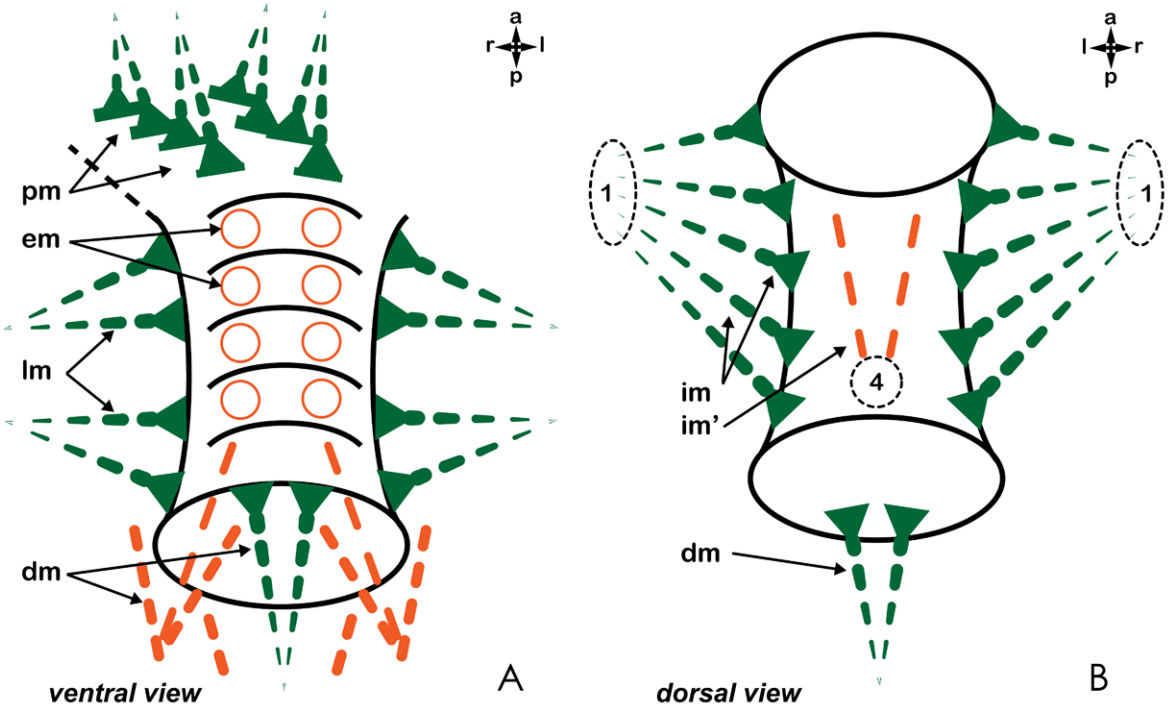

Fig. 3.2.7. Schematic illustration of labral musculature.

A – labral musculature in ventral view; **B** – labral musculature in dorsal view.

Colour code:
muscles of pyramid-like structure, muscles of regular shape, outlines of the circular muscles of oesophagus.

3.3. Early development

The developmental phase of the barnacle *Elminius modestus* described in this chapter covers the stages from 0 until the beginning of 3 (Table 3.1.1.) and takes approximately 15-17h under given conditions.

The eggs are of a drop-like shape. The embryos are oval with their anterior being oriented towards the rounded end of the egg shell.

3.3.1. Cleavage

The cleavage is total, unequal with regards to the yolky cell, and increasingly asynchronous. Asynchrony starts from the second, sometimes from the third division, and has an anterior-posterior gradient.

During the whole process of cleavage a polar body remains visible. Its position remains almost unchanged (being placed between the quadrants (and their descendants) B and C or between A, B, and C), and can be used as a landmark for the animal pole. The vegetal pole is occupied by the blastomere D which contains the majority of the embryonic yolk. It is also marked by the presence of granules stained with Sytox. The stain is, however, not present in all specimens and when it is, it frequently bleaches fast. Therefore, it may represent unspecific staining.

The nuclei of the micromeres are centrally placed within the cells, while the nucleus of the macromere lies always superficially on the yolk.

Each division is described in detail in the following subchapters and visualized with pictures and movies. The pictures of living embryos were obtained from 4D microscopic scans, unless it is specified otherwise. All the fixed samples demonstrated in this part were stained with Sytox Green, scanned with a CLSM, and reconstructed with the software Imaris.

3.3.1.1. Zygote, first division, and 2-cell stage.

Fertilization and the first division take approximately 3,5 h. There are two major processes which precede the first cleavage: the fusion of the gamete nuclei and the segregation of the cytoplasm. After the penetration of the sperm, the shape of the ovum changes from spherical to drop-like.

Fig. 3.3.1. Cell lineage of blastomeres during first five divisions.

Colour code (here and on all pictures presented in this chapter):

A quadrant and its derivatives, B quadrant and its derivatives, C quadrant and its derivatives, D quadrant and its derivatives

On the left and right there are schemes of the cleavage stages in ventral and dorsal view, respectively. The time on the grey bar on the left is given in hours (the time here and in the text is obtained on the base of averaged calculations; there were few examples of slower or faster divisions: ±20min, statistics is not provided.

.

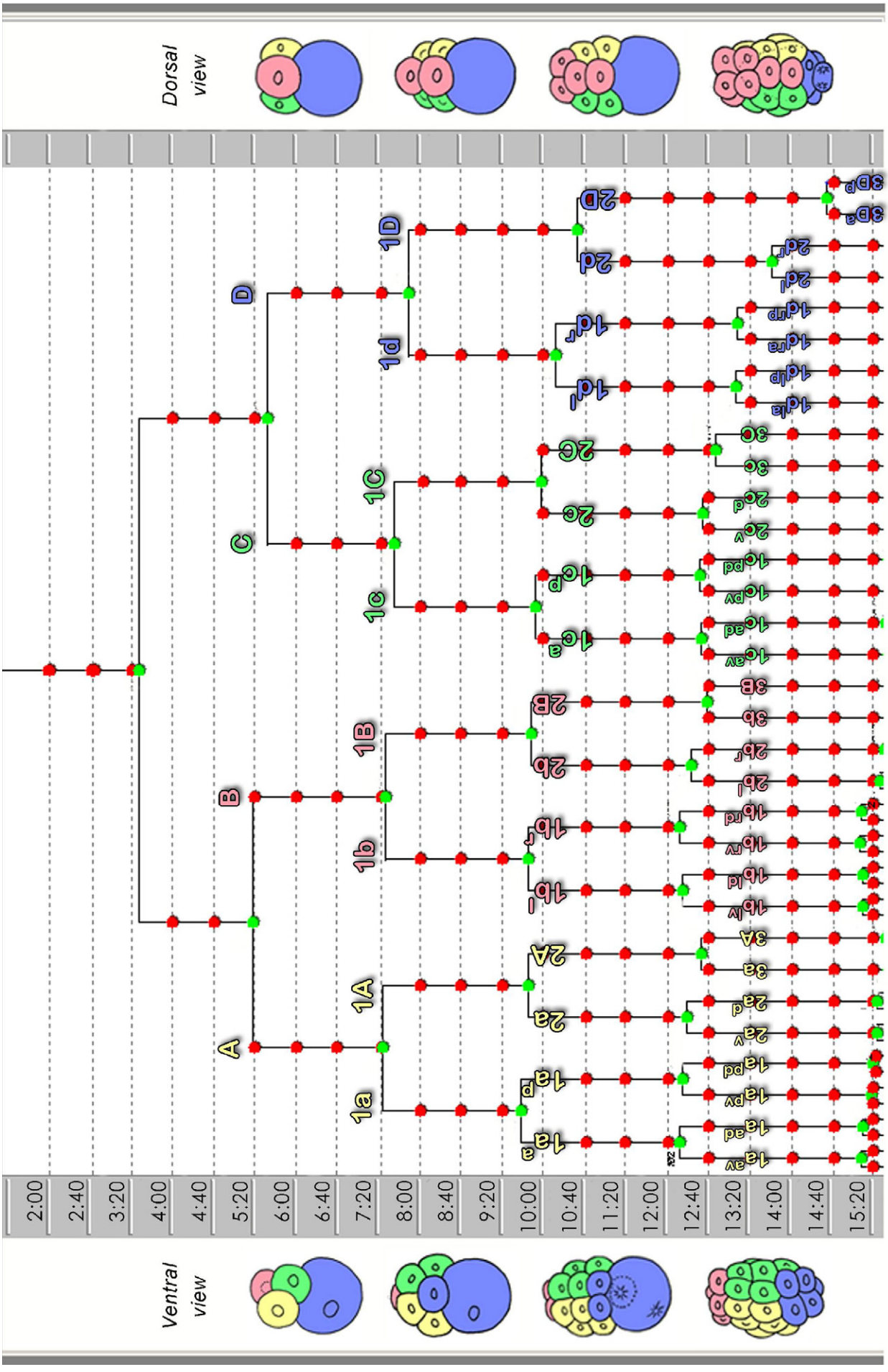
Dorsal view
Ventral view
2:00
2:40
3:20
4:00
4:40
5:20
6:00
6:40
7:20
8:00
8:40
9:20
10:00
10:40
11:20
12:00
12:40
13:20
14:00
14:40
15:20
A
B
C
D
1a
1b
1c
1d
1A
1B
1C
1D
2A
2B
2C
2D
3A
3B
3C
3D

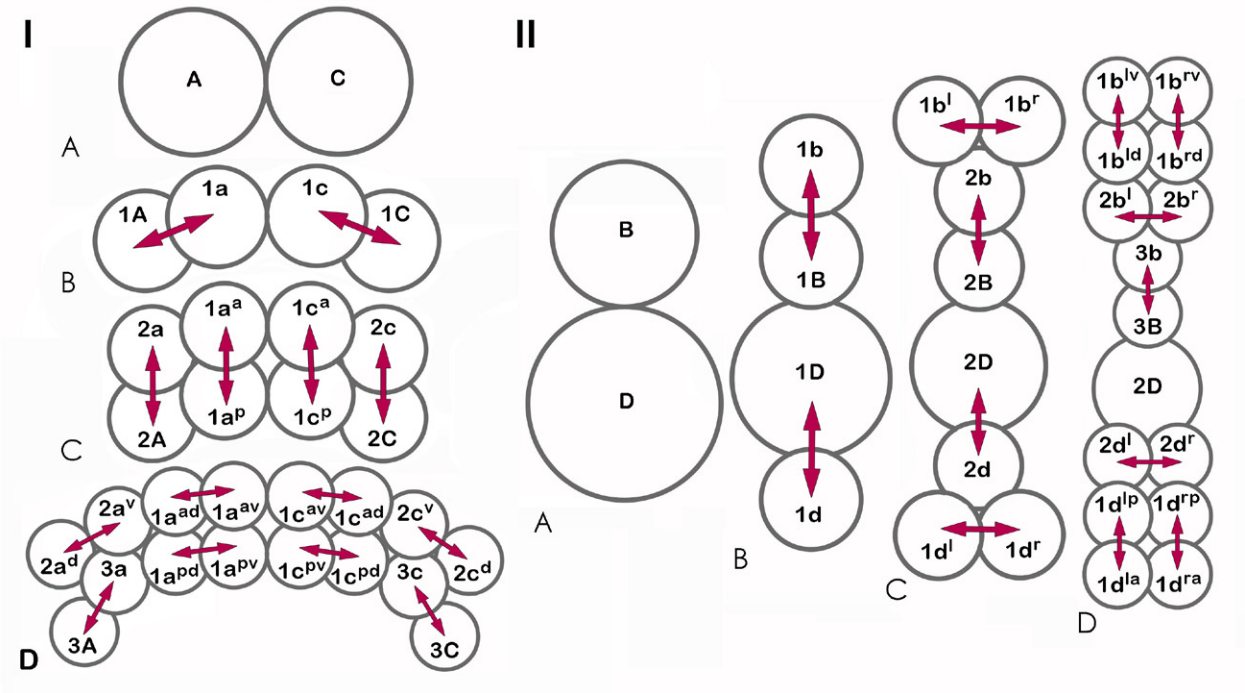

Fig.3.3.2. Orientation of cell divisions within AC (I) and BD (II) bands.

A – 4-cell stage; **B** – 8-cell stage; **C** – 16-cell stage; **D** – 31-cell stage.

During fusion of the gamete nuclei the cytoplasm undergoes undulating constrictions (Fig. 3.3.3.A). Simultaneously, the fertilization membrane is being generated, corresponding in shape to the ovum. Together with the vitelline membrane of the oocyte it forms the egg shell.

The newly-formed zygote is oval, whereas the egg shell keeps its drop-like shape until the very end of the embryonic development (Fig. 3.3.3.C). The cytoplasm is rich of yolk, which is spread quite homogeneously. The nucleus with its surrounding perinuclear plasma, which seems to be free of yolk, is placed closer to the rounded end of the egg (Fig. 3.3.3.B).

The cytoplasm of the zygote then segregates into a bright and relatively yolk-free part on the animal pole and a yellowish-brown part on the vegetal pole (Fig. 3.3.3.C, Movie 3.3.1.). The polar axis more or less corresponds to the elongated axis of the egg (Fig. 3.3.3.B-D). Sytox-stained granules are spread over the vegetal pole, close to the plasmatic membrane.

The cytoplasm segregation is closely followed by the formation of a mitotic spindle. At first, the spindle is nearly perpendicular to the animal-vegetal axis (Fig. 3.3.3.C, D; Movie 3.3.1.). However, as the division proceeds, the embryo rotates within the egg shell. As a result of this, the division plane comes to lie transversally to the elongated axis of the egg shell. The polar axis is oblique now (Fig. 3.3.3.E, G).

The first division is unequal. The zygote divides into a small and relatively yolk-free micromere AB and a big macromere CD, containing the majority of the yolk. The blastomere AB occupies the rounded part of the egg shell, whereas the CD blastomere is situated in the pointed part. The

nucleus of AB is placed almost in its center, while that of CD lies superficially regarding the yolk, in proximity to the animal pole (Fig. 3.3.3.G). The Sytox-stained granules are found now only in the CD blastomere (Fig. 3.3.3.H).

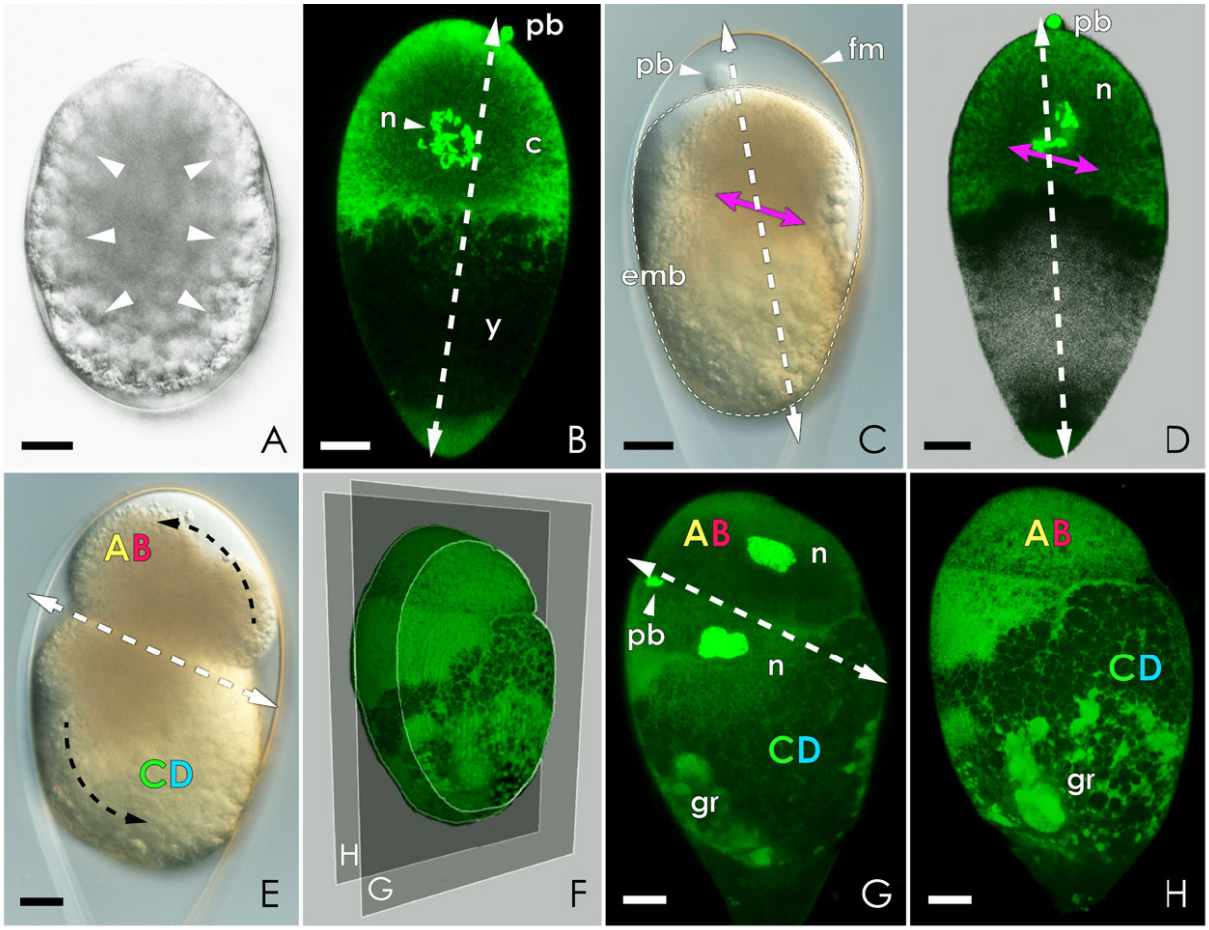

Fig. 3.3.3. Formation of the zygote and first cleavage.

White dashed arrows – embryonic axes; lilac arrows – spindle orientation in dividing blastomeres.

A – living sample during fusion of the gamete nuclei and formation of the zygote, arrows indicate undulations of the cytoplasm; **B** – section through segregated zygote, fixed and stained sample; **C**-**D** – zygote shortly before division; **C** – alive sample during first division. The embryo is of oval-round shape (outlined), while the shape of the egg is drop-like; **D** – section through the fixed sample; **E**-**H** – embryo at the 2-cell stage; **E** – alive embryo, black dashed arrows show the turn of the embryo after first division; **F** – fixed and stained embryo; **G**-**H** - sections through different regions of the embryo presented on F. Scale-bars: 20 µm

3.3.1.2. Second division and 4-cell stage.

The second cell cycle takes about 110 min for AB and 130 min for CD (measured from the beginning of the interphase in AB and CD until the beginning of the interphase in their respective daughter cells). The two blastomeres develop mitotic spindles almost synchronously (interphase lasts for about 50 min in AB and for 55 min in CD). Initially, the planes of the spindles are oblique to each other and transversal in relation to the egg shell (Fig. 3.3.4.A-D). During the on-

going division, CD rotates, so that its plane of division comes to stand nearly perpendicular to that of AB (Movie 3.3.2.). The micromere AB gives rise to the two equal micromeres A and B. The cleavage of the macromere CD is unequal and results in the micromere C and macromere D. The micromere C matches A and B in size, whereas D is three times bigger (Fig. 3.3.4.F-I). The Sytox-stained granules are now found in D (Fig. 3.3.4.F).

A and C touch on the animal pole, while B and D have contact on the vegetal pole. After completion of the divisions, their contact planes are perpendicular to each other, thus creating animal and vegetal cross-furrows, respectively (Fig. 3.3.4.H-K).

Despite some shifts in blastomere positions during further development (see below) and turns of the embryo within the egg shell during the gastrulation, it is the four-cell stage, in which the main axes of the embryo and future nauplius larva are established. The axis passing through the A and C blastomeres corresponds to the left-right axis, while the axis running through B and D represents the antero-posterior axis (with B on the anterior and D on the posterior of the embryo) (Fig. 3.3.4.L). Furthermore, the contact region between A and C indicates the future ventral side of the nauplius larva. B contacts D on the future dorsal side. Thus, the animal-vegetal axis of the embryo is under an approximately 45º angle with the dorso-ventral and the antero-posterior axes of the larva. To make future orientations within the described embryos slightly easier for readers, on the figures there will be provided small ap/dv/lr arrow-cross.

The embryos of the four-cell stage were found to be organized in two chiral variants (so called mirror images). The first morphologically detectable difference in the development of these two distinct types is found in the orientation of the unequal cleavage of the CD blastomere. When viewed from the animal pole, the direction of the division of CD is either right-anterior or left-anterior (Fig. 3.3.4.G and L). In the first case the four resulting blastomeres are ordered clockwise from A to D and in the second case counterclockwise. Correspondingly, embryos of "clockwise (right)" and "counterclockwise (left)" types were distinguished. It was impossible,

Fig. 3.3.4. Second cleavage and 4-cell stage.

Dashed arrows – embryonic axes; lilac arrows – spindle orientation in dividing blastomeres; yellow arrow or dot – the long axis of the egg; dashed lines – cross furrows.

A-**B** – living embryos during second division from two different sides, coloured spheres indicate nuclei; **C** and **D** – SimiBioCell 3D reconstructions of the embryo during second cleavage, coloured spheres correspond to the positions of the nuclei; **C** – view from the animal pole; **D** – view from the posterior pole; **E** – **I** – embryo at the 4-cell stage; **E** – fixed and stained embryo at the early 4-cell stage, the embryo is of the "clockwise type" (compare with L); **F**-**G** – sections through the embryo from E; **H**-**I** – Imaris 3D reconstructions of an embryo shortly after the completion of the second divisions; **H** – ventral view; **I** – left-dorsal view; **J** – Imaris 3D reconstruction of blastomeres A and C forming an animal cross furrow; **K** – Imaris 3D reconstruction of blastomeres B and D forming a vegetal cross furrow; **L** – fixed and stained embryo of the "counterclockwise type" (compare with E and G), the body axes of the future animal are already established. Scalebars: 20 µm.

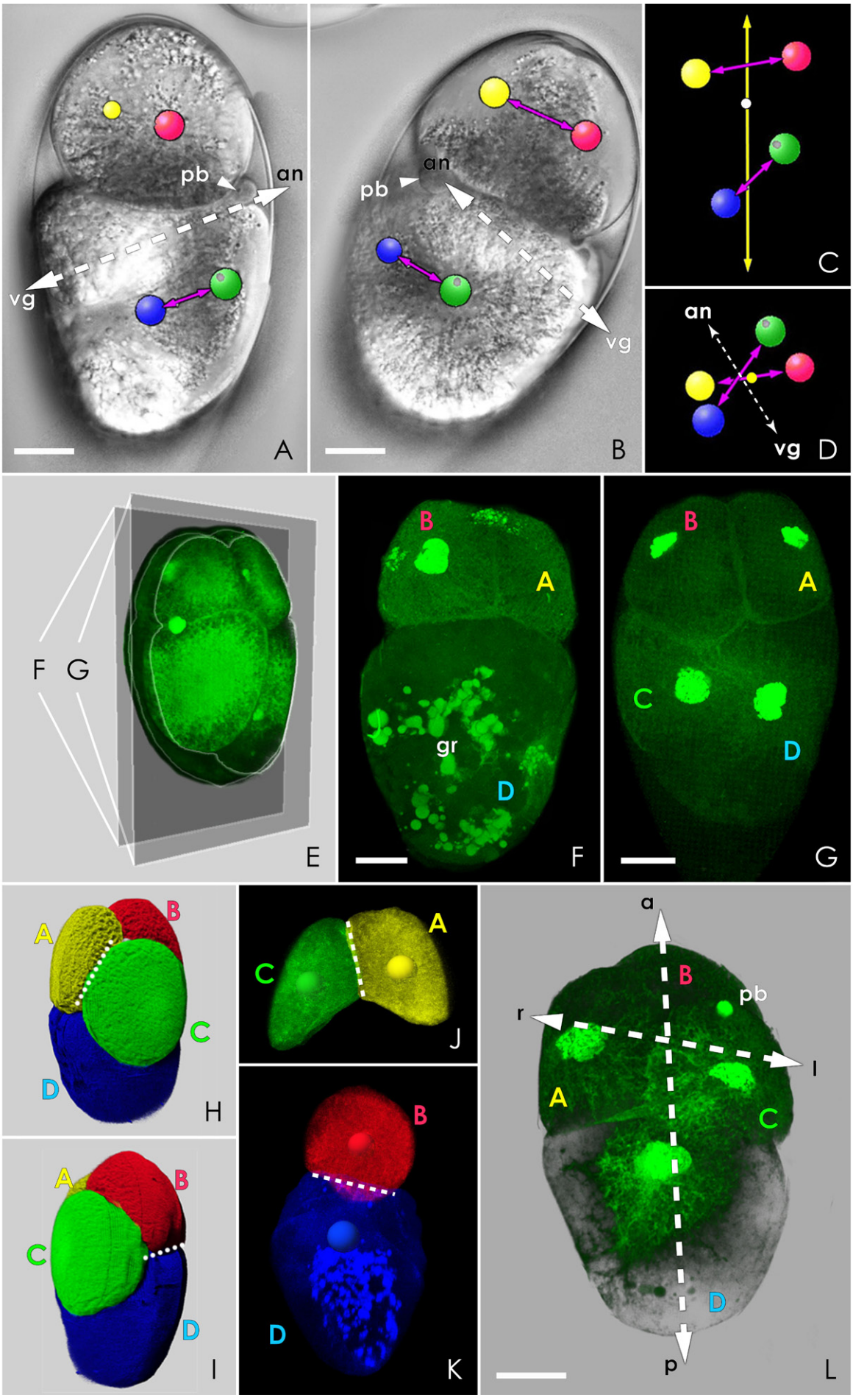
pb
an
vg
A
pb
an
vg
B
C
an
vg
D
F G
E
B
A
gr
D
F
B
A
C
D
G
A
B
C
D
H
A
C
J
A
B
C
D
I
B
D
K
a
B
pb
r
l
A
C
D
p
L

however, to provide precise statistics for the occurrence of the two types. Some egg broods contained approximately equal amounts of "left" and "right" embryos, others only "left" embryos. In contrast to this, broods with exclusively "right" embryos were never observed.

3.3.1.3. Third division and 8-cell stage

The third cell cycle lasts approximately 120 min for A, B, and C and 130 min for D. The blastomeres A and B form mitotic spindles simultaneously after 60 min interphase, being soon afterwards followed by C (with the same interphase length) and then D (interphase lasts for about 70 min).

The spindle axes of all blastomeres, except for D, are perpendicular to those of the preceding cleavage. The spindles of A and C lie in the same plane, which is the transversal plane of the egg shell and orthogonal to the elongated axis of the egg shell (Fig. 3.3.2.IB). The spindle of B stands obliquely to the spindles of A and C, being nearly parallel to the polar axis of the embryo and oblique to both axes of the egg shell (Fig. 3.3.2.IIB; Fig. 3.3.5.A-C). The D blastomere has initially its spindle almost in parallel to the plane of the A and C spindles. But as the cytokinesis occurs, the D spindle turns and the cleavage direction becomes parallel to that of B (Fig. 3.3.2.IIB; Compare 5.A and 5D; Movie 3.3.3.).

A, B, and C divide equally, giving rise to the micromeres 1a and 1A, 1b and 1B, and 1c and 1C, respectively. The cleavage of D is unequal, leading to a micromere 1d and a macromere 1D, micromere 1d is being given off towards the animal pole. Owing to this, the cells 1a and 1c (adjacent daughter cells of A and C) appear to be "pushed" to the anterior of the embryo (Fig. 3.3.5.D, E, arrowheads; Movie 3.3.3.). Together with them, also the animal pole shifts to the rounded end of the egg shell. As a consequence, the polar axis almost corresponds to the longitudinal axis of the egg from this point on (Fig. 3.3.5.D).

The size of all the micromeres is quite equal. The macromere 1D is four times bigger than the micromeres and contains most of the embryonic yolk and the Sytox-stained granules. The latter appear to be more condensed and are often located near the vegetal cross furrow (Fig. 3.3.5.C).

The A and C derivatives form a horseshoe-shaped band (Fig. 3.3.2.IB; Fig. 3.3.5.F). The animal cross furrow is in the middle of this cell band. The descendants of B and D also form a band, which is, however, slightly distorted by the conspicuous size difference of the yolky cell 1D (Fig. 3.3.2.IIB; Fig. 3.3.5.G). These two bands interlock with each other (Compare 5.F and 5.G).

In this and the following stages it is hard to discern "clock-" and "counter-clockwise" embryos, since the embryos are highly symmetrical and only sometimes the blastomeres on the left or right side slightly retard in their division. In such cases, they are believed to be descendants of the C blastomere (based on 4D observations).

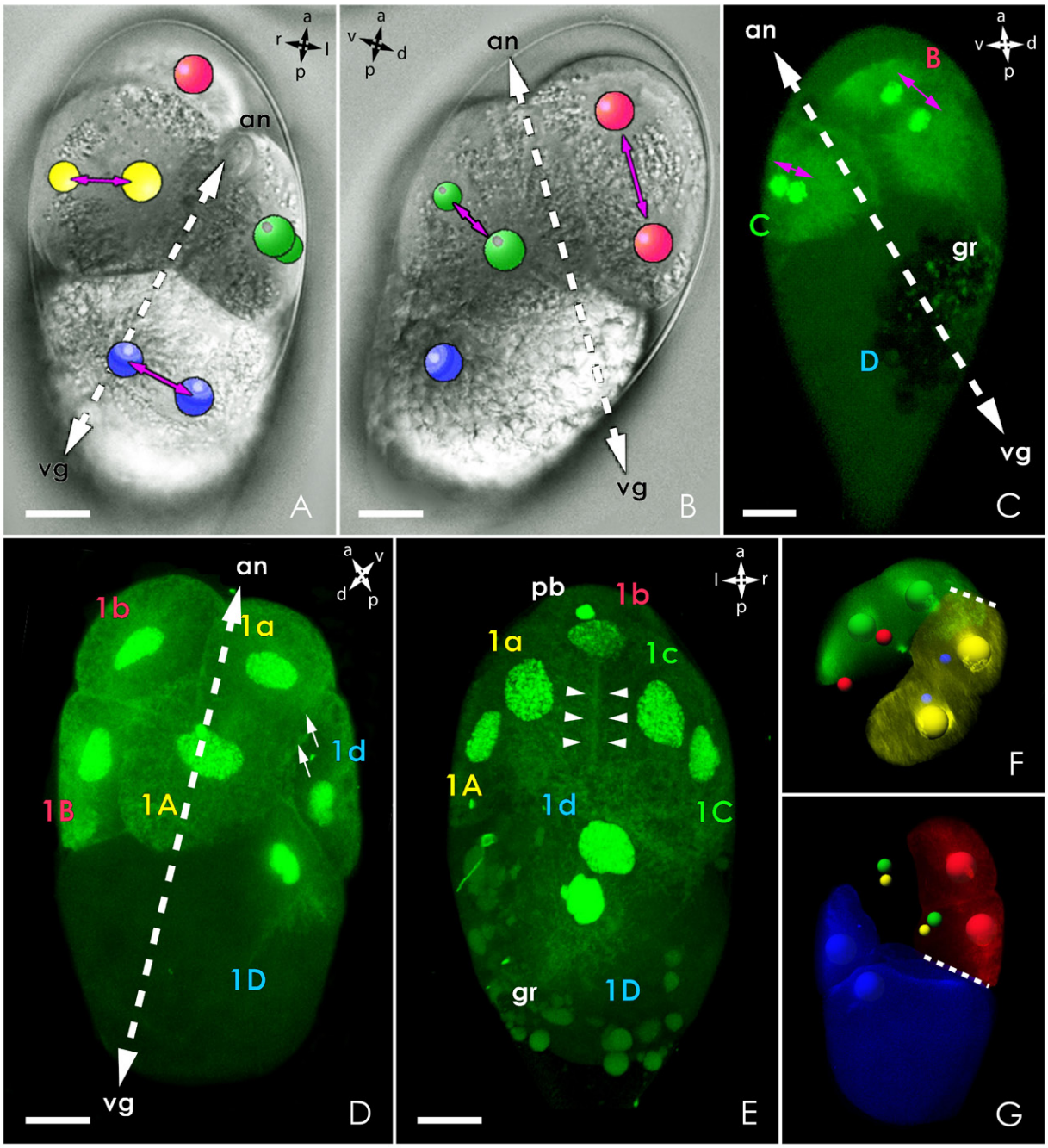

Fig. 3.3.5. Third cleavage and 8-cell stage.

Dashed arrows – embryonic axes; lilac arrows – spindle orientation in dividing blastomeres.

A–C – embryo during third division; **A** and **B** – living specimens, ventral (**A**) and left-lateral (**B**) view; C – fixed and stained embryo, left-lateral view; **D–G** – embryo at the 8-cell stage; **D-E** – fixed and stained embryo, right-lateral (**D**) and ventral (**E**) view, arrowheads in E indicate animal cross furrow; **F-G** – Imaris 3D reconstructions of blastomeres forming interlocking cell bands: descendants of A and C (**F**) and descendants of B and D (**G**), coloured spheres correspond to the positions of the nuclei. Scalebars: 20 µm.

3.3.1.4. Fourth division and 16-cell stage

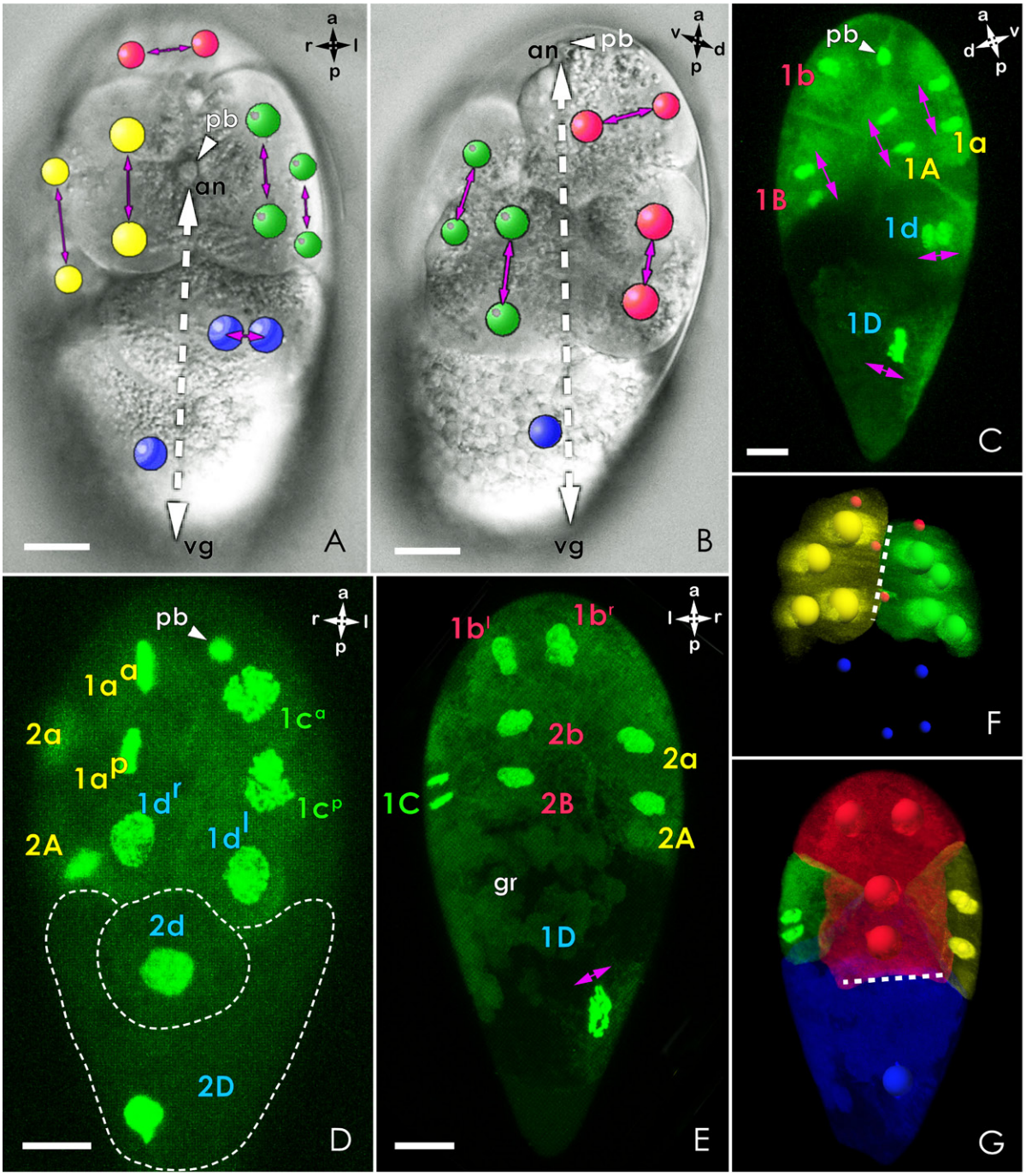

Fig. 3.3.6. Fourth cleavage and 16-cell stage

Dashed arrows – embryonic axes; lilac arrows – spindle orientation in dividing blastomeres.

A–**C** – embryo during fourth division; **A**-**B** – living specimens, coloured spheres mark the positions of the nuclei, ventral (**A**) and left-lateral (**B**) view; **C** – fixed and stained embryo, right-lateral view; **D**-**G** – embryo at the 16-cell stage; **D** – ventral view of fixed and stained embryo at the 16-cell stage, note some descendants of A enter already the next (fifth) division; **E** – dorsal view of stained and fixed embryo at the end of fourth division, note the asynchrony between descendants of different quadrants: descendants of C and D are still within mitosis, while those of A and B already have completed their fourth division; **F**-**G** – Imaris 3D reconstructions of blastomeres at the 16-cell stage forming bands interlocking with each other: descendants of A and C are forming a two-cell wide cross furrow on the animal pole (**F**) and descendants of B and D are forming a one-cell wide cross furrow on the vegetal pole (**G**), coloured spheres correspond to the positions of the nuclei. Scalebars: 20 µm

The fourth cell cycle lasts longer than the previous ones and its duration differs more significantly between the different blastomeres. It takes around 135 min in 1a, 1b, 1c, 1A, and 1B; 140-145min in 1d and 1C; and 170 min in 1D.

Except for that in 1B, the spindles of all cells are perpendicular to the ones of the preceding cleavage. The spindle of 1B is oriented in the same way as during the division of its mother cell B and is parallel to the polar axis (Fig. 3.3.2.IIC; Fig. 3.3.6.B,C). In the descendants of A and C the spindles are parallel to each other and in line with the polar axis. 1b and 1d form parallel spindles, which are perpendicular to those of the other micromeres (Fig. 3.3.2.C; Fig. 3.3.6.A-C). 1D has its spindle perpendicular to those of the other blastomeres, and it lies as before in the transversal plane of the egg (Fig. 3.3.6.C,E). Later on, during cytokinesis the division orientation in 1D changes. Thus, its daughter cell 2d is cut off towards the animal pole, where it neighbours $1d^r$ and $1d^l$, the products of the division of 1d (Fig. 3.3.6.D; Movie 3.3.4.).

All blastomeres apart from the macromere 1D cleave equally. 1D divides into a micromere 2d and a yolk-rich macromere 2D. The Sytox-stained granules are located in the yolk of the macromere (Fig. 3.3.6.E).

The horseshoe-shaped AC band keeps its organization, with the animal cross-furrow becoming two-cell wide and being formed by $1a^a$, $1a^p$, $1c^a$, and $1c^p$ (Fig. 3.3.2.IC; Fig. 3.3.6.F). In contrast, a symmetrical arrangement of the B and D descendants is not only disturbed by the big size of 2D, but additionally by the direction of the divisions of 1B and 1D. This results in a one-cell wide cross furrow on the vegetal pole created by 2B and 2D (Fig. 3.3.2.IIC; Fig. 3.3.6.G).

Tthe polar axis remains in the same position in relation to the elongated axis of the egg like at the stage before.

3.3.1.5. Fifth division and 32-cell stage

The fifth cell cycle takes an even longer time than the one before. It lasts for 160-180 min in all micromeres and for about 250 min in the macromere 2D. The asynchrony of the divisions is strongly pronounced (Fig. 3.3.7.A,B,E,F; Movie 3.3.5.). In some anterior blastomeres, mitosis starts already 10-15 min after the fourth division of 1D has come to an end. The macromere 2D, which is the last to enter the fifth division, divides 120 min later. The resulting 32-cell-stage lasts only briefly, since the completion of the 2D division is almost directly followed by the karyokinesis of the next (sixth) cell cycle in anterior blastomeres (Fig. 3.3.8.E, arrowheads). In general, the 32-cell stage represents the last stage, where all the blastomeres of one generation coexist together.

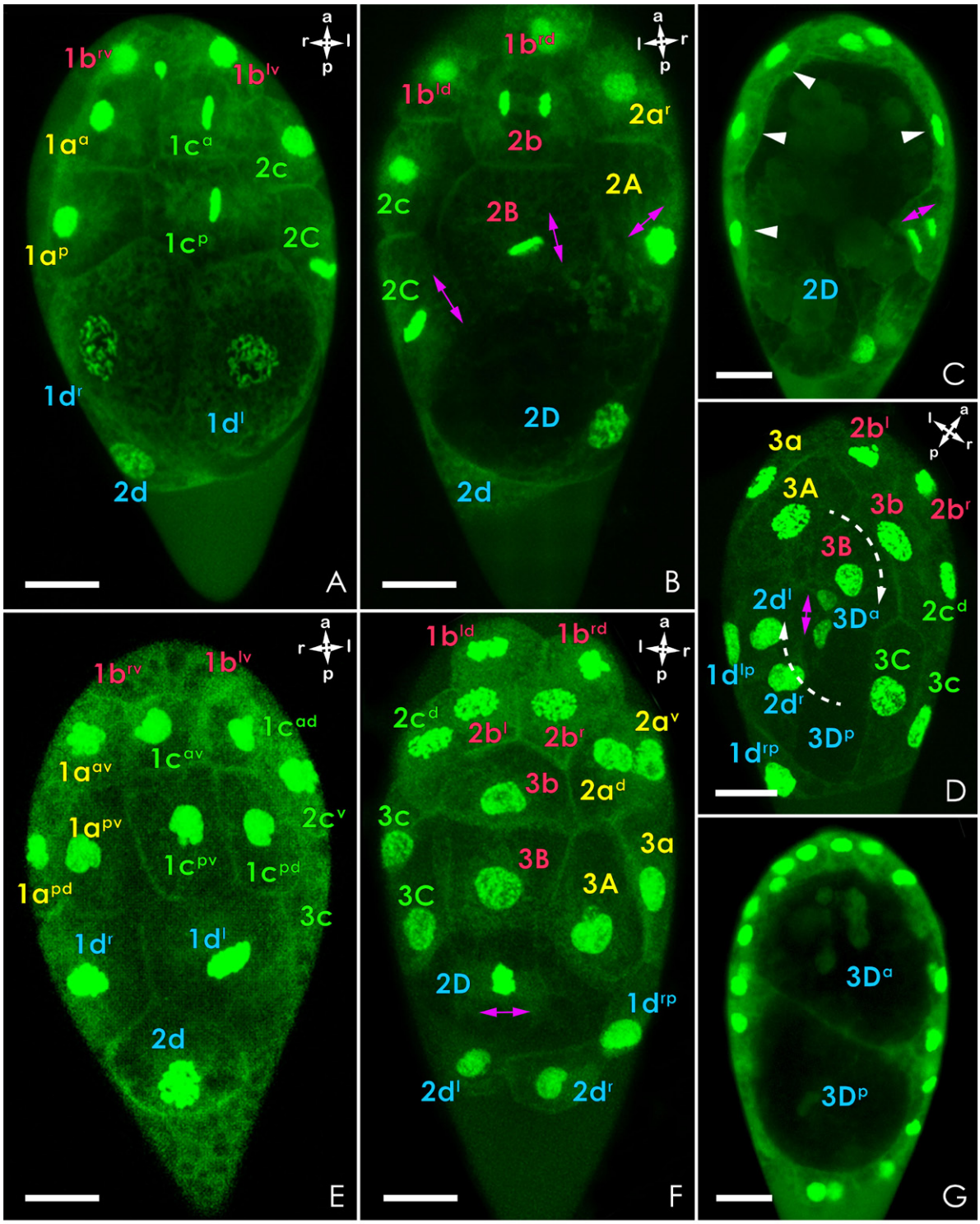

Fig. 3.3.7. Fifth cleavage, 32-cell stage, and epiboly.

Lilac arrows – spindle orientation in dividing blastomeres.

A-**G** – fixed and stained embryos during fifth division; **A**-**B** – early stage of fifth cleavage: the descendants of the A, B, and C lines are in metaphase or anaphase of mitosis, the spindles of 2A, 2B, and 2C are oriented towards the future blastopore area. Ventral (**A**) and dorsal (**B**) view; **C** – section through fixed and stained embryo. White arrowheads point to flattened blastomeres overgrowing the yolky cell 2D. Lilac arrow indicates the inwards orientated spindle in one of the blastomeres, see text; **D** – fixed and stained embryo at nearly 32-cell stage, the yolky cell, which is about to complete cytokinesis, has divided equally into $3D^a$ and $3D^p$. The lilac arrow indicates the final direction of its division. The blasto-

During the fifth cleavage, the spindles in all micromeres are perpendicular to the previous cleavage, with the exception of 2A, 2B, and 2C (Fig. 3.3.2.ID, IID). Their spindles are oriented towards the vegetal pole and the area, where the blastopore will be formed, and somewhat inside (Fig. 3.3.7.B, C). Thus, their daughter cells partly overlie each other. However, after the division is completed, the inner cells come to the surface. The direction of the cleavage in 2D is difficult to set in relation to the embryonic axes because of the ongoing process of gastrulation (see below). Its daughter cells $3D^a$ and $3D^p$ have been named after their final position within the embryo (Fig. 3.3.7.D,G).

All the blastomeres cleave equally this time, including the macromere 2D (Fig. 3.3.7G; Fig. 3.3.8.E,G). The yolk and the Sytox-stained granules are shared quite evenly between the two daughter cells $3D^a$ and $3D^p$ (Fig. 3.3.7.G).

The animal-vegetal axis corresponds to the plane of division of the yolky cell 2D and changes its orientation within the egg shell during cell division (see below).

3.3.2. Gastrulation.

Gastrulation, as the process of formation of a three-layered embryo, in the barnacle goes by three different ways: epiboly, delamination, and migration. While the first results in the internalization of the endoblast, the other two lead to internalization of mesoderm (endomesoderm and ectomesoderm, respectively).

3.3.2.2. Epiboly

Epiboly (Fig. 3.3.8A-D) starts during the fourth division. When the micromeres at the anterior end of the embryo enter cleavage, the yolky cell 1D seems to slightly squeeze itself among the micromeres with its anteriormost part, which becomes modified into a cone-like shape (Fig. 3.3.8A; Movie 3.3.6.). The cell regains a more or less round shape as soon as the spindle of the fourth division starts to form within (Fig. 3.3.8B).

After the cleavage is completed and the nuclei of all blastomeres are in their interphase (after approximately 10 min for 2d and 2D, which had been the last to finish the fourth division), epiboly starts over again. The anteriormost part of the newly formed yolky cell 2D regains a cone shape and seems to be "sucked" in between the micromeres (Fig. 3.3.8.C; Movie 3.3.6.). When

◁ derm is turned clockwise (compare with F). View from vegetal pole; **E**-**F** – late stage of fifth cleavage: the descendants of A, B, and C have completed their fifth cleavage, while those of D only start to divide. Ventral (**E**) and dorsal (**F**) view, lilac arrow indicates initial direction of division in 2D; **G** – section through an embryo after the next cycle of division in the blastoderm, one can see the final position of the nearly equal daughter cells of 2D, $3D^a$ and $3D^p$. Scalebars: 20 µm

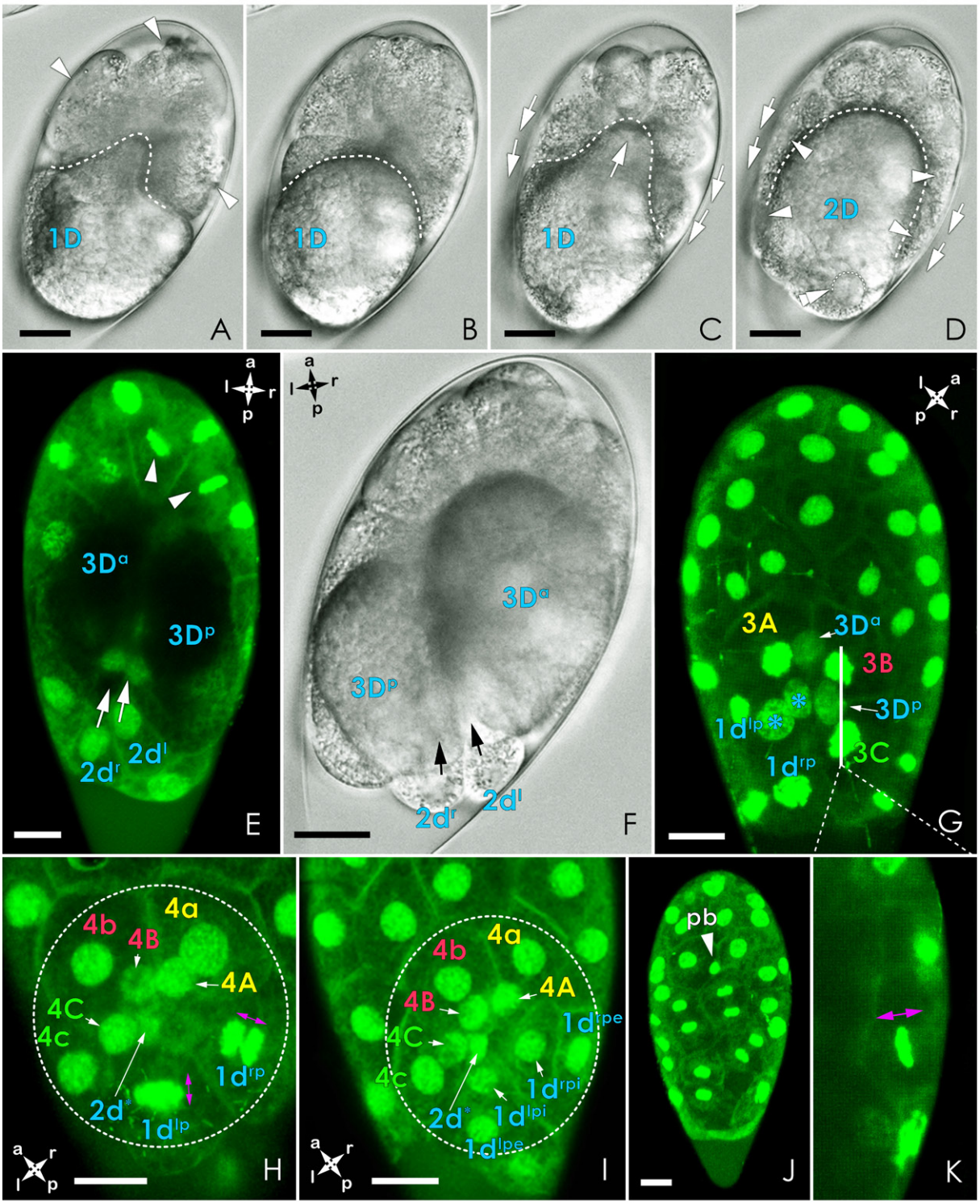

Fig. 3.3.8. Gastrulation steps.

A-**D** – section through living specimen during epiboly (for explanations see text); **A** – fourth division in the micromeres, arrowheads point at dividing blastomeres; **B** – fourth division of the macromere; **C** – fifth division of the micromeres; **D** - arrowheads indicate flattened micromeres, double arrowhead shows the nucleus of 2D; **C**-**D** – arrows show the direction of blastomere movements; **E**-**G** – migration of daughter cells of 2d, $2d^r$ and $2d^l$; **E** – section through an embryo at the end of cytokinesis in 2D, arrows indicate the direction of migration of the $2d^r$ and $2d^l$, the arrowheads point at the dividing anterior blastomeres; **F** – optical section through living embryo after the daughter cells of 2D, $3D^a$ and $3D^p$ have taken their final position in the anterior and posterior of the embryo, respectively; **G**-**I** – formation of the blastopore, vegetal pole view; **G** – blastopore-organising cells are in metaphase, daughter cells of 2d

When the ventral side of the embryo is completely covered by the blastoderm, 2D divides. Its cytokinesis seems to lead to a slight turn of the blastoderm (Fig. 3.3.7.D, dashed arrows). According to the 4D observations the blastoderm turns in the way that descendants of quadrant C move towards the posterior of the embryo and those of quadrant A towards the anterior. The embryos of right type (See chapter 3.3.1.2.), thus, perform a counter-clockwise turn and those of the left type a clockwise turn (compare Fig. 3.3.7.D and 3.3.8.G with 3.3.8.H and I).

2D has established contact with all the blastomeres from the interior of the embryo, the blastomeres 2A, 2C, $1d^r$, $1d^l$, and 2d migrate towards the vegetal pole (Fig. 3.3.8.C,D, arrows; Movie 3.3.6.). At this point, the 2D macromere has returned to a rounded shape, whereas the overgrowing blastomeres are flattened representing a blastoderm (Fig. 3.3.7.C; Fig. 3.3.8.D, arrowheads point to the flattened blastomeres). In the meantime, most of the anterior cells ($1b^r$, $1b^l$, $1a^a$, $1c^a$, $1a^p$, $1c^p$, 2b) have begun with the fifth division cycle.

With the overgrowth, the animal-vegetal axis slightly tilts in relation to the elongated axis of the egg shell (see Fig. 3.3.7.D, 3.3.8.G, and Fig. 3.3.8.J, vegetal and animal pole views respectively; Movie 3.3.6.), whereas the antero-posterior axis of the embryo almost matches the latter (Fig. 3.3.8E,F). A bit later, after the division of 2D, the polar axis is tilted under 45º to the elongated axis of the egg. The turn of the blastoderm results in inclination of both the left-right and antero-posterior embryonic axes: they are now under 45º to the transversal egg axis (Fig. 3.3.7.D).

3.3.2.3. Ingression and migration

Simultaneously with the closure of the blastopore, blastopore-organizing cells pass through the sixth division. Their division is directed towards the blastopore and slightly inwards. This way of internalization is referred here as ingression, although one could compare it with delamination. (Fig. 3.3.8.K). The newly produced sister cells partly overlay each other, like it has been described in the fifth cleavage for their mother cells. However, unlike in case of the fifth division, the inner cells do not come to the surface. In contrast, they become completely covered by their outer sister cells. The inner cells, 4 A, 4B, 4C, $1d^{rpi}$, and $1d^{lpi}$, are precursors of the mesoderm (Fig. 3.3.8.I).

Other precursors of mesoderm, the cells $2d^r$ and $2d^l$, migrate inside the embryo through the closing blastopore (Fig. 3.3.8.E,F,G). This happens during or shortly before the division of the blastopore cells. $2d^r$ and $2d^l$ do not divide till after the closure of the blastopore.

(asterisks) migrate inside; **H** - blastopore-organising cells of A,B, and C lines have divided into external and internal daughter cells, those of the D quadrant ($1d^{rp}$ and $1d^{lp}$) are in mitosis; **I** – blastopore-organising cells of the D quadrant have divided into external and internal cells; **J** – animal pole view of an embryo during formation of blastopore, polar body can be used as a landmark for the animal pole, the animal-vegetal axis is inclined in relation to the long axis of the egg; **K** – section through the dividing blastopore-organising cells, lilac arrow shows inwards directed division. Scalebars: 20 µm.

Gastrulation ends with the closure of the blastopore, which is formed by five cells: 4a, 4b, 4c, $1d^{rpe}$, and $1d^{lpe}$ (Fig. 3.3.8.I). At this stage the sixth division of all the blastoderm cells is completed. Thus, the embryo consists of 60 cells. The internal set of cells include $3D^{a}$ and $3D^{p}$ (precursors of endoderm), 4A, 4B, 4C, $1d^{lpi}$, and $1d^{rpi}$ (precursors of ectomesoderm), and $2d^{r}$ and $2d^{l}$ (precursors of endomesoderm).

3.4. Blastomere fates

3.4.1. Statistics of injections and problems encountered

The single blastomere labelings have been performed at the 4-, 8-, and 16-cell stages. As it was written above (see chapter 3.3.), the cleavage of the barnacle is patterned and the axes are established already at the 4-cell stage (what has been possible to discover by backwards lineaging). Therefore, the embryos can be oriented and the derivatives of the anterior quadrant B and the posterior quadrant D are quite easy to be individually identified. It is not, however, so simple to recognize the progeny of the blastomeres A and C because of two chiral variants of the second division (see subchapter 3.3.1.2.). For that reason the quadrants together with their offspring have been assigned letters L/l or R/r corresponding to their left or right position, respectively.

Successfully marked and normally developing embryos[♣] have been observed through the days and documented according to the stage. The fixations were not made on every stage, but within certain developmental-groups. The groups were distinguished as following: group I (stage 3), group II (stages 4-5), group III (stages 6-7), and group IV (stages 8-9).

The group sampling has varied (see Table 3.4.2.), as well as the number of the clones analyzed for each blastomere. That depended mostly on different level of interest in particular stages or cells. For example, within the group I only few embryos were fixed and investigated. On the contrary, the group III contains the biggest number of studied animals. The specimens with ectoblastic blastomeres 2a, 2b, and 2c marked are the fewest, whereas the embryos with labeled mesodermal 2d represent the biggest sampling.

A number of difficulties and problems have occurred during labeling. The first of those to be mentioned is the fast evaporation of the medium during the injection process. That has lead to higher salinity which caused shrinkage of the egg shell. When slight, the malformation was temporary, and the animals got their normal shape back as soon as they were put in water with normal salinity. The injections, therefore, had to be conducted quite fast to prevent major misdevelopment.

The injection into some particular blastomeres became another problem. For example, blastomere 2d appeared to be the most difficult cell to mark. The labeling of it led either to its immediate death, or to an abnormal development afterwards. Precise statistics of successful injections have not been performed daily, but just to give a general idea, a comparative example of the labeling applied for 1b and 2d is provided below (Table 3.4.1.).

[♣] The embryos which were fixed had a normal outer appearance, but some of them did have abnormalities in development of internal structures, which could have been observed only with assistance of CLSM

Table 3.4.1. Comparative statistics on survival between the embryos with injected 1b anord 2d blastomeres.

Numbers: alive and looks normal (fixed)/alive, but misdevelopped/dead.

Blastomere	Marked[♣]	After few hours	Next 2-3 days	Next 4-6 days	Shortly before hatching	Fixed outcome[♣♣]
1b	38	24/-/14	21(5)/1/3	15(7)/1/-	8(8)/-/-	20
2d	114	56/-/58	16(3)/17/36	8(4)/4/1	3(3)/-/1	10

One of the possible reasons for such a high sensitivity of this cell can be the constant migration during its life cycle (and any intrusion in rebuilding cytoskeleton might cause destructive for the cell consequences).

Table 4.3.2. General statistics on successfully marked and scanned embryos.

First digit: number of specimens analyzed by means of CLSM.
In brackets: total number of successfully marked and fixed embryos, which were analysed by meansof an stereo binoscope (not all of them were proceeded to CLSM).

	Fixation group	4cell stage	8 cell stage		16 cell stage				Total
Left quadrant		L	1l	1L	$1l^a$	$1l^p$	2l	2L	
	Group I	0(3)	0(0)	1(1)	0(1)	0(2)	0(0)	1(2)	
	Group II	3(5)	1(2)	2(6)	2(6)	3(5)	2(6)	4(4)	
	Group III	7(10)	6(7)	1(2)	3(3)	4(6)	1(4)	5(5)	
	Group IV	6(6)	4(4)	1(1)	3(3)	2(4)	0(0)	4(4)	
	Σ	16(24)	11(13)	5(10)	8(13)	9(17)	3(10)	14(15)	66(102)
Right quadrant		R	1r	1R	$1r^a$	$1r^p$	2r	2R	
	Group I	0(2)	0(0)	0(1)	0(2)	0(1)	0(0)	0(0)	
	Group II	6(7)	2(3)	4(5)	3(5)	2(7)	1(3)	4(6)	
	Group III	4(11)	4(4)	2(3)	3(4)	3(8)	1(3)	2(2)	
	Group IV	3(10)	6(7)	2(3)	1(1)	3(5)	0(1)	5(6)	
	Σ	13(30)	12(14)	8(12)	7(12)	8(21)	2(7)	11(14)	61(110)
B quadrant		B	1b	1B	$1b^r$	$1b^l$	2b	2B	
	Group I	1(1)	0(0)	0(0)	0(0)	0(0)	0(0)	2(2)	
	Group II	1(3)	7(7)	2(2)	1(1)	1(2)	0(3)	2(2)	
	Group III	4(8)	11(13)	3(4)	0(0)	0(0)	2(6)	5(5)	
	Group IV	5(7)	4(8)	1(2)	3(5)	1(1)	0(1)	7(9)	
	Σ	11(19)	22(28)	6(8)	4(6)	2(3)	2(10)	16(18)	63(92)
D quadrant		D	1d	1D	$1d^r$	$1d^l$	2d	2D	
	Group I	0(0)	1(1)	0(0)	0(0)	0(0)	1(1)	3(5)	
	Group II	0(1)	3(3)	3(6)	1(1)	1(2)	1(3)	2(7)	
	Group III	2(2)	8(11)	5(12)	2(4)	3(3)	6(9)	1(1)	
	Group IV	3(3)	11(14)	6(8)	0(0)	0(0)	4(6)	5(6)	
	Σ	5(6)	23(29)	14(26)	3(5)	4(5)	12(19)	11(19)	72(109)

[♣] It means the embryo looked normally directly after labeling and was transferred into a watch glass for experimental living (those with immediate death have not been counted of course).

[♣♣] There was a certain percentage of those embryos with internal misdevelopment which was invisible from outside and was observed only during the following analysis at CLSM (numbers are not given).

Unfortunately, not all fixed specimens were of a quality good enough to proceed with confocal microscopy afterwards. The main problem was related to the bleaching of the fluorescent signal of DiI. In table 4.3.2. one can find a summary on successfully performed scans.
The reason that the developmental group III is best represented is connected to another problem. The quality of the marking worsens during development and drastically drops at stage 8. Sometimes it was hard not only to say which structure was labeled, but also which quadrant was at all marked. Fixation of the stage 7 therefore gives a good balance of advanced development and marking quality.
In the following subchapters there is a description of the fate of each quadrant and additional information on the development of certain larval structures.

3.4.2. General patterns of quadrant fates

On the base of successful markings it was possible to establish the destiny for every quadrant and two generations of their daughter cells. In this chapter a short overview on their developmental fate is given. One has to keep in mind that the borders and the sizes of the areas, which are occupied by the marked descendants, vary (more detailed information will be given in the following chapter 3.4.3.). Nonetheless, despite of this variability, distinct patterns in fate and position of the derivatives of the marked blastomeres could be observed. Schemes of the generalized patterns of the development are provided in Fig. 3.4.1. A summary of the developmental origin of internal larval structures is shown in Fig. 3.4.1.C. The cell lineage of the germ layers is shown in Fig. 3.4.1.D.

3.4.2.1. Left quadrant

The left quadrant is one of the three small blastomeres in the 4-cell stage, which forms the cross furrow on the animal pole together with the right quadrant. As said above, unless the second cleavage is observed, it is impossible to identify certainly whether the left quadrant is blastomere A or C.
On the plate (Fig. 3.4.2.A,B) the outward appearance of the "left clone" at the early and late embryonic stage is presented. When the quadrant is injected with dye, its offspring is found to form most of the ectodermal and some mesodermal structures of the left body side. They include epi-

Fig. 3.4.1. Generalized patterns of developmental fates. Segregation of germ layers.

A-**B** - Epidermal descendants of the blastomeres at the 16-cell stage, **A** – ventral view; **B** – dorsal view; **C** - Generalized quadrant contribution to the internal structures of the nauplius larva; **D** - segregation and-cell lineage of the germ layers, mesectoblasts were not followed beyond 16-cell stage by means of in vivo inyections, but in the 3D reconstructions of the fixed specimens.

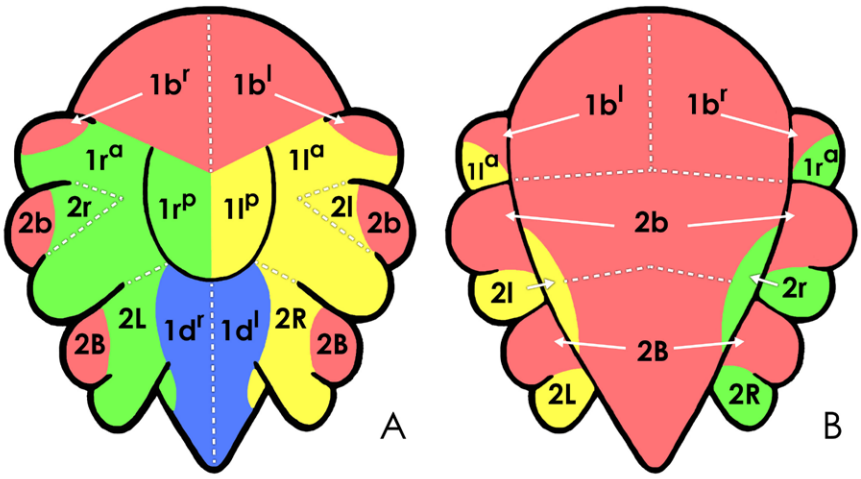

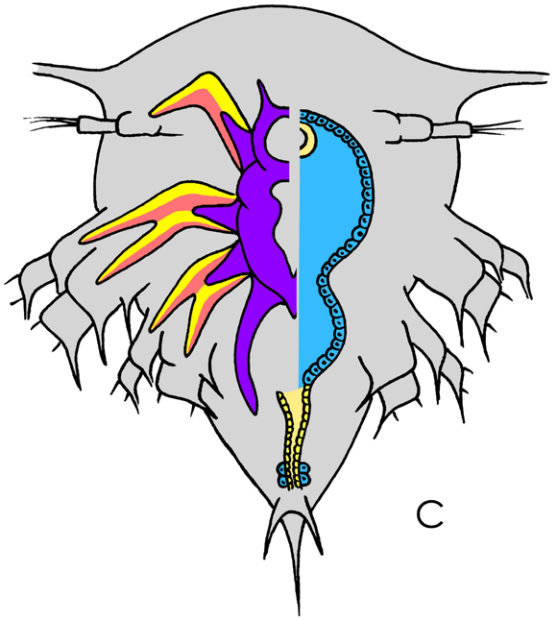

Colour code for A and B:

- descendants of L-quadrant
- descendants of B-quadrant
- descendants of R-quadrant
- descendants of D-quadrant

Colour code for C:

- descendants of L- or R-quadrants
- descendants of 2B
- descendants of 2d
- descendants of 2D

Colour code for D:

- ectoblast
- endomesoblast
- mesectoblast
- endoblast

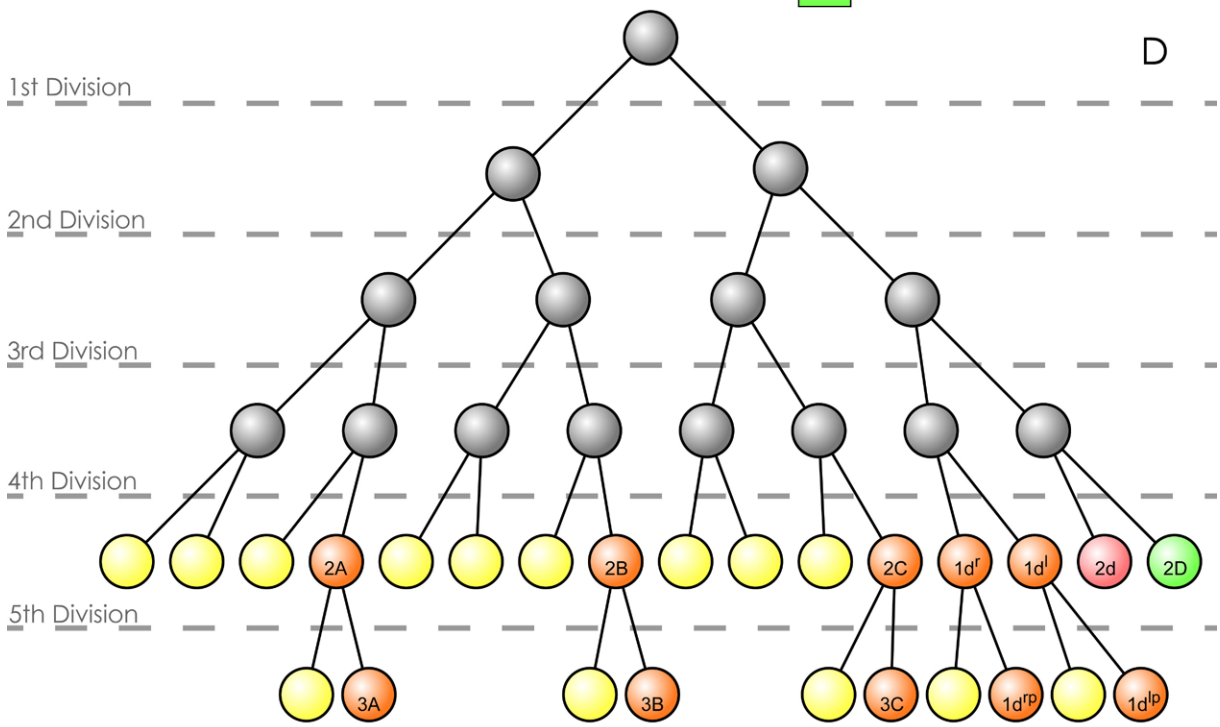

dermis of the limbs and labrum (Fig. 3.4.2.A,B), ectodermal parts of the oesophagus and proctodaeum (Fig. 3.4.3.C), the nauplius nervous system (Fig. 3.4.3.A,B), and some muscles of the limbs (Fig. 3.4.3.D).

Labelling of the blastomeres at 8- (Fig. 3.4.2.C,F) and 16-cell-stages (Fig. 3.4.2.D-H) provided more detailed data. Below the data of the 16-cell-stage labellings are provided. These data are also schematized in Fig. 3.4.1.

$1l^a$ is observed to give rise to the epidermis of the proximal and ventral side of *aI* and *aII* (including the endopodite) (Fig. 3.4.2.D). Besides that, this blastomere contributes to the formation of the nervous system in the nauplius (Fig. 3.4.3.A,B). In the majority of examined specimens the stain of DiI was found in the left somata of the deuto- and tritocerebrum, the mandibular ganglia, the left deuto-tritocerebral and tritocerebral-mandibular connectives, and also in the tritocerebral comissure (Fig. 3.4.3.A,B). Several strands in the mandibular comissure appeared to be stained as well, but rather weakly (Fig. 3.4.3.B). In all observed embryos segmental nerves going to *aI*, *aII*, and *mb* had a distinct signal of DiI (Fig. 3.4.3.A,B). Additionally, some somata from protocerebral region (like those of anterior ganglion) had also carried mark of DiI.

$1l^p$, the sister cell of $1l^a$, is also purely ectodermal. Its descendants are found on the left side of the labrum and the left parts of the oesophageal and proctodaeal epithelium of the nauplius (Fig. 3.4.3.C).

2l was observed to contribute exclusively to the ectoderm of the nauplius (Fig. 3.4.2.G). The clone of marked cells covered the dorsal and distal parts of the left *aII* (including the developing exopodite). The marked cells were also found on the left-dorsal side of the headshield (Fig. 3.4.2.G, arrowhead). The development of this blastomere is quite difficult to follow on the late stages of embryogenesis. Epidermal cells keep nearly no stain inside.

Fig. 3.4.2. Cell fate of the left quadrant. External parts of the clone.

All the images are obtained in Imaris Surpass view, Blend mode of Volume Scene, apart from B.
All the specimens presented in this chapter, if not specified otherwise, were marked by DiI (glow channel) and counterstained by DAPI or Sytox (blue or green channels).

A-**B** – 4-cell stage labelling, marked cells cover the left side of the labrum, left limbs and left epidermis of the nauplius body; **A** – Stage 5, left-lateral view; **B** – Nauplius I, ventral view, MIP(max) mode; **C** – 8-cell stage labelling, 1l marked, left-lateral view of the Stage 6, the clone is spread over the labrum, ventro-proximal part of *aI* and *aII*; **D**-**E** – 16-cell stage labelling, left-lateral ventral view; **D** – $1l^a$ marked, Stage 9, the clone covers the left-proximal part of the labrum, and the ventral-proximal parts of *aI* and *aII*; **E** – $1l^p$ marked, Stage 8, externally the clone is found only on the left-distal part of the labrum, some few epidermal cells of the ventro-proximal part of *aI* and the left side of the nauplius body in the base of *aII* are also labelled; **F** – 8-cell stage labelling, 1L marked, left-lateral view of the Stage 7, the clone is spread over the left side of the hind body, the dorsal-distal parts of *aII* and mb, one patch of marked cells is found at the midlevel of the dorsal side of the carapace; **G**-**H** – 16-cell stage labelling; **G** – 2l marked, Stage 6, left-lateral view, the clone includes the dorsal patch and the dorsal-distal side of the *aII* epidermis; **H** – 2L marked, Stage 8, latero-ventral view, the clone covers the ventral-distal part of the mandibular epidermis and the left side of the hind body. Scalebar 20 µm.

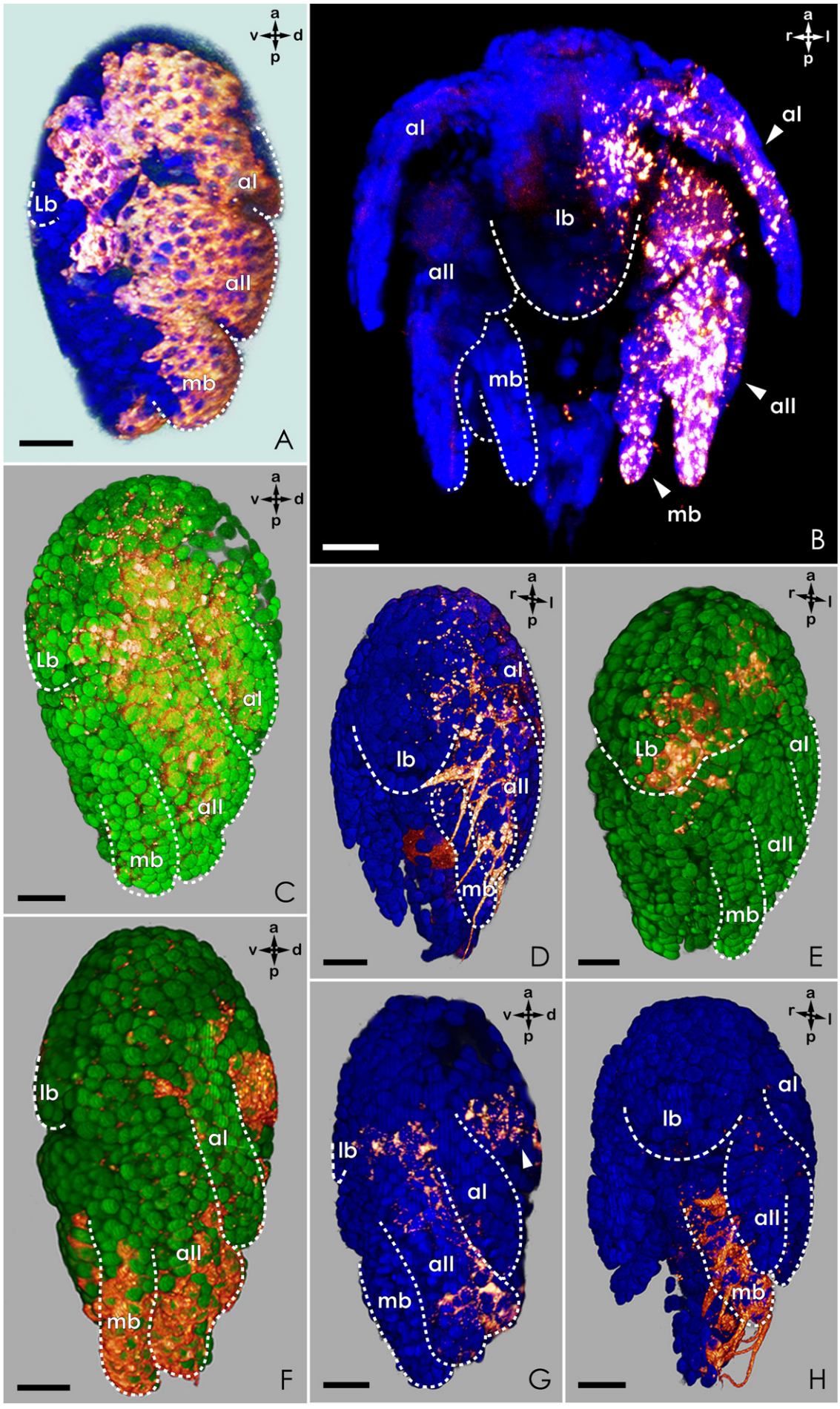
a
v
d
p
Lb
al
all
mb
A
a
r
l
p
al
lb
all
mb
al
all
mb
B
a
v
d
p
Lb
al
all
mb
C
a
r
l
p
al
lb
all
mb
D
a
r
l
p
Lb
al
all
mb
E
a
v
d
p
lb
al
all
mb
F
a
v
d
p
lb
al
all
mb
G
a
r
l
p
al
lb
all
mb
H

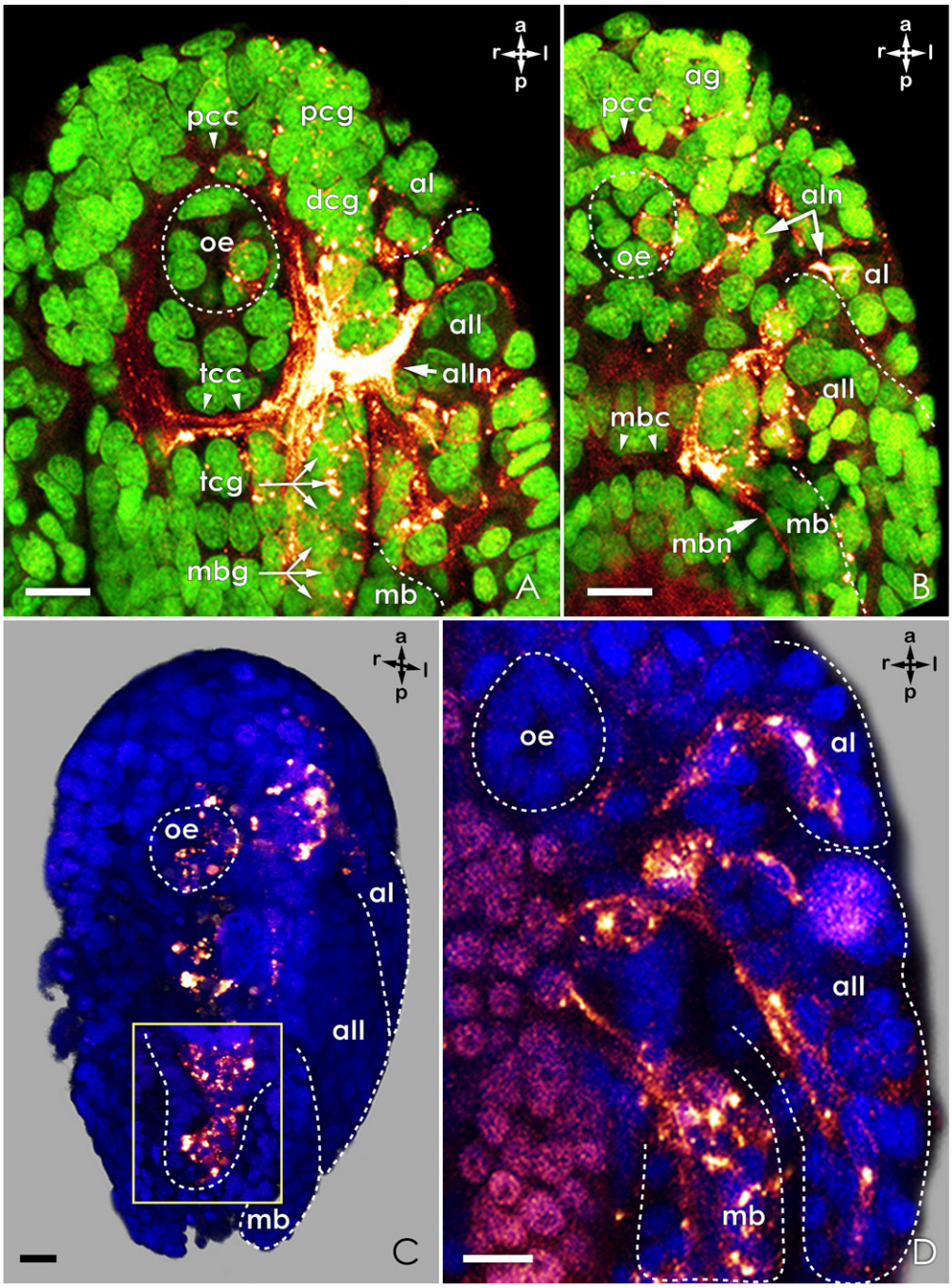

Fig. 3.4.3. Cell fate of the left quadrant. Internal parts of the clone.

All the images are obtained in Imaris Surpass view, by means of Clipping Plane scene.

A-**B** – contribution of the left quadrant to the nervous system, 1l[a] marked, Stage 9, ventral view, MIP(max) mode; **A** – marked somata are found in abundance in the regions of the deuto-, tritocerebral and mandibular ganglia, some somata with DiI occur in the proto-cerebral region as well (arrowheads here and on B), the nerve of *all* and the trito-cerebral commissure are labelled; **B** – a deeper cut of the embryo on A, the nerves leading to *al* and *mb* are shown to be labelled; **C** – contribution of the left quadrant to the digestive tract, 1lp marked, Stage 6, latero-ventral view, the left side of the oesophageal epidermis is marked; **Insertion**: deeper cut through the embryo on C, the left half of the forming hindgut is marked; **D** – contribution of the left quadrant to the musculature, 2L marked, Stage 8, ventral view, the dorsal extrinsic and intrinsic limb muscles are labelled. Scalebar 10 µm.

2L is a mesectoblastic cell. The ectoderm, which comes from it, includes the epidermis of the left hindbody and the ventral side of the mandible (including the endopodite) (Fig. 3.4.2.H). The mesodermal derivatives of 2L are intrinsic and dorsal extrinsic muscles of the left *aI*, *aII*, and *mb* (Fig. 3.4.3.D). Precise muscles are hard to identify, since very little of the dye is left in the fibres at the stages of final differentiation.

3.4.2.2. Right quadrant

According to the same principle as the one mentioned int the previous chapter the blastomere A or C, which position was on the right side of the embryo after the second division, was referred as the right quadrant and assigned with a letter R. The right quadrant contributes to two germ layers. In the position and fate of it and its progeny the right quadrant mirrors the left one. Thus, when it is labelled, most of the right side of the nauplius appears to be stained with DiI (Fig. 3.4.4.A). The following structures were observed to derive from the blastomere R: limb and labral epidermis, nauplius nervous system, epidermis of the digestive tract, muscles of the limbs. Injections on 8- (Fig. 3.4.4.B,C,E,F) and 16-cell stages (Fig. 3.4.4.D,G-I) provided us with a more detailed picture of the R-progeny. A summarized scheme is given in Fig. 3.4.1.A,B.

$1r^a$ is responsible for the formation of ectodermal structures on the right-anterior part of the nauplius. It gives rise to the epidermis on the ventral side of right *aI* (Fig. 3.4.4.D) and to the right side of the nauplius nervous ring, which includes regions of the deuto-, tritocerebrum, and mandibular ganglion. Segmental nerves leading to *aI*, *aII*, and *mb* are stained as well. The neurofibers of the tritocerebral commissure and those of the connective bundle between both deuto- and tritocerebrum, as well as tritocerebrum and mandibular ganglion demonstrate the most prominent DiI staining. In the embryo shown in Fig. 3.4.5.A the protocerebral somata and a single strand in the protocerebral commisure are labelled as well.

Fig. 3.4.4. Results of the injections into the right quadrant and its daughter cells. External parts of the clone.

All the images are obtained in Imaris Surpass view, Blend mode of Volume Scene.

A – 4-cell stage labelling, Stage 6, right-lateral side, the clone of marked cells includes the epidermis of the right limbs, the right side of the labrum and the right side of the nauplius body; **B**,**C**,**E**,**F** – 8-cell stage labelling, right-lateral view; **B**,**E** – 1r marked, Stage 5 (B) and 8 (ventro-lateral view), the clone includes epidermal cells of the left-anterior side of the nauplius and covers the ventro-proximal parts of the developing *aI* and *aII*; **C** – 1R marked, Stage 5, the marked cells cover the distal part of *aII* and the ventral part of mb; **F** – 1R marked, Stage 7, additionally to what is marked on the C clone of marked cells extends to the ventro-proximal part of *aII*, the distal part of mb, and the base of the developing labrum; **D**,**G**-**I** – 16-cell stage labelling, right-lateral view; **D** – $1r^a$ marked, Stage 7, the clone includes the ventral side of the epidermis of *aI* and a small right-anterior epithelial patch; **G** – $1r^p$ marked, Stage 8, externally the clone contributes to the epidermis of the right distal part of the labrum; **H** – 2r marked, Stage 6, the labelled descendants are found at the midlevel of the dorsal side of the nauplius (arrowhead), at the base of the labrum, and on the distal part of *aII*; **I** – 2R marked, Stage 6 (the embryo was slightly flattened during mounting), externally the clone covers the distal part of mb and a small part of the tip of the *aII* endopodite (arrowheads). Scalebar 20 µm.

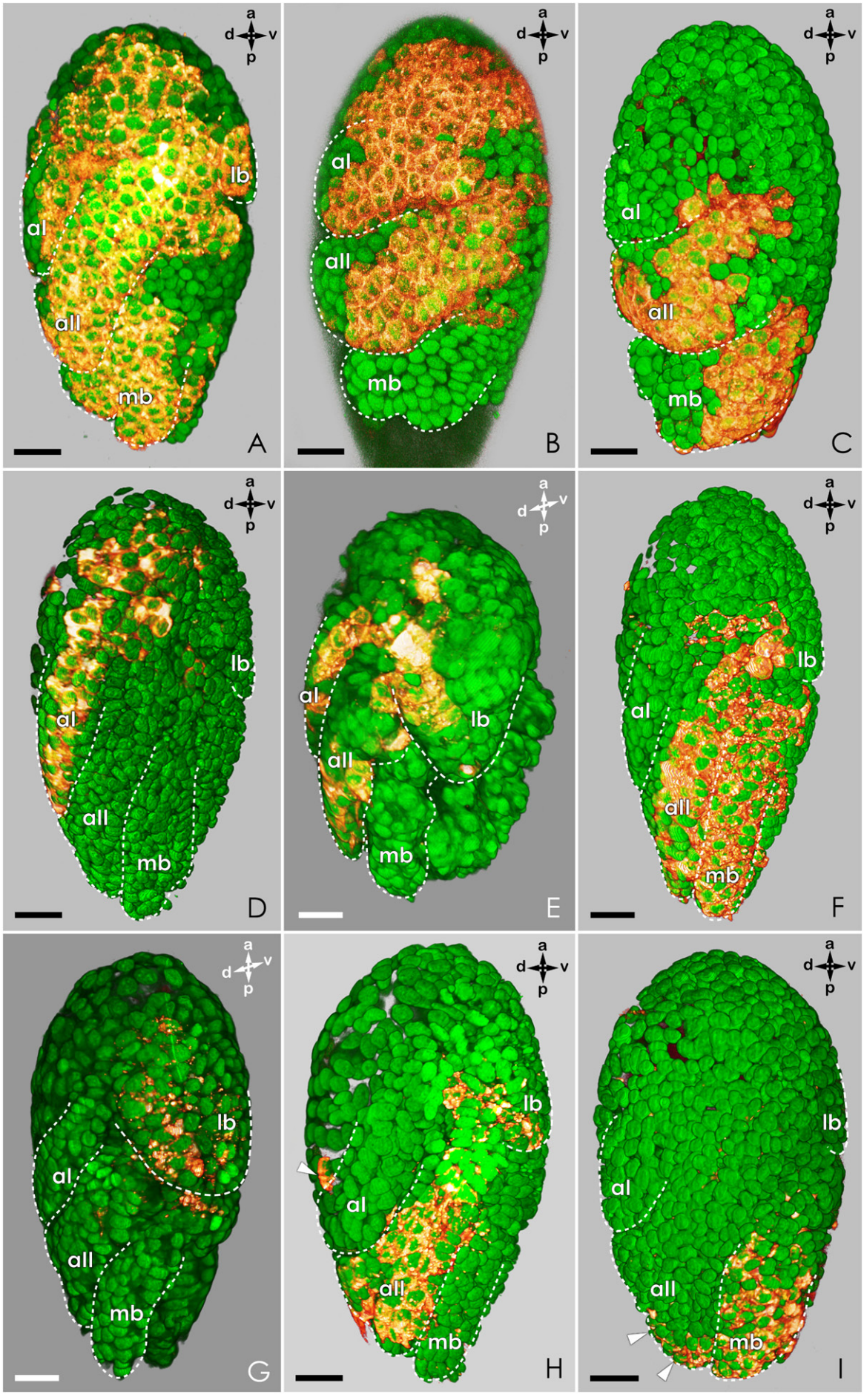
a
d
v
p
lb
al
all
mb
A
B
C
D
E
F
G
H
I

$1r^p$ is the sister blastomere of $1r^a$ and it also provides exclusively ectodermal structures. Among those: right side of the labral epidermis (Fig. 3.4.4.G) and right parts of the epidermis in stomodaeum and proctodaeum (Fig. 3.4.5.B).

8-cell stage labelling of 1r (Fig. 3.4.4.B,E; Fig. 3.4.5.A) suggests that one of its daughter cells gives rise to the epidermis of the proximal portion of the right *aII*. Taking into account that the R quadrant and its descendants show mirrored fates of the L quadrant, then the blastomere responsible for this epidermal patch would be $1r^a$. However, none of 16-cell labelled specimens had this part of the body labelled.

2r is a purely ectoblastic cell. It forms most of the epidermis on the ventral and distal side of *aII* and a little part of the epidermis on the dorso-lateral side of the headshield. As well as its mirror companion 2l, this blastomere is hard to trace till the very late embryonic stages.

2R, which is the sister cell to 2r, presents a mesectoblast. It gives rise to epidermal cells of the ventral side of the right mandible (including the entopodite) and of the right side of the hind body (Fig. 3.4.4.I; Fig. 3.4.5.C). Mesodermal structures of 2R are intrinsic and dorsal extrinsic muscles of the right limbs (Fig. 3.4.5.C).

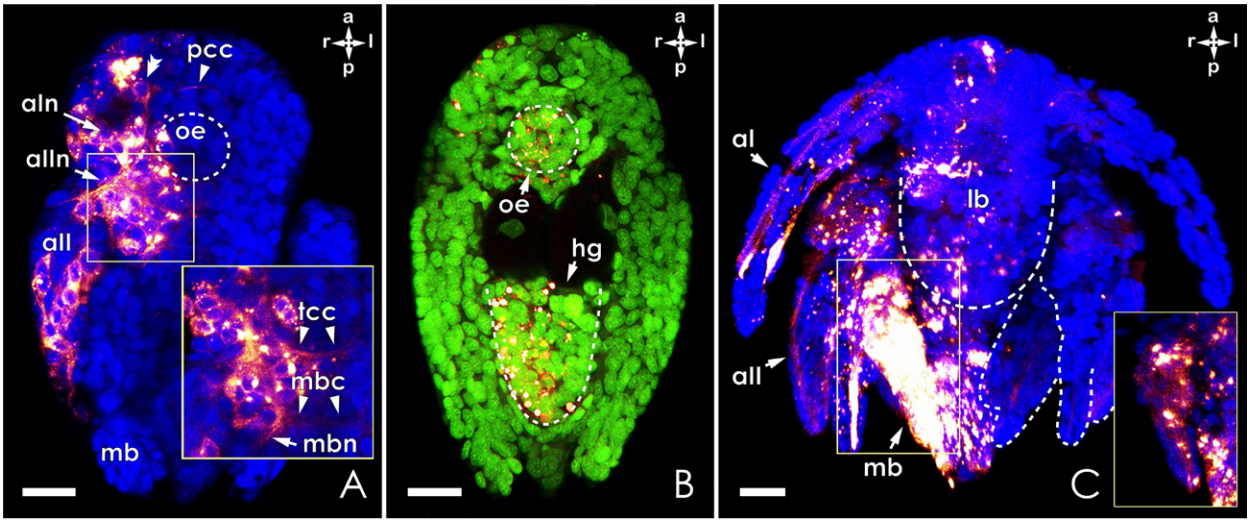

Fig. 3.4.5. Results of the injections into the right quadrant and its daughter cells. Internal parts of the clones.

All the images are obtained in Imaris Surpass view, MIP(max) mode of Volume Scene, with help of Clipping Plane scene (except for C).

A – 1r labelling, early Stage 8, ventral view, regions of the deuto-, tritocerebral, and mandibular are intensively stained including central somata, central neuropiles, and peripheral nerves leading to *aI*, *aII*, and *mb* (see **Insertion**), theprotocerebral region contains some marked cells (double arrowheads), a single strand in the protocerebral commissure seems to be stained as well (arrowhead); **Insertion**: deeper and slightly zoomed in cut of the region outlined on A; **B** – $1r^p$ marked, Stage 8, ventral view, the right half of the oesophagus and the proctodaeum are stained; **C** – 2R marked, Nauplius I, ventral view, the internal descendants of the blastomere include some of the dorsal extrinsic and intrinsic muscles of the right limbs; **Insertion**: mandibular exopodite from the outlined area on C, mandibular exopodite is cut out. Scalebar 20 µm.

3.4.2.3. B quadrant

Quadrant B is the dorsal quadrant and gives rise to the most of the dorsal and anterior structures of the nauplius. This blastomere contributes to the two germ layers, ectoderm and mesoderm. Among the structures labelled with DiI in case of B-injection one can see epidermis of the anterior and dorsal parts of the nauplius head shield, epidermis of the dorsal and distal limb parts (Fig. 3.4.6.A), the anterior region of the nervous system, and some of the extrinsic dorsal as well as intrinsic limb muscles (Fig. 3.4.7.A,F).

More detailed fates of the progeny of the B quadrant was obtained on the base of 8- and 16-cell stage labellings and is schematized in Fig. 3.4.1.

$1b^r$ and $1b^l$, the daughter cells of 1b, are involved in the formation of the same but mirrored structures, $1b^r$ on the right and $1b^l$ on the left of the forming larva. These blastomeres are purely ectodermal blastomeres. In general, externally the 1b clone includes the epidermis, covering the whole anterior of the barnacle embryo and spreading to the labrum and the anterior sides of *aI* (Fig. 3.4.6.C,D). Internally, the descendants of 1b are concentrated in the protocerebral region of the nervous system, forming the nauplius eye (the signal is seen in cups and their innervations) (Fig. 3.4.7.A) and the frontal filaments (including ag, ffn, and fft) (Fig. 3.4.7.A,B). Intensive marking by DiI was also observed in the protocerebral commissure and the circumoesophageal connective bundles (Fig. 3.4.7.A).

1B, the sister blastomere of 1b, divides into 2b and 2B. 2b represents an ectoblastic cell. Its clone is placed on the midlevel of the dorsal side of the nauplius carapace and also covers partly the exopodites of *aII* (Fig. 3.4.6.E).

2B gives rise to both ectoderm and mesoderm. Ectodermal parts include the dorsal epidermis of the hind body, dorsal and distal parts of the right and left mandibles (this includes tips of the ento- and exopodites) (Fig. 3.4.6.F). Mesoderm originating from 2B is presented by intrinsic and dorsal extrinsic musculature of both left and right naupliar limbs. Apart from this, a group of cells was found along the wall of the midgut, which carried the mark of DiI in the case of 2B labelling (Fig. 3.4.7.D,E). It was hard to identify whether these cells belong to the gut epithelium, musculature of the gut, or something else. Due to their position (at the midlevel of the midgut) one can suggest that later they might form the constriction separating the midgut into anterior and posterior portions (Walley and Rees, 1969). This is yet to be proven though.

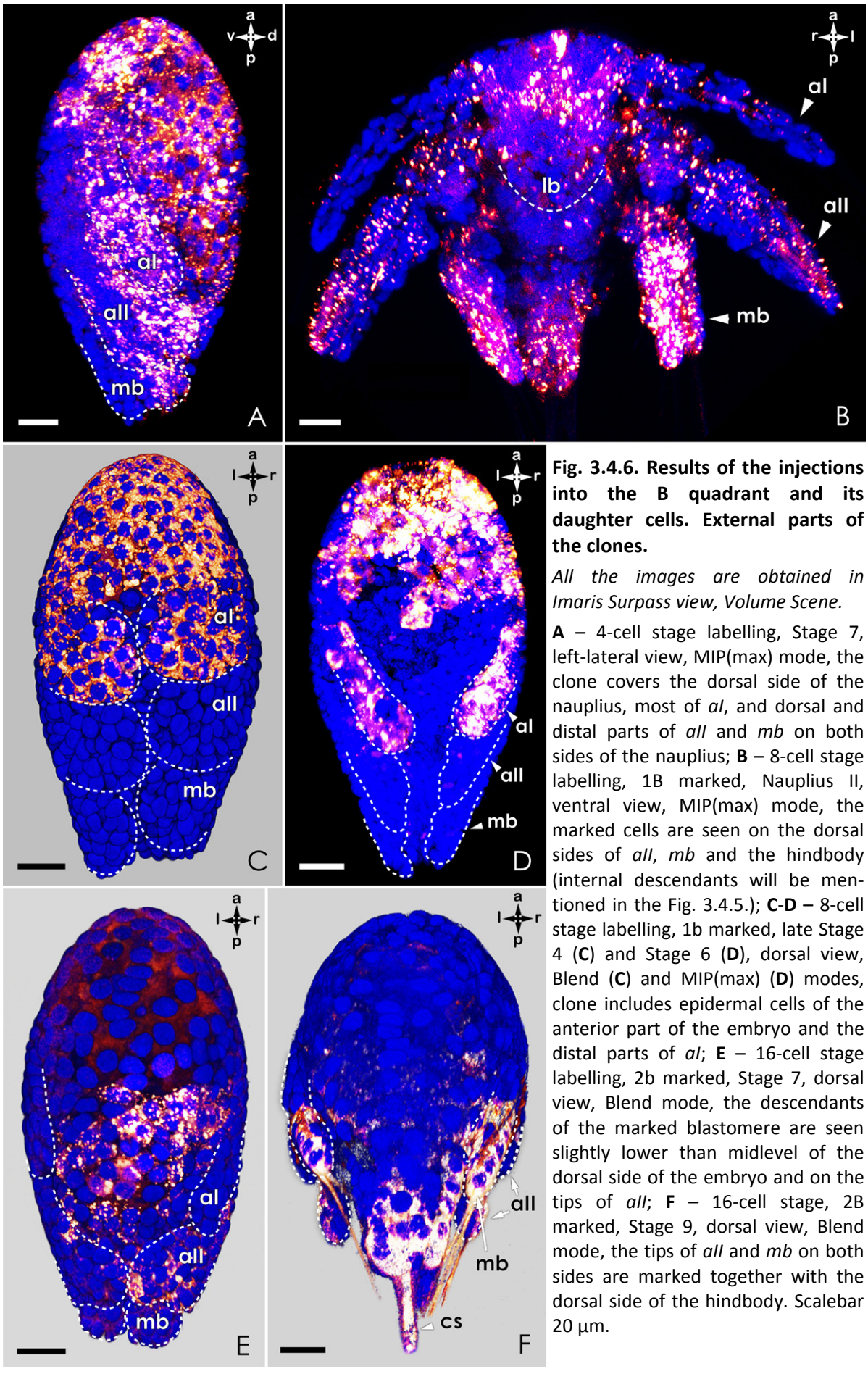

Fig. 3.4.6. Results of the injections into the B quadrant and its daughter cells. External parts of the clones.

All the images are obtained in Imaris Surpass view, Volume Scene.

A – 4-cell stage labelling, Stage 7, left-lateral view, MIP(max) mode, the clone covers the dorsal side of the nauplius, most of *al*, and dorsal and distal parts of *all* and *mb* on both sides of the nauplius; **B** – 8-cell stage labelling, 1B marked, Nauplius II, ventral view, MIP(max) mode, the marked cells are seen on the dorsal sides of *all*, *mb* and the hindbody (internal descendants will be mentioned in the Fig. 3.4.5.); **C**-**D** – 8-cell stage labelling, 1b marked, late Stage 4 (**C**) and Stage 6 (**D**), dorsal view, Blend (**C**) and MIP(max) (**D**) modes, clone includes epidermal cells of the anterior part of the embryo and the distal parts of *al*; **E** – 16-cell stage labelling, 2b marked, Stage 7, dorsal view, Blend mode, the descendants of the marked blastomere are seen slightly lower than midlevel of the dorsal side of the embryo and on the tips of *all*; **F** – 16-cell stage, 2B marked, Stage 9, dorsal view, Blend mode, the tips of *all* and *mb* on both sides are marked together with the dorsal side of the hindbody. Scalebar 20 µm.

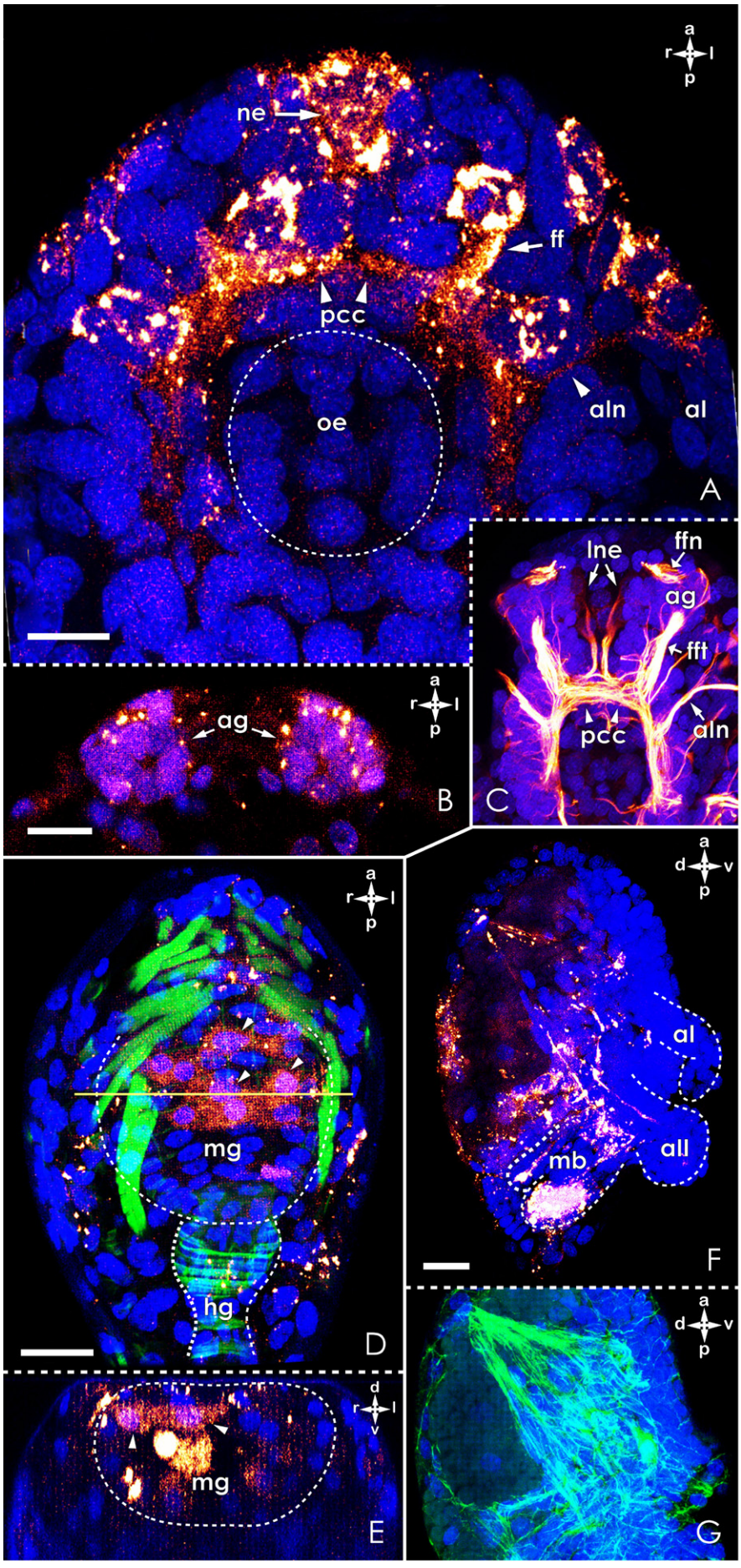

Fig. 3.4.7. Results of the injections into the B quadrant and its daughter cells. Internal parts of the clones.

All the images, apart from B and E, are obtained in Imaris Surpass view, MIP(max) mode of Volume Scene with help of Clipping Plane scene.

A – 1b marked, late Stage 7, ventral view, most of the protocerebral region is stained by DiI including the nauplius eye, fft of the frontal filament complex, some somata and the neuropile of the deutocerebral region are marked including several strands of the nerves leading to *al*; **B** – section of the embryo on A taken at the level of the globular parts of the frontal filaments which both appear to be marked, Imaris Section view, MIP(max) mode; **C** – general view of the proto- and deutocerebral regions of an embryo at the same stage as A and B (Stage 7), ventral view, acetylated α-tubulin with counter staining by Sytox; **D** – 2B marked, Stage 9, dorsal view, group of "unspecialized" cells are among the descendants of the B quadrant, they strap the midgut on the dorsal side; **E** – transversal section of the embryo on D in the position of the yellow line, Imaris Section view, MIP(max) mode, the cells seem to be placed within the midgut; **F** – 2B marked, late Stage 7, right-lateral view, some dorsal extrinsic and intrinsic muscle fibres are marked; **G** – the same embryo as on F, stained by phallocidin to demonstrate the total amount of muscle fibres in the embryo.
Scalebar A-B – 10 µm, D-G – 20 µm.

3.4.2.4. D quadrant

Blastomere D is the biggest quadrant and contains most of the embryonic yolk. It is the only quadrant which contributes to the formation of all three embryonic germ layers. When D is marked, its clone includes the ventral epidermis of the hindbody and sometimes of the limbs, the entire midgut, the musculature of the digestive tract and the ventral extrinsic limb muscles. The scheme of the fates of D descendants is given on Fig. 3.4.1.A,B.

$1d^r$ and $1d^l$ are the daughter cells of 1d, which undergoes bilaterally symmetrical division. The progeny of them is symmetrical as well and can be found on the right and left sides of the nauplius body. Together they form most of the ventral epidermis of the hindbody and also contribute to the epidermis on the ventral side of the mandibular protopodites (Fig. 3.4.8.A,B). Both $1d^r$ and $1d^l$ give rise to mesoderm of the *aII* and *mb* (Fig. 3.4.8.C) and to the circular musculature of the hindgut (Fig. 3.4.8.D). DiI presence was also observed in the two pairs of the big cells placed on both sides of the proctodaeum and right under the midgut (Fig. 3.4.8.E,F). These cells (here called uc2) will be described in chapter 3.5.3.

1D, the sister cell of 1d, is mesendoblastic (Fig. 3.4.9.A,D). It divides into endmesoblastic 2d and endoblastic 2D. The labelling of 2d leads to the visualisation of labral and oesophageal musculature, as well as the extrinsic ventral muscles of all the naupliar appendages (Fig. 3.4.9.E,F arrowheads; Fig. 3.5.5.D,E). 2D is the one to incorporate most of the embryonic yolk at the 16-cell stage. This blastomere solely forms the midgut of the barnacle (Fig. 3.4.9.B,C). Beside of this, two pairs of prominent cells emerge as descendants of 2D (Fig. 3.4.9.A,D: insertions). These cells are referred as uc1 and like uc2 will be described in the chapter 3.5.3.

Fig. 3.4.8. Labelling of blastomere 1d.

All the images, apart from E and E', are obtained in Imaris Surpass view, Volume Scene.

A-**B** – external descendants of the blastomere, Stage 5 (**A**) and Stage 9 (**B**), ventral view, Blend mode, the clone almost entirely covers the ventral side of the hindbody; **Insertion**: posterior part of the same embryo as on A viewed from the right-lateral side, some marked cells are found at the base of the forming mandible; **C** – mesodermal descendants of the blastomere, the same embryo as on A, cut by means of a Clipping Plane scene, groups of marked mesodermal cells are seen within the developing buds of *aII* and mb; **D** – mesodermal descendants of the blastomere, Stage 9, dorso-lateral view, MIP(max) mode, embryo cut by means of a Clipping Plane scene, the DiI signal is extremely poor because of the late stage, however, it is visible within the muscle elements wraping up the proctodaeum, the signal within the midgut is not related to any structure or cells and might be unspecific; **E**-**E'** – longitudinal sections through the lower part of the naupliar hindbody, Stage 5, ventral view, Imaris Section view, MIP(max) mode, "unidentified cells 2" are derivatives of the blastomere 1d. Scalebar A-C – 20 µm, D – 10 µm.

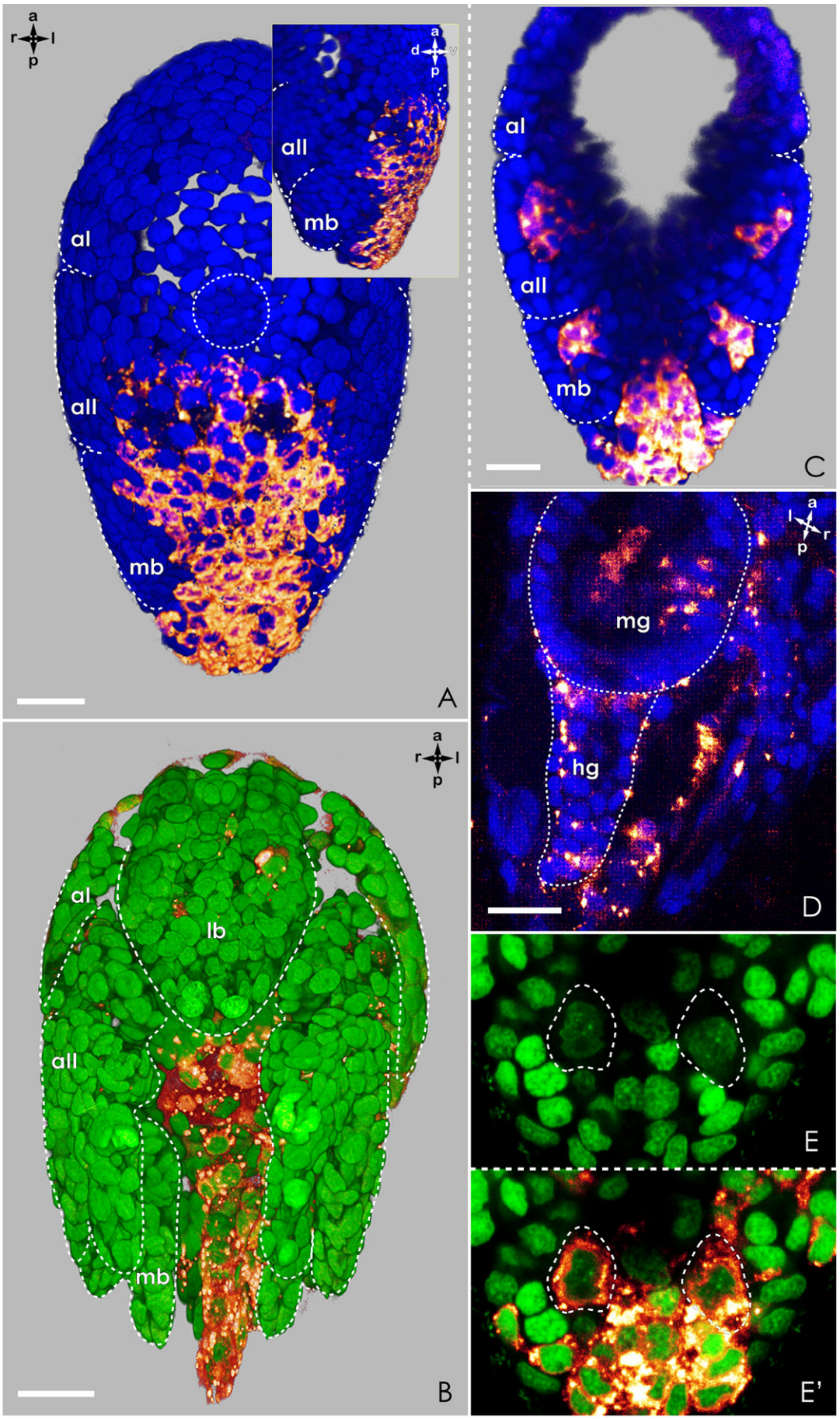
a
r
l
p
al
all
mb
A
a
d
v
p
all
mb
al
all
mb
C
a
l
r
p
mg
hg
D
a
r
l
p
al
lb
all
mb
B
E
E'

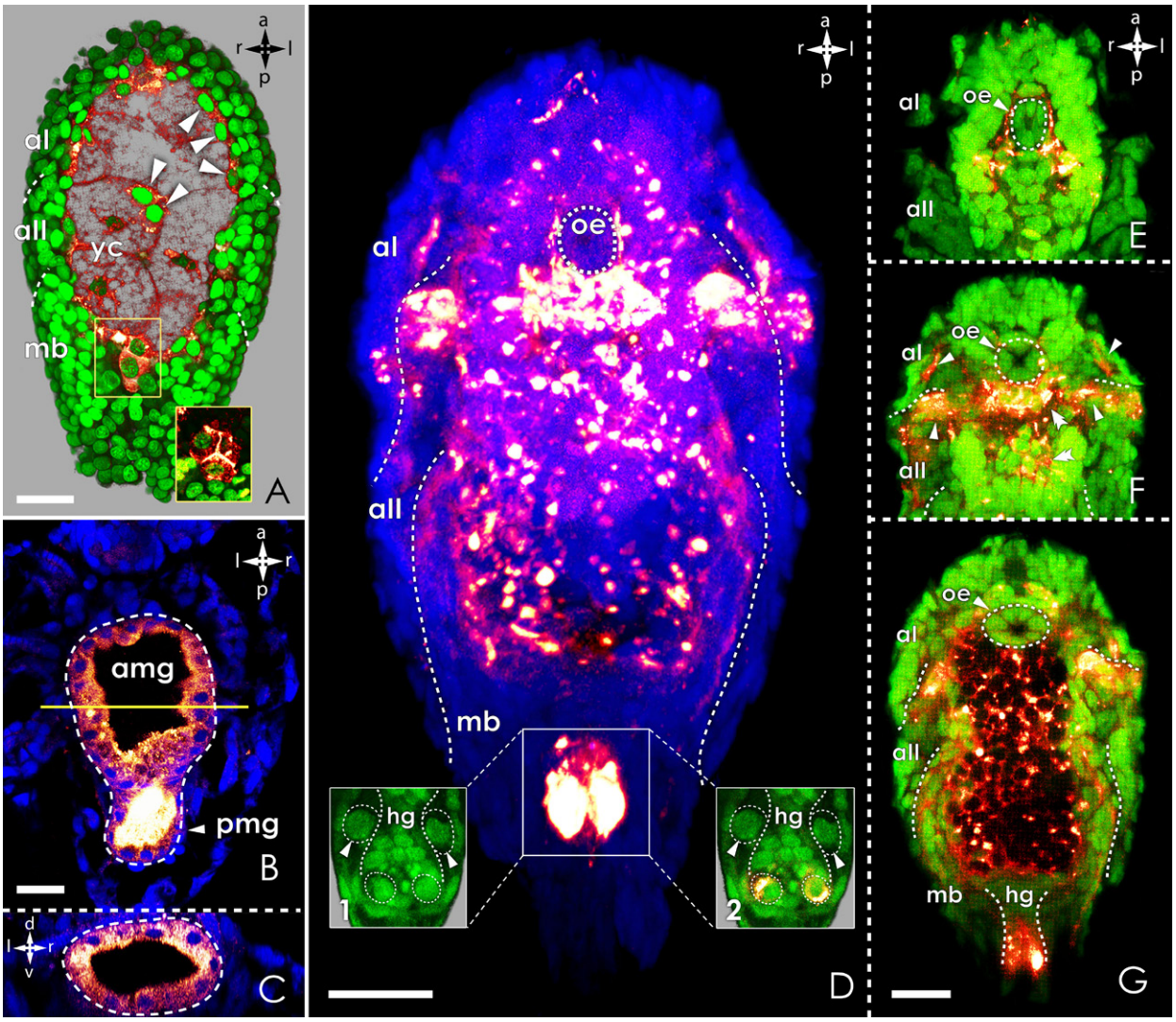

Fig. 3.4.9. Labelling of blastomere 1D and its daughter calls.

All the images, apart from D, are obtained in Imaris Section view.

A – 1D marked, section through the embryo of Stage 6, ventral view, Blend mode, the derivatives of the marked blastomere include all the yolky cells, some mesodermal cells (arrowheads), and two "unidentified cells 1" (outlined by yellow rectangular); **Insertion**: deeper section of the same embryo as on A through the outlined region, two more "unidentified cells 1" are found also labelled, making it four in total; **B** – 2D marked, longitudinal section through the midgut of the embryo of Stage 9, dorsal view, MIP(max) mode, all the cells of the midgut including its future two regions are labelled; **C** – transversal section of the embryo on B through the region of the yellow line; **D** – general view of the clone derived from 1D, Stage 8, ventral view, Imaris Surpass view, MIP(max) mode of Volume scene; **Insertions**: sections in Blend mode of the region outlined on D showing both "unidentified cells 1"(dashed circles), which are being marked (Ins. 2), and "unidentified cells 2" (arrowheads), "unidentified cells 1" are at this stage placed in the end of the hindgut and seemingly within its walls; **E**-**G** – longitudinal sections through the embryo on D, MIP(max) mode, **E** – section through the labrum, the labral and oesophageal musculature is marked; **F** – section at the level of the ventral endoskeleton, some ventral limb muscles (arrowheads) and also endoskeletal musculature (double arrowheads) are labelled; **G** – section through the developing midgut, apart from some limb muscled, the entire groups of yolk cells is labelled. Scalebar 20 µm.

3.4.3. Variability of the clones

A closer look reveals that there is a certain variability to the generalized patterns presented above. This variability is mostly related to the location, size, and shape of the clonal area. It is best visible on the example of ectodermal descendants (in Fig. 3.4.10. there is a map of quadrant fates with variable epidermal parts of the clones), although the position of the mesodermal ones can differ sometimes[♣] as well. In the following subchapters there is a description of the "most demonstrative" examples of the variability observed in different structures. To manifest an existing variability marginal cases of the entire spectrum of possible developmental patterns were mostly choosen.

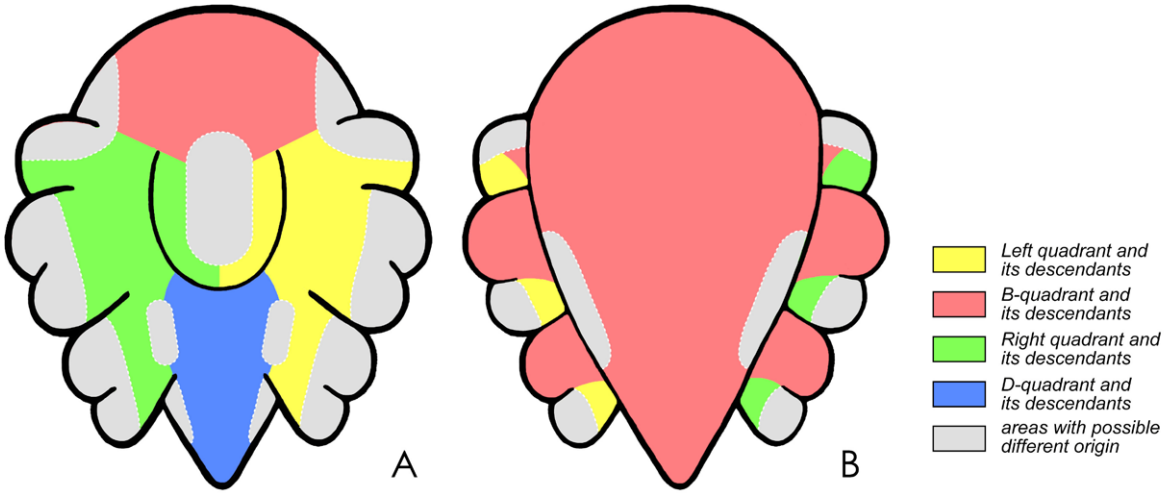

Fig. 3.4.10. Fate map of the four quadrants with variation zones.

A – ventral view; **B** – dorsal view.

3.4.3.1. Labrum

The labral epidermis is formed by descendants of three blastomeres on 8-cell stage: 1a, 1c, and 1b, derived from three quadrants. Although their clones, roughly speaking, occupy left, right, and anterior parts of the labrum, each of these cells contribute differently in every specimen.

The labelled epidermal patch on the anterior part of the labrum originating from 1b can, for example, vary in size and position. In some samples it is a small and elongated patch, running from the anterior towards the middle of the labrum (Fig. 3.4.11.A), and looks like a little extension of the most anterior naupliar epidermis, which is also derived from 1b. In one sample (Fig. 3.4.11.B) the connection between the small group of epithelial labral cells and those on the anterior seems to be broken. This case, however, could be traced back to the state of the embryo on Fig. 3.4.11.C. In some other cases the group of marked cells is large and expands to cover most of the labral surface (Fig. 3.4.11.D).

[♣] The words "some" or "sometimes" are used since the statistics of the variable clones was not performed.

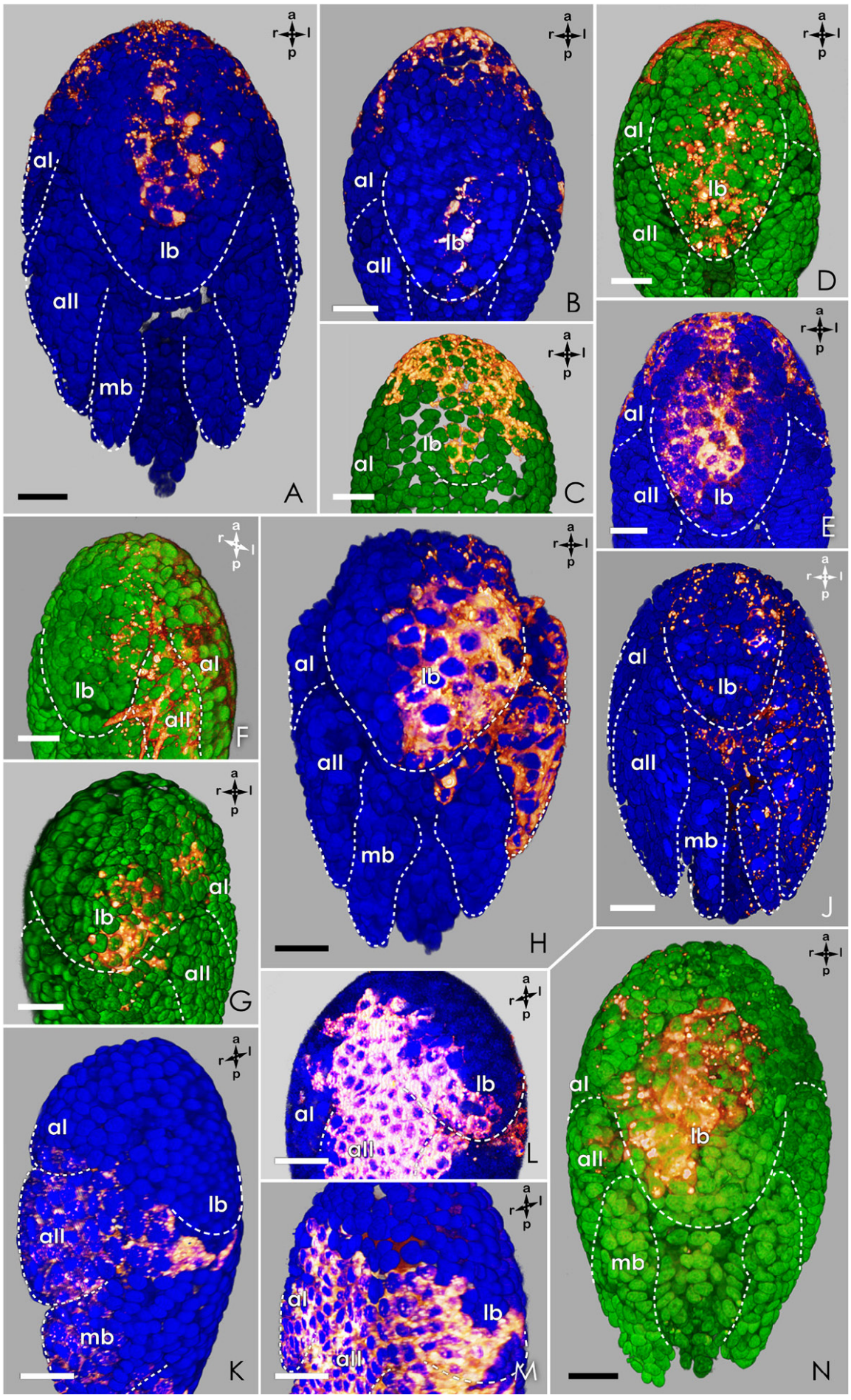
A
al
lb
all
mb
B
al
lb
all
C
al
lb
D
al
lb
all
E
al
all
lb
F
lb
al
all
G
al
lb
all
H
al
lb
all
mb
J
al
lb
all
mb
K
al
lb
all
mb
L
al
lb
all
M
al
lb
all
N
al
lb
all
mb

Differences in the position of the 1b clone is well observed in relation to the AP axis of the embryo. In general, 1b develops a bilaterally symmetrical clone, left and right parts of which come from the daughter cells $1b^l$ and $1b^r$, respectively. The clonal progeny, in this case the labral part of it, can be shifted either to the right of the embryo, like it is shown on Fig. 3.4.11.E, or to the left.

The left part of the labral epidermis can come from either 1a or 1c (here just 1l, see above). The size of the part varies from quite small, hardly taking 1/8 of the labrum surface (Fig. 3.4.11.F), to a large area covering the most of the labrum (Fig. 3.4.11.H). Its position varies as well. If it is of small or of medium size, it can be placed on the anterior-(or proximal-)left side of the labrum (Fig. 3.4.11.F), at the level of *aI-aII* or on the posterior (distal)-left side, at the level of *aII-mb*. In case of a big patch, there were two patterns observed: (1) it either extends from the anterior (proximal) to the posterior (distal) of the labrum leaving a symmetrical half on the right, which is unmarked (Fig. 3.4.11.H), or (2) it expands onto the right side covering most of the anterior (proximal) (Fig. 3.4.11.J) or posterior (distal) labral part.

The progeny of the right quadrant resembles in its distribution the mirror image of that of the left quadrant (compare Fig. 3.4.11.F and G with L and M, respectively). Among the marked specimens there were two with R quadrant labelling found, in which no cell of the labral epidermis was at all stained with DiI (Fig. 3.4.11.K; 3.4.13.F). In these embryos entire R clones had been shifted towards the dorsal side.

Fig. 3.4.11. Variability in clonal contributions in formation of the labral epidermis.

All the images are obtained in Imaris Surpass view, Blend mode of Volume Scene.

A-**E** – 1b marked, ventral view, **A** – Stage 8, marked cells occupy prominent anterior-central part of the labrum; **B** – Stage 8, marked cells occupy small central part, the cellular patch is widely separated from the rest of the clone; **C** – Stage 6, marked cells cover left-anterior part of the labrum; **D** – Stage 8, marked cells cover most of the distal part of the labrum, this part of the clone is separated from the rest; **E** – Stage 7, marked cells occupy anterior-central and right part of the labrum; **F**-**J** – L quadrant daughter cells marked, **F** – 1l marked, Stage 9, left-lateral ventral view, marked cells are few and seen only on the left side of the labrum; **G** – $1l^p$ marked, Stage 8, ventral view, marked cells are placed on the left distal half of the labrum; **H** – 1l marked, Stage 8, ventral view, marked cells occupy half of the labrum; **J** – L quadrant marked, Stage 9, ventral view, marked cells are placed on the left side, anteriorly, an additional patch of marked cells is placed on the right side of the labrum, also anteriorly; **K**-**N** – R quadrant and its daughter cells marked, **K** – R quadrant marked, Stage 5, right-lateral view, labral epidermis does not contain any marked cells, **L** – R quadrant marked, Stage 6, marked cells are placed along the right side of the labrum; **M** - R quadrant marked, Stage 5, right-lateral ventral view, marked cells occupy right distal half of the labrum; **N** – $1r^p$ marked, late Stage 8, marked cells cover central and right part of the labrum. Scalebar 20 µm.

3.4.3.2. Limbs

Here the data on the variety in the clonal composition of the *aI* and *mb* epidermis will be provided.

The epidermis of each *aI* is built by the clones of two blastomeres: $1r^a$ and $1b^r$ on the right and $1l^a$ and $1b^l$ on the left body side. The blastomeres $1b^r$ and $1b^l$ are responsible for the dorsal and distal parts of the antennular epidermis. $1r^a$ and $1l^a$ for the ventral and proximal parts on the right and left side, respectively. The main difference between the samples comes from the number of cells of each clone participating in the epidermis formation. To show possible clone appearances the earlier embryonic stages were used (stages 5-7).

The blastomeres $1b^r$ and $1b^l$ in most of the cases give symmetrical clones and form mirror structures on both sides of the embryo. Here only the left side is presented. One can see that the B clone contribution varies from a narrow cell patch extending along the dorsal side of *aI* towards its tip (Fig. 3.4.12.A) to a broad cell cluster covering almost the entire antennular anlage except for a small ventral patch (marked field on the Fig. 3.4.12.B).

Variable samples of $1l^a$ markings did not show a broad spectrum of possible clones. The smallest cell patch of the *aI* epidermis contributed by this blastomere, which was found, is presented on the Fig. 3.4.12.C and the biggest in Fig. 3.4.12.D. Although in one case it is around 1/3 of the ventral surface of the limb bud and in the other case it is more than a half of it, which is stained, on the pictures it is hard to see.

The clonal contribution of $1r^a$ into the antennular epidermis on the right side was more variable than that on the left side. The smallest patch of the clone was found in the embryo of Stage 5 (Fig. 3.4.12.F). It is located in the ventral posterior region of the developing limb bud. The opposite case is presented in Fig. 3.4.12.E. There 1 r^a gives rise to most of the ventral epidermis of *aI* leaving a small dorsal area free of mark (not shown).

The most complicated case of clonal composition can be observed in the mandibular epidermis. This is the area, where the offspring of the three quadrants come in contact. The epidermis of the right mandible originates from quadrants R (blastomere 2R), B (blastomere 2B), and D (blastomere $1d^r$). That of the left mandible comes from the quadrants L (blastomere 2L), B (blastomere 2B), and D (blastomere $1d^l$). The generalized case of the epidermal origin of a mandible would be the following: the ventral part of the developing limb bud (in the nauplius it develops into the ventral and proximal part of the protopodite) formed by the descendants of 1d; the lateral part (becomes the distal portion of the protopodite and the proximal parts of the exo- and endopodites) comes from 2L (on the left) and 2R (on the right); the dorsal part (develops into the distal parts of the exo- and endopodites) originates from 2B. This pattern is, however, variable. The

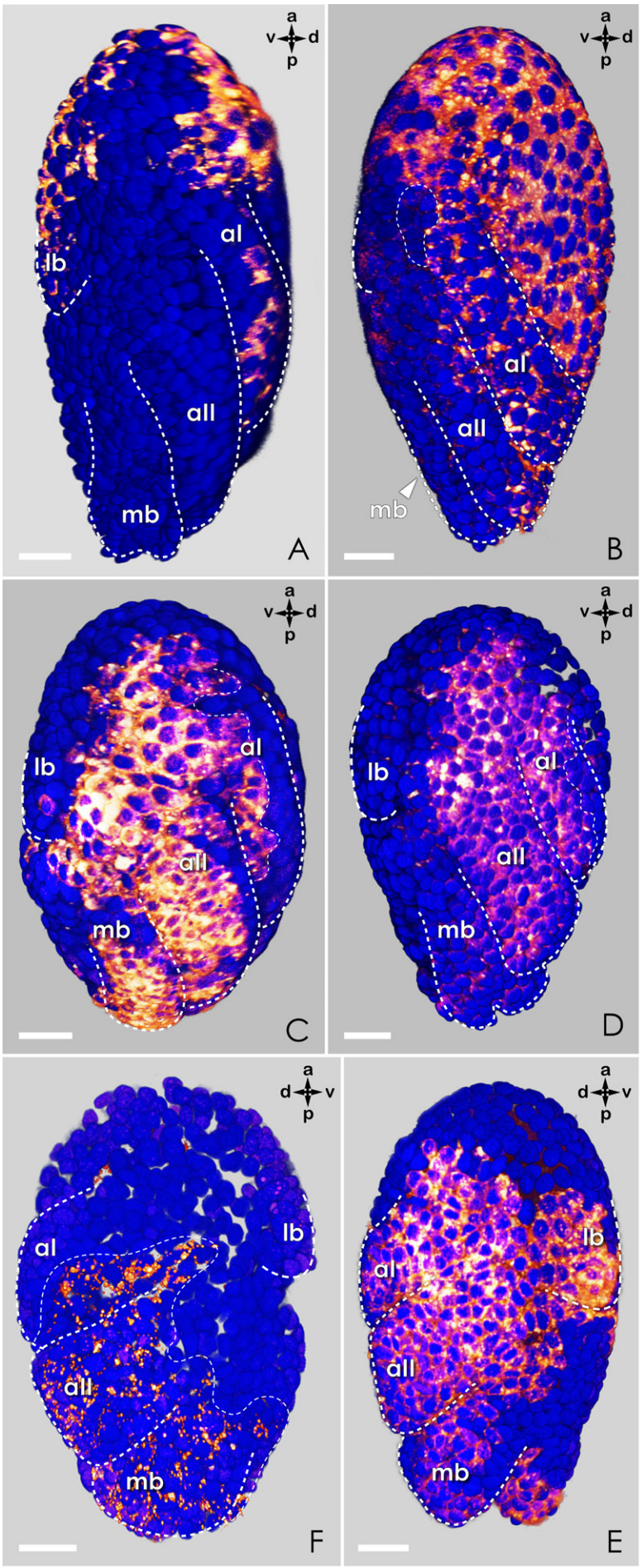

Fig. 3.4.12. Variability in clonal contributions in formation of the *al* epidermis.

All the images are obtained in Imaris Surpass view, Blend mode of Volume Scene.

A – 1b marked, Stage 7, left-lateral view, only some cells on the distal part of *al* are labelled; **B** – B quadrant marked, Stage 7, left-lateral view, nearly entire epidermis of *al* is part of the marked clone save for the outlined proximal patch; **C** – L quadrant marked, Stage 6, left-lateral view, the clone contribute to a third of the ventral epidermis of *al* (outlined), it is placed ventro-proximally; **D** – $1l^{a}$ marked, Stage 6, left-lateral view, ventral half of the *al* epidermis is labelled; **F**-**E** – R quadrant marked, Stage 5, right-lateral view, **F** - small patch of the *al* epidermis positioned posterior-ventrally is stained (outlined); **E** –entire ventral epidermis of *al* is labelled. Scalebar 20 µm.

measure of the contribution of each quadrant varies from a few cells of the mandibular epithelium (see Fig. 3.4.13.B,F,H – left mandibular anlage) to a large patch of epithelial cells covering a considerable part of the mandible (see Fig. 3.4.13.A,C,D,G,I').

In the case of the embryos shown in Fig. 3.4.13.G,H,I generally symmetrical clones appear to be assymmetrical. For example, the offspring of 1d (Fig. 3.4.13.G), while covering the right mandible excessively, is totally absent on the left mandible. In the embryo

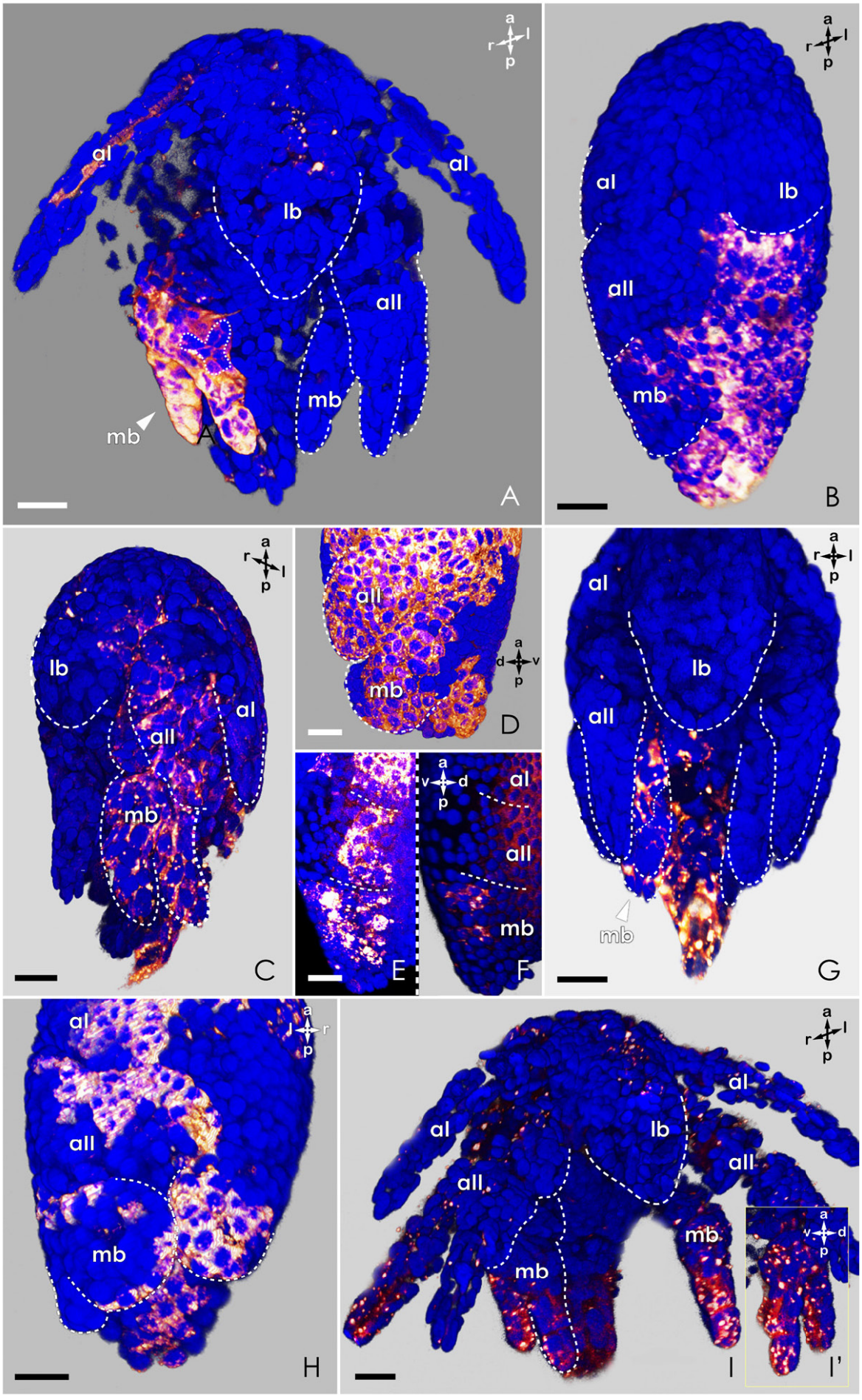
al
lb
all
mb
A
B
C
D
E
F
G
H
I
I'
a
r
l
p
d
v

shown on H the descendants of 2B cover entirely the distal part of the developing exopodite of the right mandible, whereas that of the left mandible is formed by the cells of different origin. The asymmetry of the embryo on Fig. 3.4.13.I relates to the epidermis of the mandibular endopodite. On the left side it is mostly derived from 2B (Fig. 3.4.13.I), and on the right side it is almost free of external 2B descendants (yet intrinsic muscle fibers of both endo and exopodites are labeled).

Despite of the large amount of possible clonal compositions of the mandibular epithelium due to the variability, we were able to find some probably complementary clones (try to puzzle together: Fig. 3.4.13. D,B, and H(right *mb*) or I(right *mb*); G and F or H(left *mb*)).

3.4.3.3. Nervous system

The nauplius nervous system is formed by the offspring of the three quadrants (A, B, and C), which are presented by four cells on the 16-cell stage: $1r^a$, $1l^a$, $1b^r$, and $1b^l$. In most of the observed embryos, in the case of $1r^a$ and $1l^a$ labelling, the marked progeny ends up in the deuto-, tritocerebral and mandibular ganglia and, additionally, in the innervations running from these portions of the brain♣. $1b^r$ and $1b^l$ form the complete protocerebral region (including the frontal filament complex and nauplius eye) giving contribution to its right and left sides, correspondingly. There were several samples showing different patterns though.

The two samples of the $1l^a$ clone and one of the $1r^a$ clone were found to be expanded in anterior direction (Fig. 3.4.14.A-C). Thus, the entire half of the nerve ring was stained by DiI, including

Fig. 3.4.13. Variability in clonal contributions in formation of the *mb* epidermis.

All the images are obtained in Imaris Surpass view, Blend mode of Volume Scene, except for E (MIP(max) mode).

A – 2R marked, Stage 9, ventral view, right *aII* is cut out, almost entire epidermis of right *mb* is marked, small ventral group of cells (outlined) on the mandibular endopodite is free of injected dye; **B** – 1d labelled, Stage 5, latero-ventral view, the clone includes a small group of cells placed ventro-proximally on the mandible; **C** – L quadrant marked, Stage 9, left-lateral view, *aII* exopodite is cut out, despite of the poor signal one can see that the epidermis of *mb* is almost totally marked; **D** – R quadrant marked, lower part of the embryo of Stage 6, right-lateral view, the epidermis of the developing *mb* is intensively marked by DiI leaving tips of the exopodite and endopodite and ventro-proximal part of the limb unstained; **E-F** – 2L marked, early Stage 5, left-lateral view, despite of the big internal part of the clone (**E**), externally only a small group of cells is marked (**F**), it is placed at the ventral base of the developing *mb*; **G** – 1d marked, Stage 8, ventral view, epidermis of the right mandible is marked, marked cells cover the ventro-proximal part of the exopodite and the tip of the endopodite; **H** – B quadrant marked, Stage 6, dorso-posterior view (the specimen is slightly turned by the posterior), epidermis of the developing mandibles is asymmetrically marked, the right *mb* has an intensively marked tip, while only some cells of the left one contain injected dye; **I** – 2B marked, Nauplius I, latero-ventral view, epidermis of the mandibles is asymmetrically labelled, the right mandible has only a stained endopodite and dorsal tip of the exopodite; **Insertion**: left mandible of the nauplius on I, left-lateral view, almost the entire epidermis of this mandible is marked. Scalebar 20 μm.

♣In those cases there were also some somata of the protocerebral ganglia randomly stained, but they were few in number.

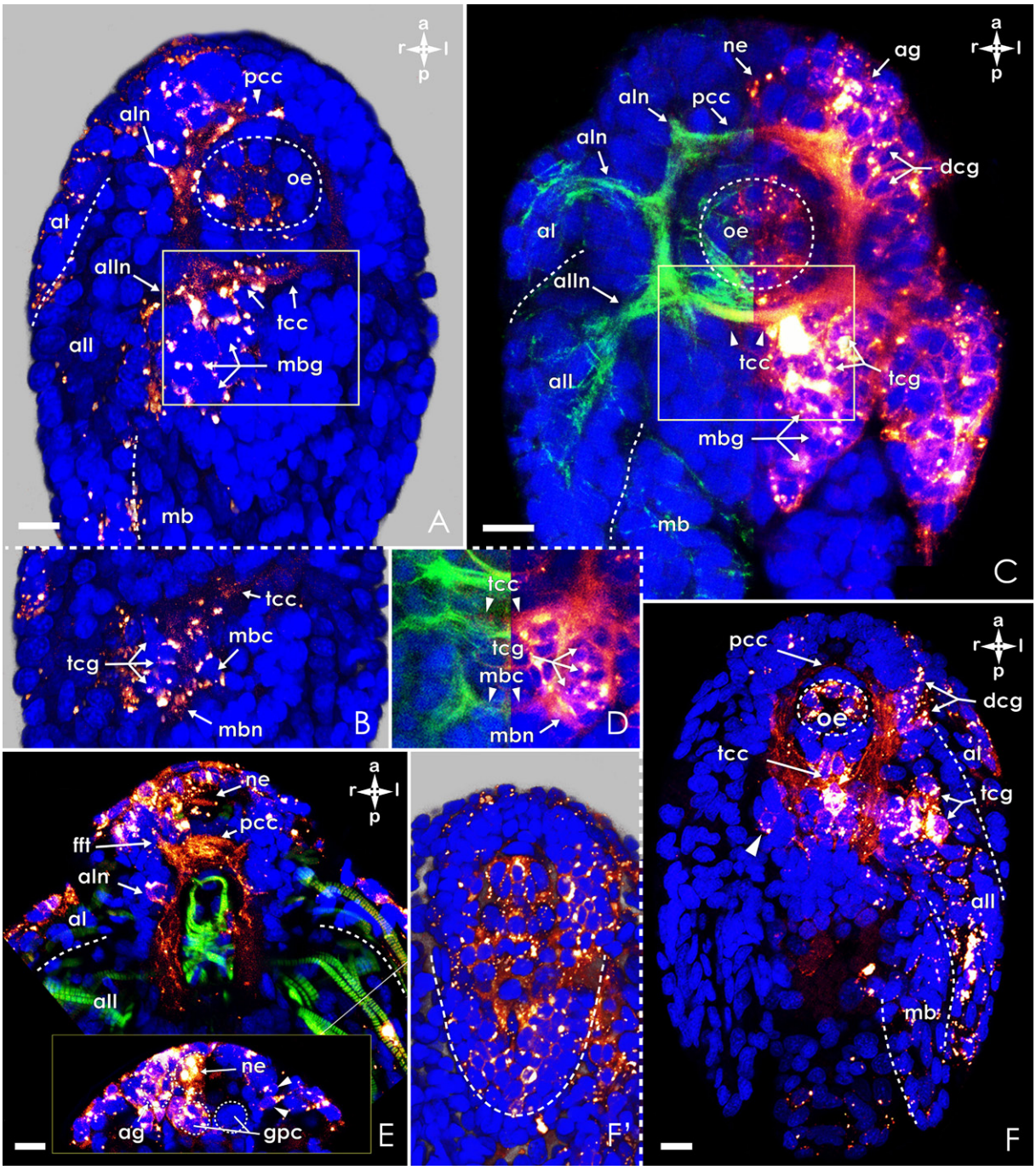

Fig. 3.4.14. Variability in clonal contributions in formation of nervous system.

All the images in ventral view, images on A, B, and F' are obtained in Imaris Surpass view, Blend mode of Volume Scene; images on C-E, F are obtain in Imaris Section view, MIP(max) mode.

A – 1r marked, Stage 8, labelling is seen in the right half of the circumoesophageal ring, including somata of proto- and deutocerebrum, mandibular ganglion, corresponding neuropiles, and innervations leading to the frontal filaments and *al* and *all*; **B** – deeper cut through the outlined area of the embryo on A, labelling is seen in the somata of the tritocerebrum, the signal in the mandibular commissure and mandibular nerve is weak but visible; **C** – 1l marked, early Stage 8, left side of the nauplius nervous ring is labelled including all the somata and innervations running from them, the right side of the embryo is stained by phallocidin to demonstrate the structure of the nervous system at this stage; **D** – deeper cut through the outlined area of the embryo on C; **E** – 1b marked, Nauplius I, the anterior part of the nauplius nervous ring is stained, the marking is asymmetrical, on the right side the nerve of the frontal filament, the lateral cup of the nauplius eye, and the nerve of *al* are labelled, while the same structures on

all the major ganglia and their innervations. In the right clone the nauplius eye was the only structure to remain not dyed (Fig. 3.4.14.A), unlike in the left clone, which appears to give rise to the entire left-ventral part of the nervous system of the first naupliar segments (Fig. 3.4.14.C,D).
Surprisingly, no anterior clone (coming from the B quadrant) had been found with unlabelled protocerebral region hence representing a complementary pattern to the two described ones. One sample presented on Fig. 3.4.14.E, nevertheless, could be interpreted as a probable match. This embryo was labelled on 8-cell-stage. The anterior epidermis is rather symmetrically stained,covering the central labral part and the anterior-dorsal side of both antennulae. The nervous system, however, appeared to be asymmetrically labelled. The protocerebral and partly the deutocerebral ganglia on the right side together with the innervations leading to the right *aI* and the frontal filament complex are intensively stained. The mirror structures on the left have, in contrast, only singular cells marked by DiI (Fig. 3.4.14.E, insertion: arrowheads). The left-lateral cup of the nauplius eye seemed to be also unmarked.
Another deviation[♣♣] from the general pattern had been found in one of the samples of $1l^a$ labelling. The clone was expanded in lateral direction to the right side of the embryo covering most of the labrum (Fig. 3.4.14.F'). Additionally to the cerebral ganglia of the left domain of the nervous system, it included some cells of those on the right side (Fig. 3.4.14.F, arrowhead).
In general, the labelled regions of nervous structures more or less correlate with the labelled epidermis covering it. This appears to be highly logical as neuroectoderm and epidermal precursors belong to the same ectodermal patch in early development.

3.4.3.4. Fore- and hindgut

The ectodermal parts of the digestive tract originate from two quadrants: L and R, and from two cells in the 16-cell stage: $1r^p$ and $1l^p$. In the general case the contribution is bilaterally symmetrical, with each cell forming either the right or left side of both foregut and hindgut. Variability of the marked group of cells was related mostly to its size and to asymmetry in its position. For example, the Fig. 3.4.15.A represents the partially stained epidermis of the developing digestive

the left side seem to be free of dye, except for a slight signal in the left frontal filament, in green colour one can see muscles stained by phallocidin; **Insertion**: deeper section through the protocerebral region of the same embryo as on E, some other protocerebral structures like the anterior ganglion of the frontal filament complex, and the globular protocerebral department are marked only on the right side of the nauplius, arrowheads show the singular labeled cells on the left; **F** – 1l marked, Stage 9, deuto- and tritocerebral regions on the left side are intensively stained, some somata (arrowhead) of the tritocerebral ganglion on the right side is marked as well as in the deuto- and tritocerebral neuropil, additionally some strands of the protocerebral commissure carry the mark, however none of the protocerebral somata appear to be labelled; **F'** – view of the labrum of the embryo on F, most of the labral epidermis is marked, leaving only some cells on the right side free of dye. Scalebar 20 µm.

[♣♣] In this case the term does not necessarily imply a misdevelopment, but just a unique appearance of the clone.

tract from an embryo with 1L labelled. There are just few cells of the future proctodaeum (arrowhead) stained and the majority of labelled cells are seen in the oesophagus. The clone shown in Fig. 3.4.15.C might be a complementary to Fig. 3.4.15.A from the right side, with most of the cells in the proctodaeal epidermis carrying the dye and only few of such in the oesophageal part

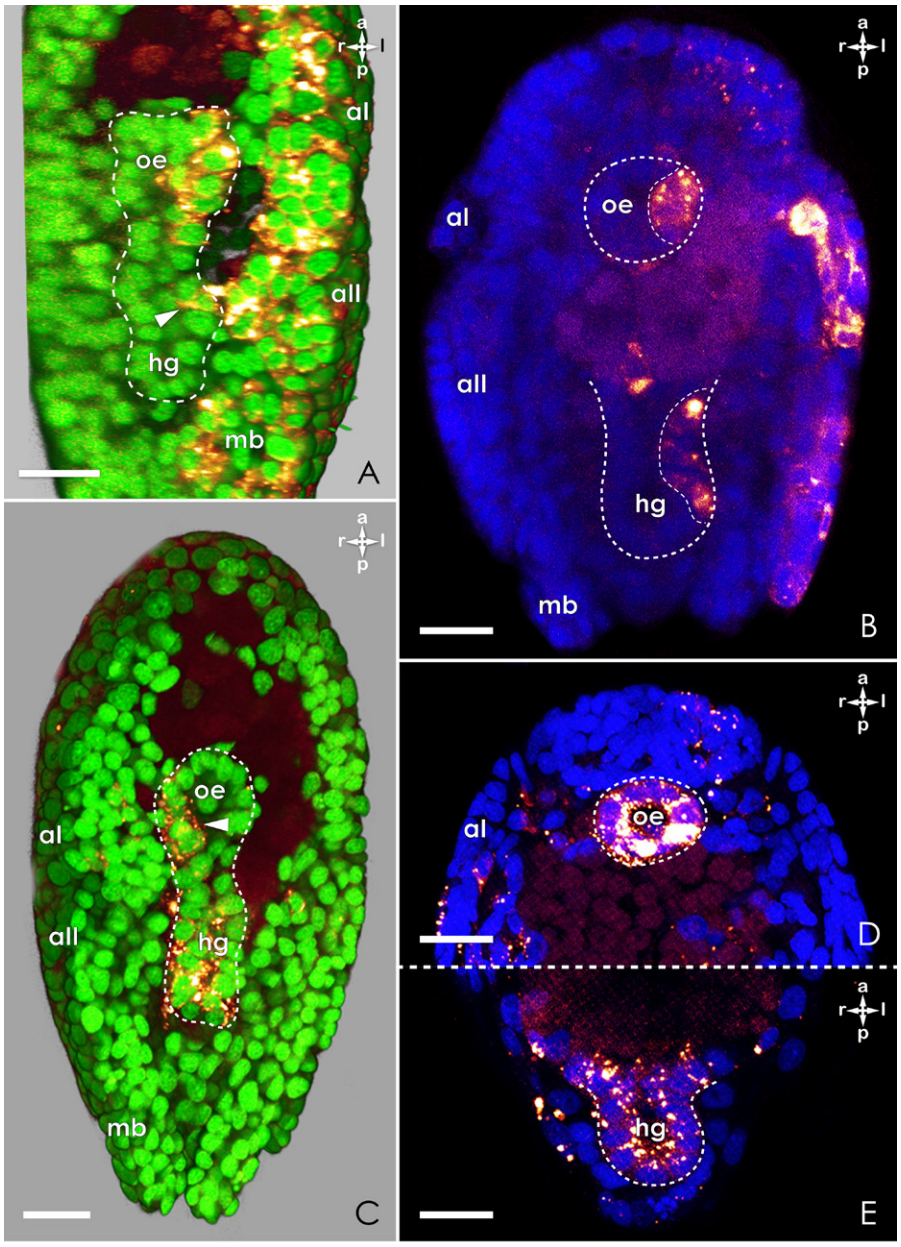

Fig. 3.4.15. Variability in clonal contributions in gut formation.

Images on A-C are obtained in Imaris Surpass view, Volume Scene, with help of Clipping Plane scene; images on D and E are obtained in Imaris Section view, MIP(max) mode.

A – R quadrant marked, late Stage 6, ventral view, Blend mode, the left epidermal part of the developing oesophagus is labeled, but only a small patch of cells in the left epidermis of the forming hindgut is marked (arrowhead); **B** – 1l marked, early Stage 8, ventral view, MIP(max) mode, only small patches of epidermal cells on the left side of the oesophagus and proctodaeum are labelled; **C** – $1r^{p}$ marked, Stage 7, ventral view, Blend mode, half of all those cells participating in fore- and hindgut formation is labelled, among them a small part is seen on the right side of the future oesophagus (arrowhead) and the majority cover the future proctodaeum; **D** -**E** – R quadrant marked, Stage 8, ventral view, MIP(max) mode, two longitudinal sections through the region of the oesophagus (**D**) and proctodaeum (**E**), the epithelium of both is entirely marked. Scalebar 20 µm.

(arrowhead). While these two pictures show rather equal input of both blastomeres into the structure, even though an asymmetrical one, the other two demonstrate a difference in the total amount of cells contributing to the ectodermal gut parts by the blastomeres. It can vary from very few and equally distributed cells between foregut and hindgut (Fig. 3.4.15.B, outlined zones) to a

large number of cells including the nearly complete (or complete – it is hard in these cases to tell for sure) epidermis of those parts of the gut (Fig. 3.4.15.D,E).

3.4.3.5. Mesodermal elements

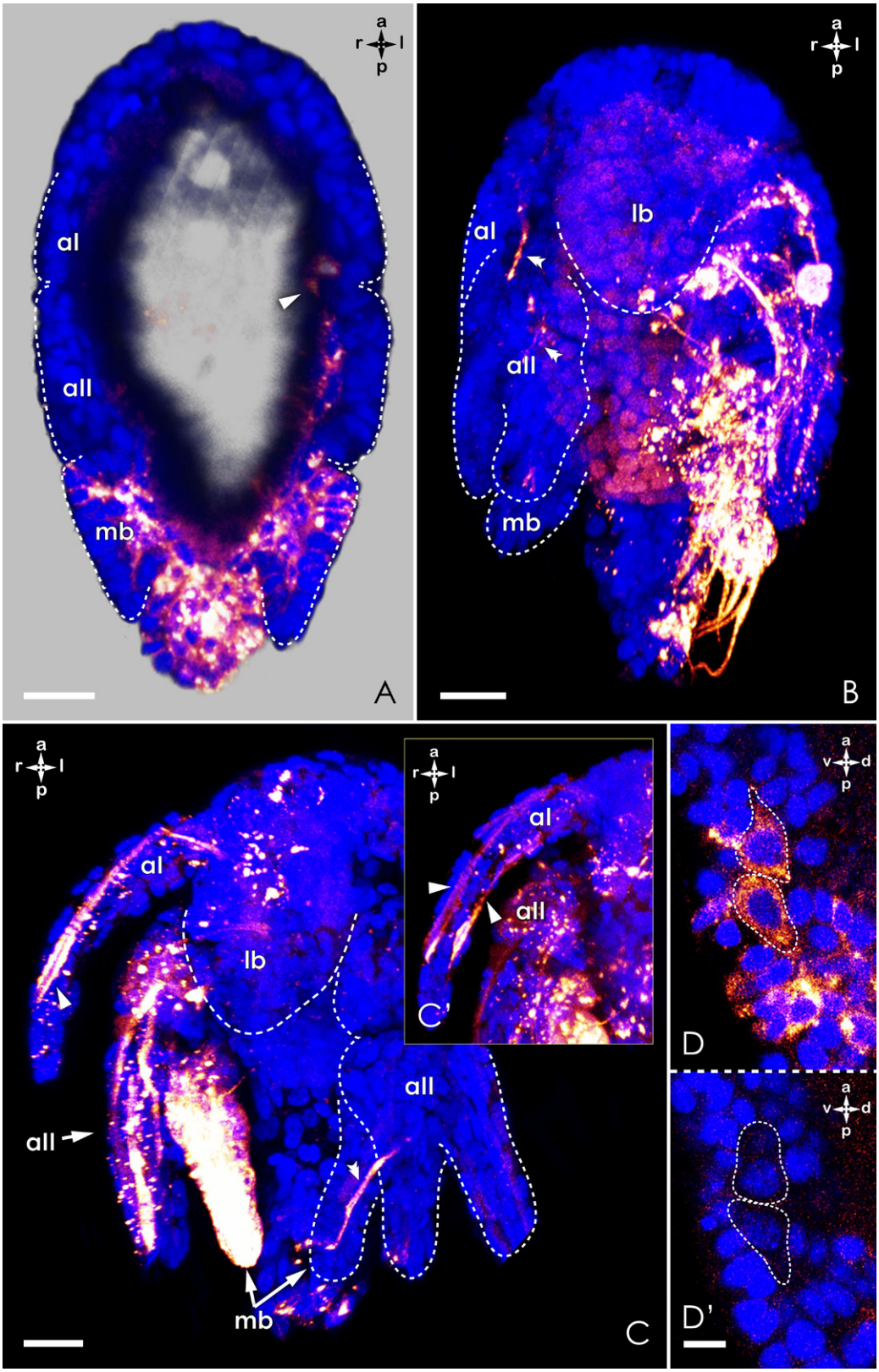

Fig. 3.4.16. Variability in clonal contributions in mesoderm.

All the images are obtained in Imaris Surpass view; apart from D and D', Volume Scene.

Variation in the clonal contribution to mesodermal structures was observed for different quadrants.

In the early development variability was found in the distribution of mesodermal cells of the clone coming from 1d. The generally bilaterally symmetrical clone in this case had symmetry only in its epidermal part (Fig. 3.4.16.A). In contrast, the mesodermal cells were unequally distributed between the right and left sides of the embryo. The limb buds of *aI*, *aII*, and *mb* on the left got input in mesoderm from the labeled 1d, whereas only the mandibular limb bud of the right side had the cluster of the 1d offspring.

In the generalized pattern left and right quadrants in contribute to the limb musculature of the corresponding side. In some samples single marked cells were found on the opposite side from the majority of labeled cells. These singular cells form limb muscle fibers (Fig. 3.4.16.B,C, double arrowheads).

Fig. 3.4.16.C and C' demonstrate also another type of variability in the clonal outcome. One can see in both examples of these R quadrant markings the intrinsic muscles of *aI* labeled. The muscle, which are marked, are, however, different in the two cases.

Apart from the described variation in the nauplius mesoderm, some differences in the origin could be also found in the cells, which are suspected to be the precursors for postnaupliar mesoderm. The cells (uc2, for details see chapter 3.5.3.) are found to originate from different quadrants. In most of the studied specimens the uc2 were the offspring of 1d (Fig. 3.4.8.E'). In the Fig. 3.4.16.D there is an example showing one pair of the cells originating from the L quadrant, while the origin of the other pair remains unknown (Fig. 3.4.16.D').

A – 1d marked, Stage 6, ventral view, Blend mode, Clipping Plane scene, mesodermal descendants of the blastomere are asymmetrically distributed between right and left sides, on the right the marking is seen only in the mandible, on the left mesoderm of all three limb buds is marked, arrowhead shows the mesodermal cluster in *aI*-segment; **B** – 2L marked, Stage 8, ventral view, MIP(max) mode, apart from the limb musculature of the left side also singular muscles on the right are labelled (arrowheads); **C** – 2R marked, Stage 9, ventral view, apart from the muscles on the right side, a singular intrinsic muscle in the left mandible (double arrowhead) is labelled; **C'** – Nauplius, ventral view of the right anterior region, the same blastomere marked as on C, but another specimen, two muscles of *aI* are labelled (compare with C, where specimen has only one labelled muscle) (arrowheads); **D**-**D'** – 2L marked, Stage 7, sagittal sections through the same embryo on different levels, Imaris Section view, MIP(max) mode, "unidentified cells 2" on the left side are labeled (**D**) and "unidentified cells 2" on the right side are not labeled (**D'**). Scalebar 20 µm, except for D-D': 5 µm .

3.5. Notes on organogenesis

While performing *in vivo* labelling, the results of which were described in the previous chapter, it was possible to additionally collect some data on the development of different organ systems and structures of the nauplius larva.

3.5.1. Muscle system

3.5.1.1. Origin

The mesoderm of the nauplius larva originates from six blastomeres (at the 16-cell stage): five mesectoblasts, 2A, 2B, 2C, $1d^{l}$, and $1d^{r}$, and one endomesoblast, 2d. Mesectoblasts are the mother cells giving rise to the blastomeres directly forming blastopore, which are 3A, 3B, 3C, $1d^{lp}$, and $1d^{rp}$. An analysis of the blastopore region in Sytox-stained samples and in 4D recordings lets suggest, that exactly these cells are responsible for the formation of ectomesoderm. However, since we could not manage to perform a successful *in-vivo* labelling on the 32-cell stage or later, it is impossible to claim that with certainty. In the Table 3.5.1. there is a summary on the origin of mesoderm in the nauplius.

Table 3.5.1. Origin of different muscle groups in the nauplius of *Elminius modestus.*

Group of muscles		Blastomere				
		2L♣	2B	2R♣	$1d^{r}$ and $1d^{l}$	2d
Limb muscles	Dorsal extrinsic	+	+	+		
	Ventral extrinsic				+♣♣	+
	Intrinsic	+	+	+		
Digestive tract muscles	Oesophagus and Labrum					+
	Midgut					?
	Hindgut				+	
Dorso-ventral muscles and muscles of endoskeleton			?			?
Postero-lateral muscles					?	

Fig. 3.5.1. Schematic view of main steps in mesodermal development.

A-**B**,**G** – migration, arrows show the direction, **A** – dorsal view; **B** – Ventral view; **G** – cross section through the middle of the embryo; **C**-**D**,**H** – clusterization, C – dorsal view, arrow show the direction of the descendants of the 2B; **D** – ventral view; **H** – cross section through the middle of the embryo, two substages of the clusterization of the mesodermal elements: according to the limb buds (upper scheme) and division into two groups within each limb anlage (lower scheme); **E** – simplified appearance of the mesodermal cells at the different stages of the myogenesis, **1** – migration, **2**-**3** – clusterization, **4** – final differentiation; **F**-**I** – final differentiation, **F** – right-lateral view; **I** – cross section through the middle of the embryo (ventral muscle elements are not shown).

♣ Progeny of 2L forms the muscles on the left side of the nauplius and that of 2R on the right side.
♣♣ They form only ventral muscles of *aII* and *mb*.

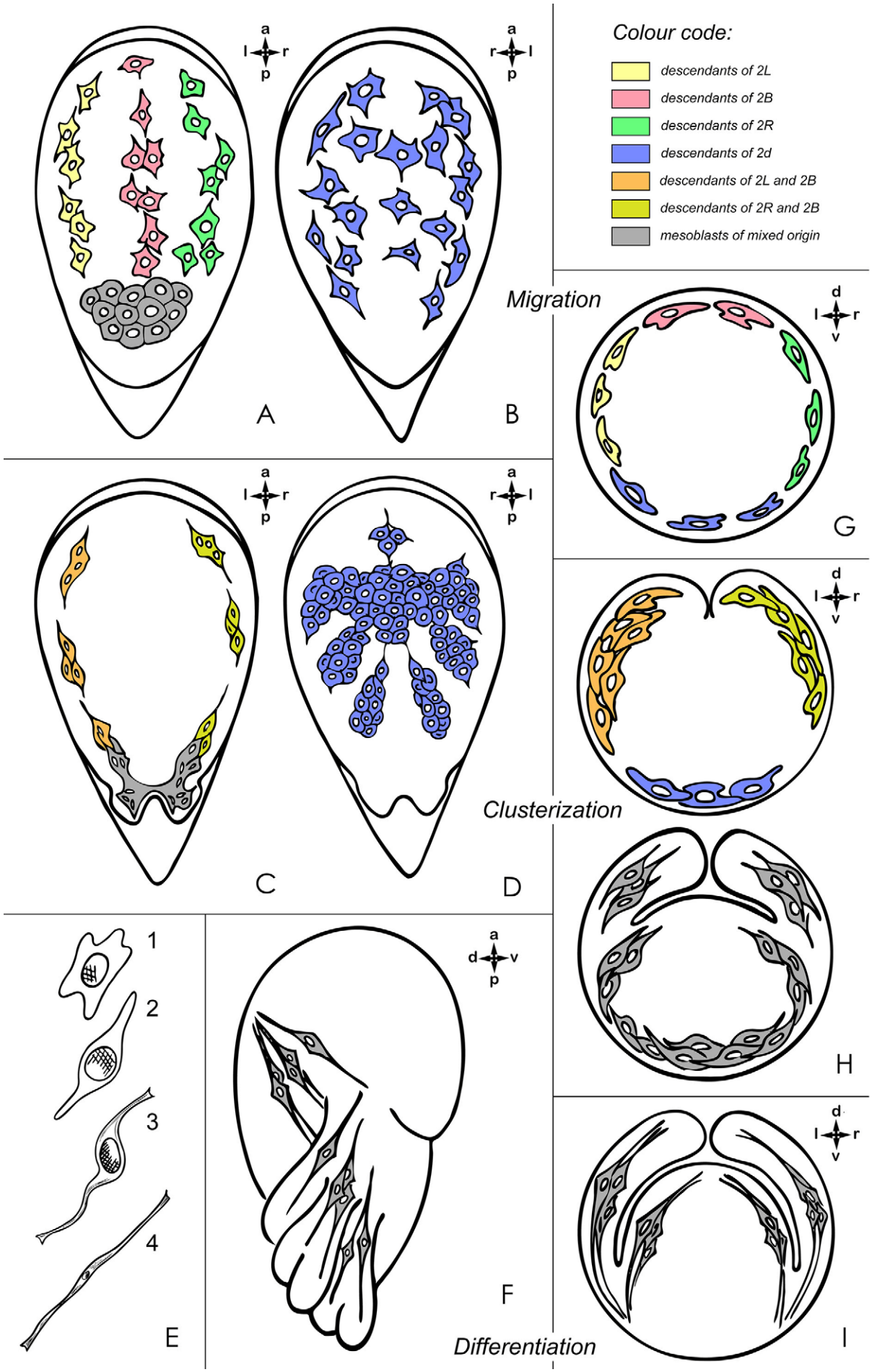
Colour code:
descendants of 2L
descendants of 2B
descendants of 2R
descendants of 2d
descendants of 2L and 2B
descendants of 2R and 2B
mesoblasts of mixed origin
Migration
Clusterization
Differentiation
A
B
C
D
E
F
G
H
I
1
2
3
4

The postnaupliar mesoderm possibly originates from the two pairs of big cells situated in the space behind the midgut and between the epidermis of the hindbody and hindgut. Several specimens we found having these cells marked by DiI. Most of them were samples of 1d (or its daughter cells) clones. However, there was also one sample with 2L labelled, which had a DiI signal in the right pair of the big cells (Fig. 3.4.15.D). Therefore, one could suggest that there is no strict blastomere lineage leading to these cells, although it seems constant that they originate from one of the mesectoblasts.

3.5.1.2. Development

We traced the development of the mesoderm through the stages of embryogenesis given in the Table 3.1.1. The whole process can be subdivided onto four main stages: division, migration, clusterization, and differentiation. The scheme of the development is given on Fig. 3.5.1.

Division

It corresponds to the embryonic stage 3. After the blastopore is closed, undifferentiated mesoblasts suffer a number of unoriented divisions (or at least it looks like this). During this phase all of them are placed in the posterior region of the embryo, behind the endoderm precursors (Fig. 3.5.2.). A more detailed location of the progeny of the certain blastomeres is hard to identify. The cells are of irregular shape at this stage. In size they are nearly equal to the blastoderm cells.

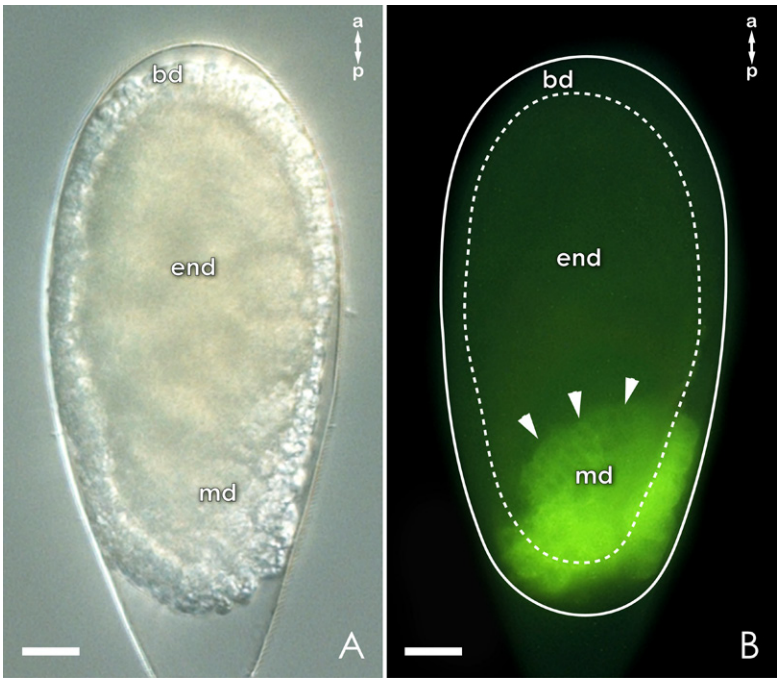

Fig. 3.5.2. Development of mesodermal germ layer. Division.
At this stage it is hard to distinguish the dorsal and ventral sides of the embryo.
A – alive embryo of Stage 3; **B** – the same embryo as on A viewed in epi-fluorescent miscroscope, 1d labelled, the mesodermal part of the clone is concentrated in the posterior part of the embryo. Scalebar 20 µm.

Migration

The migration of mesoblasts starts with the first signs of limb bud formation in the ectodermal layer. This process corresponds to the embryonic stage 4. The cells migrate between blastoderm and endoderm towards the anterior region of the embryo. In total one can distinguish four tracks of migration, and each of them is taken by the offsprings of one different blastomere (Fig. 3.5.1.A,B,G). The derivatives of 2L migrate on the

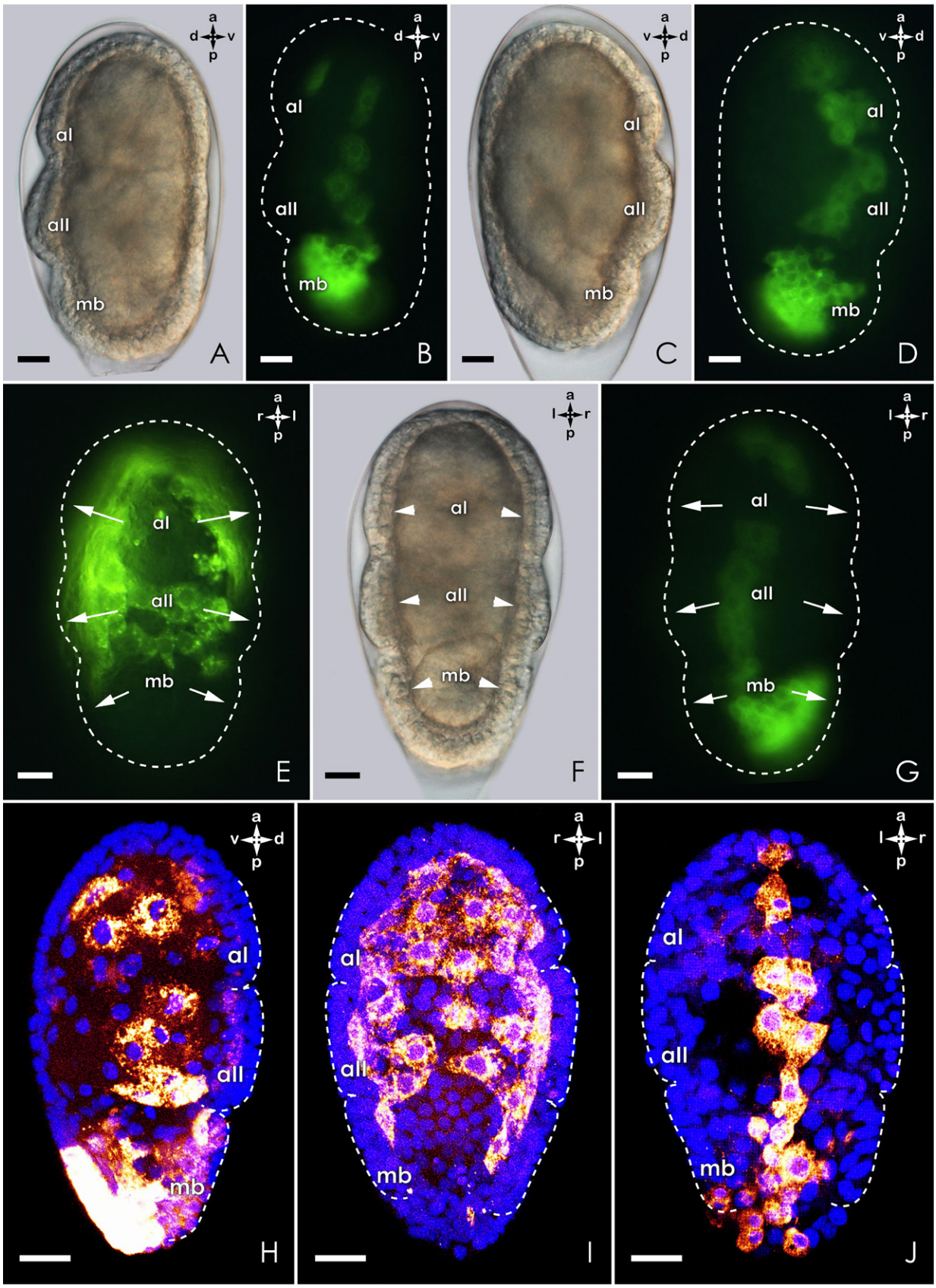

Fig. 3.5.3. Development of mesodermal germ layer. Migration.

A-**G** – alive specimen; **A**-**B** – 2R marked, right-lateral view of the embryo in DIC mode (**A**) and through fluorescent filter (**B**), a part of the marked cells start to migrate on the right side of the embryo, the track of migrating cells is still one-cell wide; **C** -**D** – 2L marked, left-lateral view of the embryo in DIC mo-

left side of the embryo (Fig. 3.5.3.D,H), 2R on the right side (Fig. 3.5.3.B), 2B dorsally (Fig. 3.5.3.G,J), 2d ventrally (Fig. 3.5.3.E,I), and those of 1d chose left and right sides according to left and right daughter cells of 1d (1d^{l} and 1dr).

The tracks of 2L and 2R are similar. In the beginning of migration they are one to two cells wide (Fig. 3.5.3.B) and reach the level of the antennular segments. In the late stage of migration they appear as relatively broad strands of scattered cells (Fig. 3.5.3.D,H). 2B descendants form a narrow (two-cell-wide) track, which extends till the very anterior of the embryo and remains narrow till the end of the migration stage (Fig. 3.5.3.G,J). On the contrary, 2d offsprings migrate from the very beginning along the whole ventral side and in the end of the stage they cover that side completely (Fig. 3.5.3.E,I). The left and right bands of the 1d derivatives are compatible in width to those of 2L and 2R, but they do not run further than the *aII* segment.

All the described mesodermal tracks, except that of 2d, lay under the ectodermal cells originating from the corresponding quadrant.

During migration the cells are quite flattened, their shape is irregular (Fig. 3.5.1.E:1). Some cells divide.

Clusterization

This stage can be subdivided on two sub-stages, which more or less correspond to the embryonic stages 5 and 6.

After the mesoblasts reach a certain point, their posterior-anterior movement stops and they form clusters. The lateral mesoblasts group in a way that the clusters match in position the ectodermal bulges of the forming limbs (Fig. 3.5.4.B,E). The dorsal mesoblasts from the B quadrant contribute to the lateral clusters. In order to do this they move from the dorsal side symmetrically to the left and right (Fig. 3.5.1.C; Fig. 3.5.4.F). The mesoderm on the ventral side demonstrates the most complicated pattern. One can discriminate three paired clusters (lateral clusters), which correspond to the forming limb buds, and one laying in the central region (central cluster) underneath the forming labrum and the invaginating ectodermal part of the digestive tract (Fig. 3.5.1.D; Fig. 3.5.4.I,I').

de (**C**) and through fluorescent filter (**D**), part of the marked cells migrate on the left side of the embryo, the track becomes broader; **E** – 2d marked, ventral view, fluorescent filter, all the marked cells migrate covering the ventral and ventro-lateral sides; **F**-**G** – 2B marked, dorsal view of the embryo in DIC mode (**F**) and through fluorescent filter (**G**), part of the marked cells migrate on the dorsal side, forming a narrow (still one-cell wide) track; **H**-**J** – fixed and counter-stained embryos; **H** – 2L marked, left-lateral view, migrating cells on the left side of the embryo, the track is broad and consist of scattered cells; **I** – 2d marked, ventral view, migrating cells are scattered across the ventral side of the embryo; **J** – 2B marked, dorsal view, narrow (now two-cell wide) track of migrating cells on the dorsal side of the embryo. Scale-bar 20 μm.

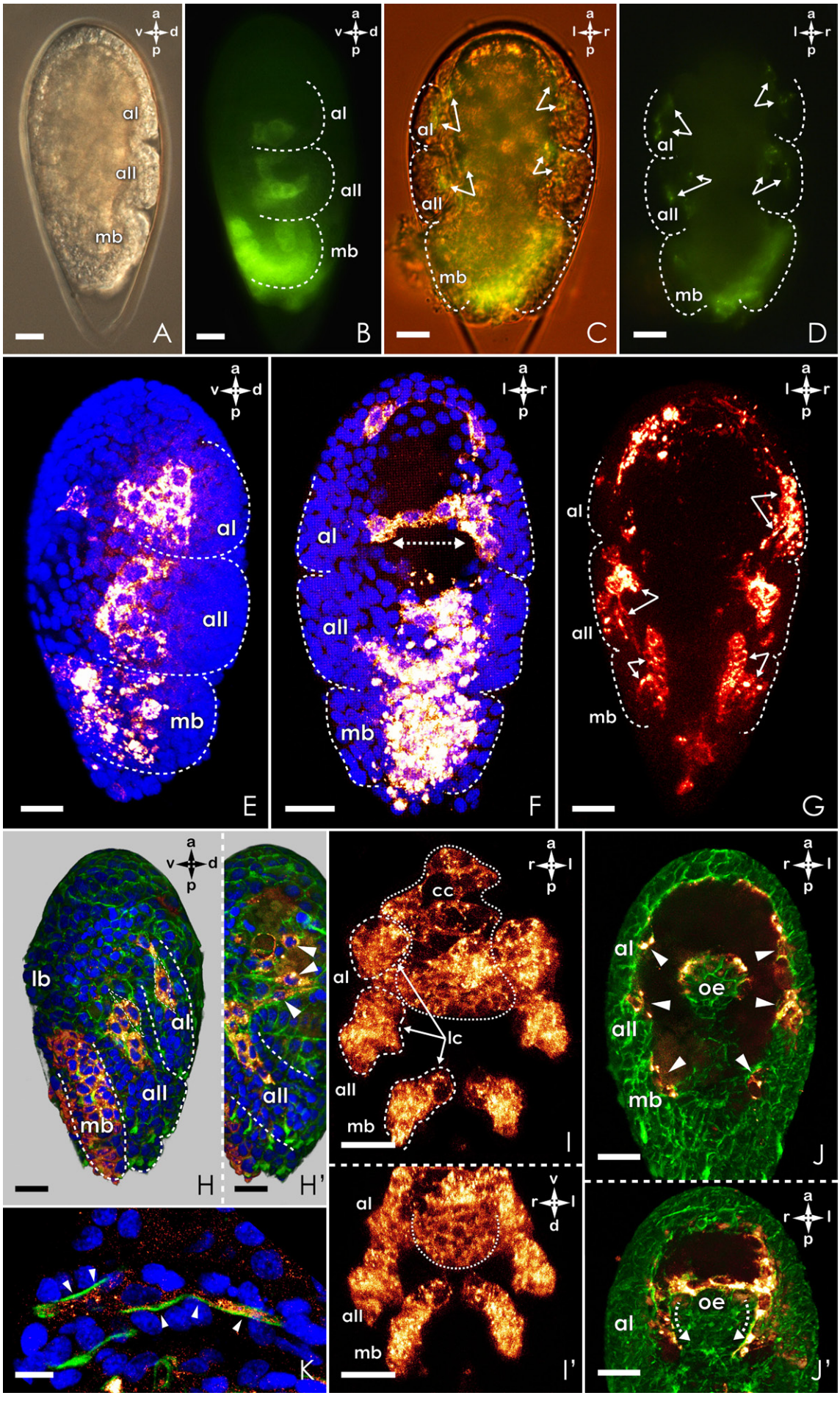
a
v
d
p
al
all
mb
A
B
C
D
E
F
G
lb
H
H'
cc
lc
I
J
oe
I'
J'
K
l
r

The mesodermal clusters of the limb buds are formed by descendants of 2L, 2B, and 2d on the left and 2R, 2B, and 2d on the right side. Additionally, derivatives of $1d^l$ and $1d^r$ contribute to the left and right anlagen of *aII* and *mb*, respectively. The central ventral cluster originates from 2d.

The next sub-stage of clusterization can be distinguished at the end of embryonic stage 5 (Fig. 3.5.4.C,D). When the ectodermal grooves outlining the limb buds sink deeper, they split mesodermal cell clusters to "external" (those which go to the limb anlagen and form the intrinsic muscles later) (Fig. 3.5.1.H; Fig. 3.5.4.D,H,G) and "internal" (those which stay within the body of the embryo and give rise to the extrinsic muscles) (Fig. 3.5.1.H; Fig. 3.5.4.D,H'G). The central ventral cluster extends around the invaginating stomodaeum (Fig. 3.5.4.J').

Thee cellular level of development was observed only in the limb clusters, and it was possible to see two sub-stages as well. During initial clusterization the myoblasts become elongated (Fig. 3.5.1.E:2). Later they take a spindle shape and start to synthesize fibrillar actin, which can be visualized by means of phallotoxin with fluorochrome (phallacidin in our case) (Fig. 3.5.1.E:3; Fig. 3.5.4.K, arrowheads). Now both tips of the cells stretch towards the attachment sites of the future muscle. At this moment some cells lay so close to each other that it looks like if they fuse. With 3D reconstructions, however, it is visible that they are still singular myoblasts, or so called mononucleate muscle precursor cells (for more detailed and complete nomenclature of the mesodermal cells see Kreissl et al., 2008).

Fig. 3.5.4. Development of mesodermal germ layer. Clusterization.

A-**D** – alive specimen; **A**-**B** – 1d marked, late Stage 4, left-lateral view of the embryo in DIC mode (**A**) and through fluorescent filter (**B**), the mesodermal descendants of the blastomere group according to the forming limb buds, in this case the mesodermal descendants of 1d reach the antennular segment (see chapter 3.4.3 for details); **C**-**F** – 2B marked, late Stage 5, dorsal view of the embryo in DIC mode (**C**) and through fluorescent filter (**D**), the group of marked cells within the limb buds are being split into internal and external groups; **E**-**J** – fixed and counter-stained embryos; **E** – 2L marked, late Stage 4, left-lateral view, the marked cells are arranged in groups according to the limb buds; **F** – 2B marked, Stage 5, dorsal view, the marked cells form groups on the dorsal side related to the bulging limb buds and start to migrate laterally (two-ended arrow); **G** – 2B marked, Stage 6, dorsal view, lateral groups of the mesodermal descendants of the blastomere, already split into internal and external parts; **H** – 2L marked, late Stage 6, left-lateral view, limb-related external groups of the marked cells, the cells are mostly elongated and of spindle-shape (outlining); **H'** – deeper cut through the embryo on H, marked cells from internal groups (arrowheads); **I** – 2d marked, Stage 5, ventral view, the marked cells are grouped forming one central cluster and three pairs of clusters related to the limb buds; **I'** – the same embryo as on I turned by the posterior, posterior-ventral view, the central cluster of marked cells invaginates according the invaginating epidermal cells of the digestive tract; **J** – 2d marked, Stage 6, ventral view, marked cells grouped according to developing limb buds (arrowheads); **J'** – another section (more ventral) of the same embryo as on J, the central complex of the marked cells embrace (the direction is shown by dashed arrows) the invaginating cells of the digestive tract; **K** – longitudinal section through a labelled muscle precursor, the cell starts to synthesize fibrillar actin placed in the peripheral cytoplasm and stained by phallacidin (here marked in green, arrowheads). Scalebar 20 µm, escept for K: 5 µm.

Final differentiation

This stage corresponds to the embryonic stages 7 – 9 and covers late myogenesis, which includes the attachment of the muscle precursors, the appearance of striation in the muscle fibers, and the formation of muscle bundles. Unfortunately, the DiI signal at this point of time becomes quite weak (Fig. 3.5.5.C,E,F). Therefore, on this stage additional data were collected on the base of embryos stained with actin-specific phallacidin.

At the stage 7 each limb muscle precursor elongates significantly and has now the shape of a straw, two ends of which are attached (Fig. 3.5.1.E:4; Fig. 3.5.5.F, insertion). The attachment sites are different for the muscles originating from "internal" and "external" cell clusters. The former ones attach with one end either dorsally or ventrally inside the nauplius body and extend the other end towards the proximal part of the limbs (Fig. 3.5.1.F,I; Fig. 3.5.5.G:1,2). The latter ones are have both ends attached within the limbs (Fig. 3.5.5.F,G2,3). For more detailed information about attachment sites see Chapter 3.2.3. At this stage one can still see nuclei within the forming muscle fibres (Fig. 3.5.5.D, arrowheads, F, arrowhead).

Soon after being attached, at the early stage 8, each limb muscle becomes a bit thicker and starts to organize cytoskeletal elements in sarcomeric pattern. This leads to the appearance of striation. At first, striation is observed in intrinsic muscles (Fig. 3.5.5.G) and a bit later during the stage 8 it develops in extrinsic ones as well (Fig. 3.5.5.H). At the embryonic stage 9 all the limb muscles are striated and appear to be able to function. At this stage some of the muscles are also united in bundles.

Fig. 3.5.5. Development of mesodermal germ layer. Final differentiation.

A-**B** – 2R marked, Stage 8, right-lateral view of alive embryo in DIC mode (**A**) and through fluorescent filter (**B**), the marked muscle elements are elongated; **C**-**H** - fixed and stained embryos, Imaris Surpass view, Volume Scene; **C** – 2L marked, Stage 8, left-lateral (slightly posterior) view, muscle elements of the left side; **D** – 2d marked, Stage 7, right-lateral ventral view, the marked muscle elements of the limbs are strongly elongated and attached, the muscle elements of the central cluster surround completely the oesophagus (see **Insertion**), in marked cells one can still see nuclei (arrowheads), here actin is marked by phallacidin, therefore cell borders, nervous system and muscles are visible; **Insertion**: transversal section through the region under the yellow line; **E** – 2d marked, Nauplius I, ventral view, the marked muscles are fully developed, the marking is clear visible only in the oesophageal and labral muscles, the marking in the limbs is not well defined; **F** – 2B labelled, late Stage 7, right-lateral view, the muscle precursors are of straw-shape, it is hard to distinguish any borders between future muscles, here actin is stained by phallacidin therefore muscles are marked in green; **Insertion**: outlined region on F with additional nuclear staining by DAPI, some nuclei of muscle precursors are visible (arrowhead), muscle fibres are attached (double arrowheads); **G** – right side of the musculature in an embryo of early Stage 8, dorso-(right-)lateral view, phallacidin staining of muscles, muscles are well defined, some intrinsic muscles become striated (double arrowheads), dashed circles outline attachment sites: **1** – attachment sites on the dorsal side, **2** – attachment sites within the protopodite of the mandible, **3** – attachment sites in the tip of the mandible; **H** – left side of the musculature in an embryo of late Stage 8, left-lateral view, phallacidin staining of muscles, extrinsic muscles become striated (double arrowheads). Scalebar 20 µm.

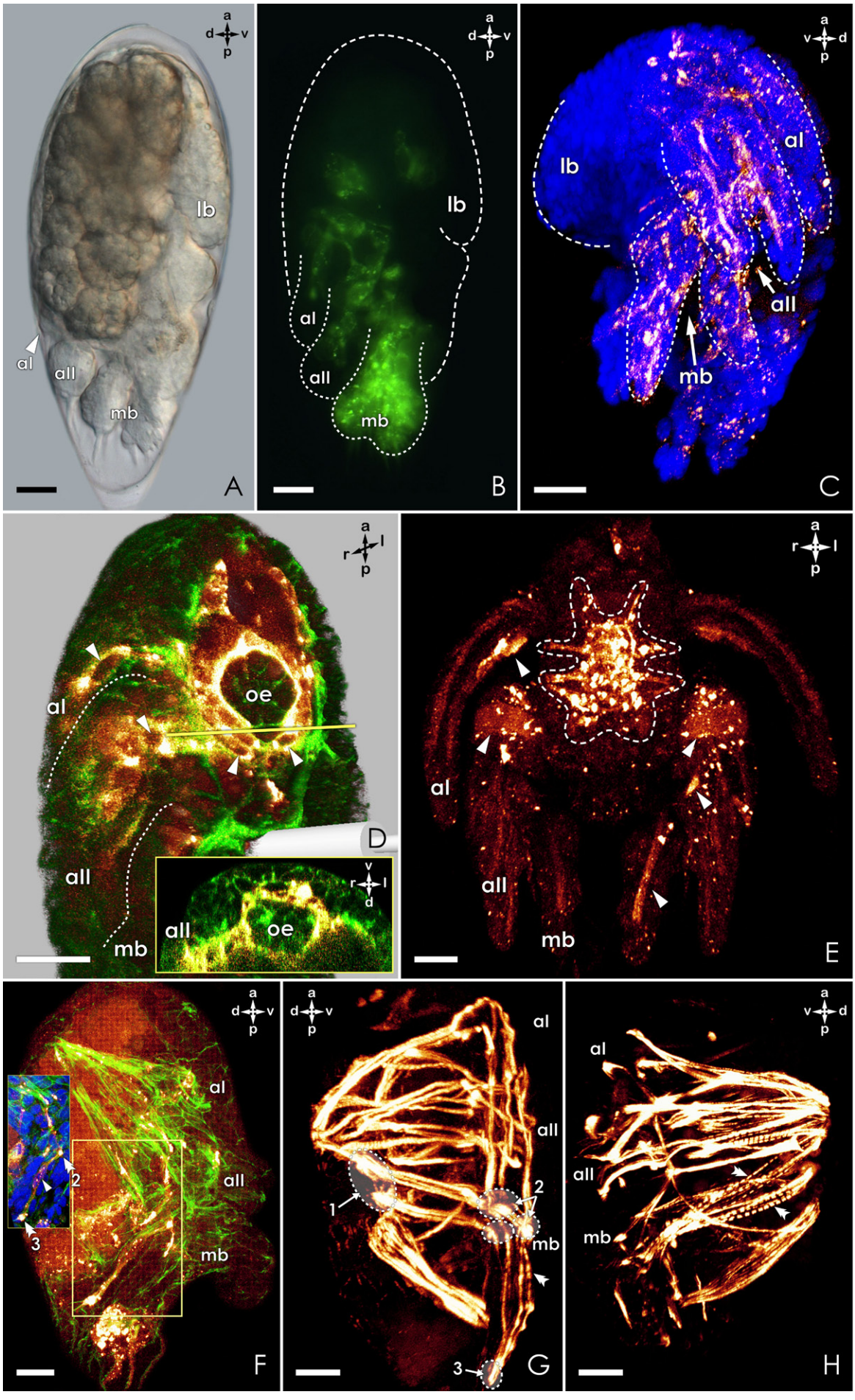
a
d
v
p
lb
al
all
mb
A
B
C
D
E
r
l
oe
F
G
H
1
2
3

The final differentiation of the mesodermal descendants of the marked blastomeres occurs in the locations, where they formed clusters before. Thus, the derivatives of the L-, R-, and B quadrants differentiate into extrinsic and intrinsic muscles of the limbs on the left, right, and dorsal side of an embryo, respectively (Fig. 3.5.5.B,C,F). The muscle precursors originating from 1d differentiate into extrinsic and intrinsic muscles of antenna II and mandible. Three paired clusters of muscle precursors derived from 2d differentiate into ventral extrinsic and intrinsic muscles of the limbs (Fig. 3.5.5.D,E, arrowheads). The central cluster differentiates into the circular muscle of the oesophagus and labral muscles (Fig. 3.5.5.D,E, outlined zone).

As well as during clusterization, at the stage of differentiation the fusion of the muscle precursors was not observed. Moreover, it was hard to say how many nuclei were placed within one developing muscle. The fact, that the cytoplasm of each forming muscle is filled with a lot of fibres of actin now, makes it impossible to distinguish the borders between different muscles. To somehow clarify the myogenetic process, the number of cells/nuclei at the stages of migration and clusterization were counted and and compared to the number of developing muscles at the late stage 8 (when the muscles are already well defined, but muscle bundles are still not formed). It was done only for the first two segments[*]. The data are given in Table 3.5.2.

The amount of cells on the early clusterization stage almost corresponds to the amount of forming muscles. This speaks for the idea that the mononucleate muscle precursors do not fuse, but develop further into one muscle each. Nonetheless, one cannot deny the possibility that during this investigation the stage of fusion was overlooked. In this case the number of muscles might have been reached by later subdivision of polynucleate muscle precursors.

Table 3.5.2. The number of muscle precursors from different quadrants within *aI* and *aII* anlagen in the two differential stages

Stage \ Cell	2B	2L	2R	2d	1d[**]
Migration	7	13	17	[***]	5-8
Clusterization	15-22	19-21	24-29	7-18	8-15

[*] The quadrants 2L, 2B, 2R, 1d, which give rise to mesoderm, give also rise to the ectoderm of the mandible and of the hindbody. That means, that the ectodermal clones of marked descendants cover the mesodermal ones exactly in the mandibular segment. This makes the thorough count of mesodermal cells within the mandibles nearly impossible.

[**] Cells contributing only to the mesoderm of *aII*.

[***] During migration stage of the 2d offspring it is hard to definitely say which cells later contribute to the lateral clusters and which to the central one.

3.5.2. Digestive system

The gut of the barnacle (as it was mentioned in Chapter 3.2.) consists of fore-, mid-, and hindgut. The midgut is of endodermal origin and is formed by the descendants of the single blastomere 2D containing most of embryonic yolk. After internalisation this blastomere undergoes the sequence of divisions and consequently gives rise to a group of yolky cells, which stay till the last embryonic stage 9 (compare Fig. 3.1.1.I and Fig. 3.5.6.H,K). At this stage the yolk is dissolved and the former yolky cells intensively divide forming the epithelium of the midgut (this process was not observed in details in the present work) (Fig. 3.4.9.B; Fig. 3.5.6.L).

Fore- and hindgut are of ectodermal origin and develop from one cell mass, which originates from the two blastomeres $1a^p$ and $1c^p$. The development of both of these regions starts at the stage 5 from epidermal invagination on the ventral side of the embryo (Fig. 3.5.6.A,B). At the stage 6 the invagination advances into a closed tube (or a pocket) turned towards the posterior (Fig. 3.5.6.C,D). With further progress the tube flattens in the middle (Fig. 3.5.6.E:3) forming a spacious anterior pocket (Fig. 3.5.6.E:1) and a small posterior enclosed chamber (Fig. 3.5.6.E:4). At the late stage 7 to early stage 8 the flattened region of the tube thins out, what results in separation of its anterior and posterior regions (Fig. 3.5.6.F,G,I). In between these two regions the yolky cells are placed now. The anterior portion represents the developing foregut, and the posterior one the developing hindgut (Fig. 3.5.6.I,J). With the transformation of the yolky cells into the midgut, the ectodermal epithelium of the fore- and hindgut establish contact with the endo dermal epithelium of the midgut, thus forming an intact digestive tract (stage 9) (Fig 3.2.6.L). The hindgut remains enclosed till hatching, when the anal opening is formed.

Additionally to the epithelial parts, the barnacle digestive tract is outlined by muscle fibres. Their structure and development are described in the chapters 3.2.2. and 3.5.1.

Fig. 3.5.6. Development of the digestive system.

All the images, apart from A, C, and F, are obtained in Imaris Extended Section view; A,C,F – in Imaris Surpass view with assistance of Clipping Plane scene.

A – Stage 5, ventral view, under the marked labral bulge there is an outlined region of invaginating cell material for the ectodermal parts of the future gut; **B** – 1r labeling, Stage 5, median section through the invaginating region, right-lateral view; **C** – 1L labeling, Stage 6, frontal clipping plane, right-lateral view, the developing ectodermal gut is represented by a tube-like invagination/pocket (outlined); **D** – 1r labelling, Stage 6, median section, the tube-like pocket turned posteriorly; **E** – late Stage 6, median section, left-lateral view, the tube-like invagination flattens in the middle (**3**), yellow lines show the regions of the transversal sections presented on **1**-**4**; **F** – $1l^p$ labeling, Stage 7, median clipping plane, left-lateral view, the middle of the tube-like invagination (outlined) flattens more, the division between anterior and posterior regions is well discernible; **G** – Stage 7, median section, the flattened region is one-cell wide; **H** – 1D labeling, Stage 6, frontal section, the yolky cells are shown, the cells of the future midgut do not show many changes since the late gastrulation stage (compare with Fig.3.1.1.I); **I** – early Stage 8, frontal section, the anterior and posterior portions of the invaginated cells are two separated parts (outlined), in the middle the yolky cells are placed; **J** – 1l labeling, Stage 8, frontal section, anterior and posterior portions of the developing gut are now in the right positions of the fore- and hindgut, the hindgut portion is representing an enclosed chamber; **K** – 1D-labelling, early Stage 9, median section, right-lateral view, the yolky cells still remain unchanged; **L** – Stage 9, median section, left-lateral view, the yolk is dissolved, but the epithelium of the midgut has not yet taken shape, the anal opening is also not yet formed. Scalebar 15 μm.

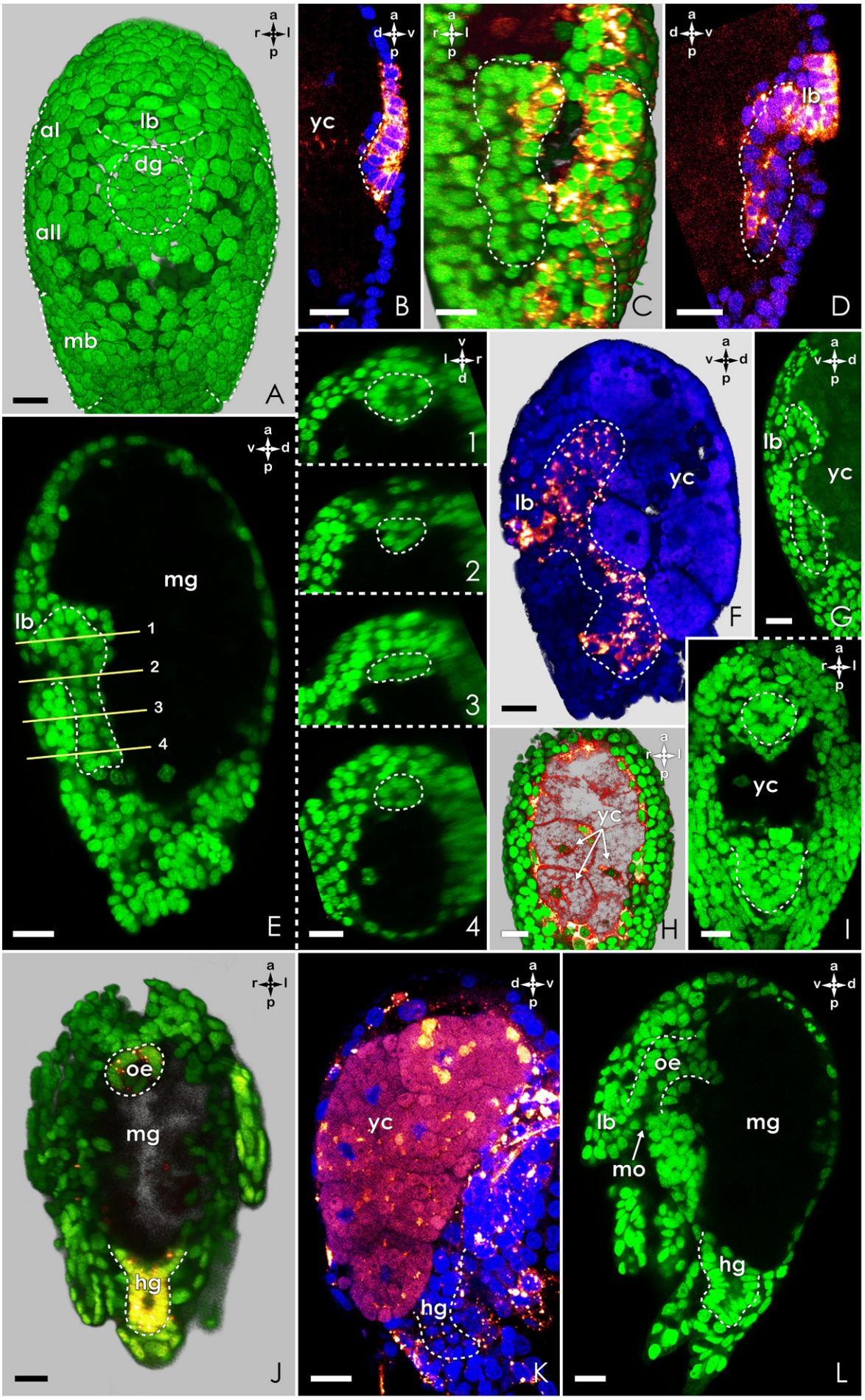
al
lb
dg
all
mb
A
yc
B
C
lb
D
1
2
3
4
mg
lb
1
2
3
4
E
lb
yc
F
lb
yc
G
yc
H
yc
I
oe
mg
hg
J
yc
hg
K
oe
lb
mo
mg
hg
L

3.5.3. Unidentified cells

During embryogenesis there were some cells found, which stayed undifferentiated till after hatching. Since current research did not go beyond nauplius I, the destiny of these cells remains unclear. The cells can be classified into two groups according their origin, history, and probable fate.

The first group (here they are referred to as unidentified cells 1, uc1) is represented by four cells and is established in early embryogenesis (late stage 2 to early stage 3). The first two cells (uc1 of the first generation) are the result of an unequal division of $3D^a$ and $3D^p$ (Fig. 3.5.7.A). Shortly afterwards they divide once again (uc1 of the second generation) and remain in the resulting number of four till the end of the present observation (Fig. 3.5.7.B). The uc1 are of round shape with big nuclei, which contain some heterochromatic DNA. In the beginning the uc1 are placed posterior to the endodermal yolky cells (Fig. 3.5.7.B,F) close to the ventral surface of the embryo. During development (stage 6 and 7) the cells move towards the posterior together with the cell material of the developing hindgut (Fig. 3.5.7.C,C'). Once the hindgut is developed the cells are situated on its wall (the cells are placed so tightly to the hindgut, that sometimes it seems as if they belong to it) (Fig. 3.5.7.H,J). Due to the position and origin these cells are suspected to be germ line cells. To prove this, however, further studies have to be conducted.

The second group of unidentified cells is also represented by four cells. The first two appear at the stage 5 (uc2 of the first generation). In most of the cases they are the descendants of blastomere 1d[♣]. It is yet unclear whether they derive from the mesodermal or ectodermal layer. The cells (referred here as unidentified cells 2, uc2) are big cells of uncertain shape and contain large euchromatic nuclei. These cells are placed ventro-posteriorly in regards to the uc1 (Fig. 3.5.7.C",F). With advancing of the gut development the uc2 remain in their position, but now they are placed between the developing hindgut and the epithelium of the hindbody. At the stage 7 they divide equally in longitudinal direction (uc2 of the second generation; Fig. 3.5.7.G). Shortly afterwards one pair of the sister cells migrate dorsally around the hindgut (Fig. 3.5.7.D,D',E, arrow). They remain in the number of four and placed around the hindgut till hatching (Fig. 3.5.7.I,J). In the nauplius these cells become hard to identify. On the base of their position the uc2 are assumed to be the mother cells of the postnaupliar mesoderm. To be able to claim that with certainty one has to trace these cells during the larval development of a barnacle.

[♣] There were two cases found which speak for a different origin of the uc2. One is shown on Fig. 3.4.16.D (Chapter 3.4.3), where the cells on the left come from the L quadrant. In that case the ancestor blastomere of the cells on the right remained unknown. In another case the origin of the cells on both sides was not identified, as they were not among the labelled descendants of the blastomere 1d (the case is not shown).

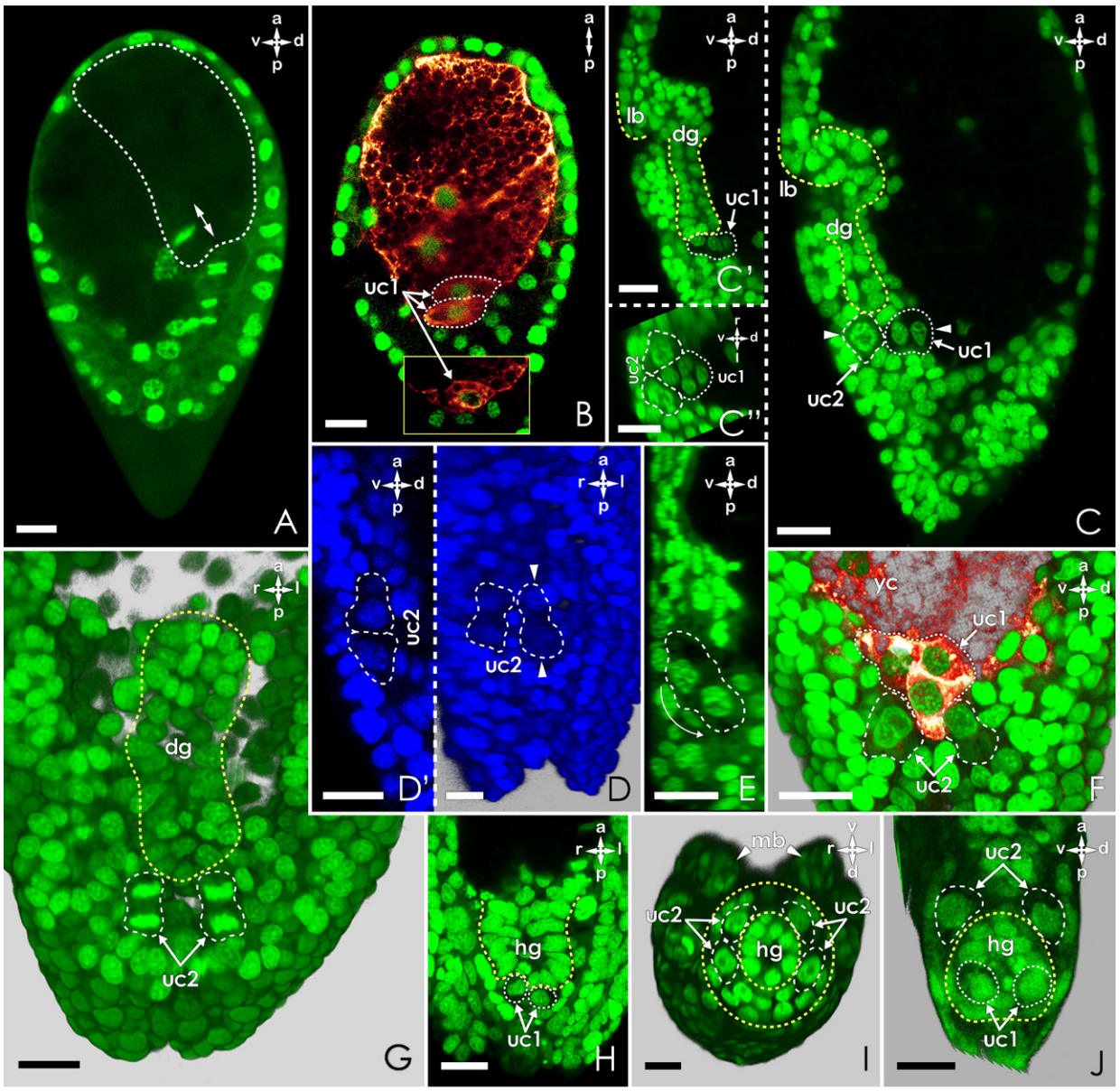

Fig. 3.5.7. History of unidentified cells.

All the images, apart from D,G, I, and J, are obtained in Imaris Extended Section view, MIP(max) mode; D,G,I,J– in Imaris Surpass view, Blend mode of Volume scene with assistance of Clipping Plane scene.

A – Stage 2, metaphase of asymmetrical division in yolky cell 3D[a], **B** – 2D labeling, late stage 2, shortly after the division of the uc1 of the first generation, four cells of uc1 are presented, only three are shown; **C**,**C'**,**C"** – late Stage 6, relative positions of the unidentified cells to each other and to the developing midgut and hindgut, sagittal (close to median) section (**C**,**C'**) and transverse section (**C"**) through the region pointed by arrowheads on C; **D**,F' – stage 7, shortly after the formation of the uc2 of the second generation, all four cells are placed ventrally, frontal cut (F) and sagittal section of the region marked on D by arrowheads (**D'**); **E** – late stage 7, sagittal section, one sister cell of the left pair of the uc2 migrates dorsally, arrow; **F** – stage 6, frontal cut, relative positions of the unidentified cells to each other and to the yolky cells; **G** – Stage 7, frontal cut, longitudinal division of the uc2; **H** – Stage 8, frontal section, the uc1 are "pushed" posteriorly by the cell material of the developing hindgut; **I** – Stage 8, transverse cut of the midlevel of the hindbody, the uc2 of the second generation surround the hindgut ventrally and latero-dorsally; **J** – early Stage 9, fronto-transversal cut of the posterior hindbody, relative positions of the unidentified cells to each other. Scalebars: 20 μm.

4. DISCUSSION

The discussion is organized in three parts:

1. – comparison of the obtained data on the development of *E. modestus* with that of other thecostracans in order to work out a developmental pattern of the group;
2. – comparison of the development of *E. modestus* and Cirripedia in general with that of other crustaceans. The goal of this chapter is to find common characteristics with the perspective to contribute to the search of the developmental ground pattern of Crustacea;
3. – comparison of some developmental features of *E. modestus* and other Crustacea with those in different groups across Protostomia and some possible evolutionary scenarios on the base of this comparison.

The very last part of the discussion is more a pile of sophisticated speculations and has to be addressed and judged as such.

4.1. Three of a kind

Comparison of Elminius modestus with other Thecostraca

Within Thecostraca the embryonic development has been described for Ascothoracida and all the groups of Cirripedia (the evolutionary system of thecostracans is presented on the Fig. 4.1.1.). The exceptions are the representatives of Facetotecta, for which there is no known record of the early stages as well as the adult ones. All the observations and the analyses for this group are based exclusively on the larval stages (for review see Grygier, 1987). Most of the available studies on cirriped development concentrate mainly on the morphogenesis of the embryo giving only slight attention to the early stages like cleavage and gastrulation (Nussbaum, 1890; Groom, 1894; Batham, 1945; Crisp, 1959; Bocquet-Vedrine, 1961, 1964; Anderson, 1965). And only few works thoroughly followed the development identifying the single blastomeres and establishing the cell lineage (Bigelow, 1902; Delsman, 1917; Krüger, 1922; Vagin, 1949; Anderson, 1969; Turquier, 1967).

Elminius modestus (Cirripedia: Thoracica) investigated in this work demonstrates a stereotypic cleavage pattern with a determined cell specification. When compared with the rest of the relevantly studied thecostracans, the high number of similarities is revealed (Table 4.1.1.). As a resume to the table the common features for embryonic development of thecostracans could be stated as following:

1. Unequal cleavage with respect to the yolky cell.

There are two groups, which exhibit an exception to the general pattern. These are the parasitic barnacles Rhizocephala (Shirase and Yanagimachi, 1957; Bocquet-Vedrine, 1961, 1964; Scholtz

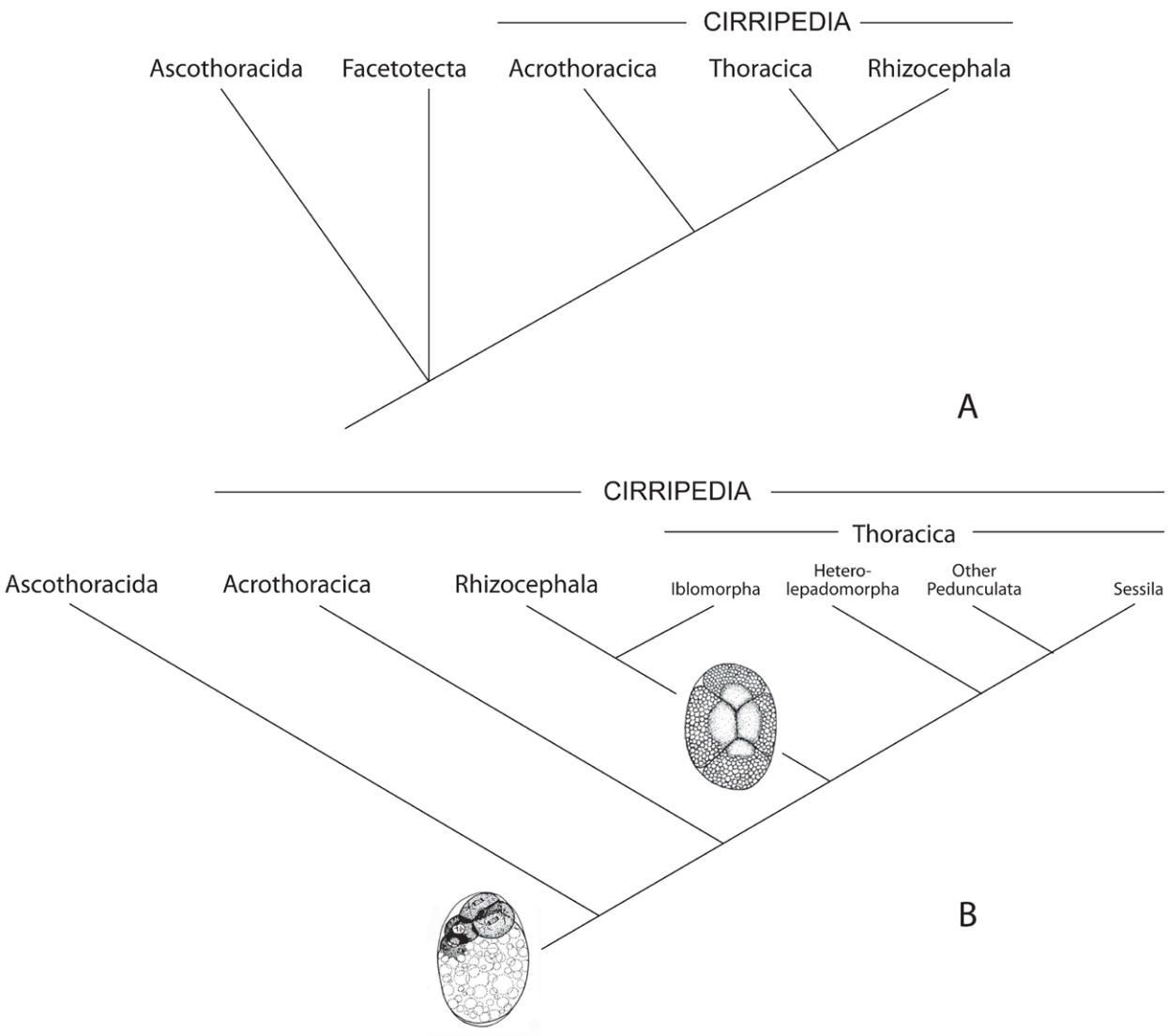

Fig. 4.1.1. Phylogenetic system of Thecostraca. Possible approaches.

A – modified from Høeg and Kolbasov (2002); **B** – modified from Scholtz et al. (2009), a suggestion on relationshis between Iblomorpha and Rhizocephala.

et al., 2009) and the stalked thoracican *Ibla quadrivalvis* (Anderson, 1965). The embryos of these groups are characterized by equal first two cleavages and the formation of quartets of micro- and macromeres after the third cleavage. It has been suggested, that this way of early development might represent a synapomorphy for a group comprising rhizocephalans and iblomorphs and being in sister relationship to the rest of Thoracica (Scholtz et al., 2009).

2. Asynchronous cleavage (with animal-vegetal gradient).

This developmental aspect seems to be consistent across all the observed specimens in Thecostraca. The only exception is shown in the work of Anderson (1969). His results on the first four divisions are congruent with those of other studies. From the fifth division on, however, the 2D blastomere (the yolky cell) in the specimens observed by him starts to divide faster than the other cells. Thus, the division sequence becomes reverse. The closure of the blastopore occurs at

the 33-cell stage, with the yolky 3D (according to Anderson's identification) already divided into 4D and 4d.

Interestingly, this difference in the sequence of the divisions during cleavage leads to a different "cell composition" of the 28-cell stage. In the case of *E. modestus*, *Lepas anatifera* (Bigelow, 1902), and *Semibalanus balanoides* (Delsman, 1917), when the 28-cell stage is reached, the clones of A, B, and C consist of 8 blastomeres each, while the D quadrant has produced only 4 derivatives so far. These are the micromeres $1d^r$, $1d^l$, 2d and the yolky 2D. In "Anderson's case" the 28 blastomeres include 8 derivatives of the D quadrant, 7 cells of the A and C quadrants (the most anterior $1a^a$ and $1c^a$ are still undivided), and 6 cells of the line B (including two blastomeres $1b^r$ and $1b^l$ being arrested at the fourth cell cycle).

Table 4.1.1. Comparative data on the early development within Thecostraca.

Thecostracan group		Species/Author	Gradient of asynchrony	Mirror image	Blastopore		endomesoderm/ endoderm origin
					organizing cells	position	
Cirripedia	Thoracica	*Lepas anatifera*, *L. peciinata*, *Gonchoderma virgata*, *Diohelaspis*, *Chthamalus stellatus*, *Balanus perforatus* (Groom, 1884)	an-vg	present	n/a	posterior-ventral	n/a
		L. anatifera (Bigelow, 1902)	an-vg	not present	3A,3B,3C,$2d^r$,$2d^l$ daughter cell of 3b	posterior-ventral	2d/2D
		Semibalanus balanoides (Delsman, 1917)	an-vg	n/a	4A,4B,4C,$2d^r$,$2d^l$	posterior-ventral	2d, $3D^a$ and $3D^p$
		Scalpellum scalpellum (Krüger, 1922)	an-vg	n/a	n/a	posterior	2d/2D
		Tetraclita rosea, *T. purpurascens*, *C. antennatus*, *Chamaesipho columna* (Anderson, 1969)	an-vg vg-an (after 4^{th} div)	n/a	4A,4B,4C,$2d^r$,$2d^l$	posterior-ventral	not present/ 4D
		Elminius modestus (present study)	an-vg	present	3A,3B,3C,$1d^{rp}$,$1d^{lp}$ and their external daughter cells	posterior-dorsal/ dorsal	2d/2D
	Acro-thora-cica	*Trypetesa nassarioides* (Turquier, 1967)	an-vg	n/a	n/a	posterior	2d/2D
Ascotho-racida		*Ascothorax* (Vagin, 1949)	an-vg	n/a	n/a	posterior	2d/2D

Most unfortunately, Anderson does not provide pictures of these fast divisions of the yolky cell. Moreover, if not for his identifications of the blastomeres, the embryos in his illustrations are strikingly similar to those from other studies (Bigelow, 1902; Delsman, 1917; current work). Based on this it is concluded here that the observations of Anderson (1969) on the reverse cleavage sequence and the existence of 4d and 4D were erroneous, perhaps, because of work with fixed material. His 4d cell is hereby equalized with 2d, and 4D with 2D.

3. Differentiation of endoderm and endomesoderm after the fourth cleavage. The blastomeres responsible for these germ layers are 2D and 2d, respectively.

In the works on Ascothoracida (Vagin, 1949), Acrothoracica (Turquier, 1967), and *Scalpellum scalpellum* (Thoracica) the conclusion of the fates of 2d and 2D has been done on the base of homologization of their cell lineage with that of *L. anatifera* (Bigelow, 1902). The blastomeres have not been traced in their differentiation.

4. Epibolic gastrulation in association with the migration of the endomesoderm precursors

There was no endomesoderm described in the research performed by Anderson (1969) (Table 4.1.2.), but this will be addressed later.

One can see from the table that there is also a number of disagreements in the results of different works. The most important ones are related to blastopore position, limb development (not shown in the tables), and cell fate (Table 4.1.2.).

4.1.1. Blastopore

While the authors of the works on cirriped development largely agree upon the cell composition of the blastopore (or their illustrations are), their views on the blastopore position itself vary (Table 4.1.1.).

As it was described earlier in this thesis, the embryos of *E. modestus* undergo certain turns within the egg shells (Chapter 3.3.). Exactly in the time of the blastopore closure the anterior-posterior embryonic axis is tilted in relation to the elongated axis of the egg (Fig. 3.3.7.). If the position of the blastopore is considered in relation to the egg shell, then it is placed on the future posterior-dorsal side. However, if one observes the development *in vivo* or traces the descendants of the blastopore initiating cells, the blastopore area corresponds approximately to the posterior part of the nauplius. In any case, the blastopore is not placed on the future “ventral side” of the developing embryo as it was described by Bigelow (1902), Delsman (1917), and Anderson (1969).

The precise placement of the blastopore has been possible to identify only by means of 4D microscopy. Since most of the previous descriptions were performed on the base of fixed material,

there might have been a mistake made concerning this subject. Nonetheless, one cannot exclude the possibility of differences between the different species and therefore the exact position of the blastopore for the other barnacles has to be verified.

4.1.2. Limb formation

Many of the early researchers (reviewed in Groom, 1894) observed that the limbs in cirriped embryos form on the ventral side, where "the mesoderm band is situated". Such opinion is shared also by Anderson (1969), and has been supported by his study on the embryonic development of four thoracican species. Other cirripedologists, like Groom (1894), Bigelow (1902), and Delsman (1917), describe a dorsal formation of the limb buds. The same holds true for the specimens of *E. modestus* investigated in the present study. The limb development starts with longitudinal and transverse grooves on the dorsal half of the embryo. Later, as the ectodermal grooves separate the distal parts of the appendages from the body, their proximal parts are placed laterally. In the case of *Scalpellum scalpellum* (Kaufmann, 1965), *Trypetesa nassarioides* (Turquier, 1967), and *Ascothorax* (Vagin, 1949) the eggs contain large amount of yolk and the embryo develops out of some sort of a germ disc. There the limbs are directed first laterally and later dorsally.

Thus, the question remains, whether the findings of a ventral limb formation are incorrect. Possibly, those in favour of ventral limb formation observed the formation of the limbs on the same side where the blastopore has been formed before and which they interpreted as ventral side. One can observe the same situation in *E. modestus*. Later, however, this side appears to be dorsal, and that is very well visible as soon as the area of the future mouth starts to invaginate. At this point in development Anderson (1969), however, describes that the limbs turn dorsally. This limb turn is not observed in any other barnacle study though.

Coming back to the conclusion made by Groom (1894) more than a hundred years ago: such observation of ventral limb buds can be just an initial mistake in the orientation of the embryo.

4.1.3. Blastomere fate

For the further discussion it is necessary to make a summary on blastomere specification in cirripedes. Data on this are even fewer than those on cleavage and gastrulation. The general origin of the germ layers can be concluded on the base of several publications (most detailed are the ones by Bigelow, 1902; Delsman, 1917; Anderson, 1969; and the present one). (Table 4.1.2.). The further differentiation of the cells within each germ layer has however been investigated only once before the current work (Anderson, 1969).

Ectodermal differentiation has never been traced in much detail for barnacles. Anderson (1969) is the only one who gives outlines of the fates of ectodermal blastomeres. His data, however, significantly differs from the data obtained in the course of this research. This concerns particularly the derivatives of the B and D quadrants. For example, in *E. modestus* 1d develops mainly on the ventral side of the hind body and sometimes at the bases of the limbs. In *T. rosea*, *T. purpurascens*, *Ch. columna*, and *Cht. antennatus*, according to Anderson, 1d produces dorsal ectoderm of *aI* of the nauplius together with the dorsal ectoterm of a headshield. Another ectodermal blastomere, 1b, in *E. modestus* is mostly responsible for the anteriormost ectoderm and sometimes takes part in the formation of the labrum. The offspring of 2b occurs exclusively in the middorsal area of the head shield covering some dorsal parts of the antennae II. 1b and 2b in Anderson's study contribute to the ectoderm of the labrum and ventral parts of the limbs.

In general, as Anderson (1969) describes, the descendants of B can be mostly found on the ventral side of the embryo, whereas those of D are spread over the dorsal side. This is almost totally

Table 4.1.2. Comparative data on the origin of germ layers and their time of segregation in Thoracica.

* It is hard at this stage to make homology assessments between the blastomeres described by Delsman and those in the present work.

** It was not specified in this work, which daughter cells give rise to mesoderm, but on the base of the illustrations one can assume, that they are 4A-4C.

div – division.

Species	Ectoderm	Endoderm	Mesoderm	
			Ecto mesoderm	Endo-mesoderm
Lepas anatifera (Bigelow, 1902)	3rd div: 1a-1d 4th div: 2a-2c 5th div: 3a,3c 6th div: derivative of 3b	4th div: 2D	derivatives of 3b, 3A-3C**	4th div: 2d
Semibalanus balanoides (Delsman, 1917)	3rd div: 1a-1c 4th div: 2a-2c 5th div: 3a-3c, 1d^{ra}, 6th div: 4a-4c, daughter cells of 1d^{rp}, 1d^{la}, 1d^{lp}* 7th div: derivatives of 1d^{rp}, 1d^{la}, 1d^{lp}**	6th div: the bigger daughter cells of 3D^{a} and 3D^{p}	6th div: 4A-4C 7th div: derivatives of 1d^{rp}, 1d^{la}, 1d^{lp}*	4th div: 2d 6th div: the smaller daughter cells of 3D^{a} and 3D^{p}
Tetraclita rosea, *T. purpurascens*, *Chtamalus antennatus, Chamaesipho columna* (Anderson, 1969)	3rd div: 1a-1d 4th div: 2a-2d 5th div: 3a-3d 6th div: 4a-4c	6th div: 4d,4D	6th div: 4A-4C	not present
Elminius modestus (present study)	3rd div: 1a-1c 4th div: 2a-2c 5th div: 3a-3c, 1d^{ra}, 1d^{la} 6th div: 4a-4c, 1d^{rpe}, 1d^{rpe}	4th div: 2D	6th div: 4A-4C, 1d^{rpi}, 1d^{rpi}	4th div: 2d

opposite to the barnacle investigated in this work. This contradiction seems to be a logical result of different orientation of the embryos in his studies (see above).

Additionally, there are some differences related to the ectodermal derivatives of the A and C quadrants. According to Anderson (1969) these blastomeres are always responsible for the structures on the right and left body sides, correspondingly. In the species investigated in this work there were specimens observed having the A offspring on the left side of the animal and that from the C quadrant on the right. This is undoubtedly related to the presence of the two mirror images of developing embryos, which has not been noted in the species studied by Anderson.

Endoderm and mesoderm. Endoderm and endomesoderm lineages in barnacles represent the most consistent results among the available studies (Tables 4.1.1. and 4.1.2.). Nevertheless, as it is shown in the Table 4.1.2., there are some differences in the investigations. For example, Delsman (1917) reported two sources of endomesoderm. He observed the asymmetrical division of $3D^a$ and $3D^p$ and claimed the bigger sister cells to give rise to endoderm and the smaller ones to be the endomesoderm precursors. Embryos of *E. modestus* undergo the same unequal division, but here the smaller cells are assumed to be responsible for the formation of the future germ line cells uc1 (see Chapter 3.5.3, Fig. 3.5.7.).

The differences in the case of Anderson's (1969) results are, firstly, due to the false identification of the blastomeres (see above), resulting in 4d and 4D presence. Secondly, he claims that 4d (2d here), is responsible for the formation of the posterior midgut. Thus, the blastomere 3D (1D here) represents a pure endoblast and endomesoderm is not present at all. However, the position and the appearance of the cells, which are indicated on the pictures of Anderson's paper as the derivatives of 4d/2d and the material for the future posterior midgut, strongly resemble the product of the unequal seventh division of $3D^a$ and $3D^p$ (just described in the previous paragraph). To say for sure, nevertheless, one has to retrace the embryonic development in the species studied by Anderson (1969).

The ectomesoderm origin varies in all the studies. There is, nevertheless, one stable feature: the ectomesoderm originates always from the blastopore organizing cells. One can see this correspondence in Tables 4.1.1. and 4.1.2.

4.1.4. Muscle anatomy

To assist in future analyses on muscle differention and muscle establishment within crustacean, the attempt was made to homologize muscles of the nauplius larvae of different cirripedes. The relevant data are available only for four species of Thoracica. No information of the muscle anatomy is known for the other two groups of Cirripedia: Acrothoracica and Rhizocephala. The

known data are restricted only to the two groups of muscles: extrinsic limb musculature and supporting muscles.

From the Table 4.1.3. and Fig. one can see that in general the muscle anatomy of the extrinsic limb muscles in the investigated species is to great extent similar. It is hard to explain the reasons for existing differences though. Some speculations on this matter are provided by Semmler et al. (2009).

Table 4.1.3. Homologous extrinsic limb muscles in the nauplii of four barnacle species.

In brackets – the number of muscles included in one bundle.
* On the pictures of the publication mdv1 has clearly two muscles.
** Different muscles and muscle bundles under the same name.
*** See Table 4.1.4.:
omd1+omd2=sk5
mdpl = sk7
mdd4=sk2=23

appendage	*E. modestus*	*B. improvisus*, Semmler et al., 2009	*S. balanoides*, Walley and Rees, 1969	*I. quadrivalvis*, Anderson, 1987	*E. modestus*	*B. improvisus*, Semmler et al., 2009	*S. balanoides*, Walley and Rees, 1969	*I. quadrivalvis*, Anderson, 1987
	dorsal				ventral			
aI	d1	d1	5	aa1d	v1	-	25	-
	d2	d2	12	pa1d	v2	v1	26	a1v
	d3	d3	7	aa1d(2)				
	d4	d4	8					
aII	d1	d1	3	aa2d(3)	v1	v3	27	-
	d2	d2	4		v2	v4	28	a2v
	d3	d3	6		v3	-	-	-
	d4	d4	14	2x pa2d(3)	v4	v1	31	a2m (3)
	d5	d5	13		v5	v2	32	
	d6	d6	15		v6		29	
	d7	d7	9		v7	v5	34	-
	d8	-	17		-	-	33	-
	d9	-	18					
	d10	d8	16	-				
mb	"d1"	mdd3	10	amd (4)	v1	mdv1*	36	
		-	11		v2		37	mmβ**
	"d2"	mdd1	19		v3	-***	38	mmα (3)
	"d3"	mdd5	20	pmd	v4	-***	39	
					v5	mdv2		
					-	-	-	mmβ**
					-	-	-	mmβ**

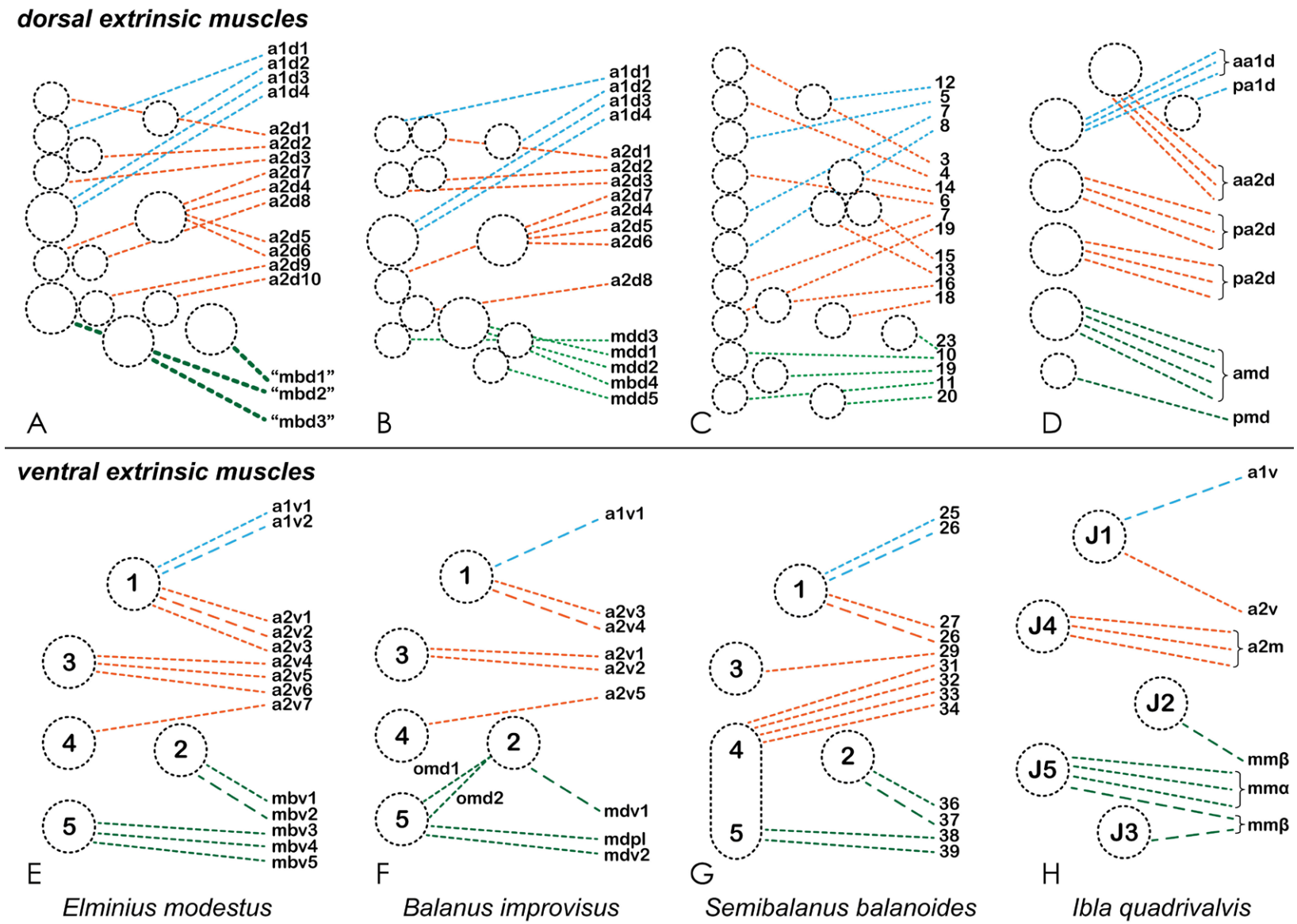

Fig. 4.1.2. Schematic comparative illustration of dorsal and ventral extrinsic muscles in the four species of Cirripedia: Thoracica

Colour code: muscles of antenna I, muscles of antenna II, muscles of mandible.

A-**D** – schematic placement of dorsal extrinsic muscles, **E**-**H** – schematic placement of ventral extrinsic muscles; dashed circles are attachment sites, smaller circles stay for attachments site of single muscles, bigger circles are for the attachment sites shared by several muscles;
A – *E. modestus*, mandibular muscles are represented by muscle bundles; **B** – *B. improvisus*, attachment sites are slightly different to those *E. modestus*, two muscles of *aII* – a2d9 and a2d10 – are not present, with a2d8 is homologous to a2d10 of *E. modestus* and *S. balanoides*, *mb* muscles are five singular

The so called “supporting muscles” or the muscle of the endoskeleton are described in detail only for *I. quadrivalvis* (Anderson, 1987). However, in the works on *B. improvisus* (Semmler et al., 2009) and *S. balanoides* (Walley and Rees, 1969) some muscles were mentioned, which are possible to be homologized with the supporting muscles of *E. modestus* (Table 4.1.4.). The long-sarcomeric muscles (a1v1, a2v2, mbv2) are under question. In the work of Walley and Rees, 1969 on *S. balanoides* they describe these muscles as the ones, which "tie [endosternites] ventrally to the protopodites of the limbs". However, they do not speak of the function for these muscles, what could help classifying them. For *I. quadrivalvis* the similar muscles are described in the group of supporting musculature (Anderson, 1987). Their real function is not clear and has to be verified by live observations.

Table 4.1.4. Homologous supporting muscles in thenauplii of four barnacle species.

E. modestus	*B. improvisus,* Semmler et al., 2009	*S. balanoides,* Walley and Rees, 1969	*I. quadrivalvis,* Anderson, 1987
plm	plm	21	dva
dv	ffm	1	ell
sk1	-	2	J1b/d
sk2	-	22	J2b/d
sk3	mdpl	23	J3d
sk4♣	-	24	a (est)
sk5	omd1 omd2	35	J25α/β
sk6	-	30	J12
sk7	mdpl	-	d (est)
sk8	-	-	b (est)

muscles; **C** – *S. balanoides*, attachment sites are nearly identical to *E. modestus*, but every muscle has its own attach-ment site, the number of *aI* and *aII* muscles is the same as in *E. modestus*, the mandibular muscles are singular and in number equal to those in *B. improvisus*; **D** – *I. quadrivalvis*, the scheme is made on the base of a written description, therefore the precise attachment sites are not clear, muscles of *aII* are nine, *mb* muscles are five, but arranged differently than in *S. balanoides* and *B. improvisus*; **E** – *E. modestus*; **F** - *B. improvisus*, attachment sites are the same as in *E. modestus*, the number of muscles is smaller in each limb; **G** – *S. balanoides*, attachment sites 4 and 5 are united in one, *aII* muscles are the same in number as in *E. modestus*, but arranged differently; *mb* muscle mbv5 is not present; **H** – *I. quadrivalvis*, the attachment sites are placed somewhat different, *aI* and *aII* muscles are fewer in number, *mb* muscles are in contrast more numerous than those in *E. modestus*.

♣ This muscle does not show striation, therefore one cannot exclude the possibility that it is not a muscle but just a structure positively stained against fibrillar actin

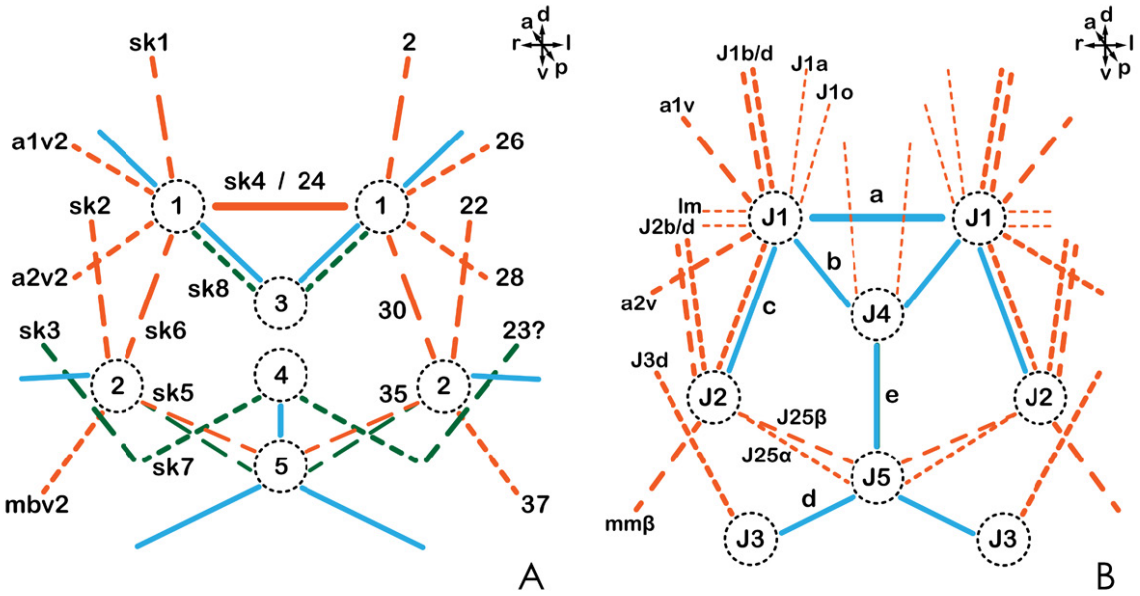

Fig. 4.1.3. Schematic comparative illustration of supporting muscles and endoskeleton in three species of Thoracica (Cirripedia).

Colour code: endoskeletal structures, muscles, muscles found in both species.

A – united scheme of the supporting muscles in *Elminius modestus* and *Semibalanus balanoides* (Walley and Rees, 1969),
Colour code: muscles found in both species, additional muscles found in E. modestus, endoskeletal structures described for S. balanoides, encircled numbers – ventral attachment sites, long dashed lines – muscle fibres with long sarcomeres, short dashed lines – muscle fibres with short sarcomeres;
B – scheme of the supporting muscles in *Ibla quadrivalvis* (Anderson, 1987),
Colour code: muscles, endoskeletal structures, encircled numbers – ventral attachment sites, long dashed lines – muscle fibres with long sarcomeres, short dashed lines – muscle fibres with short sarcomeres.

4.2. Full house

Comparison of Elminius modestus with other crustaceans

The phrase, that the Crustacea demonstrate a huge variety of the developmental patterns, has been said probably more times than the number of the described patterns itself is. Naturally, almost every time the phrase has been told, the logical attempt followed to find some common pattern in this variety. Reviews on the crustacean development and on the different aspects of it have been done through years and can be found for example in Korschelt, 1936; Weygoldt, 1960; Ivanova-Kazas, 1979; Anderson, 1979; Scholtz, 1997; Gerberding and Patel, 2004. The comparison of the embryonic development in *E. modestus* with the relevant data on other crustaceans provided in this chapter is no exception to the rule. And below there is an attempt to slightly contribute to the search of the developmental ground pattern of Crustacea (if any exists) and to the on-going dispute on the relationships between major crustacean groups.

However, one has to pay attention to the different phylogenetic views on the group of Crustacea itself. In the past years classical monophyly of the crustaceans has been compromised by ever growing counter evidence from the molecular field. The crustaceans come out as a paraphyletic group in the most of the modern phylogenies. On the Fig. 4.2.1. one can compare the "older", morphologically based, view on arthropod phylogeny and that of the last decade. It is obvious, that molecular data unanimously unite crustaceans with hexapods into one phylum Pancrustacea, or Tetraconata. However, its internal relationships, especially when it comes to crustacean groups, represent total mess (summarized in Jenner, 2010). Some very general agreements can be found among major part of works, which are demonstrated on the Fig.4.2.1.A. It relates, for example, to the close relationships between Copepoda, Thecostraca, and Malacostraca, forming together Multicrustacea, or Ostracoda, Branchyura, and Mystacocarida, united in Oligostraca. The more refined relationships between them as well as the positions of other important groups, like Branchiopoda, or Remipedia, are under constant dispute. There are also other works, which provide completely alternative views to major pancrustacean phylogeny (check Lavrov et al., 2004; Jondeung et al., 2012).

Another big question regards the sister group of Pancrustacea (see discussions in Dohle, 2001; Richter, 2002; Edgecomb, 2010; Giribet and Edgecombe, 2012). According to some works, the closest group to the phylum is Myriapoda and together they form Mandibulata (Giribet et al., 2001; Regier et al., 2010; Rota-Stabelli et al., 2011). According to others, Myriapoda is closely

Fig. 4.2.1. Phylogenetic relationships within and outside of Crustacea. Recent and older analyses.

A – the summarized tree from the references listed in the right upper corner, some developmental characters are mapped (descriptions see in the text). ThRh – the data are available only for the groups of Thoracica and Rhizosephala. Phylogeny of Malacostraca is based on Richter and Scholtz, 2001 (simplified); **B** – the consensus tree from Štys and Zrzavý, 1994; **C** – one of the older view on the phylogeny of Arthropoda and the position of Crustacea (Dogiel, 1981).

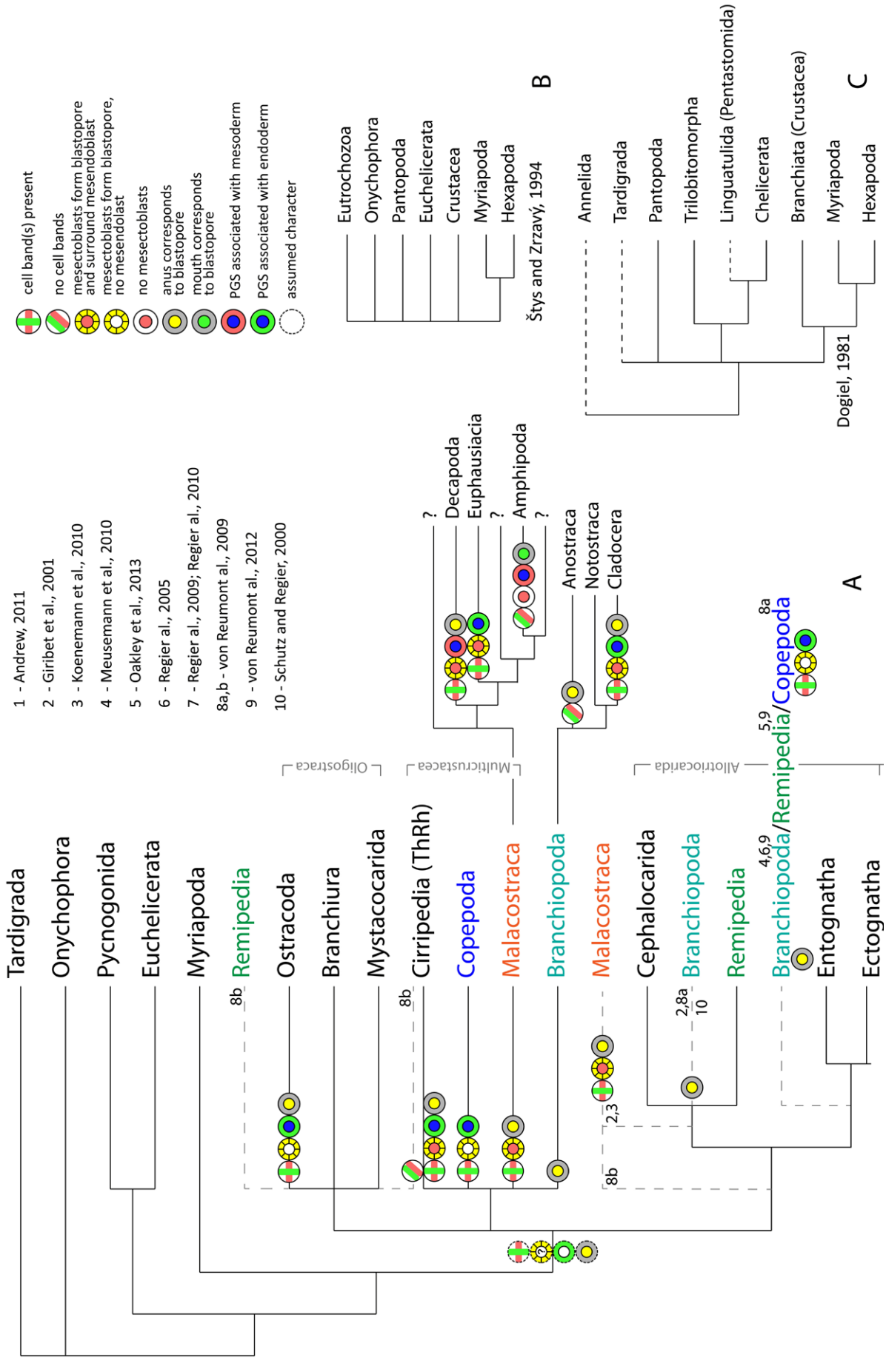
cell band(s) present
no cell bands
mesectoblasts form blastopore and surround mesendoblast
mesectoblasts form blastopore, no mesendolast
no mesectoblasts
anus corresponds to blastopore
mouth corresponds to blastopore
PGS associated with mesoderm
PGS associated with endoderm
assumed character
1 - Andrew, 2011
2 - Giribet et al., 2001
3 - Koenemann et al., 2010
4 - Meusemann et al., 2010
5 - Oakley et al., 2013
6 - Regier al., 2005
7 - Regier al., 2009; Regier al., 2010
8a,b - von Reumont al., 2009
9 - von Reumont al., 2012
10 - Schutz and Regier, 2000
Tardigrada
Onychophora
Pycnogonida
Eucheliceratа
Myriapoda
Remipedia
Ostracoda
Branchiura
Mystacocarida
Cirripedia (ThRh)
Copepoda
Malacostraca
Branchiopoda
Malacostraca
Cephalocarida
Branchiopoda
Remipedia
Branchiopoda/Remipedia/Copepoda
Entognatha
Ectognatha
Oligostraca
Multicrustacea
Allotriocarida
8b
8b
8b
2,3
2,8a
10
4,6,9
5,9
8a
?
Decapoda
Euphausiacia
?
Amphipoda
?
Anostraca
Notostraca
Cladocera
A
Eutrochozoa
Onychophora
Pantopoda
Euchelicerata
Crustacea
Myriapoda
Hexapoda
Štys and Zrzavý, 1994
B
Annelida
Tardigrada
Pantopoda
Trilobitomorpha
Linguatulida (Pentastomida)
Chelicerata
Branchiata (Crustacea)
Myriapoda
Hexapoda
Dogiel, 1981
C

related to Chelicerata, forming a monophylum Paradoxopoda, or Myriochelata (Dunn et al., 2008; Reumont et al., 2009; Meusemann et al., 2010). However, as long as the results of the current work in no way contribute to the clarification of the major arthropod relationships, it will be left out of the further discussion.

4.2.1. 4-cell stage

Cleavage variety found in crustaceans reviewed many times and discussed elsewhere (Costello and Henley, 1976; Siewing, 1979; Ivanova-Kazas, 1979; Scholtz, 1997). In this chapter I want to address to exclusively spatial arrangement of the cells during the cleavage.

A tetrahedral arrangement of the blastomeres at the 4-cell-stage leading in the course of further cleavage to the formation of two broadening interlocking cell bands (so called "tennis ball" pattern) has been carefully proposed to be a developmental characteristic of the crustaceans (Alwes, 2008).

This suggestion, however, has to be dealt with caution, since the first half of it (regarding the 4-cell stage) can be true for various animals and does not necessarily lead to the second half. Indeed, a tetrahedral 4-cell stage has been reported for some other arthropods: pycnogonids (Ungerer and Scholtz, 2009), ecdysozoans: nematodes (Malakhov, 1986; Schierenberg, 2005), and even within other protostomian groups like some flatworms (Willems et al., 2009; Caspari, 2010) and chaetognaths (Elpatievsky, 1907; Shimotori and Goto, 2001). Clearly, such cell arrangement might be an ancient cleavage feature preserved in development for many recent animals. Additionally, some curious fossil findings support this idea (Xiao et al., 1998). If the neoproterosoic fossils are indeed from an animal embryonic stage, as it was interpreted by the authors, the tetrahedral 4-cell stage evolved long before the major arthropod split. Nevertheless, such blastomere arrangement could have been lost and evolved independently along the evolutionary way of different arthropod and crustacean groups. On the base of the current data it is, unfortunately, hard to prove either way.

On the other hand, what can in fact be considered as a crustacean feature is a "tennis ball" organisation of the blastula (for detailed review on occurrence of this pattern among crustaceans see Alwes, 2008 as well as on the Fig. 4.2.2.). This pattern can without question be observed from the 16-cell stage on, when cross furrows become two-cell wide (for example, see Hertzler and Clark, 1992; Alwes and Scholtz, 2004; Biffis et al., 2009; Pawlak et al., 2010)

Within Thecostraca *E. modestus*, together with some other investigated thoracican species (Bigelow, 1902; Delsman, 1917), show some similarity to the "tennis ball" arrangement. The blastomeres of the A-C band follow all the rules of a "typical" cell band: their divisions are always in the same direction (and perpendicular to those in the blastomeres of the other band, which follow the pattern – see below), the spindles of cleavages alternate between transversal and longitudinal

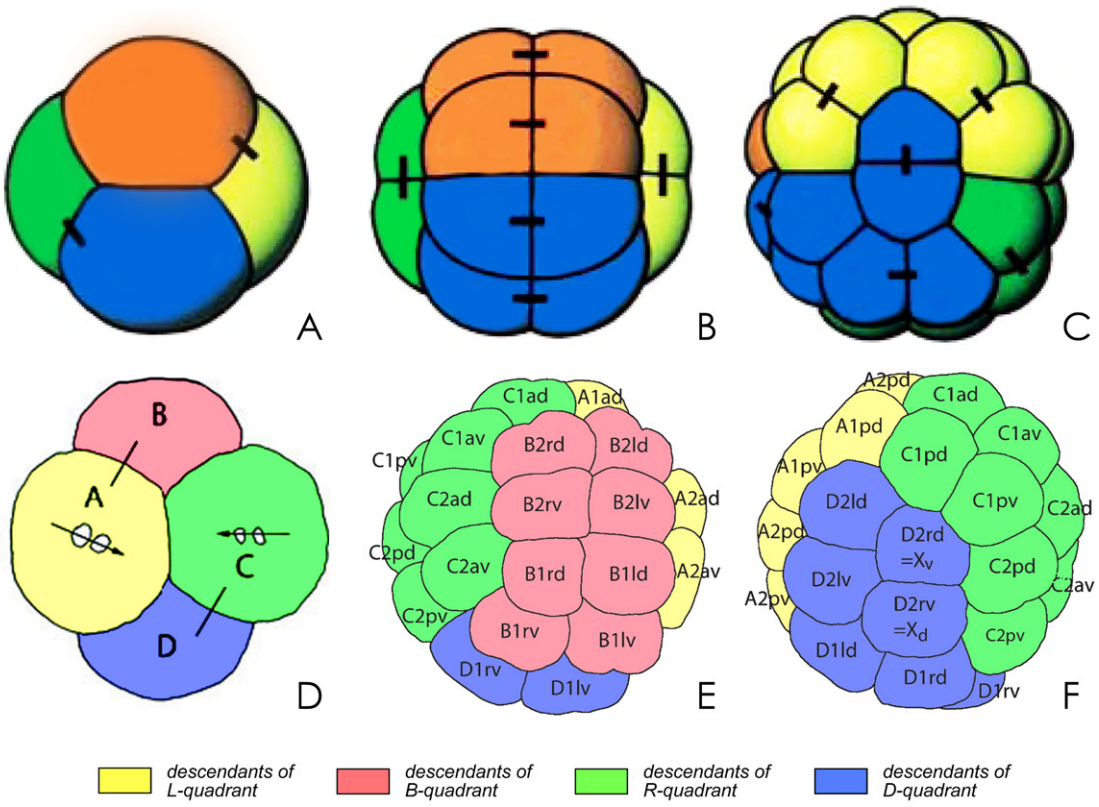

Fig. 4.2.2. Blastomere arrangement during cleavage in the crustacean embryos. Cell bands.

A-**C** – *Meganyctiphanes norvegica*, modified from Alwes and Scholtz (2004), **A** – 4-cell stage, vegetal cross furrow; **B** – 16-cell stage, vegetal pole; **C** – 32-cell stage, the side view of the A-C band; **D**-**F** – *Marsupenaeus japonicus*, modified from Pawlak et al. (2010), **D** – 4-cell stage, animal cross furrow; **E** – 32-cell stage, the side view of the vegetal cross furrow; **F** – 32-cell stage, the side view of the animal cross furrow.

in relation to the band itself, the contact zone (an animal cross furrow) is getting broader every second division from fourth division on (Fig. 3.3.2.). The B-D band is, however, distorted in the middle, although the blastomeres placed on the "ends" of the band do divide according to the just listed rules. Those derivatives of the B and D quadrants, which form the vegetal cross furrow, divide always in the same direction. Thus, the cross furrow is always of a one-cell width (details see in Chapter 3.3.1.).

The cleavage of *Tetraclita rosea* and the other three species described by Anderson (1969) differs significantly in the arrangement of blastomeres and it is impossible to observe any cell bands. However, as it was referred in the Chapter 4.1., the Anderson's identification of the cells might have been wrong.

On the other hand, the number of thecostracans, which do not show cell band arrangement is rather big. First of all, it is the embryos of *Ibla quadrivalvis* (Anderson, 1965) and of the different rhizocephalans (Shirase and Yanagimachi, 1957; Bocquet-Vedrine, 1961; 1964; Scholtz et al., 2009). They do not seem to have an invariant division pattern beyond the 8-cell stage at all

(Fig. 4.2.4.). However, taking into account the suggestion about the derived state of the early development for these two groups within Cirripedia (Scholtz et al., 2009), the absence of the bands could possibly be an evolutionary loss.

Second, the cleavage in the thoracican *S. scalpellum* (Krüger, 1922), the acrothoracican *Trypetesa nassarioides* (Turquier, 1967), and ascothoracidian *Ascothorax* (Vagin, 1949) does not lead to formation of any recognizable cell bands either (Fig. 4.2.3). One cannot deny though, that in *Scalpellum* and *Ascothorax* the arrangement of the blastomeres of the A and C quadrant at the 16-cell stage and their two-cell wide cross furrow do resemble vaguely the cell band (Fig. 4.2.3.D,F). The placement of the blastomeres on the following stages does not show this pattern anymore. Due to the phylogenetical placement of Thoracica within Thecostraca (Fig. 4.1.1.A), one naturally comes to the question, whether the A-C band observed in thoracicans can be homologized with that of other crustaceans or it is a secondarily acquired condition with the loss of

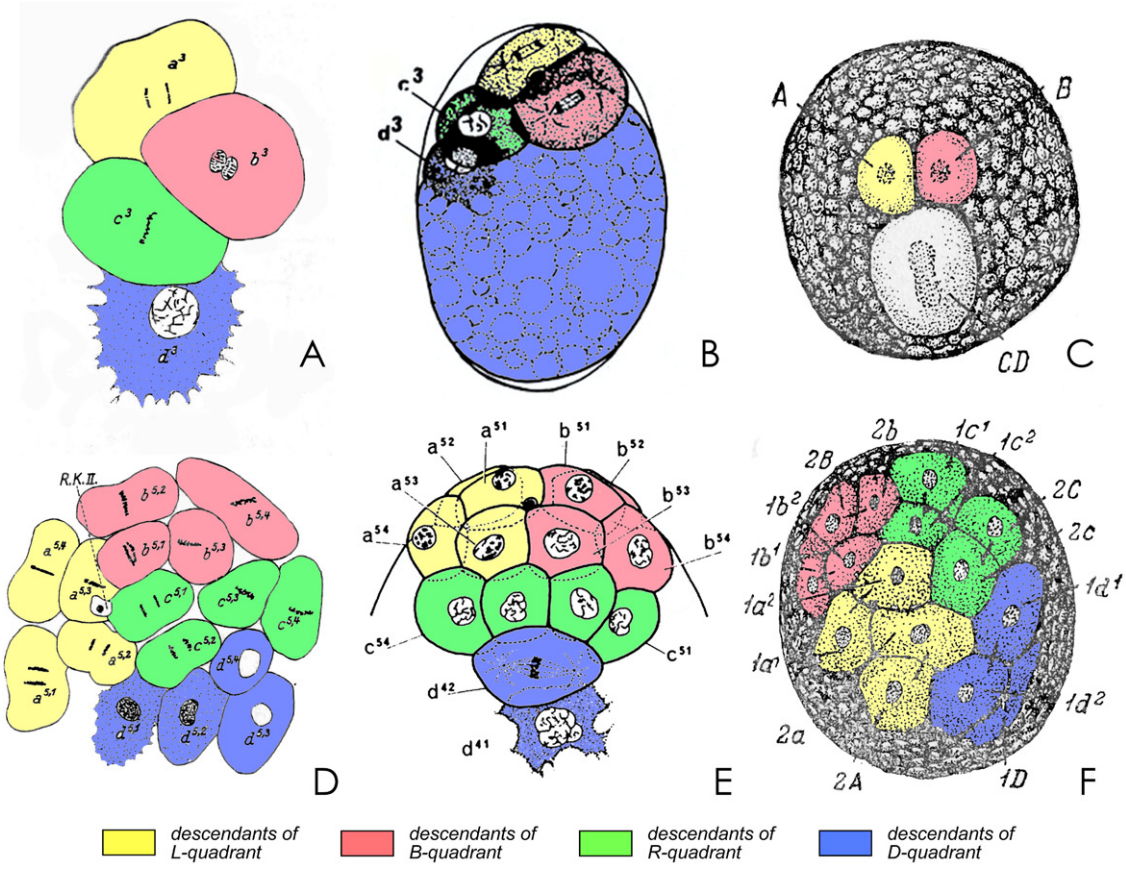

Fig. 4.2.3. Blastomere arrangement during cleavage in the thecostracan embryos. Cell bands?

A,**D** – *Scalpellum scalpellum*, modified from Krüger, 1922, **A** – 4-cell stage; **D** – 16-cell stage, it is possible to recognize the two-cell wide animal cross furrow, the A-C band is modified though; **B**,**E** – *Trypetesa nassarioides*, modified from Turquier (1967), **B** – 4-cell stage, **E** – 14-cell stage, no band is recognizable; **C**,**F** – *Ascothorax*, modified from Vagin (1949), **C** – 3-cell stage, **F** – 15-cell stage, the two-cell wide animal cross furrow, one can see the A-C band.

some yolk[♣] as it logically appears from the Fig. 4.1.1. Unfortunately, the data for Acrothoracica and Ascothoracida are known for one species each (Turquier, 1967; Vagin, 1949). And these data have been obtained by means of light microscopy. Not to show disrespect for the method, but by now the information appears to be insufficient to make far going conclusions on the ancestral pattern of cleavage in Thecostraca.

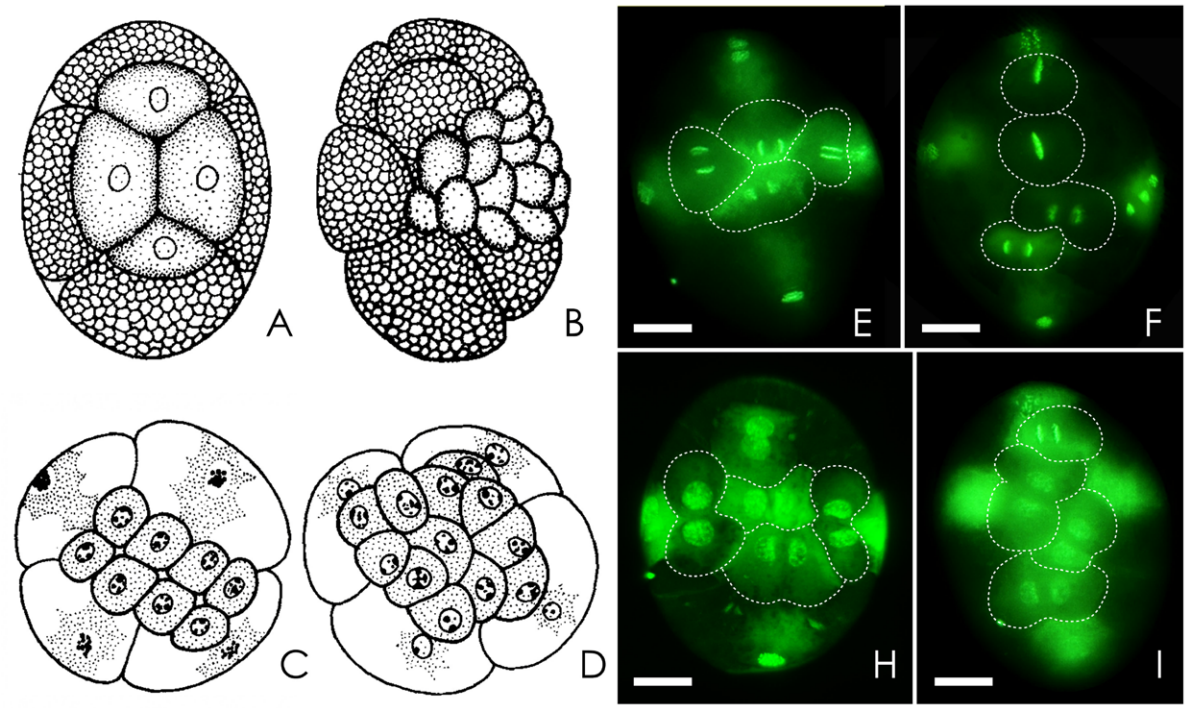

Fig. 4.2.4. Blastomere arrangement during cleavage in the rhizocephalans and iblomorph embryos. No cell bands.

A-**B** – *Ibla quadrivalvis*, modified from Anderson (1965), **A** – 4-cell stage, animal pole view; **B** – late stage of cleavage, side vie; **C**-**D** – *Sacculina carcini*, modified from Bocquet-Védrine (1964), **C** – 4-cell stage, animal pole view; **D** – 16-cell stage view, animal pole view; **E**-**H** – *Peltogasterella gracilis* (see Appendix II for explanation), animal pole view, micromeres are outlined, note the various arrangements of the micromeres, **E**-**F** – fourth division; **G**-**H** – end of fourth division, 15-16-cell stage.

4.2.2. Mirror images

Another characteristics of *E. modestus* shared with some crustaceans is the presence of two chiral versions of cleavage, which leads to so-called mirror image embryos. Within cirripedes this has been first described by Groom (1894), but his observations were considered erroneous by Bigelow (1902). Afterwards no other researcher mentioned the presence of mirror imaged barnacle embryos. Within crustaceans, however, eggs of two chiral types have been discovered

[♣] It is suggested, that amount of yolk does not really influence the type of cleavage (Ivanova-Kazas, 1979; Scholtz, 1997). However, in the mentioned species the reason for extremely unequal divisions and late gastrulation is thought to be relatively bigger yolk amount compared to the majority of thoracicans (Krüger, 1922; Vagin, 1949). The same reason can also cause more or less chaotic placement of the blastomeres and absence of "bands".

for Euphausiacea: *Euphausia* (Taube, 1909), *Meganyctiphanes norvegica* (Alwes and Scholtz, 2004); Dendrobrancheata: *Penaeus monodon* (Biffis et al., 2009), Amphipoda: *Orchestia cavimana* (Scholtz and Wolff, 2002), Cladocera: *Polyphemus pediculus* (Kühn, 1912), *Holopedium gibberum* (Baldass, 1937), *Daphnia pulex* (Baldass, 1941), and some others. Yet again as well as with the pattern of tetrahedral 4-cell stage, the sampling of animals demonstrating two mirror images of early development extends far beyond crustaceans and includes some molluscs, annelids (see short review in Luetjens and Dorresteijn, 1995), chaetognath (Shimotori and Goto, 2001) and others as well.

Apparently, the presence of the two mirror images in the development is a quite common feature for many animals and it has been persistently reported in the crustacean descriptions. Nevertheless, it is hard to use it in any way, unless the reasons and the purpose of this event are understood. There are some speculations on this matter (Scholtz and Wolff, 2002), but none of them are proven so far.

4.2.3. Blastopore and ectomesoderm formation

The presence of ectomesoderm originating from mesectoblasts has been described for many crustaceans (Bigelow, 1902; Taube, 1909; Kühn, 1912; Fuchs, 1914; Delsman, 1917; Cannon, 1921; Anderson, 1969; Hertzler, 2002), as well as for some other ecdysozoans (Sulston et al., 1983; Houthoofd et al., 2003), and most of the spiralians[♣] (for a short review see Hejnol et al., 2007; Table 4.3.1.). Interestingly, the early formation of ectomesoderm shows a similarity, which is restricted exclusively to some crustaceans: it originates from the blastopore surrounding cells. In fact, in the case of the cirriped *E. modestus* (present work), copepod *Cyclop viridis* (Fuchs, 1914), cladoceran *Simocephalus vetulus* (Cannon, 1921), dendrobranchiates *Sicyonia ingentis* (Hertzler, 2002) and *Litopenaeus vannamei* (Hertzler, 2005), and euphausiacean *Meganyctiphanes norvegica* (Alwes, 2008) <u>all</u> the blastopore cells give rise to ectomesoderm. These cells in some malacostracans (Euphausiacea and Dendrobranchiata) have been referred to as crown cells and their number is considered to be of importance for the phylogeny of the groups (Taube, 1909; Zilch, 1978; Hertzler and Clark, 1992; Alwes and Scholtz, 2004; Hertzler, 2005; Biffis et al., 2009 – not for all of the described crown cells the lineage was traced till their differentiation).

For the cirripedes apart from *E. modestus* this was described differently. In the table 4.1.1. one can see that some researchers considered endomesoblasts ($2d^l$ and $2d^r$) to form a blastopore. On

[♣] Here and further the name "spiralian" is used for the group classically comprising Annelida, Echiura, Kamptozoa, Sipunculida, Mollusca, Nemertini, and Platyhelminthes (currently subdivided into Trochozoa, Polyzoa, and Platyzoa, see fig. 4.4.1.)

the base of the results of live observations conducted in the present study, it could be concluded, that the blastopore is formed by mesectoblasts, while the endomesoblastic cells just migrate inside through the closing blastopore. Among other non-malacostracans it was described, that additionally to the mesectoblastic cells the endoblast participates in the organization of the blastopore (reviewed in Manton, 1928; 1949; Baldass, 1941; Weygoldt, 1960b). On the base of the illustrations in the literature it could be speculated though, that the next step leading to the internalization of the endoblast would also lead to the blastopore surrounded exclusively by mesectoblastic cells. This, however, has to be proven by live examination.

The number of crustaceans, which do not show the same pattern of the ectomesoderm formation, is on the other hand, rather big. First of all, in the entire group of malacostracans, which form a germ disc during embryogenesis, a "typical" blastopore cannot be identified and the cell lineage of cells surrounding the blastopore as the internalization locus is poorly established (for reviews see Manton, 1926; Gerberding and Patel, 2004). Gastrulation together with the cell lineage is well documented only for *Orchestia cavimana* (Wolff and Scholtz, 2002; Hunnekuhl and Wolff, 2012) and *Parhyale hawaiensis* (Gerberding et al., 2002; Alwes et al., 2011). The cell lineages of both animals are highly similar save for different nomenclature. Yet one major difference can be outlined. *O. cavimana* does not seem to have an ectomesoderm, as the three blastomeres (A, ba, and da) contribute to both mesoderm and endoderm. *Prh. hawaiensis*, in contrast, has exclusively ectomesoderm. This difference is explained by various interpretation of the origin of midgut glands, originating from these blastomeres. They are considered to be the product of endoderm in studies on *O. cavimana* and the product of mesoderm in those on *Prh. hawaiensis*. Regardless of the lineage, the "typical" blastopore is not formed in either of the two. Moreover, in *O. cavimana* and *Prh. hawaiensis* the internalization of mesodermal mass happens through different zones: through the central the central gastrulation center/"rosette" and additionally through either the locations placed lateral to the "rosette" (Gerberding et al., 2002; Alwes et al., 2011) or the groove extended along the germ disc (Wolff and Scholtz, 2002). These observations do not fit the pattern of a mesectoblastic blastopore, but this could be considered as another supportive detail to the view, that *Orchestia cavimana* and *Parhyale hawaiensis* possess a derived mode of the early development (Scholtz and Wolff, 2002).

Presumably, the blastopore of *Ascothorax* (Vagin, 1949), *Trypetesa* (Turquier, 1967), and *Scalpellum* (Krüger, 1922) is also not formed by mesectoblasts as there has not been ectomesoderm reported for these animals. However, the cells, which are to form the blastopore, are interpreted as mesodermal. To clarify this and to identify the origin of the mesoderm in these species for sure, the cell tracing experiments are required.

The absence of relevant data on other non-malacostracans does not allow concluding the origin of their blastopore cells either. It is described for branchiopods *Daphnia pulex* (Baldass, 1941) and *Artemia salina* (Benesch, 1969), an ostracod *Cyprideis litoralis* (Weygoldt, 1960a), and a copepod *Lernaeocera branchialis* (Kohler, 1976) that the mesoderm comes exclusively from the region of the blastopore, although the detailed cell lineage of the mesodermal cells have not been performed. In these species there also can be a complication with defining a "true" blastopore, since there are two locations of internalisation of the germ layers: one for the mesoderm and the germ-line cells and another for the endoderm. And according to Manton's (1949) definition, only the place of endoderm internalization can be considered as a true blastopore.

After mapping the occurrence of the blastopore formed by mesectoblasts on the generalized tree, it appears to be reasonable to suggest its presence also in the last common ancestor of Multicrustacea (Fig. 4.2.1.). It is, nevertheless, not very clear how to interpret such blastopore in the cladoceran (Cannon, 1921). Its presence would be quite coherent, when Branchiopoda is placed together with Multicrustacea. However, in case of the branchiopods being part of Allotriocarida, the ectomesoblastic blastopore either derived independently for the cladocerans or is a more ancient characteristic and could have been present in the pancrustacean ancestor. These suggestions hold true also if the malacostracans or the copepods form a sister group to the branch, which includes Hexapoda. Clearly, the data at hand do not allow make a proper analysis so far.

4.2.4. Fore- and hindgut development

In crustaceans gut formation (the development of the endodermal midgut is not considered here) has been investigated mostly in relation with the question on the mouth and anus position and their relation to the blastopore (reviews are in Manton, 1949; Weygoldt, 1960b; Benesch, 1969; Scholtz and Wolff, 2002). In most of the crustaceans the classical protostomy, when the blastopore develops directly into a stomodaeum, is absent. After the blastopore closure the epidermal cells of its region form the hindgut (Reichenbach, 1886; Agar, 1908; Manton, 1928; Hickman, 1936; Weygoldt, 1960a; Fioroni, 1970). The mouth is opened anew at the anterior-ventral region of the embryo (Fig. 4.2.5.A). In *Cherax* it is slightly different, and proctodaeum develops somewhat anterior to the zone of closing blastopore (Scholtz, 1992). In the case of the two-phased gastrulation described for *Artemia salina* (Benesch, 1969) and *Cyprideis litoralis* (Weygoldt, 1960a), the mouth location corresponds to the endoderm internalization location, while the anus is formed in the area of mesoderm internalization. In some exceptional cases, like that of amphipods *Gammarus pulex* (Weygoldt, 1958; Scholtz, 1990), *Parhyale hawaiensis* (Gerberding et al., 2002; Alwes et al., 2011), and *Orchestia cavimana* (Scholtz and Wolff, 2002), the mouth cor-

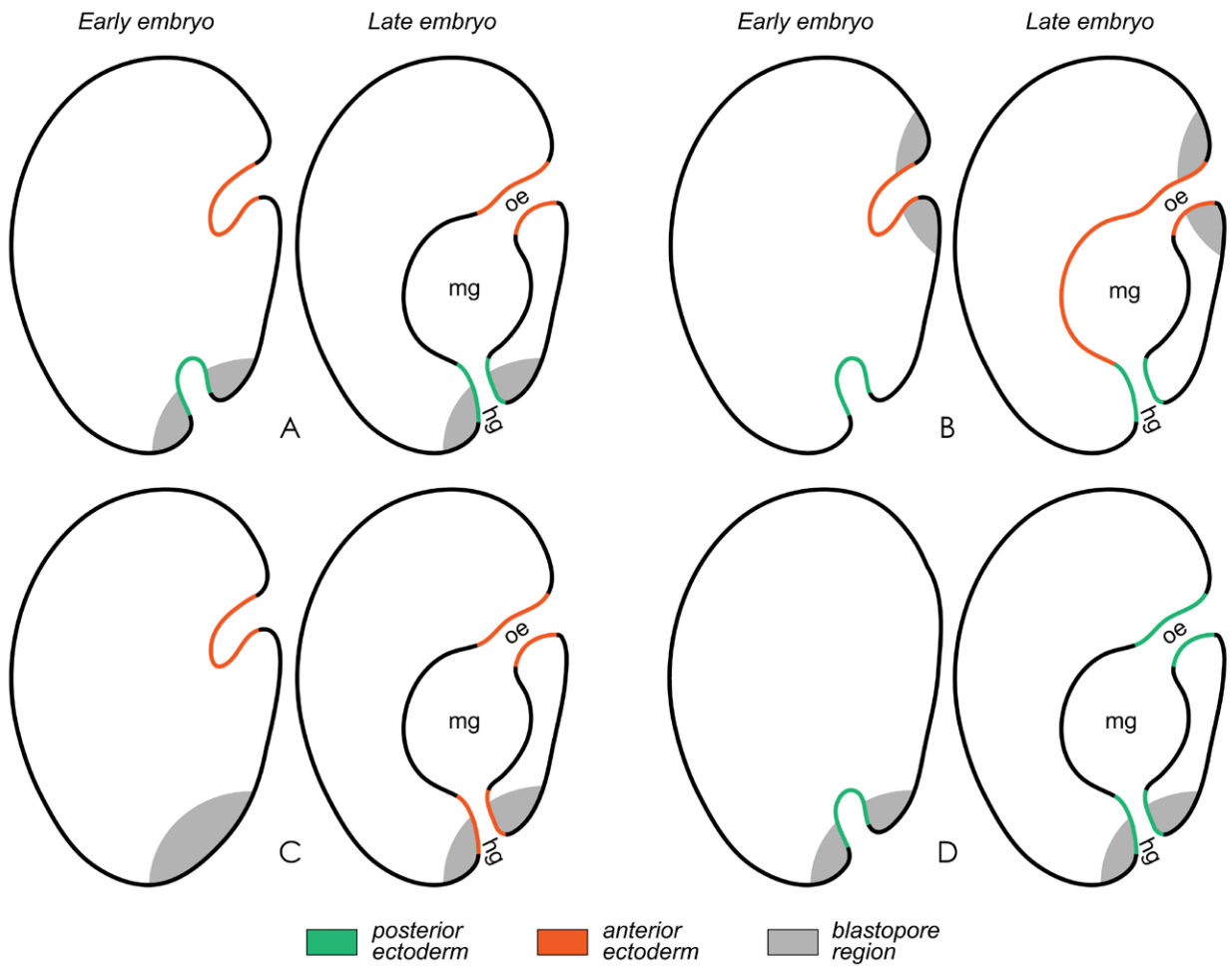

Fig. 4.2.5. Variety of the fore- and hindgut formation in relation to the blastopore among the crustaceans.

A – the hindgut develops in the area of the blastopore, the foregut is formed by the invagination of the anterio-ventral ectoderm (condition for many crustaceans, see text for references); **B** – the hindgut develops posterior to the blastopore, foregut is formed in the area of the blastopore, condition found in Amphipoda (Weygoldt, 1958; Scholtz, 1990); **C** – the fore- and hindgut develop together from a singular invagination of the anterio-ventral ectoderm, the position of the hindgut later corresponds to the area of the blastopore, condition found for *Semibalanus balanoides* (Delsman, 1917) and *E. modestus* (present study); **D** – the foregut develops from the cell material of the blastopore area, its final position of it is, however, anterior to the blastopore; the hindgut position corresponds to the area of the blastopore, condition described for *Holopedium gibberum* (Agar, 1908) and *Cyprideis litoralis* (Weygoldt, 1960a).

responds to the area of the blastopore and the hindgut opens posterior to it (Fig. 4.2.5.B). Such "protostomy" has been recently observed on the example of *Priapulus caudatus* (Ecdysozoa: Priapulida) and has been suggested to be a derived condition within Ecdysozoa (Martín-Durán et al., 2012). Similarly, if one concludes that "deuterostomy" is a plesiomorphic character for Crustacea as well as Ecdzsoyoa, then the development of mouth in amphipods is also a derived condition within Crustacea as well as Malacostraca.

Generally, the situation in *E. modestus* is similar to the most of the crustaceans. By means of cell tracing it has been shown, that the position of the anal opening corresponds to the area of the

former blastopore. The mouth opens anterior-ventrally to it. However, the development of the ectodermal parts of the alimentary canal follows a rather interesting pattern. Both the fore- and the hindgut start to develop together on the anterior-ventral side of the embryo as a common invagination of the ectoderm. This side is opposite to the side where the blastopore was closed. The invagination deepens, elongates, turns posteriorly, and cuts the posterior part off (Fig. 3.5.6.; Fig. 4.2.5.C). The latter will become the hindgut (details see in the Chapter 3.5.2.). The cell material for both the stomo- and the proctodaeum has been traced to originate from two blastomeres in the 16-cell stage ($1a^p$ and $1c^p$, each contributing to the left or right epidermis of both gut portions). The only record of the same way of gut development in cirripedes comes from Delsman (1917) for *Semibalanus balanoides* (Fig. 4.2.6.A). Anderson (1969) also illustrates an intermediate stage of the gut formation (Fig. 4.2.6B.), but he does not provide any notation or comment to the cell material of the hindgut. At the very late stage of the embryonic development the hindgut is interpreted as a posterior midgut of endodermal origin (the offspring of the blastomere 2d, in his description 4d) (Fig. 4.2.6E, marked as hindgut.). The hindgut development itself he describes later in his review paper as following: "A proctodaeum also invaginates at the posterior midpoint of the postnaupliar ectoderm... The ingrowing proctodaeum pushes through the posterior mass of mesoderm..." (Anderson, 1979). Surprisingly, it happens completely different in the species observed by Delsman (1917) and in the present work. Moreover, when one compares the figures of Anderson (1969), Delsman (1917), and those form the current study (Fig. 4.2.6.A-C, compare developing hindgut on A and C with outlined region on B), it appears as if they illustrate the same process, but with different interpretations.

In other crustaceans, as has been mentioned above, attention was mostly paid to the relation in positions of the mouth, anus, and blastopore. Cell material contributing to the formation of the stomodaeum and hindgut was described briefly or not at all. On the base of the provided illustrations it can be inferred though. In most of the studies these two portions of the alimentary canal develop separately as epidermal invaginations of the corresponding regions (Reichenbach, 1886; Manton, 1928; Hickman, 1936; Nair, 1956; Fioroni, 1970; Benesch, 1969, and others) (Fig. 4.2.5.A). Similar to the thoracicans, as it was already suggested by Weygoldt (1960a), the same cell material seems to contribute to the fore- and the hindgut of *Holopedium gibberum* and *Cyprideis litoralis* (Agar, 1908; Weygoldt, 1960a). The development of the different parts of the alimentary canal happens, however, in a reverse way. The cell material invaginating in the area of the blastopore moves towards the anterior along the ventral midline (Fig. 4.2.5.D). The final anterior position of the migrating cells corresponds to the future stomodaeum. Furthermore, one could also speculate regarding the illustrations on crayfish development by Reichenbach (1886).

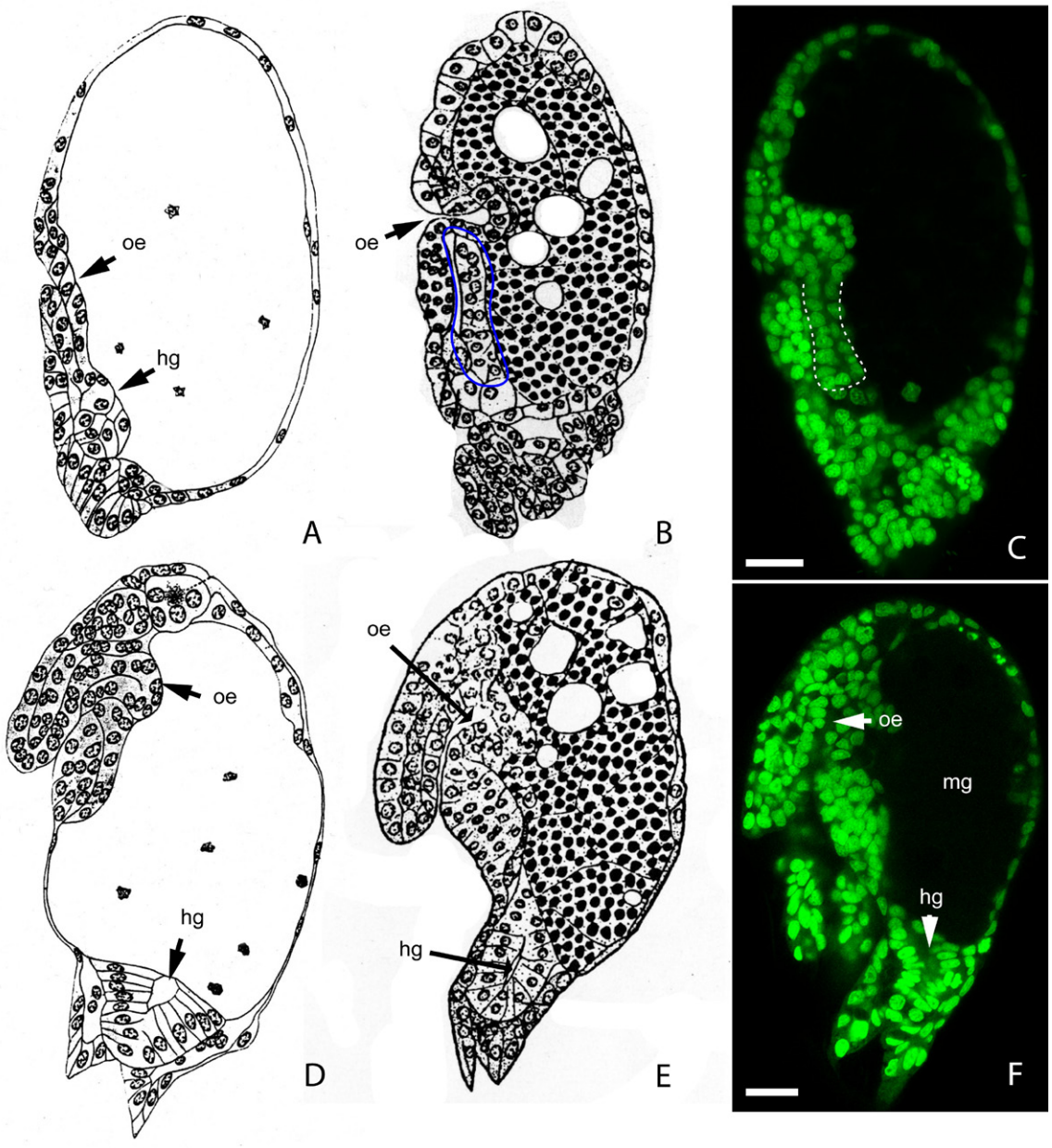

Fig. 4.2.6. The gut formation in Thoracica.

All the images – median section, view from the left.

A-**C** – embryonic stage 7, **D**-**F** – embryonic stage 9; **A**,**D** – *Semibalanus balanoides*, modified from Delsman (1917), **A** –anterio-ventral invagination of fore- and hindgut, **D** – hindgut is formed; **B**,**E** – *Tetraclita rosea*, modified from Anderson (1969), **B** –only invagination of the oesophagus is marked by the author, note the set of nuclei right under the ventral epidermis of the hindbody, outlined by the blue shape; **E** – the hind gut is formed; **C**,**F** – *E. modestus*, **C** – the posterior part of anterio-ventral invagination (outlined) will develop into a hindgut. Scalebar 20 μm.

Fore- and hindgut seem to invaginate from one region of the germ disc, which might mean that the invaginating cells have a big chance to have a common origin.

The unique way of hindgut development in some thoracicans can represent an interesting model for further investigations. To a certain degree it shows not only the secondary mouth presence

(deuterostomy), but also the presence of a secondary gut (deuteroprocty(?)). An understanding of its molecular background might possibly provide some additional material to the ongoing discussion on mouth-anus evolution (Arendt et al., 2001; Hejnol and Martindale, 2008; 2009; Martín-Durán et al., 2012). For example, it is known that the gene expression of *brachyury* (bra) is associated with the blastopore and the hindgut area of ecdysozoans, and that of *goosecoid* (gsc) with the animal pole and the stomodaeum region (based on nematodes, insects, and *Priapulus*). Where would these genes express in the embryos of thoracicans? Will gsc products be found in the hindgut? Could the expression of bra be missing after the blastopore closure? Might it possibly lead to the conclusion of non-homologous hindguts across Crustacea? Some questions to work on.

4.2.5. Postnaupliar mesoderm

The data on postnaupliar mesoderm (PNM) in crustaceans are quite misbalanced. There is a huge amount of literature on the development of the PNM, mostly for malacostracans (reviewed in Dohle et al., 2004), while there are just a very few data concerning their origin and again only for malacostracans. According to the literature, in dendrobranchiates *Sicyonia ingentis* and *Litopenaeus vannamei* as well as euphausiacean *Meganyctiphanes norvegica* the mesoderm of the postnaupliar segments comes from the derivatives of a single mesendoblastic cell X_v (Hertzler and Clark, 1992; Hertzler, 2005; Alwes, 2008). The only difference is that in *S. ingentis* and *P. vannamei* mesoteloblasts can be traced back to the one descendant of X_v (Hertzler and Clark, 1992; Hertzler, 2005). In contrast, in *Meganyctiphanes norvegica* it is two non-sister cells which differentiate into mesoteloblasts (Alwes, 2008). A mesendoblastic origin of the PNM has been also shown in *Orchestia cavimana* (Wolff and Scholtz, 2002; Hunnekuhl and Wolff, 2012). However, in this case PNM is tracked back to the two cells, ba and da, which are derived from two non-sister quadrants. The cell lineage leading to the PNM in *Parhyale hawaiensis* is very similar to that of *O. cavimana* (Gerberding et al., 2002; Alwes et al., 2011), with the mentioned above exception related to the nature of midgut glands.

Unfortunately, there is no data on the lineage of the PNM for non-malacostracans. In *E. modestus* it has not been followed in detail either, as the study has not proceeded much further than to the nauplius I. Nevertheless, there are some candidates for possible precursors of the PNM. These are the two pairs of cells (uc2, see chapter 3.5.3 and Fig. 3.5.7.) placed in the embryo posterior to the midgut in the space between the walls of the hindgut and the body. Their line was traced back to the ectomesoblasts originating from 1d (or 2R).

By comparison with the few data that exist, one can conclude that the ectomesodermal origin of the PNM in *E. modestus* represents a rather unusual character. Clearly, the species, which have been reported not to have an endomesoderm♣: the cladocerans (*Polyphemus pediculus* (Kühn, 1912) and *Holopedium gibberum* (Baldass, 1937), *Daphnia pulex* (Baldass, 1941)) and the copepods (*Cyclops viridis* (Fuchs, 1914) and *Tisbe furcata* (Witschi, 1934)), would develop the PNM from ectomesoderm as well. However, the embryos of *E. modestus* are by now the only known ones to develop the PNM from ectomesoblasts, while endomesoblast contributes to the formation of the naupliar muscles.

Unfortunately, having data only for the two closely (most likely) related groups (Cirripedia and Malacostraca) does not help much in the overall analysis of PNM in Crustacea. Therefore one could only suggest a more broad and profound investigations on the subject.

Regarding the claim of Anderson (1969) about the presence of mesoteloblasts in cirripedes, it is not proven by the results of this study. The nauplius I and II have scattered mesodermal cells in the hindbody, which presumably descend from the two pairs of the uc2, depicted also by Anderson as mesoteloblasts. The position of their products and the equal appearance of them speak, however, in favour of a non-teloblastic nature of these cells. That can be also supported by the observation of the formation of thoracic segments in the rhizocephalans *Sacculina carcini* and *Peltogasterella gracilis* (unpubl. data). To prove it for thoracicans for certain the division pattern should be thoroughly investigated. In general, mesoteloblasts as well as ectoteloblasts are not yet found outside malacostracans (for review see Dohle et al., 2004).

4.2.6. Notes on myogenesis

Most detailed data on myogenesis for crustaceans are available for malacostracans: isopods (Kreissl et al., 2008), marbled crayfish (Jirikowski et al., 2010), and american lobster (Harzsch and Kreissl, 2010). Myogenesis in non-malacostracan has been described for the branchiopod *Artemia salina* (Benesch, 1969; Anderson, 1967) and also for the cirripedes *Ibla quadrivalvis* and *Tetraclita rosea* (Anderson, 1965, 1969). The studies for non-malacostracans are restricted to the description of the morpho-anatomical process of mesoderm differentiation without going into a cellular level.

During the study on the mesodermal lineage in *E. modestus* it was possible to obtain some results on the myogenesis in the naupliar limbs. According to the observations, muscle differentiation starts at the embryonic Stage 5. With outpocketing of the limb buds the myoblasts, placed laterodorsally, are subdivided into the "internal" and "external" groups (Fig. 3.5.1.). Correspondingly, these groups of mesodermal elements will develop into extrinsic and intrinsic limb muscles. In

♣ In general, the absence of endomesoderm in so different crustacean groups would suggest the possible absence of it in the pancrustacean ancestor as well (Fig. 4.2.1.). However, this issue will be discussed below.

the process of elongation of the limb buds, the myoblasts, or muscle precursors (MP), stretch towards the future attachment sites and eventually attach. Many myoblasts of the internal and external groups seem to attach from different sides of the same attachment sites placed at the base of the protopodites (Fig. 3.5.1.; Fig. 3.5.5.G:2). During the myogenetic process it was impossible either to observe when the fusion of the mesodermal elements happens if at all or to identify any muscle precursor, which could play a role of a single muscle founder. On the contrary, all the myoblasts appeared the same at all the stages of myogenesis till the formation of muscle bundles. Additionally, the number of mesodermal cells at the stage of clusterization roughly corresponds to the number of forming muscles (not muscle bundles)♣. This suggests that every mesoderm cell can be considered a muscle precursor and develops into a single muscle. The possibility of a temporary fusion and later subdivision into separate fascicles (like it happens in some muscles of a grasshopper, Jellies, 1990) seems very unlikely, although not impossible.
On the base of all the available studies one can outline three different models of muscle development described for crustaceans until today (Fig. 4.2.7.).

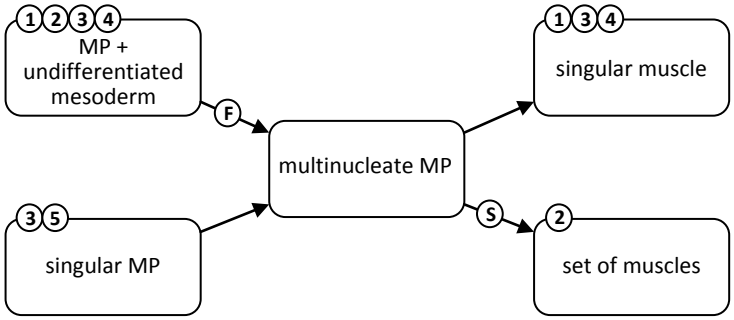

Fig. 4.2.7. Schematized myogenesis in crustaceans
1 – Decapoda (Marble crayfish)
2 – Decapoda (American lobster)
3 – Isopoda
4 – Amphipoda (*O. cavimana*)
5 – Cirripedia (*E. modestus*)
F – fusion
S – subdivision

1. A single muscle founder cell, or mononucleate MP, initiates the muscle formation by fusing with surrounding undifferentiated mesoderm cells and forming a syncitial muscle primordium, or multinucleate MP. The multinucleate precursor develops further into a single muscle. This model was observed in crayfish (Jirikowski et al., 2010) and also in some insects (Ho et al., 1983; reviewed in Jellies, 1990; Bate, 1990). The same way of myogenesis was also suggested for amphipod *O. cavimana*, although it was not documented (Hunnekuhl and Wolff, 2012).
2. A mononucleate MP develops into a binucleate MP and later into a multinucleate MP. Every multinucleate MP differentiates into a single muscle. This scenario has been described for isopods♣♣ (Kreissl et al., 2008) and cirripedes (present work).

♣ count has only been performed for the segments of *aI* and *all*
♣♣ According to personal comments by Jirikowski, the multinucleate MP in isopods is formed by fusion with surrounding undifferentiated mesoderm (what is not specified in the paper of Kreissl et al., 2008). This makes the model 2 in isopods highly similar to the model 1.

3. Multinucleate primordia are formed by means of fusion with surrounding cells. These later subdivide into a set of muscles as it was exemplified by the studies on the american lobster (Harzsch and Kreissl, 2010) and insects (reviewed in Jellies, 1990).

In *E. modestus* the state of multinucleate primordia has not been observed. Nevertheless, the developed muscles had numerous nuclei placed along the actin-myosin frame. Logically, with no fusion observed one could conclude that nuclei just pass sequential divisions. Additionally, it was shown earlier in the literature that the muscles of the nauplius larvae in cirripedes do not subdivide during later larval development (Walley and Rees, 1969; Anderson, 1987). They either correspond to the muscles in the following cypris (with slight modification) or are being histolyzed during the last molt.

On the base of the available data it is impossible to sum up the diversity of muscle development pathways observed in crustaceans in regards of a possible evolutionary scenario. To make a proper analysis, one has to establish a set of different muscles, which can be homologized between different crustacean groups, and investigate the myogenesis for each of these muscles. In addition to the problem of diversity, there is also a problem with fragmented data. Myogenesis within the mentioned crustacean groups was observed for muscles in different body zones. One cannot exclude that muscle formation within the nauplius and the postnaupliar region might involve various mechanisms. For example, in case of cirripedes one cell/one muscle model could be explained by the small amount of cells in the embryo. Thus, in the late nauplius and cypris larva, which are built of more cells than the embryo, thoracic muscles might follow the same model as they do in malacostracans.

So far it has been suggested that the mode of syncitial MP subdividing into separate subunits as found in the american lobster represents the ancestral state for crustacean muscle development (Kreissl et al., 2008; Harzsch and Kreissl, 2010). The way of development observed in isopods has been assumed to be derived by the same authors. This assumption is based on the comparison of late myogenesis in the american lobster with that in the dendrobranchiate shrimp *Sicyonia ingentis*[♣♣] (Kiernan and Hertzler, 2006). The embryos of *Sicyonia* have been shown to develop extrinsic muscles, which extend from inside the nauplius body into the distal parts of the limbs (Kiernan and Hertzler, 2006). There have not been any intrinsic muscles reported. According to the suggestion of Kreissl and colleagues (2008), the elongated muscles of the naupliar limbs in *S. ingentis* might subdivide later in development and represent, thus, a condition similar to what had been reported for *H. americanus*. However, to be able to really claim that the conditions of

[♣♣] Unfortunately, the observation on the myogenesis in *S. ingentis* starts from the late stage, when the muscle precursors are already attached and contain fibrillar actin.

muscle development in *S. ingentis* and *H. americanus* are homologous and represent the ancestral pattern at least for malacostracans, one has to (first) study myogenesis within the naupliar segments of *H. americanus* and (second) observe the further muscle development of *S. ingentis* to prove whether any subdivision of the muscles takes place.

In general, the absence of intrinsic muscles is a rather unusual condition for a nauplius or it might as well be a derived condition for a malacostracan nauplius. The latter could possibly speak in favour of the existing idea that malacostracan nauplius is non-homologous to that of other crustaceans (Scholtz, 2000). Among non-malacostracan nauplii the muscle anatomy was investigated for two groups: branchiopods (*Artemia salina* (Benesch, 1969), *Branchinecta ferox* (Fryer, 1983), *Triops longicaudatus* (Williams and Müller, 1996)) and cirripedes (*I. quadrivalvis* (Anderson, 1987), *S. balanoides* (Walley and Reese, 1969), *B. improvisus* (Semmler et al, 2009), *E. modestus* (present study)). Intrinsic muscles are always present in these crustaceans. Most of the extrinsic muscles insert within the protopodites of the limbs, and only few are extending further into the distal portion. The myogenesis for most of these species has not been traced, therefore it is impossible to say whether these muscles are the product of the subdivision of a multinucleate MP. For the thoracic limbs of *T. longicaudatus* (Williams and Müller, 1996) it was described that the intrinsic and extrinsic muscles are formed from two separate groups of muscle precursors, similar to the observation in *E. modestus*. This is a strong supportive argument, that in other species, nauplii of which have both extrinsic and intrinsic muscles, the muscles develop in a comparable way.

4.2.7. Primordial germ cells

The early differentiation of the primordial germ cells (PGC) has been described for the number of other crustaceans, both non-malacostracans: cladocerans *Polyphemus pediculus* (Kühn, 1912), and *Holopedium gibberum*, anostracans *Daphnia pulex* (Baldass, 1937, 1941) and *D. magna* (Sagawa, 2005), copepods *Cyclops viridis* (Fuchs, 1914) and *Tisbe furcata* (Witschi, 1934), and malacostracans: decapods *Penaeus kerathurus* (Zilch, 1978), *Sicyonia ingentis* (Hertzler, 2002), *Litopenaeus vannamei* (Hertzler, 2005), and *Penaeus japonicus* (Pawlak et al., 2010; Grattan et al., 2013), euphasiacean *Meganyctiphanes norvegica* (Alwes, 2008), amphipods *Orchestia cavimana* (Wolff and Scholtz, 2002) and *Parhyale hawaiensis* (Gerberding et al., 2002; Extavour, 2005; Alwes et al., 2011). Most of these results, except of those on *Daphnia magna* (Sagawa, 2005) and *Parhyale hawaiensis* (Extavour, 2005; Alwes et al., 2011), have been based on the observation of cytoplasmic markers associated with the lineage of the germ line cells. Among those markers one can mention ncr (nutrition cell remnant), ds (dense spot), icb (intracellular

body), granulated cytoplasm and some others (for detailed review see Extavour and Akam, 2003; Alwes, 2008; Extavour, 2007).

The segregation of PGC has not been thoroughly followed in the present study. On the base of some by-product observations, however, the unidentified cells uc1 (see Chapter 3.5.3) have been suggested to represent the PGC. These cells are the products of the unequal 7th division of the two yolky endoblastic cells. They divide once more and remain in the number of four until after hatching. In the nauplius I they are placed on both sides of the posterior part of a hindgut. In *E. modestus* there have not been observed any intracellular markers defined for the PGC. Nevertheless, prior to the segregation of the zygote, some granules appear within the yolk. One could observe these granules till the epibolic stage of gastrulation. Visualization of the granules was possible due to a weak staining by Sytox Green. Clearly, a number of molecular investigations would be highly desirable in order to check whether the cells in question are the PGC.

If the uc1 are indeed the PGC, that would be another case for crustaceans where the germ cells are connected in their origin to the endoderm. The similar situation has been shown for *P. pediculus* (Kühn, 1912), *C. viridis* (Fuchs, 1914), *T. furcata* (Witschi, 1934), *H. gibberum*, *D. pulex* (Baldass, 1937, 1941) (Fig. 4.2.1.). In contrast, for the malacostracans the line of PGC is usually associated with that of the mesoderm. This was demonstrated at the examples of *P. kerathurus* (Zilch, 1978), *L. vannamei* (Hertzler, 2005), *S. ingentis* (Hertzler, 2002), *P. japonicus* (Grattan et al., 2013). There is an exception to this pattern. For the euphaseacean *M. norvegica* (Alwes, 2008) the PGC has been shown to derive from a cell related to the endoderm line. The results on *O. cavimana* (Wolff and Scholtz, 2002) and *Prh. hawaiensis* (Gerberding et al., 2002; Extavour, 2005; Alwes et al., 2011) again slightly vary (see above). The blastomere a, or g, responsible for the formation of germ cells in future, is a sister cell to the mesendoblast (*O. cavimana*) or to the mesoblast (*Prh. hawaiensis*).

Given that the connection of the germ cells with tmesodermal line is broadly eyewitnessed for many protostomes (reviewed in Extavour and Akam, 2003), the PGC originating from the endoblastic line can represent a derived condition within crustaceans. It is also possible that the connection of the germ line with endoderm has evolved independently for malacostracans and non-malacostracans (Fig. 4.2.1.).

On the base of this comparison of certain crustacean developmental features presented above one can draw some conclusions. The development of *E. modestus* follows the typical pattern of Cirripedia. It includes an unequal total cleavage with the persistence of one large cell on the vegetal pole, which incorporates the most of the embryonic yolk; epibolic gastrulation; early segregation of germ layers.

When compared with other crustaceans, the development of *E. modestus* reveals a set of similarities. Among those one can mention the 4-cell-stage arrangement, the A-C cell band, the mesectoblastic blastopore, the anal opening corresponding to the blastopore area, and that PGC line being in a sister relationship with endoderm. Some of these characters are most likely plesiomorphic for crustaceans (Fig. 4.2.1.), such as the tetrahedral 4-cell-stage and the placement of the anus. Others seem to be derived within certain crustacean groups, for example the germ line cells associated with the endoblast in their origin. Few characteristics, like the presence of cell bands during cleavage and the blastopore formed by mesectoblasts, might be qualified for the set of apomorphies present in the last common pancrustacean ancestor. Naturally, to confirm this further investigations in crustaceans and groups related to them are necessary.

4.3. Royal Flush

Comparison of cirripedes with the whole world, or "hopeful monsters" in action

4.3.1. Why spiral?

Notes on spiral cleavage and the relation of cirripedes to it

The original goal of the present study was to reinvestigate a barnacle species in regards to its mode of development. The reason for this was simple: the cirripedes were the "guilty" ones for the claim that the mode of crustacean cleavage is derived from the spiral cleavage (Delsman, 1917; Anderson, 1969; Costello and Henley, 1976; Nielsen, 1995).

Currently, due to the nowadays accepted phylogenetical system hardly anyone believes that the cirripedes might have spiral cleavage (Valentine, 1997; Nielsen, 2010). However, "retracing (previous) steps is a wise place to begin" (Klove, 2004). Therefore, it is worth to refer to the two questions: (1) what does make a spiral cleavage spiral? and (2) what would make a crustacean cleavage spiral?

To answer the first question one has to just open a text book on animal embryology or to take a relevant review (Siewing, 1969; 1979; Zilch, 1978; Dohle, 1989; Nielsen, 2004, 2005; Nielsen, 2010; van den Biggelaar et al., 1997). The set of features of spiral cleavage most likely would include:

- the two first planes of division are meridional, which leads to the nuclei of the four blastomeres positioned more or less in one plane and with non-sister blastomeres contacting each other on the animal and vegetal poles;
- the directions of cleavages from the third division on are either clock- or counterclockwise, when observed from the animal pole (exactly this feature was the cause for the name "spiral", first used by Selenka (1881) and Lang (1884) in their studies on flatworms);
- from the third division on the macromeres bud off quartets of micromeres towards the animal pole;
- blastomeres of the animal pole form an "animal cross" with annelid- or mollusc-typical cell composition[♣];
- certain derivatives of the micromeres leading to a set of ciliatory structures of the trochophore;
- blastomere 2d, "primary somatoblast", giving rise to most of the ectodermal structures of the trunk;
- blastomere 4d, "secondary somatoblast", producing trunk mesoderm.

[♣] Although some authors consider an animal cross as an uninformative by-product of the oblique divisions (Jenner, 1999; Maslakova et al., 2004; Nielsen, 2010), the others keep on investigating the variety of the animal crosses among spiralians (Merkel et al., 2012).

The second question leads us naturally to Delsman (1917) and Anderson (1969), who were the ones to interpret the cleavage in cirripedes as spiral. Below there is a list of the features of a barnacle development, which were described by Anderson (1969) as the ones of spiral cleavage:

1. *The first two cleavage divisions segregate four cells as anterior, posterior, left and right quadrant cells, of which the former, B and D, retain transverse contact ventrally while the latter, A and C, retain median contact dorsally in the typical spiral cleavage manner.*

As it was mentioned in the chapter 4.2.1., such an arrangement of the blastomeres at the 4-cell-stage occurs in many crustaceans. The exception is that for some species, for example, *Polyphemus pediculus* (Kühn, 1912; Kühnemund, 1929; Baldass, 1941), the B-D axis is reverse. Quadrant B is responsible for the formation of the posterior, and quadrant D for the anterior of the embryo.

Moreover, similar relations between the axes of the 4-cell-stage and those of the adult were described for chaetognaths (Shimotori and Goto, 2001). Apparently, such broad sampling suggests that this arrangement of the quadrants might have been present in the protostomian ancestor, although it needs to be proved with further investigations.

Clearly, this does not reject the idea that the barnacles might have spiral cleavage, as this developmental mode could have been ancestral (see below). On the other hand, the characteristic of 4-cell stage arrangement does not group the crustaceans together with the “typical” spiralians against other animals.

On the scheme (Fig. 4.3.1.) one can see the ventral and dorsal contact zones of quadrant descendants presented for different animals. It is related to another feature of the barnacles marked by Anderson as a spiral characteristic. In cirripedes the derivatives of A and C border on the ventral side. This arrangement is not only different from that in spiralians, but represents a rather unique mode compared even with some crustaceans. It would certainly be interesting to trace the development of other crustaceans in attempt to reconstruct the evolutionary way, which led to the dorso-ventral switch found in cirripedes. Another animal, in which the descendants of the left and right quadrants contact on the ventral side is the chaetognath (Shimotori and Goto, 2001; Fig. 4.3.1.C). How this similarity is related within these two groups for now it is hard to guess.Cell lineage studies in broader range of animals would be highly required here.

2. *... the division of each cell is perpendicular to the previous division, as it is in the alternating dexiotropic, laeotropic and dexiotropic divisions of spiral cleavage*

Divisions alternating under a right angle are not exactly a feature typical of spiral cleavage, but can be seen in many animals. Clock- and counterclockwise alternations in regards to the animal-

vegetal axis is the characteristic of the spirally cleaving embryos. This way of divisions is not observed in the barnacle embryos.

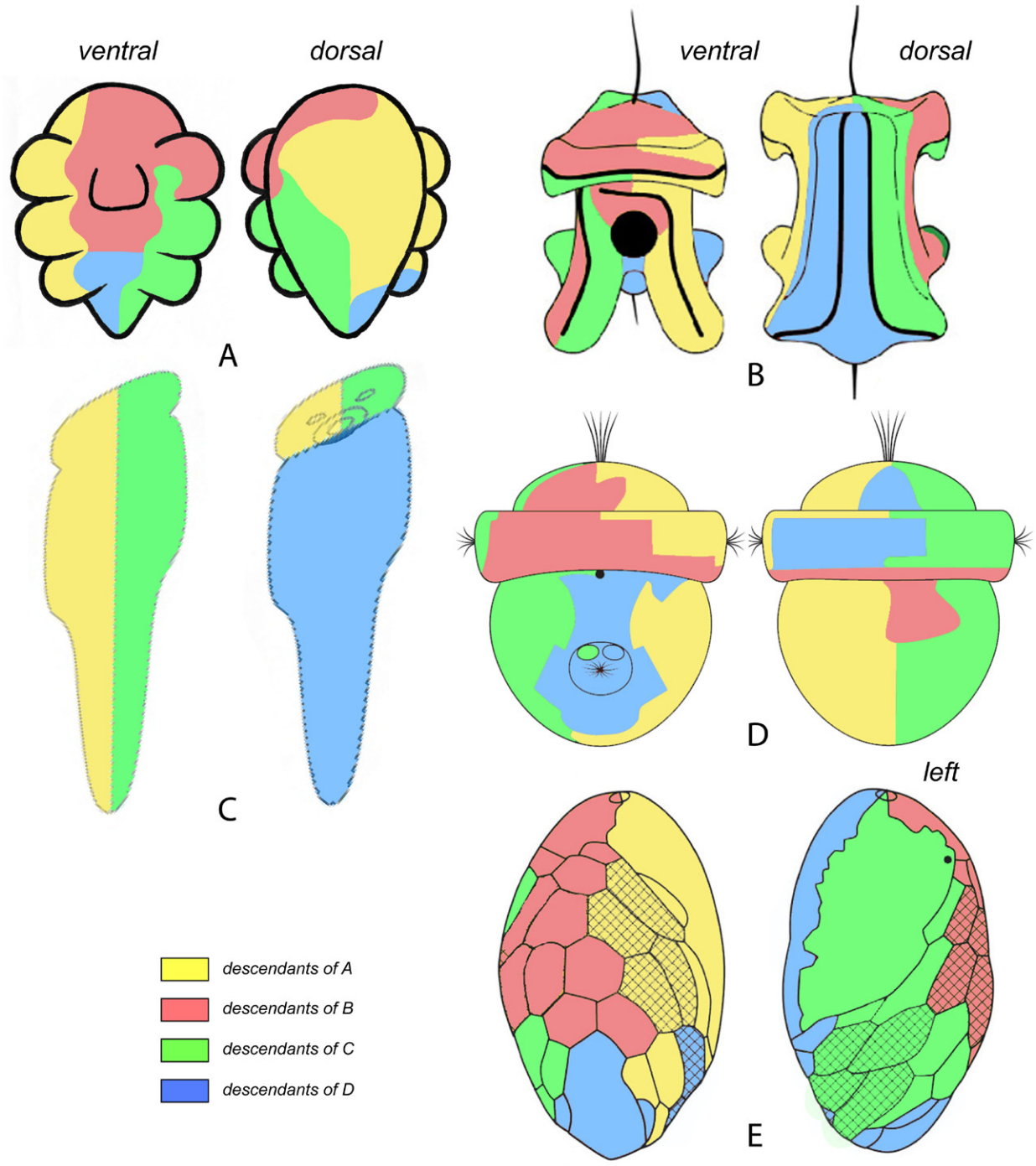

4.3.1. The epidermal descendants of the four quadrants in the larvae of different animals.

A – dendrobranchiate decapod *Sicyonia ingentis*, modified from Hertzler et al., 1994; **B** – flatworm Hoploplana inquilina, modified from Boyer et al. (1998); **C** - chaetognath *Paraspadella gotoi*, modified from Shimotori and Goto (2001); **D** – gastropod *Patella vulgata*, modified from Dictus and Damen (1997); **E** - nemertine *Carinoma tremaphoros*, modified from Maslakova et al. (2004).

3. *... the most ventral cells of the quadrants remain in contact as a ventral group of four, becoming 3A, 3B, 3C and 3D, and the transverse ventral contact between the B and D quadrants persists, as in the stem cells of the spiral cleavage sequence*

As it was mentioned several times above, the B and D quadrants have their contact zone on the vegetal pole. However, this place will later be found on the posterior-dorsal side of the barnacle embryo. Additionally, in most of the investigated thoracicans there is never in development a group of 3A, 3B, 3C and 3D. At the stage when 3A, 3B, and 3C appear, the D derivative on the vegetal pole is represented by 2D and is already totally internalized.

4. *... the ectodermal, mesodermal and midgut rudiments are segregated from one another by the end of the fifth cleavage division, a characteristic spiral cleavage feature*

First of all, in cirripedes the germ layers finish segregation by the end of the 6th division cycle (if not to take into account the segregation of the PGC, which happens after the 7th division) (Table 4.1.2.). Second, in spiralians only endoderm from the A, B, and C lines separates by the end of the 5th division. The endoderm and the endomesoderm of the D-line segregate at different stages of development (Fig. 4.3.3.). So does the ectomesoderm as well.

Thus, the last two points provided by Anderson in support of spiral cleavage in cirripedes are not validated by the comparative analysis. Regarding the others, they could be considered as a result of modification from the original spiral cleavage as it was proposed. Indeed, a certain variety in spiral cleavage can be observed in those groups, for which the presence of the spiral cleavage is of no doubt (reviewed in Boyer and Henry, 1998; Henry and Martindale, 1999; Hejnol, 2010; Pennerstorfer and Scholtz, 2012)

The most often observed modifications are related to the size of the blastomeres. For example, in some molluscs and polychaetes, the D quadrant and its derivatives are bigger than the other quadrants (Wilson, 1889; Woods, 1931; reviewed in Anderson, 1966). In some Hirudinea the blastomeres 2d and 4d happen to be bigger than any of the other cells including the macromere 4D (Tannreuther, 1915; Weisblat and Huang, 2001; for a review see Anderson, 1966; Dohle, 1999). In oligochaetes, leeches, and some molluscs, the difference between macro- and micromeres is so extreme, that one can hardly observe a spiral pattern (Conklin, 1907; Weisblat et al., 1984; Sandig and Dohle, 1988; Dohle, 1999). On the contrary, in some spiralians, like nemertines (Henry and Martindale, 1998; Maslakova et al., 2004) all the blastomeres are of more or less equal size and there is no pronounced difference between the micro- and macromeres. Moreover, in some sipunculids (Gerould, 1907) and flatworms (only after the 5th division) (Martín-Durán and Egger, 2012) the macromeres are smaller than the micromeres.

Another modification of the spiral cleavage is related to the asynchrony of divisions. With progress of cleavage in the most of spiralians the blastomeres on the vegetal pole divide faster than

those on the animal pole. And the derivatives of the D quadrant overtake those of other quadrants in speed (van den Biggelaar, 1996). In some derived representatives, like Oligochaeta and Hirudinea, the descendants of the A, B, and C quadrants after two to three cycles stop to divide at all and only the D quadrant proceeds with the cleavage (Whitman, 1886; 1887; Wilson, 1889; reviewed in Anderson, 1966; Dohle, 1999; Weisblat and Huang, 2001).

Taking into account the possibility of such variations in size and spatial arrangement of the blastomeres in spiralians, one can forcibly compare the early cleavages of the barnacles to the spiral mode. The anterior-posterior gradient of the divisions observed in cirripedes, however, does not fit the general direction of the modifications in asynchrony of spiral cleavage. Moreover, on the later stages of cleavage the barnacle embryo follows a certain pattern of development. The blastomere lineages and their arrangement on the animal pole can be compared to that of other crustaceans (see Chapters 3.3. and 4.2.1.), which are concluded as not having a spiral developmental mode (Zilch, 1978; Alwes and Scholtz, 2004; Alwes, 2008; Biffis et al., 2009). The arrangement of blastomeres on the vegetal pole, as it has been also suggested above, is most likely modified due to the highly unequal distribution of yolk.

The argumentation does not die out with the characteristics of cleavage divisions. As it was listed above, spiral cleavage means an entire complex of features. The part regarding the cell destinies was so far considered to have the biggest weight in the definition of spiral cleavage. The comparison of the blastomere fate between crustaceans and spiralians is not easy. First of all, it is hard to make any homology assumptions between the cells during cleavage. Second, there is a significant number of structures peculiar to each group. Therefore the comparison can go no further than the germ layer specification.

For example, most of the micromeres of the first and third quartets in a spiral cleaving embryo become trochoblasts (Nielsen, 2004, 2005). Their fates are impossible to compare with the fates of crustacean blastomeres, as the latter do not possess any of the ciliatory structures. Furthermore, the lineages of the nervous system, oesophagus, and proctodaeum originating from the micromeres are also quite different between spiralians and crustaceans (compare chapter 3.4. and 3.5.2. with Nielsen, 2004, 2005). On the one hand, this could be considered as a strong argument in favour that the cleavage observed in barnacles and in all crustaceans in general is not a modified version of the cleavage reported for the spiralians. On the other hand, there are two micromeres, 2d and 4d, which show a great deal of similarity between barnacles and spiralians. This could either put some doubt on the previous conclusion or might as well be considered as a characteristic conserved within the entire group of Protostomia. This issue will be reviewed in the subchapters below.

Table 4.3.1. Comparative data on cell lineage in some spiralians.

(?) – The author is not sure or does not give precise description.

The appreviations used only in this table:

QMa – quartet of macromeres
QMi – quartet of micromere
der - derivatives
E – Echiunra
S – Sipuncula

	Author	Species	Endoderm	Ectomesoderm	Endomesoderm
Platyhelminthes	Lang, 1884	*Discocoelis*	3rd QMa (A-C), 4D	2nd,3rd,4th quadrants	none(?)
	Wilson, 1898	*Leptoplana*	3rd QMa	2nd or 3rd quart QMi(?)	none(?)
	Surface, 1907	*Planocera inquilina*	4d der (after 7-9th div)	2a,2b,2c,2d	4d2der (9th div)
	van den Biggelaar, 1996	*Prostheceraeus giesbrechtii*	4d2 and 4d1der	(?)	4d 1 der
	Boyer et al., 1996; 1998	*Hoploplana inquilina*	4d, yolk mass from 4a-4c	2b	4d der
Mollusca	Conklin, 1897	*Crepidula*	3rd QMa (A-C), 4D, 4d der	2a,2b,2c	derivatives 4d (after 2nd div)
	Heath, 1899	*Ischnochiton magdalensis*	4th QMa (all)	(?)	4d(?)
	Conklin 1907	*Fulgur*	3rd QMa (A-C), 4D, 4d der	(?)	4d der
	Delsman, 1914	*Littorina obtusata*	3rd QMa (A-C), 4D, 4d der(?)	3a, 3b	4d der
	Dictus and Damen, 1997	*Patella vulgata*	3rd QMa (A-C), 4D	2b, 3a, 3b	4d
	Render, 1997	*Ilyanassa obsoleta*	3rd QMa (A-C), 4D	2a, 2b, 2c,2d, 3c, 3d, 3A, 3C	4d der
	Henry et al., 2004	*Chaetopleura apiculata*	3rd QMa (A-C), 4D	none	4d(?)
	Hejnol et al., 2007; Lyons et al., 2012	*Crepidula fornicata*	3rd QMa (A-C), 4D, 4d der	2c,3a,3b	4d der
	Lillie, 1895	*Unio*	3rd QMa (A-C), 4D	2a	4d
	Meisenheimer, 1901	*Dreissensia polymorpha*	3rd QMa (A-C), 4D	(?)	4d
	Woods, 1931	*Spaerium striatum*	3rd QMa (A-C), 4D	(?) (2b, 2c – Boyer et al., 1996)	4d
Nemertini	Henry and Martindale, 1998	*Cerebratulus lacteus*	4 quadr	3a,3b	4d der
	Maslakova et al., 2004	*Carinoma tremaphoros*	derivatives of 2nd QMa	(?)	2D der
E	Torrey, 1903	*Thalassema*	3rd QMa (A-C), 4D	1a, 1b, 1c, 3a, 3c, 3d	4d der
S	Gerould, 1907	*Phascolosoma*	3rd QMa (A-C), 4D	(?)	4d

	Author	Species	Endoderm	Ectomesoderm	Endomesoderm
Annelida	Wilson, 1892; 1898	*Nereis* *Aricia faetida* *Spio fulginosus*	3rd QMa (A-C), 4D, 4d der	none	derivatives of 4d
	Child, 1899	*Arenicola* *Sternapsis*	3rd QMa (A-C), 4D	none	4d
	Treadwell, 1901	*Podarke obscura*	3rd QMa (A-C), 4D, 4d der	3a, 3c, 3d	4d der
	Nelson, 1904	*Dinophilus*	3rd QMa (A-C), 4D	1st quadr	4d
	Ackermann et al., 2005	*Platynereis dumerilii*	3rd QMa (A-C), 4D	2a,2c,3a,3b,3c,3d	4d
	Meyer et al., 2010	*Capitella teleta*	3rd QMa (A-C), 4D	2a, 2c, 3a, 3b, 3c, 3d, 4d	none
	Whitman, 1886; 1887	*Clepsine*	3rd QMa (A-C)	none	3D
	Tannreuther, 1915	*Bdellodrilus philadelficus*	3rd QMa (A-C), 4D	none	4d
	Goto et al., 1999; Gline et al., 2011	*Tubifex (oligo)*	(?)	(?)	4d - mesoblast
	Weisblat et al.,1984; Gline et al., 2011	*Helobdella*	3rd QMa (A-C), 4D	3c, 3d	4d der (4th div)

4.3.2. Lineage of endoblast

As it was just concluded above, the cirripedes together with crustaceans in general do not possess a spiral mode of development. This is, however, far from being the most novel conclusion. Another problem, which is far more interesting to deal with, is whether cirriped studies could contribute to the search for common developmental features among Ecdysozoa (Ungerer and Scholtz, 2009; Scholtz and Wolff, 2013). One of the possibly relevant features is analysed in this chapter and is related to the lineage of the endoblast.

The endoderm of *E. modestus* as well as of several other investigated cirripedes originates from a singular blastomere at the 16-cell stage, 2D, derived from the D quadrant (Table 4.1.1.). The similar situation is observed in many other crustaceans: Cladocera (*Polyphemus pediculus* (Kühn, 1912), *Simocephalus vetulus* (Cannon, 1921), *Holopedium gibberum* (Baldass, 1937)), Copepoda (*Cyclops viridis* (Fuchs, 1914), *Tisbe furcata* (Witschi, 1934)), Decapoda (*Melicertus kerathurus* (Zilch, 1978), *Sicyonia ingentis* (Hertzler, 2002), *Litopenaeus vannamei* (Hertzler, 2005)), Amphipoda (*Parhyale hawaiensis*[♣] (Gerberding et al., 2002)), Euphausiacea (*Meganyctiphanes norvegica* (Alwes, 2008)). The endoderm of the dendrobranchiates and euphasiaceans does not have a singular cell origin, as it comes from the cells X_d and some descendants of X_v (Zilch, 1978; Hertzler, 2002; Alwes, 2008). Both of these blastomeres, nevertheless, can be traced back to a singular D quadrant.

The exceptions are found within Cirripedia and Amphipoda. Studies on the development of iblomorphs and rhizocephalans did not follow the cell lineage in great detail, but it was assumed that the endoderm (or the yolky endoderm in rhizocephalans) is derived from all four quadrants (Shirase and Yanagimachi, 1957; Bocquet-Vedrine, 1961, 1964; Anderson, 1965). The amphipod *Orchestia cavimana*[♣] has its endodermal tissue descended from three mesendoblasts at the 8-cell stage (A, ba, da, the daughter cells of the three quadrants) (Wolff and Scholtz, 2002). Taking into consideration the general pattern observed among crustaceans (Fig. 4.2.1.A.), it is reasonable to conclude that the condition found in these three groups is derived.

The relation of the endoblast to the D quadrant as a characteristic for all crustaceans has been first proposed by Weygoldt (1960a). However, a broad comparison of the endoblastic lineage across the different animals outside the crustaceans has never been done. That is of no surprise, as the relevant data on most of the groups are missing. In another arthropod with total cleavage, the pantopod *Pycnogonum litorale*, the gastrulation is initiated by one cell, which supposedly

[♣] As it was mentioned above the lineage of amphipods regarding endoderm and mesoderm varies between different species due to the different interpretation of the midgut gland nature. If midgut glands are considered as a product of endoderm, then *P. hawaiensis* as well as *O. cavimana* has three quadrants giving rise to the endoderm.

gives rise to the endoderm later (Ungerer and Scholtz, 2009). This, however, needs further investigation to be proven.

The lineage studies on Nematoda, a representative of Cycloneuralia, show striking similarities to that of Crustacea in regard to the endoderm origin. In all the investigated species, even in those with a variant cell lineage (Voronov and Panchin, 1998), the endoderm can always be traced back to a single blastomere at the 8-cell stage (Sulston et al., 1983; Malakhov, 1986; Houthoofd et al., 2003, Schulze and Schierenberg, 2011). The origin of the endoblast itself, however, varies. In some nematodes (Sulston et al., 1983; Houthoofd et al., 2003) it is the daughter cell of the EMS, which is the offspring of the posterior blastomere at the 2-cell-stage, P1. In others the endoblast belongs to the line of AB, the anterior blastomere at the 2-cell stage (Drozdovskii, 1975; Malakhov and Spiridonov, 1981). Experimental studies demonstrated, that in some nematodes with determined cell lineage and endoblast originating from P1, the anterior blastomere AB is also capable of endoderm formation (Wiegner and Schierenberg, 1998).

Different data were obtained in the study on development of the priapulid *Priapulus caudatus* (Wennberg et al., 2008). The tracing of the cell lineage showed that it is the derivatives of the non-sister B and D lines, which initiate gastrulation and are the first to be internalized. Presumably, these two cells contribute to the mesendoderm. The study did not proceed further to show which descendants produce which germ layers. In the developmental studies in other cycloneuralian groups, like Kinorhyncha (Kozloff, 2007) and Nematomorpha (Montgomery, 1904; Muhlendorf, 1914), the cell lineage had never been traced.

The similarity between the endoblast formation in Crustacea and Nematoda naturally provokes the question, whether the endoblast descending from one quadrant might represent a feature of the last common ancestor of Ecdysozoa. Another question is when exactly this feature evolved and if it in fact can be considered as an apomorphy for the entire Ecdysozoa.

The endoderm in the Spiralia, a sister group to Ecdysozoa, as it is shown in the Table 4.3.1. and Fig. 4.4.1.A, originates from the four macromeres, descendants of all four quadrants (references from the Table 4.3.1.). Nevertheless, there are some exceptions within this group. First one is found in some flatworms (Surface, 1907; Boyer et al., 1998; Caspari, 2010; Martín-Durán and Egger, 2012). The endoderm of those originates from a singular micromere, descendant of the D quadrant, while all the macromeres either degenerate or form the hull. Additionally, the endodermal lineage of the rotifers might possibly represent an exception to the “typical” spiralian lineage of the endoderm. The studies on Rotifera are quite many: Tessin, 1886; Zelinka, 1891; Jennings, 1896; Beauchamp, 1956; Tannreuther, 1920; Nachtwey, 1925; Lechner, 1966. Despite this fact, there is not much concordance in regards to the endodermal lineage. According to the

older studies, the endoderm originates from a singular quadrant (assigned as well D in rotifers). The newer research works report, that endoderm forms in the process of delamination from the dorsal blastoderm, the origin of which can be traced back to several quadrants (Nachtwey, 1925; Lechner, 1966). The D quadrant in the latter case does not participate in the endoderm formation and gives rise to the mesoderm and the germ-line cells. Which account is correct is a matter for future proper investigations. The very recent research, for example, based on live observation by means of the 4D microscopy mentions that the digestive system is formed by the descendants of all four quadrant (Schiemann and Hejnol, 2011). However, it is not clearly specified, whether only endodermal parts are meant or mesodermal ones as well.

Whether the similarity in the lineage of endoderm between ecdysozoans and platyzoans is a result of convergent evolution is not clear on the base of the current data. The first question to be answered is whether the multi-quadrant origin of endoderm is a conserved feature among the spiralians or is a novelty acquired during the evolution of this developmental mode (van den Biggelaar, 1997). The recent molecular based phylogenies suggest that the branches of flatworms (and rotiferans) are nested deeply within the spiralian tree (Fig. 4.4.1.). If these relationships are correct, then the ability to form the endoderm from the four quadrants is a conserved spiralian feature and both Platyhelminthes and Rotifera have most likely lost it. This logically leads to the assumption that the similarity to the ecdysozoans is homoplastic.

Another interesting question to clarify is what the condition of endoderm origin in the basal protostomian. This is, however, a matter of even bigger and more obscure speculations and will be addressed below.

4.3.3. Some considerations on ectomesoderm♣

That mesoderm might have two sources was first discovered by Lillie in the bivalve mollusc *Unio* (1895). He has named the blastomere contributing to both ecto- and mesoderm as ectomesoblast. It was also Lillie, who was the first to make a difference between the two types of mesoderm. He referred to the ectomesoderm as a secondary, or larval mesoblast, as it formed mostly larval muscles, and to the endomesoderm as a primary mesoblast, since it gave rise to the segmental mesoderm of the adult body.

After the study of Lillie (1895) the dual source of mesoderm has been reported for multiple organisms including representatives of other molluscs, flatworms, annelids, crustaceans, and nematodes (Table 4.3.1). Together with these reports a long going discussion has been initiated. Main directions of this discussion included: which of the mesodermal types has evolved earlier,

♣ It is not directly related to the goal of the work, neither it is related to the cirripeds, but as a by-product of a literature review, it appears interesting.

whether the ectomesoderm is homologous to the endomesoderm, and whether the ectomesoderm can be considered as a true mesoderm at all (Conklin, 1897; Wilson, 1898; Tannreuther, 1915; Siewing, 1977).

Apart from the origin and the outcome (which both will be addressed below) between the two mesodermal types there is a set of other differences. First of all, it is the way of the division of mesoblasts. Endomesoblasts in many of the described cases, which include malacostracan crustaceans and spiralians, are characterized by teloblastic divisions (Anderson, 1979; Dohle et al., 2004). The resulting mesodermal layer is segmentally and bilaterally organized. On the contrary, ectomesoblasts divide rather chaotically producing a mesodermal layer with no clear structure (reviewed in Woods, 1931).

There are some examples of deviation to this. For example in the barnacle *E. modestus* studied in this work ectomesodermal and endomesodermal cells are in distinguishable and might even form the same muscles (Chapter 3.4.3.). For nematodes there were no reported difference in the divisions of the products of ecto- and endomesoblasts either (Sulston et al., 1983). Another exception would be found among the animals, which have exclusively ecto- or endomesoderm (Table 4.3.1.). This would ultimately condition the origin of "organized" and "non-organized" mesoderm. One such example is the development of the polychaete *Capitella* (Eisig, 1898; Meyer et al., 2010). Its adult musculature originates from mesectoblasts, while mesendoblast does not seem to be present at all. The case of amphipod mesoderm differentiation outlines another case. Regardless of the affinity of the mesodermal layer itself (it is either endomesoderm or ectomesoderm, see above) it is one type, which is present within the embryos of *O. cavimana* or *Prh. hawaiensis*. Nevertheless, this type of mesoderm develops in different ways in nauplius and post-naupliar segments (Hunnekuhl and Wolff, 2012).

One more difference between endo- and ectomesoderm is found at the genetic level. It has been shown, for example, for *C. elegans* (Good et al., 2004; Broitman-Maduro et al., 2006) or *Patella vulgata* (Lartillot et al., 2002a,b; Nederbragt et al., 2002). In the nematode the molecular mechanism for the specification of ectomesoderm involves TBX-37 and TBX-38, whereas the endomesoderm formation seems to be conducted via TBX-35. For the mollusc the expressions of such genes as *goosecoid*, *fork head*, and *twist* appear to be restricted to the mesectoblasts and *brachyury* to mesendoblast. Clearly, apart from the mentioned genes, there is an enormous in its complexity cascade of the genes behind the mesoderm specification and differentiation. Many of them are functioning in both types of the mesoderm. Nevertheless, the reported genetic differences are of high interest and will be addressed once again below.

4.3.3.1. Origin of ectomesoderm

The blastomeres giving rise to the ectomesoderm vary within even closely related groups. Most of the investigations in this respect are devoted to spiralians (Table 4.3.1.). Also within Spiralia a number of attempts have been performed to use the origin of ectomesoderm as a phylogenetically valuable feature (e.g. Tannreuther, 1915; Boyer et al., 1996; Hejnol et al., 2007). The high variety in ectomesoblast lineages has complicated this task. Currently, there are two suggestions regarding the evolution of the ectomesodermal origin. According to one, the ectomesoderm originating from the second quartet of micromeres, namely from 2b, represents the conserved state within spiralians (Boyer et al., 1996). Another one suggestion regards the trochozoans and proposes to consider the third quadrant of micromeres to be the plesiomorphic ectomesodermal origin within Trochozoa (Hejnol et al., 2007). How these two ideas correlate and what is the evolutionary way of the mesectoblasts for Spiralia is irrelevant for the current discussion.

Apart from spiralians, the ectomesodermal origin has been traced for some species of Crustacea and Nematoda. For malacostracan crustaceans the lineage of ectomesoderm is known for Decapoda: Dendrobranchiata and Euphausiacea[♣]. Mesectoblasts for these groups are mostly derived from the quadrants C and D and are 8 or 9 in number (Hertzler, 2002; 2005; Alwes and Scholtz, 2004; Biffis et al., 2009). For non-malacostracans the ectomesodermal lineage has been clearly established only for cirripedes (Table 4.1.2.) and one species of Cladocera (*Polyphemus pediculus*, Kühn, 1912). In both groups all fours quadrants produce ectomesoblasts. As one can see in the Table 4.1.2., within the cirripedes some interspecific differences have been reported. Unlike for spiralians, within crustaceans the ectomesoblast lineage has never been used in the broad phylogenetical analyses. The reason for this is possibly a lack of suitable data.

Nematode lineages of ectomesoderm were described for several species (Sulston et al., 1983; Houthoofd et al., 2003; Schulze and Schierenberg, 2011). Ectomesoderm originates mostly from the two sister quadrants A and B[♣♣], with some cells descending from P_3. Many of the species are closely related, but the lineages of ectomesoderm varies considerably (compared in Houthoofd et al., 2003).

Due to the vast variety in the lineage of ectomesoderm within the protostomian groups, it would be impossible and most likely incorrect to homologize the mesectoblasts across protostomia. Consequently, one can conclude that the homologous ectomesodermal structures within each

[♣] Additionally, the origin of the mesoderm is shown also for Amphipoda (Wolff and Scholtz, 2002; Gerberding et al., 2002; Hunnekuhl and Wolff, 2012). However, taking into account the idea that the amphipod development is of a highly derived mode and that origin of mesoderm is interpreted differently for both species, data on these two animals are not considered here.

[♣♣] According to the nomenclature developed for Nematoda (Sulston et al., 1983)

group have different cellular origin, which would support the existing view on the ontogenetic criteria of homology (Scholtz, 2005).

4.3.3.2. Ectomesoderm vs. anterior mesoderm

Another interesting point about the mesoderm is that in the bilaterians it can be subdivided into anterior and posterior types depending on its differentiation place in the embryo. Such subdivision was found in spiralians, crustaceans, phoronids, hemichordates, and vertebrates (shortly reviewed in Lartillot et al., 2002a; Temereva and Malakhov, 2007).

In most of the spiralians it is the ectomesoderm that forms the anterior mesodermal structures and endomesoderm – the posterior ones. During the early development, shortly before gastrulation, one could also observe a spatial separation of the blastomeres: mesectoblasts are placed anterior to the endoblasts and mesendoblast – posterior to it (references from Table 4.3.1.; reviewed in Anderson, 1979; Nielsen, 1995).

Interestingly enough the genetical studies showed that the genes involved in the patterning of the mesoderm in the early embryos appear to be homologous across the bilaterians. The genes, expressions of which are found in prechordal (anterior) mesoderm of vertebrates, are restricted to the mesectoblasts of the spiralians (*fork head*, *goosecoid* – Lartillot et al., 2002a; *twist* – Nederbragt et al., 2002), whereas the mesendoblast expresses the genes found in posterior mesoderm of the deuterostomes (Lartillot et al., 2002; reviewed in Technau, 2001; Rodaway and Patient, 2001; Technau and Scholz, 2003). Such gene expressions led to two assumptions. The first was that ecto- and endomesoderm of spiralians is one to one homologous to the anterior and posterior mesoderm of the vertebrates, which was extended to a conclusion that these mesoderm types are homologous across the entire group of bilaterians. The second idea was that the observed gene expressions are specific to the cell lineages and not to the the position of the cells along the AP axis. Here, however, one could argue, as there are a lot of results showing, for example, the expression of *brachyury* exclusively in the posterior structures of the body regardless of their origin (reviewed in Technau, 2001).

Regarding the possible homology of the mesodermal types, there was an impressive number of the studies conducted on this matter. Their direction was pretty logical. In order to support the suggested relations between the types of the mesoderm, it was necessary to know what a last common ancestor of the bilaterians had. And as the situation with possible basal group is maybe even more problematic than the evolution of the mesoderm (see the references from Fig. 4.3.1.), the investigators turned to the bilaterian closest relatives, cnidarians and ctenophores (e.g. Martindale et al., 2004; Röttinger et al., 2013).

These two groups include the diploblastic animals, which means these organisms do not possess a well organized mesodermal layer. There is a huge discussion going on, whether the entocodon of cnidarians or the muscles described for ctenophores can be homologous to the real mesoderm of bilaterian (Scholtz, 2004; Seipel and Schmid, 2005; reviewed in Burton, 2008; Steinmetz et al., 2012). It is, however, not the point of the current work. What is more important is that in cnidarians the expressions of the genes in question (like *twist*, *snail*, *brachyury* etc) were reported and these expressions were restricted mainly to the endoderm in the region of the blastopore (Martindale et al., 2004; Röttinger et al., 2013; reviewed in Technau, 2001; Burton, 2008).

These data resulted in another set of suggestions, one of which was that the anterior placement of the mesoderm was ancestral condition for bilaterians. The split into the anterior and posterior mesodermal types happened via amphistomic gastrulation in a basal bilaterian (Lartillot et al., 2002). Thus, the asymmetry of the mesoderm in relation to the AP axis was established at the level of the blastopore[♣]. In Fig. 4.3.2. one can see the suggested scenario of the evolution of the mesoderm specification in the area of the blastopore. It is clear, that to prove it one need broad data from many animals. The data on cell lineage of the cells in in the area of forming blastopore is only a first step, which should be followed by experimental studies dealing with the molecular mechanisms of the cell interactions. For example, some studies have already shown that in the blastopore area of ascidian embryos (reviewed in Nishida, 2005) the induction of the marginal cells comes from endodermal precursors and follows oriented way.

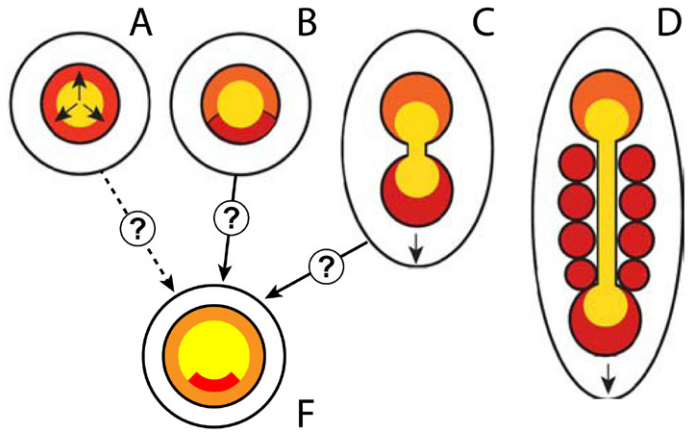

Fig. 4.3.2. The scenario of the mesoderm induction (modified from Lartillot et al., 2002a)

A – radial induction in the marginal zone, the arrows show a signal emitted from endoderm; **B** – appearance of AP axis in the blastopore area; **C** – amphistomous gastrulation causes the separation of the mesodermal field into two; **D** – posterior mesoderm becomes segmented (more detailed description see in Lartillot et al., 2002a); **F** – a condition of mesoderm specification suggested for crustaceans: the ectomesoderm (orange) surrounds the endoblast (yellow) and the posterior endomesoderm (red). Please note, the orange on **A**-**D** stays for the anterior mesoderm, whereas in **F** it marks the ectomesoderm. As in Lartillot et al., 2002a these two types were homologised, it appeared possible to make a scheme for Crustacea using the same colour code.

[♣] The differences of the blastopore organization (or germ layer specification in the region of the blastopore) within bilaterians are not addressed here. What is meant is that the blastopore area became asymmetrically arranged in regards to AP axis.

After this long way, it is time to come back to the "hopeful monsters" (in this case as "hopeful monsters" one could possibly consider all crustaceans). Among the crustaceans the spatial separation in the mesoderm occurs at the stage of muscle differentiation (Hertzler et al., 1994; Hertzler, 2005; Hunnekuhl and Wolff, 2012), but it is not observed at the gastrulation stage. As it was already discussed and summarized in the Chapter 4.2.3., in many crustaceans including *E. modestus* the mesectoblasts surround the endoblast and mesendoblast (Hertzler et al., 1994; Hertzler, 2005; Pawlak et al., 2010; reviewed in Manton, 1928; Baldass, 1941). However, the mesendoblast(s) are placed posteriorly to the endoblast in a similar to other animals way.

If one tries to apply the theory of the "asymmetric blastopore" being a characteristic of the basal bilaterian, what scenario could be suggested for the ectomesoderm of crustaceans? The generalized state of the crustacean blastopore is shown in Fig. 4.3.2.F. All the possible scenarios are rather speculative. The scenario B-F seems to be the most attractive with current data. In this case the asymmetric blastopore of the basal bilaterian would have to change back to the "radial" induction of the ectomesoderm within Ecdysozoa, while preserving the posterior specification of the endomesoderm. The A-F way appears, on the other hand, to be slightly less parsimonious than the others. This scenario would imply that the ancestor of proto- and deuterostomes had a radial induction of the mesoderm and the AP arrangement of the blastopore region evolved independently within spiralians and deuterostomes. On the other hand, the posterior specification of the mesoderm in basal bilaterian might have evolved additionally to the existing radial induction. Yet, the evolution of the secondary mesoderm induction went independently within proto- and deuterostomes. Whereas the ecdysozoans (only crustaceans are considered) preserved the radial way of induction, a zone of the posterior specification of the mesectoblasts in spiralians would have been lost (apparently not in all though, see Table 4.3.1. for the species with ectomesoderm originating from D quadrant).

The amphistomy being an attribute of the bilaterian ancestor (C-F scenario) is not considered here due to the possibility of the additional broad discussion (for arguments in favour and against see e.g. Dunn et al., 2008; Hejnol and Martindale, 2009). However, the argumentation provided in the A-F scenario might, in general, be considered as an argument against.

4.3.3.3. Specification of ectomesoderm

To identify the specification way of the ectomesoderm a set of interesting experiments have been performed in *C. elegans* almost almost three decades ago. First it was suggested, that the cells in order to take the secondary fate[♣] and give rise to the mesoderm need the presence of the EMS blastomere (the mesendoblast, appears after the second division at the 4 cell stage) (Priess and

[♣] The terms of primary and secondary cell fate are taken from Priess (2005).

Thomson, 1987). Later studies supported it and provided more detailed information. It was shown, that it is the MS cell (the endomesoblast and the daughter cell of EMS) that causes the ectoblasts to differentiate into mesoderm (Schnabel, 1991). The conditional specification occurs via the Notch signalling pathway (reviewed in Priess, 2005). Unfortunately, nematodes are about the only protostomes, for which data on ectomesodermal specification are known so far. The studies on ectomesoderm induction in deuterostomes are reviewed in Rodaway and Patient (2001).

The investigation based on ablation of the mesodermal precursors in *Parhyale hawaiensis* demonstrated that mesodermal specification occurs before 8-cell-stage (Price et al., 2010). However, which cell(s) exactly is (are) necessary for the blastomeres to take the mesodermal fate has not been described.

The fact that in many crustaceans, like Cirripedia (Bigelow, 1902; Delsman, 1917; Anderson, 1969; present study), Cladocera (Kühn, 1912), Copepoda (Fuchs, 1914), Euphausiacea (Alwes, 2008), and Dendrobranchiata (Zilch, 1978; Hertzler and Clark, 1992; Hertzler, 2005) all the mesectoblasts are in contact with the endoblast(s), makes the latter a good candidate for the initiation of mesodermal specification. In *Sicyonia ingentis*, for example, it is the mesendoblastic cells that triggers the mesectoblasts to divide in oriented way and initiate gastrulation (Wang et al., 2008). With the mesendoblast removed the internalization of ectomesoderm does not happen. That can be a supportive sign that mesendoblast plays a crucial role in the specification of mesodermal fate as well. This suggestion, nevertheless, has to be proven by further experiments.

For other crustaceans, for example branchiopods *Daphnia pulex* (Baldass, 1941) and *Artemia salina* (Benesch, 1969) and ostracod *Cyprideis litoralis* (Weygoldt, 1960), the endoblast does not seem to contact the cells producing mesoderm until the late gastrulation, when the mesoderm is already internalized. Therefore, in these species the determination can follow either autonomous specification or be a result of a different conditional specification, which is hard to guess without proper investigations.

If in some crustaceans it is in fact the endodermal precursor that is responsible for the mesoderm initiation, that would be rather different from the pattern described for *C. elegans*, where it is endomesoblast, that induces the ectomesodermal specification, and it might represent another model of conditional specification. In addition, in some nematodes the specification of the cells towards the mesodermal fate happens relatively late in development and seems to be a case of the regional specification (Houthoofd et al., 2003). The cells, which have an ectodermal primary fate, migrate to the final locations of the future structures and only then they take on the meso-

dermal secondary fate. In this case neither the cells responsible for initiation, nor the germ layer, which they belong to, are known.

Which of the three ways is an ancestral one for crustaceans or for ecdysozoans, is impossible to say. To draw some conclusions one could try to compare the ectomesoderm formation with some other organisms outside the ecdysozoans. However, by now there are not enough data to deal with. The studies on blastomere specification performed in some spiralians, for example, have been mostly devoted to the specification of D quadrant or its role in the differentiation of the particular ectodermal structures derived from the micromeres (van den Biggelaar, 1976; 1977; Henry and Martindale, 1987; van den Biggelaar and Faber, 1994; Henry et al., 2004). In the experiments on the stepwise deletion of the D quadrant the authors, unfortunately, do not mention the presence of the ectomesodermal products at all (Cather and Verdonk, 1979).

In general, the extra-cellular induction of the ectomesodermal specification has been proven so far only for *C. elegans*. In case it takes place in other organisms, the cell origin of ectomesoblasts might be of little value for a macro-scale phylogeny. Indeed, the arrangement of the blastomeres as well as their contacts can be an "easy" subject for modification as a result of "mechanical"/"spatial" adaptation of the embryo. Therefore it can vary between closely related taxa, as it does within spiralians.

4.3.4. Spiralian somatoblasts in crustaceans?

Historically, the somatoblasts are two: the primary (blastomere 2d, which gives rise to most of the ectodermal tissues) and the secondary (blastomere 4d, which gives rise to the somatic mesoderm, or endomesoderm). These blastomeres are claimed to be homologous among all the spiralians (which is most likely true) or even more, a "super-phylotypic"[♣] for this group (this, however, might be rather questionable: see below).

4.3.4.1. Fate of somatoblasts

The cell lineage of the *blastomere 2d* was first thoroughly studied by Wilson in Nereis (1892). Afterwards, a number of studies paid high attention to this cell (for review see Meyer and Seaver, 2010). While the homology of this cell among the spiralians is of no doubt, there has never been a report on a possible homologous cell in other groups of animals. Therefore this cell is without a question considered as one of the characteristics for the spiral mode of development.

The results of the current work, however, awaken some doubts in this respect. In *E. modestus* the cell 1d is responsible for most of the ectoderm on the ventral side of the hindbody. With further development this region will form the ectoderm of the thoracic segments in the cypris larva. In a

[♣] The "super-phylotypic" term is taken from Gline et al., 2011.

way one could consider this cell as a "mother ectoblast". The cell lineage studies on malacostracans have yielded results totally different to those in cirripedes. In decapod crustacean *Sicyonia ingentis* (Hertzler et al., 1994) the cell injections at the four cell stage showed that the epidermis of the hindbody originates from derivatives of the C and D lines. The cell material of the hindbody participates in the formation of postnaupliar segments of the zoea. The adult epidermis in amphipods originates from several quadrants (three for *Parhyale hawaiensis*, Gerberding et al., 2002; two for *Orchestia cavimana*, Wolff and Scholtz, 2002).

Clearly, by now there are way too few data on cell lineage across the crustaceans, which in fact studied an early ectoderm differentiation and could have reported the presence or absence of such "mother-ectoblast". Therefore it is impossible to perform an accurate evolutionary analysis of this cell. Within Arthropoda as well as in closely related groups the relevant data are missing. The only ecdysozoan group, which can be used, is Nematoda. In nematodes a cell, similar to that in cirripedes, is absent and adult epidermis is produced by the descendants of three quadrants (Sulston et al., 1983; Houthoofd et al., 2003). Another group of protostomes with known fates of quadrants but uncertain phylogenetical position is Chaetognatha (Fig. 4.3.2.; Fig. 4.4.1.A) (Shimotori and Goto, 2001). The epidermis of adult chaetognaths originates from three quadrants.

Therefore, with the data at hand it is logical to assume that the cell observed in *E. modestus* most likely evolved within cirripedes only and does not have a common history with the primary somatoblast of the spiralians, although this matter has to most certainly be investigated further.

The *blastomere 4d* appears later in the development of spiralians than 2d, but is definitely more famous (Lambert, 2008). This cell is known to produce most of the adult mesoderm in spiralians save for some exceptions (see Table 4.3.1.). The mesoderm in this case is referred as endomesoderm, since the line of the mesoderm originating from 4d is associated with the line of the endoderm. The mesendoblastic nature of 4d was first noted by Conklin (1897) in gastropods of the *Crepidula* genus. A first thorough investigation and analysis of the 4d lineage was performed by Wilson (1898). The resulting idea was that 4d might have originally been purely endodermal. In the process of evolution it started to contribute to mesoderm minimizing or reducing completely its ability to give rise to endoderm. Later works addressed this idea several times and tried to use it for some phylogenetic analyses within spiralians (Torrey, 1903; Table 4.3.1.).

Interestingly, the endomesoblasts in different spiralians are represented by different cells. Thus, if one relies only on the cell lineage, one has to give up the idea of the 4d blastomere. As it is shown on the scheme (Fig. 4.3.3.), the number of endomesoblasts as well as the division cycle of their emergence varies. Therefore, it would be more correct to speak of a singular mesendoblast cell derived from the D quadrant. This would not be a problem whatsoever and one could keep

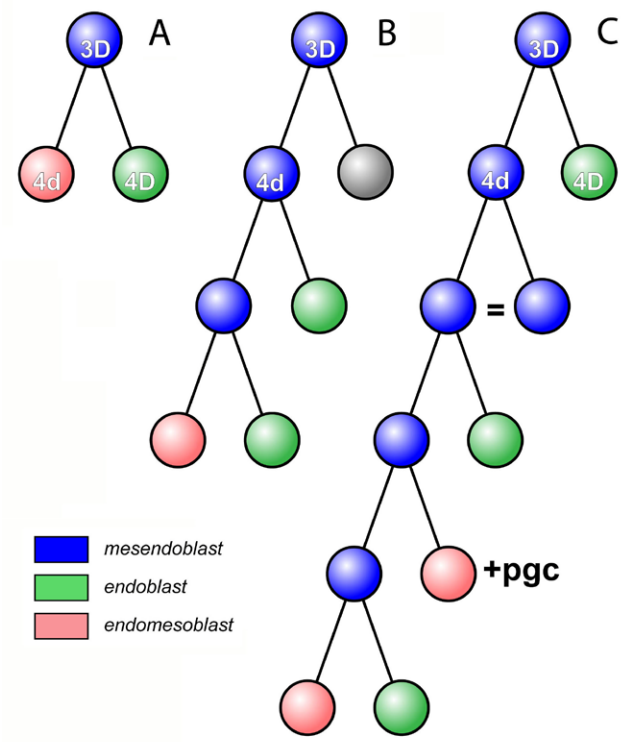

Fig. 4.3.3. The cell lineages of the mesendoblasts 3D in different spiralians.

A –polychaete *Platynereis dumerilii*, after Ackermann et al., 2005; **B** – some flat worms (Surface, 1907; van den Biggelaar, 1996); **C** – gastropod *Crepidula*, after Lyons et al., 2012. The lineages of the 4d contributing to the ectodermal structures, like those of the leach *Helobdella* (Weisblat et al., 1984; Gline et al., 2011) or the polychaete *Capitella* (Meyer and Seacer, 2010), are not shown.

on considering 4d as a "super-phylotypic" cell further, if it were not for other animal groups having a similar cell in their development.

Mesendoblastic cells have been found in two groups of Crustacea: 1D in Cirripedia (Bigelow, 1902; Delsman, 1917; present study) and X_v in Malacostraca (Euphausiacea and Decapods: Dendrobranchiata[♣], Zilch, 1978; Hertzler et al., 1994, Hertzler, 2002; 2005; Alwes, 2008). Among the analysed crustaceans the cell lineage of the mesendoblastic cell varies as well as it does in spiralians. In malacostracans it can also contain one or more endomesoblasts. Moreover, the final products of endomesoderm are also different. In cirripedes the endomesoblast gives rise mostly to the naupliar musculature, whereas that of *Sicyonia ingentis* is responsible for the musculature of the postnaupliar segments (Hertzler, 2002). Despite of these varieties, the entire endomesoderm can be traced back to a singular mesendoblast.

A mesendoblastic cell is present also in some nematodes (the cell EMS) (Sulston et al., 1983; Houthoofd et al., 2003; reviewed in Schulze and Schierenberg, 2011). It has been reported though, that the derivatives of EMS partly contribute to the ectodermal structures as well (Sulston et al., 1983). This, however, could be a secondarily evolved function. A similar case was described for the polychaete *Capitella* (Meyer et al., 2010) and the leech *Helobdella* (Weisblat et al., 1984). The descendants of 4d give rise to the ectodermal epithelium of the hindgut in these animals in addition to some mesodermal structures). Such observations have been suggested to "represent traits more recently derived within certain organisms" (Lyons, 2012). This conclusion is logically drawn from the idea that the mesendoblastic 4d is a feature of the ground pattern of spiralians (Wilson, 1898; Dohle, 1979; Lambert, 2008).

♣ The cell X_d is also called mesendodermal, although it has been shown so far to give rise exclusively to the yolk endoderm

It has, nonetheless, never occurred to the recent investigators to look for a common origin of the mesendoderm within protostomes. In the old literature (Bigelow, 1902) the mesendoblastic cell of crustaceans has been sometimes carefully compared with that found in annelids and molluscs, without far going conclusions though. Unfortunately, after the new system of Protostomia has been introduced (Aguinaldo et al., 1997) all the possible homologies in the cell fates between arthropods and spiralians have been forgotten. However ridiculous it might sound, I would still like to propose that a mesendoblastic blastomere is in fact a conserved feature within protostomes (Fig. 4.4.1). It is impossible by now to identify when exactly this feature has evolved, but it most likely has been present in the last common ancestor of Ecdysozoa and Spiralia.

Naturally, there is a number of counter-arguments to this hypothesis. For example, such groups as Phoronida and Brachiopoda, which are nested deeply within the phylogenetic trees of Protostomia and most likely belong with spiralians, according to the recent molecular analyses (Fig. 4.4.1.), do not have a single mesoderm precursor. Their mesoderm is suggested to be specified regionally during gastrulation on the border between ecto- and endoderm (Freeman, 1991; Freeman and Martindale, 2002). Some other accounts report the mesoderm of phoronids to have different locations of origin (Malakhov and Temereva, 1999; Temereva and Malakhov, 2007). Here one can always speculate that either these animals lost the peculiar specification of the D quadrant or that their position within protostomes might be up for reconsideration. Indeed, the idea of a mesendoblast as a protostomian feature and what is more important inductive mechanism similar (possibly) to deuterostomes (Rodaway et al., 1999; Rodaway and Patient, 2001; Nishida, 2005) support older views on the Phoronid and Brachiopod placement among Deuterostomia (Fig. 4.4.1.B,C; Dogiel, 1981; Nielsen, 1995; 2005). However, it is certainly beyond the scope of the present work to argue about the phylogenetic positions of these groups.

Another contradicting case is observed in Acoelomorpha. These organisms have quite an intriguing fate map compared to other animals: they have two mesendoblasts originating from non-sister cells at the 4-cell-stage (Bresslau, 1904; Henry et al., 2000). Some deletion experiments also showed that each blastomere at the two cell stage is fully capable of forming normal embryo, although of smaller size (Boyer, 1971). In the light of the undecided phylogenetical position of the acoelomorphs it is hard to interpret the presence of the two non-related mesendoblasts. On the one hand, it does not support the traditional placement of acoels within the flatworms, which, despite of most of the recent molecular analyses (Fig. 4.4.1.A), is still favoured by some studies (Egger et al., 2009). Most of the investigated flatworms demonstrate a cleavage pattern and the cell fates characteristic for the spiral mode of development including a singular mesendoblastic cell (Surface, 1907; Boyer et al., 1996; Martín-Durán and Egger, 2012; for the

same cleavage see also Selenka, 1881; Lang, 1884; Wilson, 1898). Clearly, due to the existing variety (Surface, 1907; Martín-Durán and Egger, 2012) in the embryonic development within Platyhelminthes, it is possible to consider the condition of the cell fate specification within acoels as derived compared to the ground pattern of the group of Platyhelminthes.

On the other hand, according to some phylogenetic analyses (Philippe et al., 2007; 2011), acoels and nemertodermatids belong with Ambulacralia within the deuterostomes. Unfortunately, neither the cleavage pattern nor the cell lineage of Acoela are similar to those of Echinodermata and Hemichordata (based on cell lineage studies of sea urchin and enteropneust) (Bresslau, 1904; Colwin and Colwin, 1951; Wray and Raff, 1990; Wray, 1994; Henry et al., 2000; 2001). Moreover, recent study on the mesoderm development performed for *Isodiametra pulchra* showed, that in the acoel development there are no traces of the coelom, which would be an attribute for the common deuterostome ancestor (Chiodin et al., 2013). Interestingly, the development of acoels can somewhat be compared with that of Ascidia (Conklin, 1905; Zalokar and Sardet, 1984; Nishida and Satoh, 1983; Stach et al., 2008). Both groups have the first division plane corresponding to the median plane of the future animal, although this is described for one species of enteropneust as well (Colwin and Colwin, 1951). The two resulting blastomeres are responsible for the left and right halves of the embryo. Additionally, both of these blastomeres give rise to the mesendoblasts in the future, but in ascidians they are more than two (at the 4-cell stage all four quadrants give mesendodermal descendants).

Placement of the acoelomorphs as a basal branch to all the bilaterians, which is found in most of the relevant phylogenetic studies of the past ten years will be addressed below (e.g. Hejnol et al., 2009; Edgecombe et al., 2011; Boll et al., 2013).

There are some other animals among protostomes with studied cell lineages, which possess more than one mesendoblast. First ones to be mentioned are the amphipods *Orchestia cavimana* (and possibly *Parhyale hawaiensis*), the development of which has already been considered to be of a derived mode (Scholtz and Wolff, 2002; Wolff and Scholtz, 2002; Hunnekuhl and Wolff, 2012). Another one is a chaetognath (Shimotori and Goto, 2001), whose phylogenetical position remains under constant dispute (Fig. 4.4.1.A; Marlétaz et al., 2006; Matus et al., 2006; Papillon et al., 2006). It is, however, not quite clear, whether chaetognaths have two mesendoblast or just one. Experiments on cell injections have not been performed beyond the 4-cell stage. It has been shown, that both anterior and posterior quadrants contribute to endoderm and mesoderm. The detailed origin and relation between the two germ layers remains unknown though.

Furthermore, quite an impressive amount of species do not have mesendoblastic cells at all. The mesoderm of the adults in this case is derived from mesectoblasts and is therefore representing

purely ectomesoderm. Among these animals are crustaceans (see Chapter 4.2.5.), nematodes (Drozdovskii, 1975; Malakhov and Spiridonov, 1981; Malakhov, 1986), and possibly rotiferans (although the origin of the germ layers is not thoroughly investigated (reviewed in Tannreuther, 1920; Nachtwey, 1925; Lechner, 1966). The idea of mesendoblast to be a feature presented in the protostome ancestor would lead to a non-parsimonious conclusion about multiple parallel losses of endomesoderm. Naturally, no one denies the other non-parsimonious possibility that mesendoblastic cells have evolved independently along the way of evolution within different protostome groups. With current knowledge it is hard to approve either way.

4.3.4.2. Division pattern of somatoblasts:

The specialty of the blastomeres 2d and 4d in spirally cleaving embryos rests not only in their responsible fates, but also in the way of their divisions. In contrast to that of other cells, at some point in development the division pattern of these cells becomes bilaterally symmetrical in relation to the animal-vegetal axis. Since old days this feature helped to trace the cells without difficulties. Given the similarity in the fate of 1d and 2d of *E. modestus* with 2d and 4d of spiralians, I could not help comparing the ways of their division. Both 1d and 2d in the barnacle divide bilaterally symmetrical[♣]. It is not that striking as in spiralians though, since the entire embryo cleaves in a bilaterally symmetrical way. Unfortunately, it is impossible to compare the spiralian 2d with any of the blastomeres in *Sicyonia ingentis* due to the absence of detailed data on the ectodermal lineage. However, it has been described that the endomesoblastic cell M2 (derivative of X_v) divides in fact bilaterally symmetrical to produce two mesoteloblasts (Hertzler, 2002; 2005; Pawlak et al, 2010).

Consequentially, one could suggest that the ancestral way of division in the blastomeres responsible for the ecto- and mesoderm formation was bilaterally symmetrical in relation to the animal-vegetal axis. This idea, however, has a far weaker basis that the one proposed in the previous subchapter. That is mostly due to the well known and widely accepted view, that radial cleavage is the ancestral condition for protostomes, with all other types of cleavage being derived from it, including bilateral features (Siewing, 1979; Nielsen, 1995; Valentine, 1997).

On the other hand, as it was just mentioned in the subchapter above, acoelomorphs are considered a basal bilaterian group in the most of recent phylogenies (references from Fig. 4.4.1.). The early cleavages in both groups of Acoelomorpha are bilaterally symmetrical (Bresslau, 1904; Henry et al., 2000; Jondelius et al., 2004). The later cleavage in Nemertodermatida becomes radial (Jondelius et al., 2004). The cleavage in deuterostomes is classically referred as

[♣] only the first divisions of the blastomeres are considered and compared, the later division pattern is referred as a different embryological stage and therefore is a subject to independent analysis (Scholtz, 2005)

radial (Nielsen, 1995; Valentine, 1997). However, the cleavage described for ascidians, for example, is rather bilateral[♣] (Conklin, 1905; Nishida and Satoh, 1983; 1985; Stach et al., 2008). The cleavage of ctenophorans, which are by some researchers considered as a sister group to bilaterians (Zrzavy et al., 1998; Peterson and Eernisse, 2001), is of a biradial type (Martindale and Henry, 1999).

The bilateral way of cleavage in acoels, ascidians, and ctenophores has been already compared and the similarities were pointed out in Henry et al., 2000. However, there was no a clear suggestion made. Hereby, I would like to propose the possibility that the ancestral mode of the protostomian cleavage was of a bilateral type, and that radial as well as spiral cleavage derived from it. This idea is not exactly new and was discussed before (Hadži, 1963), but obviously was not favored much. Following this hypothesis one could see the bilaterally symmetrical divisions of 2d and 4d of spiralians as a heritage from the ancestral cleavage type.

Given the above considered circumstances, the very presence of the certain blastomeres with a specific fate and dividing in a bilaterally symmetric way should not be taken as a definition for spiralians. One can, for example, refer to a unique cell lineage of the D blastomere, with somatoblasts being produced after the fourth and the sixth cell cycles. It is not, however, a goal of the present work to make a list of the characteristics of spiral cleavage.

Regarding the relation of the development of Cirripedia (and possibly of Crustacea) to the spiral mode, let's stay at that: spiral is spiral, and the crustacean mode is not spiral. Although some features, which were considered to be conserved for the spiral developmental mode, are rather conserved within Protostomia.

[♣] In general radial cleavage can also be considered as a form of bilateral, but bilateral can not be viewed as radial.

4.4. What if... a high card

This chapter includes some speculations on possible evolutionary scenarios for the cell lineages and the origin of the germ layers. In Fig. 4.4.1. one can see some developmental data mapped on a generalized phylogenetic tree of Metazoa. Certainly, it is far too obvious that the information is scarce and fragmented. Nevertheless, it is possible to make some suggestions regarding the developmental ground patterns of some metazoan groups (Fig. 4.4.1.A). Even though some of them have been discussed above, they are resumed here as following:

- a singular quadrant responsible for the formation of the endoderm is a characteristic for the "urecdysozoan";
- the way of the ectomesoderm formation in Crustacea represents a derived mode within Protostomia;
- a singular mesendoblastic cell is a characteristic for the protostomian ancestor;
- cleavage of the urbilaterian was bilateral.

The last point have been just addresses in the Chapter 4.3.4. and therefore will be omitted here.

4.4.1. One endoblast

To test the proposed "one-endoblast-apomorphy" for ecdysozoans one has to analyze possible ways of the evolution of the endoderm origin within protostomes. One of the main questions is which condition might be ancestral for protostomes. Within bilaterians three different patterns of endoblast origin occur: from one, two, and four quadrants (Fig. 4.4.1.). The state of two endoblastic lines is found in acoels (according to the recent data, the group is placed close to the bilaterian root, Fig. 4.4.1.A) and in chaetognaths (unclear position within protostomes, Fig. 4.4.1.A) (Bresslau, 1904; Henry et al., 2000; Schimotori and Goto, 2001). The pattern with one (most of the ecdysozoans) blastomere capable of endoderm formation (Fig. 4.4.1.) is described in Protostomia, mostly for ecdysozoans (see chapter 4.3.2.). The endoderm, which is formed by four quadrants, is found in many bilaterian groups both deuterostomes and protostomes (Fig. 4.4.1.). Based on known data it is possible to outline three scenarios for the endoblast evolution.

First scenario: The embryo of the protostomian ancestor is similar to that of acoels and has two endoblasts (Fig. 4.4.2.(1); 4.4.3:ScI). To reach the pattern with one endoblast one blastomere would have to lose the ability to give rise to endoderm. For some nematodes, for example, expe-

Figure 4.4.1. Phylogenetical analysis of Metazoa with mapped developmental characteristics
Groups with unclear position are written in different colours.
Colour code of developmental characteristics: cleavage, endoderm, ectomesoderm, endomesoderm.
A – generalized tree of Metazoa based on 19 sources; **B** - **C** – two selected versions of the older phylogenetical analyses.

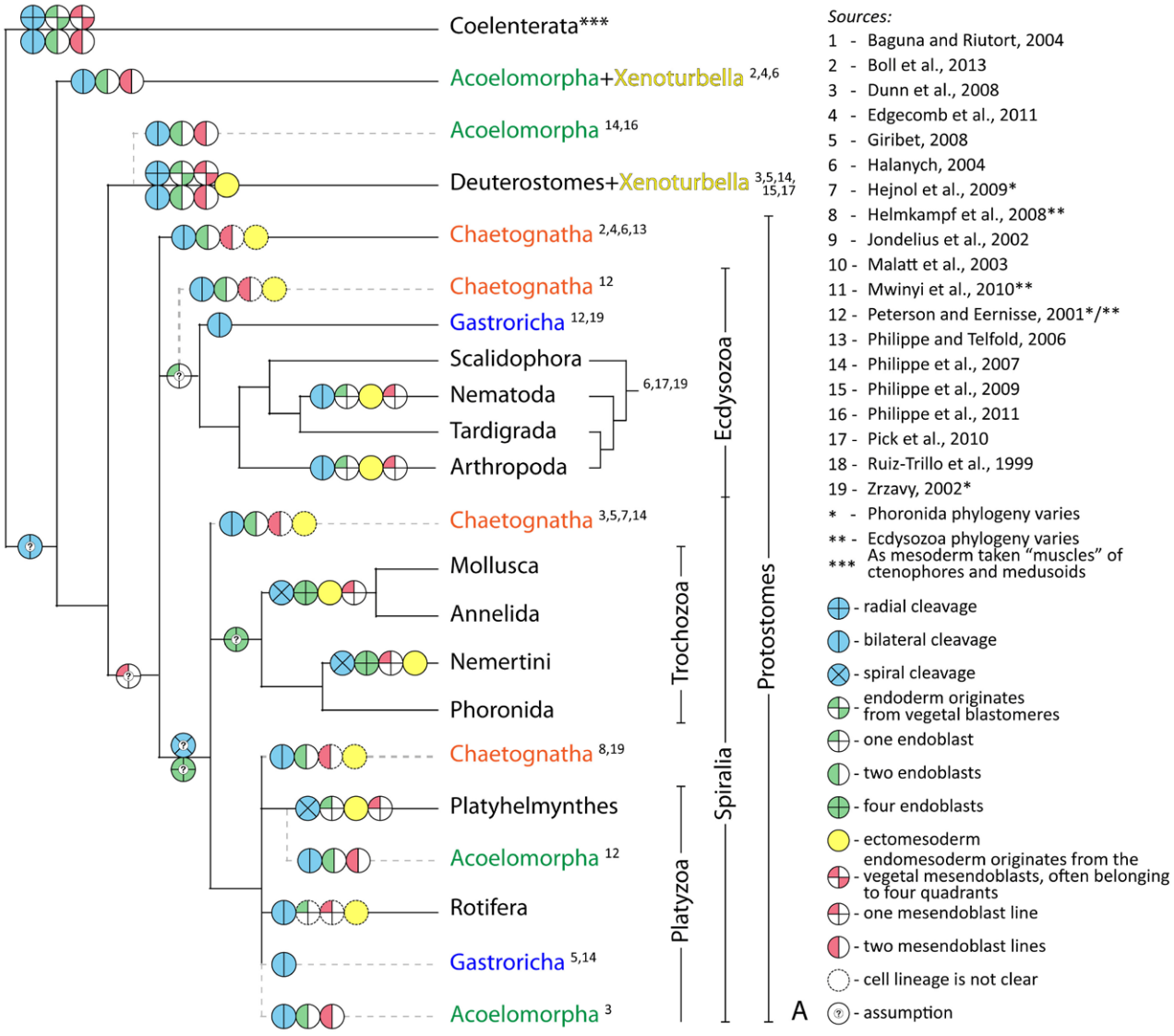
Coelenterata***
Acoelomorpha+Xenoturbella 2,4,6
Acoelomorpha 14,16
Deuterostomes+Xenoturbella 3,5,14, 15,17
Chaetognatha 2,4,6,13
Chaetognatha 12
Gastroricha 12,19
Scalidophora
Nematoda
Tardigrada
Arthropoda
6,17,19
Chaetognatha 3,5,7,14
Mollusca
Annelida
Nemertini
Phoronida
Chaetognatha 8,19
Platyhelmynthes
Acoelomorpha 12
Rotifera
Gastroricha 5,14
Acoelomorpha 3
Trochozoa
Platyzoa
Spiralia
Ecdysozoa
Protostomes
A
Sources:
1 - Baguna and Riutort, 2004
2 - Boll et al., 2013
3 - Dunn et al., 2008
4 - Edgecomb et al., 2011
5 - Giribet, 2008
6 - Halanych, 2004
7 - Hejnol et al., 2009*
8 - Helmkampf et al., 2008**
9 - Jondelius et al., 2002
10 - Malatt et al., 2003
11 - Mwinyi et al., 2010**
12 - Peterson and Eernisse, 2001*/**
13 - Philippe and Telfold, 2006
14 - Philippe et al., 2007
15 - Philippe et al., 2009
16 - Philippe et al., 2011
17 - Pick et al., 2010
18 - Ruiz-Trillo et al., 1999
19 - Zrzavy, 2002*
* - Phoronida phylogeny varies
** - Ecdysozoa phylogeny varies
*** As mesoderm taken "muscles" of ctenophores and medusoids
- radial cleavage
- bilateral cleavage
- spiral cleavage
- endoderm originates from vegetal blastomeres
- one endoblast
- two endoblasts
- four endoblasts
- ectomesoderm
- endomesoderm originates from the vegetal mesendoblasts, often belonging to four quadrants
- one mesendoblast line
- two mesendoblast lines
- cell lineage is not clear
- assumption

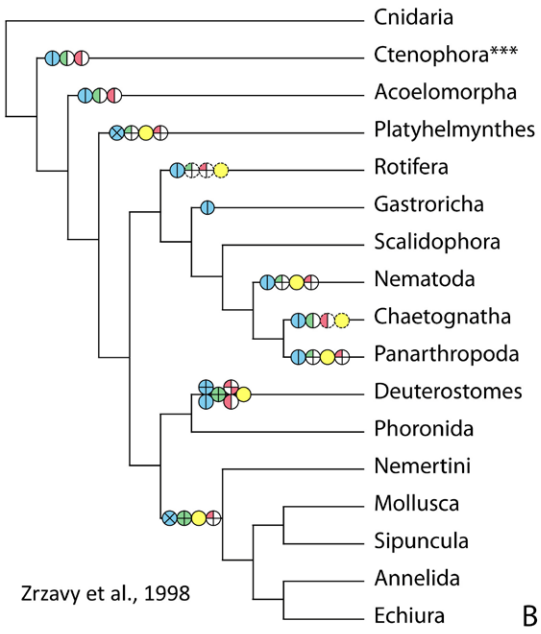
Cnidaria
Ctenophora***
Acoelomorpha
Platyhelmynthes
Rotifera
Gastroricha
Scalidophora
Nematoda
Chaetognatha
Panarthropoda
Deuterostomes
Phoronida
Nemertini
Mollusca
Sipuncula
Annelida
Echiura
Zrzavy et al., 1998
B

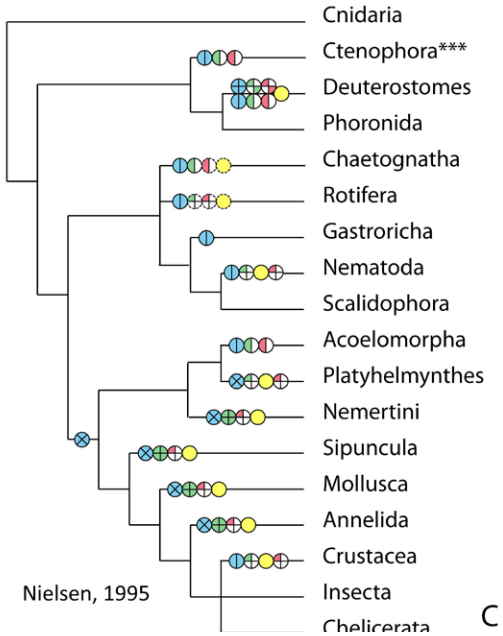
Cnidaria
Ctenophora***
Deuterostomes
Phoronida
Chaetognatha
Rotifera
Gastroricha
Nematoda
Scalidophora
Acoelomorpha
Platyhelmynthes
Nemertini
Sipuncula
Mollusca
Annelida
Crustacea
Insecta
Chelicerata
Nielsen, 1995
C

rimental studies have shown that both anterior and posterior blastomeres at the 2-cell stage have endodermal potential, whereas under normal conditions the endoblast originates exclusively from the posterior blastomere (Wiegner and Schierenberg, 1998). On the way to four-endoblast-model of development all four quadrants have to become capable of the endoderm specification. Furthermore, one could always go for the idea of adding or skipping some cleavages with postponing or fastening of the germ layer separation (such ideas have been popular for over a century: Bigelow, 1902; Costello and Henley, 1976; Henry et al., 2000).

Second scenario: The loss of the ability of one blastomere of the two to differentiate into endoderm or the skip of cleavages has happened already in protostomian ancestor, which might have been derived from a common bilaterian ancestor similar in the cell lineage to the modern Acoela (Fig. 4.4.2.:2; 4.4.3: possible in ScenarioII). In this case the developmental pattern observed in the most of trochozoans is a derived condition (Fig. 4.4.1.A). Multiple quadrant origin of the endoderm is observed, for example, in several crustacean groups: Iblomorpha, Rhizocephala, Amphipoda (Bocquet-Vedrine, 1961; Anderson, 1965; Scholtz and Wolff, 2002), while an endoderm in the ground pattern of Crustacea supposedly originates from a singular D quadrant (Weygoldt, 1960a). Interestingly, this scenario is better supported by older metazoan phylogenies (Fig. 4.4.1.B,C; see also Halanych, 2004).

Third scenario: This scenario is opposite to the second one (Fig. 4.4.2: 3; 4.4.3. possible in ScenarioII). The embryo of the protostomian ancestor forms its endoderm from four quadrants. A derived condition with the endodermal fate restricted to a singular blastomere is found in ecdy-

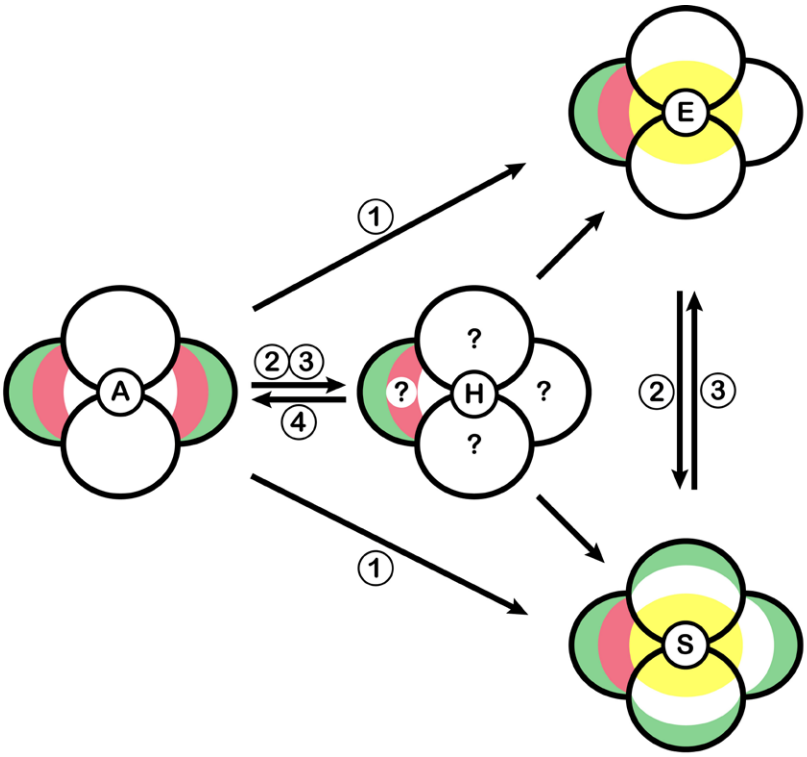

Fig. 4.4.2. Hypothetical transformations between quadrant fates within protostomes.

Colour code: endoderm, ectomesoderm, endomesoderm.

Circles with letters represent developmental patterns similar to those found in:

A – acoels;
E – ecdysozoans;
H – hypothetical ancestor;
S – spiralians.

Circles with numbers represent evolutionary scenarios (explanation in the text).

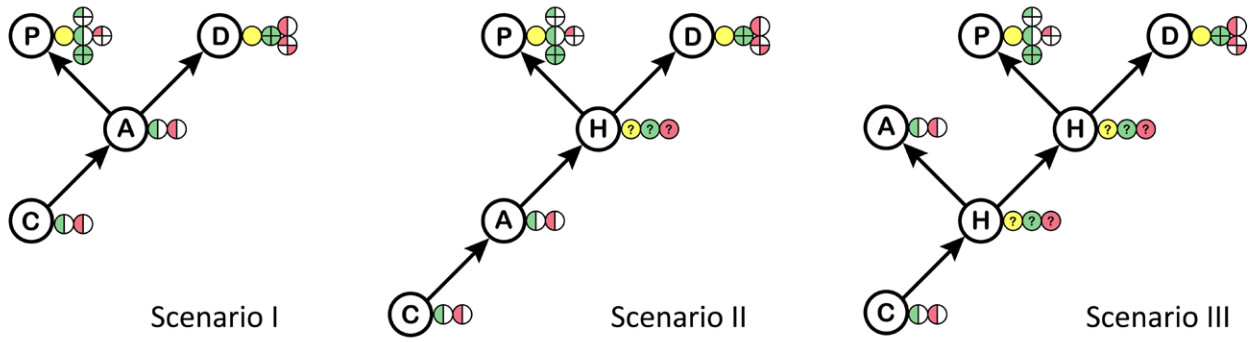

Fig. 4.4.3. Hypothetical transformations between developmental patterns within bilaterians.

Colour code: endoderm, ectomesoderm, endomesoderm.

Circles with letters represent developmental patterns similar to those found in:
A – acoels; **C** – ctenophorans*; **D** – deuterostomes; **H** – hypothetical ancestor; **P** – protostomes.

*Ctenophora is suggested as a sister group to all Bilateria e.g. in Zrzavy et al., 1998; Peterson and Eernisse, 2001.

Scenario I: the developmental pattern of acoels represents an ancestral state within bilaterians, the patterns of protostomes and deuterostomes being derived from it.
Scenario II: the developmental pattern of acoels represents an ancestral state within bilaterians. The pattern (not known) of the last common nephrozoan ancestor (H) was derived from it. The patterns of protostomes and deuterostomes evolved from the latter.
Scenario III: the developmental patterns of both bilaterian and nephrozoan ancestors are not known (possibly identical, (H)). The pattern of acoels was derived from the former one, while the patterns of proto- and deuterostomes were derived from the latter one.

sozoans, some platyzoans and polychaetes (Fig. 4.4.1.A). Such way of evolution is possibly exemplified in flatworms and polychaetes (only if the ground pattern for all the spiralians is in fact the presence of four endoblasts). In these animals the four macromeres are formed, but they degenerate and the endodermal fate is entirely carried out by the micromere 4d (Surface, 1907; Nielsen, 1995; Boyer et al., 1998).

Naturally, it is quite possible that the evolutionary way for bilaterian embryos was close to the one shown in Fig. 4.4.2.:4 and Fig. 4.4.3:Scenario III, when the state of embryological characters found in acoels is also derived from the unknown ones. In this case the endodermal pattern of the protostomian ancestor becomes even more speculative than those, which have just been discussed.

4.4.2. Once again about ectomesoderm

Due to the present variety in ectomesoderm products, from total absence till the formation of the complete mesoderm, and the occurrence of such variety within closely related groups, it is hard to identify general direction of the ectomesoderm evolution. It is as well complicated when it comes to the origin of it. Historically (and the evidence grows ever stronger) the mesoderm seems to originate from endoderm. It is by now supported by the cell lineages of the ctenophores

(Martindale and Henry, 1999) and the acoels (possibly basal bilaterian) (Henry et al., 2000). Both of these organisms lack ectomesoderm (or in the case of ctenophores, to be on a safe side, the muscle elements originate from endodermal lineage). Additional supportive data come from molecular research. As it was mentioned in the Chapter 4.3.3. most of the genes involved in the early mesoderm specification and patterning in high bilaterians (like *brachyury*, *fork head*, *twist*, *snail* etc...) were found expressing in the endoderm close to the blastopore region of cnidarians. All of it suggests that ectomesoderm was evolved in some early bilaterian animals.

The question, which comes next, is whether the ectomesoderm of protostomes is homologous to that of deuterostomes. Here one has to clarify, that it is cellular relations what is meant and not genetical network behind the fate specification (even if it might be incorrect to make such distinction). The data on ectomesoderm of protostomes have been provided in the Chapter 4.3.3.1. The reports on the ectomesoderm, or the secondary mesoderm, within deuterostomes come from some tunicates (Conklin, 1905; Nishida and Satoh, 1985; Nishida, 1987) and vertebrates (reviewed in Rodaway and Patient, 2001).

If one assumes that the ectomesoderm was evolved only once on the clade of bilaterians and the ectomesoderm of proto- and deuterostomes is in fact homologous (Fig. 4.4.3. Scenario II and III), then its absence in some polychaetes (Wilson, 1898; Child, 1899), chitons (Henry et al., 2004), amphipods (Wolff and Scholtz, 2002; Hunnekuhl and Wolff, 2012), enteropneusts (Henry et al., 2001), ambulacralians (Cameron et al., 1987; Wray and Raff, 1990; Wray, 1994) should be considered as a loss. It is not, however, clear with Acelomorpha. Their developmental pattern might be indeed similar to that in the ancestral bilaterian, with no traces of ectomesoderm. This leads to the two scenarios. According to one, the ability to develop mesoderm from ectodermal cells evolved anew in higher bilaterians (Fig. 4.4.3: Scenario II). According to the second, although not very parsimonious one, it is possible to suggest the independent way of ectomesoderm evolvement within Protostomia and Deuterostomia (Fig. 4.4.3: Scenario I). On the other hand, the urbilaterian might have already evolved the ectomesodermal line and the acoels lost it during their evolution (Fig. 4.4.3: Scenario III).

4.4.3. Important blastomere

A singular blastomere capable of giving rise to both endo- and mesoderm has been proposed in the present work to be considered a characteristic of developmental ground pattern for protostomes. Indeed, such a cell has been so far described exclusively within protostomes. The way of specification of the mesendoblast is not quite clear yet. The studies demonstrated that this cell is restricted to a certain blastomere, which might be defined at different stages of cleavage (Free-

man and Lundelius, 1992). When the blastomere is specified and its deletion is done, the mesendoblastic cell is never formed by any other quadrants and their descendants (Cather and Verdonk, 1979; Render, 1997). The motheR quadrant of the mesendoblast can be specified differently: either via cytoplasmic determinants or via cellular interactions (van den Biggelaar, 1976; 1977; Henry and Martindale, 1987; van den Biggelaar and Faber, 1994; Henry et al., 2004; reviewed: Freeman and Lundelius, 1992). Regardless of the way of specification it is always a singular blastomere, which gives birth to a singular mesendoblast.

On the contrary, in the animals outside of protostomes the mesendoblasts are more in number and they originate either from two non-sister blastomeres (at the 4-cell stage) or from all four quadrants (Fig. 4.4.1.). The state with mesendoblasts originating from two blastomeres we find outside bilaterians (Ctenophora) (Martindale and Henry, 1999), in Acoelomorpha (Acoela) (Bresslau, 1904; Henry et al., 2000), in deuterostomes (some Enteropneusta) (Colwin and Colwin, 1951), and also in protostomes (Chaetognatha) (Shimotori and Goto, 2001). In all of these animals (apart from Chaetognatha) the first cleavage corresponds to the bilateral symmetry plane of the adult and divides the zygote into two potentially equal blastomeres (both giving rise to endomesoderm). Interestingly, the experimental studies performed on acoels have shown, that any of the two blastomeres is able to form entire animal (Boyer, 1971).

It would be interesting to study the reasons and ways, which really lead to the restriction of the "important" cell fates not only to one quadrant but also to one cell. At present one can just hypothesize evolutionary paths on the basis of the existing phylogenetical analyses. On the Fig. 4.4.3. several possible scenarios of transformations from one set of developmental characters to another are present.

Clearly, these scenarios are pure speculations and none of them answers the questions, when this characteristic (singular mesendoblast) has evolved and whether the mesendodermal cell could indeed be an apomorphy for protostomes. For example, rather the curious cell lineage described for chaetognaths might provide contradicting material (Shimotori and Goto, 2001). The first two blastomeres of the chaetognath embryo are capable of giving rise to all three germ layers. According to some phylogenetical views (Fig. 4.4.1.A; see additionally: Marlétaz et al ., 2006; Papillon et al., 2006), chaetognaths are placed at the base of protostomes. However, as it was mentioned above, it is not clear, whether mesoderm from both of the blastomeres at the 2-cell stage is really endomesoderm. If it is so, the basic phylogenetic position suggests that the protostome ancestor might have had two mesendoblasts. The condition has changed either in the common ancestor of Spiralia and Ecdysozoa (Fig. 4.4.2.:2,3) or in both of these groups independently (Fig. 4.4.2.:1).

One has to be aware that the analysis provided in this chapter is nothing more than speculations lacking any evidence as well as the connection to the other characters used for analyses of such kind. Still, unless proven wrong these ideas/hypotheses have right to exist, or at least the author thinks so. To all the readers: this chapter can be easily skipped...

5. SUMMARY

English

The present work is devoted to the embryonic development of the thoracican barnacle *Elminius modestus* (Thecostraca: Cirripedia). The developmental process was investigated by means of different techniques like 4D microscopy, *in vivo* labelling, fluorescent histochemistry, and confocal laser scanning microscopy combined with 3D reconstructions. The entire embryonic development could roughly be subdivided into the stages of cleavage, germ layer differentiation, and morphogenesis.

The cleavage of *E. modestus* is total, unequal with regards to the yolky cell, and asynchronous with an anterior-posterior gradient. The entire process appears to follow a strict pattern of divisions with very little variability, one of which includes the occurrence of mirror image embryos from the 4-cell stage on. The nomenclature, which was applied to distinguish blastomeres, was adopted from Conklin (1897) and Anderson (1969). The gastrulation of *E. modestus* proceeds in a stepwise way with consecutive internalization of the endoblast, the endomesoblasts, and at last the mesectoblasts. All of this happens in the area of the blastopore.

The germ layer differentiation was mainly studied by means of *in vivo* labelling. The segregation of the endodermal and the endomesodemal germ layers are shown to happen after the fourth division, whereas the ectomesoderm segregates after the sixth division. The primordial germ cells are suggested to be a product of the seventh cleavage division of the yolky cells ($3D^a$ and $3D^p$). During the research the cell lineage of each germ layer was established, the fates of the quadrant descendants are described up to the 16-cell stage. The ectoderm originates from four quadrants, as does the ectomesoderm (the last identified mesectoblasts are 3A, 3B, 3C, $1d^{rp}$, and $1d^{lp}$). The endoderm and the endomesoderm develop from single precursors at the 16-cell stage (2D and 2d, respectively).

The obtained results on the early embryonic development and cell fates are in great accordance with those of some previous researchers (Groom, 1894; Bigelow, 1902; Delsman, 1917), although they contradict in many points the study of Anderson (1969). The comparison of the cleavage and gastrulation processes as well as the germ layer origin of the barnacles with those of the other crustaceans outlined some major similarities. The descendants of two quadrants (A and C) divide in an organized manner, thus producing a patch of cells highly resembling the cell band described for some other crustaceans. A gastrulation with temporal differences in germ layer internalization was also reported for many other crustaceans. In addition, the cell lineage of the resulting blastopore seems to represent another “crustacean feature”, the mesectoblastic blastopore. This is discussed in a broad comparative way and might be a derived characteristic within Protostomia (or maybe Ecdysozoa). One further similarity in the development of *E. modestu*s and other crustaceans, namely the presence of only a single endoblastic cell, might represent an apomorphy for the entire group of Ecdysozoa. A singular mesendoblast is suggested to be a possible feature in the developmental ground pattern of all Protostomia.

Additionally, some interesting information was obtained on the mesoderm differentiation, the hind gut development, and the postnaupliar mesoderm. The general process of mesoderm development in the naupliar segments, from cleavage stages until early myogenesis, is described here for the first time for a non-malacostracan. The singular muscle precursors most likely differentiate into the muscles omitting the step of fusion. The hind gut originating from the same blastomeres as the foregut and invaginating from the region opposite to the blastopore represents for now a rather unique mode of development and is hard to be interpreted. Presumtive postnaupliar-mesoblasts are not characterized by teloblastic divisions and are descending from the ectomesodermal line.

Deutsch

Die vorliegende Arbeit behandelt die Embryonalentwicklung des Rankenfußkrebses *Elminius modestus* (Thecostraca: Cirripedia). Der Entwicklungsprozess wurde mithilfe unterschiedlicher Methoden wie 4D Mikroskopie, *in vivo* Einzelzellmarkierungen, Fluoreszenzhistochemie und konfokaler Laserscanningmikroskopie in Verbindung mit 3D Rekonstruktionen untersucht. Die gesamte Embryonalentwicklung kann grob in die Stadien der Furchung, der Keimblattdifferenzierung und der Morphogenese unterteilt werden.

Die Furchung von *E. modestus* ist total, inequal in Bezug auf die Dotterzelle und asynchron mit einem anterior-posterioren Gradienten. Der gesamte Prozess folgt einem strengen Teilungsmuster mit nur sehr geringer Variabilität. Eine davon stellt das Auftreten spiegelbildlicher Embryonen ab dem 4-Zell Stadium dar. Die zur Benennung der Blastomeren verwendete Nomenklatur wurde von Conklin (1897) und Anderson (1969) übernommen. Die Gastrulation vollzieht sich in einem Prozess, in dem die Internalisierung des Endoblasten, der Endomesoblasten und schließlich der Mesectoblasten aufeinander folgen. All das erfolgt in der Region des Blastoporus.

Die Keimblattdifferenzierung wurde vor allem mittels *in vivo* Zellmarkierungen untersucht. Die Trennung der endodermalen und endomesodemalen Keimblätter erfolgt nach der vierten Furchungsteilung, die Trennung des Ectomesoderm nach der sechsten Teilung. Die Urkeimzellen sind aller Wahrscheinlichkeit nach ein Produkt der siebten Furchungsteilung der Dotterzellen ($3D^a$ und $3D^p$). Im Zuge der Untersuchung konnte die Zelllinie jedes Keimblattes rekonstruiert werden, die Zellschicksale der Abkömmlinge der Quadranten wurde bis zum 16-Zell Stadium beschrieben. Das Ectoderm entspringt allen vier Quadranten, ebenso das Ectomesoderm (die letzten identifizierten Mesectoblasten sind 3A, 3B, 3C, $1d^{rp}$ und $1d^{lp}$). Endoderm und Endomesoderm entwickeln sich aus einzelnen Vorläuferzellen im 16-Zell Stadium (2D bzw. 2d).

Die Ergebnisse zur frühen Embryonalentwicklung und Zellschicksalen stimmen weitgehend mit früheren Studien überein (Groom, 1894; Bigelow, 1902; Delsman, 1917), widersprechen allerdings in etlichen Punkten der Studie von Anderson (1969). Ein Vergleich der Furchung und Gastrulation sowie des Ursprungs der Keimblätter zeigt große Übereinstimmungen zwischen dem untersuchten Rankenfüßer und anderen Krebstieren. Die Abkömmlinge zweier Quadranten (A und C) teilen sich in einem Muster, das zur Ausbildung eines Zellbandes führt, welches auch für andere Krebse beschrieben wurde. Ebenso ist auch eine Gastrulation mit zeitlichen Unterschieden in der Keimblattinternalisierung bei vielen Krebsen bekannt. Darüber hinaus scheint die Zelllinie des Blastoporus (mesectoblastischer Blastoporus) ein „Krebsmerkmal“ dazustellen. Dieses wird umfassend vergleichend diskutiert und stellt möglicherweise gar eine Apomorphie der Protostomia (oder der Ecdysozoa) dar. Eine weitere Übereinstimmung in der Entwicklung von *E. modestus* und der der übrigen Krebstiere, nämlich das Auftreten nur eines einzelnen Endoblasten, stellt eine mögliche Apomorphie aller Ecdysozoa dar. Das Vorhandensein eines einzelnen Mesendoblasten wird als mögliches Merkmal des Grundmusters aller Protostomia in Betracht gezogen.

Zusätzlich konnten einige interessante Erkenntnisse über die Mesodermdifferenzierung, die Entwicklung des Hinterdarms und des postnauplialen Mesoderms gewonnen werden. Der Prozess der Mesodermentwicklung in den nauplialen Segmenten wird hier erstmalig von den Furchungsstadien bis zur frühen Myogenese für einen Nicht-Malakostraken beschrieben. Anscheinend differenzieren die einzelnen Muskelvorläufer zu Muskeln ohne dass es dabei zu einer Zellfusion kommt. Die Tatsache, dass Hinter- und Vorderdarm aus denselben Blastomeren entspringen und an der Region gegenüber des Blastoporus invaginieren, stellt einen zum jetzigen Zeitpunkt einzigartigen und schwer zu interpretierenden Entwicklungsmodus dar. Mutmaßliche postnaupliale Mesoblasten entstehen nicht durch teloblastische Proliferation, sondern entstammen der ectomesodermalen Zellinie.

6. REFERENCE LIST

Ackermann, C., Dorresteijn, A., Fischer, A. **2005.** Clonal domains in postlarval *Platynereis dumerilii* (Annelida: Polychaeta). *Journal of Morphology*. 266: 258-280.

Agar, W.E. 1908. Note on the early development of a cladoceran (*Holopedium gibberum*). *Zoologischer Anzeiger.* 33: 420-427.

Aguinaldo, A.M., Turbeville, J.M., Linford, L.S., Rivera, M.C., Garey, J.R., Raff, R.A., Lake, J.A. **1997**. Evidence for a clade of nematodes, arthropods and other moulting animals. *Nature.* 387(6632): 489-493.

Alwes, F., Scholtz, G. **2004**. Cleavage and gastrulation of the euphausiacean *Meganyctiphanes norvegica* (Crustacea, Malacostraca). *Zoomorphology*. 123: 125-137.

Alwes, F. 2008. Cell lineage studies in Crustacea - Aspects of the early development and germ layer formation in *Meganyctiphanes norvegica* (Malacostraca, Euphausiacea) and *Bythotrephes longimanus* (Cladocera, Branchiopoda). *Dissertation*. Humboldt-Universität zu Berlin, Berlin.

Alwes, F., Hinchen, B., Extavour, C. **2011**. Patterns of cell lineage, movement, and migration from germ layer specification to gastrulation in the amphipod crustacean *Parhyale hawaiensis*. *Developmental Biology*. 359: 110-123.

Anderson, D.T. 1959. The embryology of the polychaete *Scoloplos armiger*. *Quarterly Journal of Microscopical Science*. 100(1): 89-166.

Anderson, D.T. 1965. Embryonic and larval development and segment formation in *Ibla quadrivalvis* Cuv. (Cirripedia). *Australian Journal of Zoology*. 13(1): 1-15.

Anderson, D.T. 1966. The comparative early embryology of the Oligochaeta, Hirudinae and Onychophora. *Proceedings of the Linnean Society of New South Wales*. 91(1): 10-43.

Anderson, D.T. 1966. The comparative embryology of the polychaeta. *Acta Zoologica*. 47: 1-42.

Anderson, D.T. 1967. Larval development and segment formation in the branchiopod crustaceans *Limnadia stanleyana* King (Conchostraca) and *Artemia salina* (L.) (Anostraca). *Australian Journal of Zoology*. 15: 47-91.

Anderson, D.T. 1969. On the embryology of the cirrepede crustacean *Tetraclita rosea* (Krauss), *Tetraclita purpurascens* (Wood), *Chthamalus antennatus* (Darwin) and *Chamaesipho columna* (Spengler) and some considerations of crustacean phylogenetic relationships. *Philosophical Transactions of the Royal Society of London, series B: Biological Sciences.* 256(806): 183-235.

Anderson, D.T. 1979. Embryos, fate maps, and the phylogeny of arthropods. in (ed. Gupta, A.P.) *Arthropod phylogeny*. Van Nostrand Reinhold, New York.

Anderson, D.T. 1987. The larval musculature of the barnacle *Ibla quadrivalvis* Cuvier (Cirripedia, Lepadomorpha). *Proceedings of the Royal Society of London, series B: Biological Sciences.* 231: 313-338.

Andrew, D.R. 2011. A new view of insectecrustacean relationships II. Inferences from expressed sequence tags and comparisons with neural cladistics. *Arthropod Structure and Development*. 40: 289-302

Arendt, D., Technau, U., Wittbrodt, J. **2001**. Evolution of the bilaterian larval foregut. *Nature*. 409: 81-85.

Baguñá, J., Riutort, M. **2004**. The dawn of bilaterial animals: the case of acoelomorph flatworms. *BioEssays*. 26: 1046-1057.

Baldass, von F. 1937. Entwicklung von *Holopedium gibberum*. *Zoologische Jahrbücher. Abteilung für Anatomie und Ontogenie der Tiere*. 63: 399-454.

Baldass, von F. 1941. Entwicklung von *Daphnia pulex*. *Zoologische Jahrbücher. Abteilung für Anatomie und Ontogenie der Tiere.* 67: 1-60.

Bate, M. 1990. The embryonic development of larval muscles in *Drosophila*. *Development.* 110: 791-804.

Batham, E.J. 1945. *Pollicipes spinosus* Quoy and Gaimard. II. Embryonic and larval development. *Transactions of the Royal Society of New Zealand*. 75: 405-418.

Beauchamp, P. 1956. Le de´veloppement de *Ploesoma hudsoni* (Imhof) et l'origine des feuillets chez les Rotiferes. *Details - Bulletin de la Société zoologique de France*. 81: 374-383.

Benesch, R. 1969. Zur Ontogenie und Morphologie von *Artemia salina* L. *Zoologische Jahrbücher. Abteilung für Anatomie und Ontogenie der Tiere.* 86: 307-458.

Biffis, C., Alwes, F., Scholtz, G. **2009**. Cleavage and gastrulation of the dendrobranchiate shrimp *Penaeus monodon* (Crustacea, Malacostraca, Decapoda). *Arthropod Structure and Development*. 38: 527-540.

Bigelow, M.A. 1902. The early development of *Lepas*. A study of cell-lineage and germ-layers. *Bulletin of the Museum of Comparative Zoology at Harvard College*. 40(2): 62-143.

Blochman, F. 1882. Über die Entwicklung der Neritinia fluviatilis Mül. *Zeitschrift für Wissenschaftliche Zoologie*. 36: 125-174.

Bocquet-Védrine, J. 1961. Monographie de *Chtamalophilus delagei* J. Bocquet-Védrine, rhizocéphalan parasite de *Chtamalus stellatus* (Poli). *Cahiers Biologie Marine*. 2: 455-593.

Bocquet-Védrine, J. 1964. Embryologie précoce de *Sacculina carcini* Thompson. *Zoologische Mededelingen.* 39: 1-11.

Boll, P., Rossi, I., Amaral, S., Oliveira, S., Müller, E., Lemos, V., Leal-Zanchet, A. **2013**. Platyhelminthes ou apenas semelhantes a Platyhelminthes? Relações filogenéticas dos principais grupos de turbelários. *Neotropical Biology and Conservation.* 8(1): 41-52.

Boyer, B.C. 1971. Regulative development in a spiralian embryo as shown by cell deletion experiments on the acoel, Childia. *Journal of Experimental Zoology.* 176(1): 97-105.

Boyer, B.C., Henry, J.Q. **1998**. Evolutionary modifications of the spiralian developmental program. *American Zoologist*. 38: 621-633

Boyer, B.C., Henry, J.Q., Martindale, M.Q. **1996**. Dual origins of mesoderm in a basal spiralian: cell lineage analyses in the polyclad turbellarian *Hoploplana inquilina*. *Developmental Biology*. 179: 329-338.

Boyer, B.C., Henry, J.J., Martindale, M.Q. **1998**. The cell lineage of a polyclade turbellarian embryo reveals close similarity to coelomate spiralians. *Developmental Biology*. 204: 111-123.

Bresslau, E. 1904. Beiträge zur Entwicklungsgeschichte der Turbellarien. I. Die Entwicklung der Rhabdocoelen und Äcoelen. *Zeitschrift für Wissenschaftliche Zoologie*. 76: 213-332

Broitman-Maduro, G., Lin, K.T., Hung, W.W., Maduro, M.F. **2006**. Specification of the *C. elegans* MS blastomere by the T-box factor TBX-35. *Development.* 133(16): 3097-3106.

Burton, P.M. 2008. Insights from diploblasts; the evolution of mesoderm and muscle. *Journal of Experimental Zoology, Part B: Molecular and Developmental Evolution.* 310B(1): 5-14.

Cameron, R.A., Hough-Evans, B.R., Britten, R.J., Davidson, E.H. **1987**. Lineage and fate of each blastomere of the eight-cell sea urchin embryo. *Genes and Development*. 1: 75-84.

Cannon, H.G. 1921. The early development of the summer egg of a cladoceran (*Simocephalus vetulus*). *Quarterly Journal of Microscopical Science*. 65: 627-642.

Caspari, F. 2010. Aspekte der Ontogenese von *Macrostomum lignano* (Plathelminthes, Macrostomida). *Diplomarbeit*. Humboldt-Universität zu Berlin, Berlin.

Cather, J., Verdonk, N. **1979**. Development ofDentalium following removal of D quadrant blastomeres at successive cleavage stages. *Wilhelm Roux's archives of developmental biology.* 187(4): 355-366.

Child, C.M. 1900. The early development of *Arenicola* and *Sternaspis*. *Wilhelm Roux' Archiv für Entwicklungsmechanik der Organismen.* 9: 587-723.

Chiodin, M., Børve, A., Berezikov, E., Ladurner, P., Martinez, P., Hejnol, A. **2013**. Mesodermal gene expression in the acoel *Isodiametra pulchra* Indicates a low number of mesodermal cell types and the endomesodermal origin of the gonads. *PLoS ONE.* 8(2): e55499.

Colwin, A.L., Colwin, L.H. **1951**. Relationships between the egg and larva of *Saccoglossus kowalevskii*: axes and planes; general prospective significance of the early blastomeres. *Journal of Experimental Zoology*. 117: 111-137.

Conklin, E.G. 1897. The embryology of Crepidula - A contribution to the cell lineage and early development of some marine gastropods. *Journal of Morphology*. 13(1): 1-227.

Conklin, E.G. 1905. The organization and cell-lineage of the Ascidian egg. *Journal of the Academy of Natural Science of Philadelphia*. 13: 1-119.

Conklin, E.G. 1907. The embryology of *Fulgur*: a study of the influence of yolk on development. *Proceedings of the Academy of Natural Sciences of Philadelphia*. 59: 320-359.

Costello, D.P., Henley, C. **1976**. Spiralian development: a perspective. *American Zoologist*. 16: 277-291.

Crisp, D.J. 1954. The breeding of *Balanus porcatus* (da Costa). *Journal of the Marine Biological Association of the United Kingdom.* 33. 473-494.

Darwin, C. 1854. *Cirripedia I and II.* The Ray Society.

Delsman, H.C. 1914. Entwicklungsgeschichte von *Littorina obtusata*. *Tijdschrift der Nederlandsche Dierkundige Vereeniging.* 2(13): 170-340.

Delsman, H.C. 1917. Die Embryonalentwicklung von *Balanus balanoides* Linn. *Tijdschrift der Nederlandsche Dierkundige Vereeniging*. 15(2): 419-520.

Dictus, W.J.A.G., Damen, P. **1997**. Cell-lineage and clonal-contribution map of the trochophore larva of *Patella vulgata* (Mollusca). *Mechanisms of Development*. 62: 213-226.

Dogiel, V.A. 1981. *Invertebrate zoology*. 7th Edition (ed. Polyanskii, Yu.N.). Vysshaya Shkola Press, Moscow.[in Russian]

Dohle, W. 1979. Vergleichende Entwicklungsgeschichte des Mesoderms bei Articulaten. *Zeitschrift für zoologische Systematik und Evolutionsforschung*. 1: 120-140.

Dohle, W. 1989. Zur Frage der Homologie ontogenetischer Muster. *Zoologische Beiträge.* 32(3): 355-389.

Dohle, W. 1999. The ancestral cleavage pattern of the clitellates and its phylogenetic deviations. *Hydrobiologia*. 402: 267-283.

Dohle, W. 2001. Are the insects terrestrial crustaceans? A discussion of some new facts and arguments and the proposal of the proper name „Tetraconata“ for the monophyletic unit Crustacea + Hexapoda. in: *Origin of the Hexapoda* (ed. Deuve, T.). 37. Annales de la Société entomologique de France. 85-103.

Dohle, W., Gerberding, M., Hejnol, A., Scholtz, G. **2004**. Cell lineage, segment differentiation, and gene expression in Crustaceans. in (ed. Scholtz, G.) *Crustacean Issues, 15. Evolutionary Developmental Biology of Crustacea*. A.A. Balkema Publishers, Lisse. 95-133.

Drozdovskii, E.M. 1975. Blastulation in species of *Eudorylaimus* and *Mesodorylaimus* (Nematoda, Dorylaimida) and the role of blastulation in determining the composition of nematode subclasses. *Doklady Akademii Nauk.* 222(4): 1005-1008.

Dunn, C.W., Hejnol, A., Matus, D.Q., Pang, K., Browne, W.E., Smith, S.A., Seaver, E., Rouse, G.W., Obst, M., Edgecombe, G.D., Sorensen, M.V., Haddock, S.H., Schmidt-Rhaesa, A., Okusu, A., Kristensen, R.M., Wheeler, W.C., Martindale, M.Q., Giribet, G. **2008**. Broad phylogenomic sampling improves resolution of the animal tree of life. *Nature.* 452(7188): 745-749.

Edgecombe, G.D. 2010. Arthropod phylogeny: An overview from the perspectives of morphology, molecular data and the fossil record. *Arthropod Structure and Development.* 39(2-3): 74-87.

Edgecombe, G., Giribet, G., Dunn, C., Hejnol, A., Kristensen, R., Neves, R., Rouse, G., Worsaae, K., Sørensen, M. **2011**. Higher-level metazoan relationships: recent progress and remaining questions. *Organisms Diversity and Evolution.* 11(2): 151-172.

Egger, B., Steinke, D., Tarui, H., De Mulder, K., Arendt, D., Borgonie, G., Funayama, N., Gschwentner, R., Hartenstein, V., Hobmayer, B., Hooge, M., Hrouda, M., Ishida, S., Kobayashi, C., Kuales, G., Nishimu-

ra, O., Pfister, D., Rieger, R., Salvenmoser, W., Smith, J., Technau, U., Tyler, S., Agata, K., Salzburger, W., Ladurner, P. **2009**. To be or not to be a flatworm: the acoel controversy. *PLoS ONE.* 4(5): e5502.

Eisig, H. 1898. Zur Entwicklungsgeschichte der Capitelliden. *Mittheilungen aus der Zoologischen Station zu Neapel*. 13: 1-292.

Elpatiewsky, V.W. 1907. Die Urgeschlechtszellenbildung bei *Sagitta*. *Anatomischer Anzeiger*. 35: 226-239.

Extavour, C.G. 2005. The fate of isolated blastomeres with respect to germ cell formation in the amphipod crustacean *Parhyale hawaiensis*. *Developmental Biology*. 277(2): 387-402.

Extavour, C.G. 2007. Evolution of the bilaterian germ line: lineage origin and modulation of specification mechanisms. *Integrative and Comparative Biology*. 47(5): 770-785.

Extavour, C.G., Akam, M. **2003**. Mechanisms of germ cell specification across the metazoans: epigenesis and preformation. *Development*. 130: 5869-5884.

Fioroni, P. 1970. Die organogenetische und transitorische rolle der vitellophagen in der darmentwicklung von *Galathea* (Crustacea, Anomura). *Zeitschrift für Morphologie der Tiere*. 67(3): 263-306.

Freeman, G. 1991. The bases for and timing of regional specification during larval development in *Phoronis*. *Developmental Biology*. 147: 157-173.

Freeman, G., Lundelius, J.W. **1992**. Evolutionary implications of the mode of D quadrant specification in coelomates with spiral cleavage. *Journal of Evolutionary Biology*. 5(2): 205-247.

Freeman, G., Martindale, M.Q. **2002**. The origin of mesoderm in phoronids. *Developmental Biology*. 252: 301-311.

Fryer, G. 1983. Functional ontogenetic changes in *Branchinecta ferox* (Milne-Edwards) (Crustacea: Anostraca). *Philosophical Transactions of the Royal Society of London, series B: Biological Sciences.* 303: 229-343.

Fuchs, K. 1914. Die Keimbahnentwicklung von *Cyclops viridis* Jurine. *Zoologische Jahrbücher. Abteilung für Anatomie und Ontogenie der Tiere*. 38: 103-156.

Gerberding, M., Browne, W.E., Patel, N.H. **2002**. Cell lineage analysis of the amphipod crustacean *Parhyale hawaiensis* reveals an early restriction of cell fates. *Development*. 129: 5789-5801.

Gerberding, M., Patel, N.H. **2004**. Gastrulation in crustaceans: Germ layers and cell lineages. in *Gastrulation: From cells to embryo* (ed. Stern, C.D.). Cold Spring Harbor Laboratory Press. 79-89.

Gerould, J.H. 1907. The development of *Phascolosoma*. *Zoologische Jahrbücher. Abteilung für Anatomie und Ontogenie der Tiere*. 23: 77-162.

Giribet, G. 2008. Assembling the lophotrochozoan (=spiralian) tree of life. *Philosophical Transactions of the Royal Society of London, Section B: Biological Sciences.* 363(1496): 1513-1522.

Giribet, G., Edgecombe, G. D. **2012**. Reevaluating the Arthropod Tree of Life. *Annual Review of Entomology*. 57(1): 167-186.

Giribet, G., Edgecombe, G.D., Wheeler, W.C. **2001**. Arthropod phylogeny based on eight molecular loci and morphology. *Nature.* 413: 157-161.

Gline, S., Nakamoto, A., Cho, S.-J., Chi, C., Weisblat, D. **2011**. Lineage analysis of micromere 4d, a superphylotypic cell for Lophotrochozoa, in the leech *Helobdella* and the sludgeworm *Tubifex*. *Developmental Biology*. 353(1): 120-133.

Good, K., Ciosk, R., Nance, J., Neves, A., Hill, R.J., Priess, J.R. **2004**. The T-box transcription factors TBX-37 and TBX-38 link GLP-1/Notch signaling to mesoderm induction in *C. elegans* embryos. *Development.* 131(9): 1967-1978.

Goto, A., Kitamura, K., Shimizu, T., Nakamoto, A. **1999**. Cell lineage analysis of pattern formation in the *Tubifex* embryo. I. Segmentation in the mesoderm. *International Journal for Developmental Biology*. 43: 317-327.

Grattan, R.M., McCulloch, R.J., Sellars, M.J., Hertzler, P.L. **2013**. Ultrastructure of putative germ granules in the penaeid shrimp *Marsupenaeus japonicus*. *Arthropod Structure and Development.* 42(2): 153-164.

Grygier, M.J. 1987. New records, external and internal anatomy, and systematic position of Hansen's y-larvae (Crustacea: Maxillopoda: Facetotecta). *Sarsia*. 72: 261-278.

Hadži, J. 1963. *The Evolution of Metazoa*. A Pergamon Press Book. The MacMillan Company, Ney York.

Halanych, K.M. 2004. The new view of animal phylogeny. *Annual Review of Ecology, Evolution, and Systematics*. 35: 229-256.

Harzsch, S., Kreissl, S. **2010.** Myogenesis in the thoracic limbs of the American lobster. *Arthropod Structure and Development.* 39(6): 423-435

Heath, H. 1899. The development of *Ischnochiton*. *Zoologische Jahrbücher. Abteilung für Anatomie und Ontogenie der Tiere.* 12: 567-656.

Hejnol, A. 2010. A Twist in Time - The Evolution of Spiral Cleavage in the Light of Animal Phylogeny. *Integrative and Comparative Biology*. 50: 695-706.

Hejnol, A., Martindale, M.Q. **2008**. Acoel development indicates the independent evolution of the bilaterian mouth and anus. *Nature*. 456: 382-387.

Hejnol, A., Martindale, M.Q. **2009**. The mouth, the anus and the blastopore - open questions about questionable openings. in: *Animal Evolution: Genomes, Fossils and Trees*, (ed. Littlewood, D.T.J., Telford, M.J.). Ox ford University Press. 33-40.

Hejnol, A., Martindale, M.Q., Henry, J.Q. **2007**. High-resolution fate map of the snail *Crepidula fornicata*: the origins of ciliary bands, nervous system, and muscular elements. *Developmental Biology*. 305: 63-76.

Hejnol, A., Obst, M., Stamatakis, A., Ott, M., Rouse, G.W., Edgecombe, G.D., Martinez, P., Baguna, J., Bailly, X., Jondelius, U., Wiens, M., Muller, W.E., Seaver, E., Wheeler, W.C., Martindale, M.Q., Giribet, G., Dunn, C.W. **2009**. Assessing the root of bilaterian animals with scalable phylogenomic methods. *Proceedings of the Royal Society, Series B: Biological Sciences.* 276(1677): 4261-4270.

Helmkampf, M., Bruchhaus, I., Hausdorf, B. **2008**. Phylogenomic analyses of lophophorates (brachiopods, phoronids and bryozoans) confirm the Lophotrochozoa concept. *Proceedings of the Royal Society, Section B: Biological Sciences.* 275: 1927-1933.

Henry, J.J., Martindale, M.Q. **1987**. The organizing role of the D quadrant as revealed through the phenomenon of twinning in the polychaete, *Chætopterus variopedatus*. *Roux's Archives. Developmental Biology.* 196: 499-510.

Henry, J.J., Martindale, M.Q. 1998. Conservation of the spiralian developmental program: cell lineage of the nemertean, *Cerebratulus lacteus*. *Developmental Biology*. 201: 253-269.

Henry, J.J., Martindale, M.Q. **1999**. Conservation and innovation in spiralian development. *Hydrobiologia*. 402: 255-265.

Henry, J.Q., Martindale, M.Q., Boyer, B.C. **2000.** The unique developmental program of the acoel flatworm, *Neochildia fusca*. *Developmental Biology*. 220: 285-295.

Henry, J.Q., Tagawa, K., Martindale, M.Q. **2001**. Deuterostome evolution: early development in the enteropneust hemichordate, *Ptychodera flava*. *Evolution and Development*. 3(6): 375-390.

Henry, J.Q., Tagawa, K., Martindale, M.Q. **2001**. Deuterostome evolution: early development in the enteropneust hemichordate, *Ptychodera flava*. *Evolution and Development.* 3(6): 375-390.

Henry, J.Q., Okusu, A., Martindale, M.Q. **2004**. The cell lineage of the polyplacophoran, *Chaetopleura apiculata*: variation in the spiralian program and implications for molluscan evolution. *Developmental Biology*. 272(1): 145-160.

Hertzler, P.L. 2002. Development of the mesendoderm in the dendrobranchiate shrimp *Sicyonia ingentis*. *Arthropod Structure and Development*. 31: 33-49.

Hertzler, P.L. 2005. Cleavage and gastrulation in the shrimp *Penaeus* (*Litopenaeus*) *vannamei* (Malacostraca, Decapoda, Dendrobranchiata). *Arthropod Structure and Development.* 34: 455-469.

Hertzler, P.L., Clark, W.H.J. **1992**. Cleavage and gastrulation in the shrimp *Sicyonia ingentis*: invagination is accombined by oriented cell division. *Development*. 116: 127-140.

Hertzler, P.L., Wang, S.W., Clark, W.H.J. **1994**. Mesendoderm cell and archenteron formation in isolated blastomeres from the shrimp *Sicyonia ingentis. Developmental Biology*. 164: 333-344.

Hickmann, V.V. 1936. The embryologyof the syncarid crustacean, *Anaspides tasmaniae*. *Papers and Proceedings of the Royal Society of Tasmania*. 1-35.

Ho, R.K., Ball, E.E., Goodman, C.S. **1983**. Muscle pioneers: large mesodermal cells that erect a scaffold for developing muscles and motorneurones in grasshopper embryos. *Nature.* 301: 66-69.

Høeg, J.T. 1992. Rhizocephala. *Microscopic anatomy of invertebrates*. Wiley-Liss Inc. New York. 9: 313-345.

Høeg, J.T., Kolbasov, G.A. **2002**. Lattice organs in y-cyprids of the Facetotecta and their significance in the phylogeny of the Crustacea Thecostraca. *Acta Zoologica*. 83: 67-79.

Houthoofd, W., Jacobsen, K., Mertens, C., Vangestel, S., Coomans, A., Borgonie, G. **2003**. Embryonic cell lineage of the marine nematode *Pellioditis marina*. *Developmental Biology*. 258: 57-69.

Hunnekuhl, V., Wolff, C. **2012**. Reconstruction of cell lineage and spatiotemporal pattern formation of the mesoderm in the amphipod crustacean *Orchestia cavimana*. *Developmental Dynamics*. 241: 697-717.

Ivanova-Kazas, O.M. 1979. Comparative Embryology of the Invertebrates. Arthropoda. Nauka, Moscow. [in Russian]

Jeffery, W.R. 1985. Specification of cell fate by cytoplasmic determinants in ascidian embryos. *Cell.* 41(1): 11-12.

Jellies, J. 1990. Muscle assembly in simple systems. *Trends in Neuroscience*. 13: 126-131.

Jenner, R.A. 1999. Metazoan phylogeny as a tool in evolutionary biology: current problems and discrepancies in application. *Belgian Journal of Zoology.* 129(1): 245-262.

Jenner, R.A. 2010. Higher-level crustacean phylogeny: consensus and conflicting hypotheses. *Arthropod Structure and Development.* 39(2-3): 143-153.

Jennings, H.S. 1896. The early development of *Asplanchna herrickii* De Guerne – A contribution to developmental mechanics. *Bull Mus Comp Zool*. 25: 1-117.

Jirikowski, G., Kreissl, S., Richter, S., Wolff, C. **2010.** Muscle development in the marbled crayfish – insights from an emerging model organism (Crustacea, Malacostraca, Decapoda). *Development Genes and Evolution*. 220(3): 89-105.

Jondelius, U., Ruiz-Trillo, I., Baguñà, J., Riutort, M. **2002**. The Nemertodermatida are basal bilaterians and not members of the Platyhelminthes. *Zoologica Scripta*. 31(2): 201-215.

Jondelius, U., Larsson, K., Raikova, O. **2004**. Cleavage in *Nemertoderma westbladi* (Nemertodermatida) and its phylogenetic significance. *Zoomorphology*. 123: 221-225.

Jondeung, A., Karinthanyakit, W., Kaewkhumsan, J. **2012**. The complete mitochondrial genome of the black mud crab, *Scylla serrata* (Crustacea: Brachyura: Portunidae) and its phylogenetic position among (pan)crustaceans. *Molecular Biology Reports.* 39(12): 10921-10937.

Kiernan, D.A., Hertzler, P.L. **2003**. Muscle development in dendrobranchiate shrimp, with comparison to *Artemia*. *Evolution and Development*. 8(6): 537-549.

Knight-Jones, E.W., Waugh, G. **1949**. On the larval development of *Elminius modestus* Darwin. *Journal of the Marine Biological Association of the United Kingdom*. 28 (2): 413-428.

Koenemann, S., Jenner, R.A., Hoenemann, M., Stemme, T., von Reumont, B.M. **2010**. Arthropod phylogeny revisited, with a focus on crustacean relationships. *Arthropod Structure and Development.* 39(2–3): 88-110.

Kohler, H.-J. 1976. Embryologische Untersuchungen an Copepoden: Die Entwicklung von *Lernaeocera*

branchialis L. 1767 (Crustacea, Copepoda, Lernaeoida, Lernaeidae). *Zoologische Jahrbücher. Abteilung für Anatomie und Ontogenie der Tiere*. 95: 448-504.

Korschelt, E. 1936. *Vergleichende Entwicklungsgeschichte der Tiere.* (ed. Korschelt, E., Heider). 1 und 2. Gustav Fischer Verlag.

Kozloff, E.N. 2007. Stages of development, from first cleavage to hatching, of an *Echinoderes* (Phylum Kinorhyncha: Class Cyclorhagida). *Cahiers de Biologie Marine.* 48: 199-206.

Kreissl, S., Uber, A., Harzsch, S. **2008**. Muscle precursor cells in the developing limbs of two isopods (Crustacea, Peracarida): an immunohistochemical study using a novel monoclonal antibody against myosin heavy chain. *Development Genes and Evolution*. 218: 253-265.

Krüger, P. 1922. Die Embryonalentwicklung von *Scalpellum scalpellum* L. I. Furchung und Anlage der Keimblätter. *Archiv für Mikroskopische Anatomie.* 96: 355-386.

Kühn, A. 1912. Die Sonderung der Keimesbezirke in der Entwicklung der Sommereier von *Polyphemus pediculus* de Geer. *Zoologische Jahrbücher. Abteilung für Anatomie und Ontogenie der Tiere.* 35(2): 243-340.

Kühnemund, E. 1929. Die Entwicklung der Scheitelplatte von *Polyphemus pediculus* De Geer von der Gastrula bis zur Differenzierung der aus ihr hervorgehenden Organe. *Zoologische Jahrbücher. Abteilung für Anatomie und Ontogenie der Tiere.* 50: 385-432.

Lambert, D.J. 2008. Mesoderm in Spiralians: the organizer and the 4d cell. *Journal of Experimental Zoology Part B: Molecular and Developmental Evolution.* 308B: 1-9.

Lang, A. 1884. Polycladen - Zweiter Abschnitt. Ontogenie. in *Flora und Fauna des Golfes von Neapel*. 317-347.

Lartillot, N., Le Gouar, M., Adoutte, A. **2002a**. Expression patterns of *fork head* and *goosecoid* homologues in the mollusc *Patella vulgata* supports the ancestry of the anterior mesendoderm across Bilateria. *Development Genes and Evolution.* 212(11): 551-561.

Lartillot, N., Lespinet, O., Vervoort, M., Adoutte, A. **2002b.** Expression pattern of *Brachyury* in the mollusc *Patella vulgata* suggests a conserved role in the establishment of the AP axis in Bilateria. *Development.* 129(6): 1411-1421.

Lavrov, D.V., Brown, W.M., Boore, J.L. **2004**. Phylogenetic position of the Pentastomida and pan(crustacean) relationships. *Proceedings of the Royal Society London, series B: Biological Sciences.* 271: 537-544.

Lechner, M. 1966. Untersuchungen zur Embryonalentwicklung des Rädertieres *Asplanchna girodi* de Guerne. *Wilhelm Roux' Archiv für Entwicklungsmechanik der Organismen.* 157: 117-173.

Lillie, F.R. 1895. The embryology of the Unionidae. *Journal of Morphology*. 10(1): 1-100.

Luetjens, C.M., Dorresteijn, A.W.C. **1995**. Multible, alternative cleavage patterns precede uniform larval morphology during normal development of *Dreissena polymorpha* (Mollusca, Lamellibranchia). *Roux's Archive of Developmental Biology*. 205: 138-149.

Lyons, D., Perry, K., Lesoway, M., Henry, J. **2012**. Cleavage pattern and fate map of the mesendoblast, 4d, in the gastropod *Crepidula*: a hallmark of spiralian development. *EvoDevo.* 3(1): 21.

Malakhov, V.V. 1986. *Nematodes: their morphology, development, system, and phylogeny*. Nauka, Moscow. [in Russian]

Malakhov, V.V., Spiridonov, S.E. **1981**. Embryonic development of *Gastromermis* sp. (Nematoda, Mermithida). Zoologicheskii Zhurnal. 60(10): 1574-1577. [in Russian]

Malakhov, V.V., Temereva, E.N. **1999**. Embryonic development of the phoronid *Phoronis ijimai* (Lophophorata, Phoronida): two sources of the coelomic mesoderm. *Doklady Biological Sciences*. 365(4): 166-168.

Mallatt, J.M., Garey, J.R., Shultz, J.W. **2004**. Ecdysozoan phylogeny and Bayesian inference: First use of nearly complete 28S and 18S rRNA to classify the arthropods and their kin. *Molecular Phylogenetics and Evolution*. 31: 178-191.

Manton, S.M. 1928. On the embryology of a mysid crustacean, *Hemimysis lamornae*. *Philosophical Transactions of the Royal Society of London, series B: Biological Sciences.* 216: 363-463.

Manton, S.M. 1949. Studies on the Onychophora. VII. The early embryonic stages of *Peripatopsis*, and some general considerations concerning the morphology and phylogeny of the Arthropoda. *Philosophical Transactions of the Royal Society of London, Section B: Biological Sciences.* 233(606): 483-580.

Marlétaz, F., Martin, E., Perez, Y., Papillon, D., Caubit, X., Lowe, C.J., Freeman, B., Fasano, L., Dossat, C., Wincker, P., Weissenbach, J., Le Parco, Y. **2006**. Chaetognath phylogenomics: a protostome with deuterostome-like development. *Current biology.* 16(15): R577-R578.

Martindale, M.Q., Pang, K., Finnerty, J.R. **2004**. Investigating the origins of triploblasty: `mesodermal´ gene expression in a diploplastic animal, the sea anemone *Nematostella vectensis* (phylum, Cnidaria; class, Anthozoa). *Development.* 131(10): 2463-2474.

Martindale, M.Q., Henry, J.Q. **1999**. Intracellular fate mapping in a basal metazoan, the Ctenophore *Mnemiopsis leidyi*, reveals the origins of mesoderm and the existence of indeterminate cell lineages. *Developmental Biology*. 214: 234-257.

Martín-Durán, J.M., Egger, B. **2012**. Developmental diversity in free-living flatworms. *EvoDevo*. 3(7): 1-19.

Martín-Durán, J.M., Janssen, R., Wennberg, S., Budd, G.E., Hejnol, A. 2012. Deuterostomic Development in the Protostome *Priapulus caudatus*. *Current Biology.* 22(22): 2161-2166.

Maslakova, S.A., Martindale, M.Q., Norenburg, J.L. **2004**. Fundamental properties of the spiralian developmental program are displayed by the basal nemertean *Carinoma tremaphoros* (Palaeonemertea, Nemertea). *Developmental Biology*. 267: 342-360.

Matus, D.Q., Pang, K., Marlow, H., Dunn, C.W., Thomsen, G.H., Martindale, M.Q. **2006**. Molecular evidence for deep evolutionary roots of bilaterality in animal development. *Proceedings of National Academy of Science USA*. 103(30): 11195-11200.

Mead, A.D. 1897. The early development of marine annelids. *Journal of Morphology*. 13(2): 227-326.

Meisenheimer, J. 1901. Entwicklungsgeschichte von *Dreissensia polymorpha* Pall. *Zeitschrift für Wissenschaftliche Zoologie*. 69: 1–137, pls. 1–13

Merkel, J., Wollesen, T., Lieb, B., Wanninger, A. **2012**. Spiral cleavage and early embryology of a loxosomatid entoproct and the usefulness of spiralian apical cross patterns for phylogenetic inferences. *BMC Evolutionary Biology*. 12(11): 2-11.

Meusemann, K., von Reumont, B.M., Simon, S., Roeding, F., Strauss, S., Kück, P., Ebersberger, I., Walzl, M., Pass, G., Breuers, S., Achter, V., von Haeseler, A., Burmester, T., Hadrys, H., Wägele, J.W., Misof, B. **2010.** A phylogenomic approach to resolve the arthropod tree of life. *Molecular Biology and Evolution.* 27(11): 2451-2464.

Meyer, N. P., Seaver, E. C. **2010.** Cell lineage and fate map of the primary somatoblast of the polychaete annelid *Capitella teleta*. *Integrative and Comparative Biology*. 50(5): 756-767.

Meyer, N.P., Boyle, M.J., Martindale, M.Q., Seaver, E.C. **2010.** A comprehensive fate map by intracellular injection of identified blastomeres in the marine polychaete *Capitella teleta*. *EvoDevo*. 1(8): 27.

Montgomery, T.H. 1904. The Development and Structure of the Larva of *Paragordius*. *Proceedings of the Academy of Natural Sciences of Philadelphia*. 56: 738-755

Mühldorf, A. 1914. Beiträge zur Entwicklungsgeschichte und zu den phylogenetischen Beziehungen der Gordiuslarve. *Zeitschrift für Wissenschaftliche Zoologie*. 111: 1-75.

Mwinyi, A., Bailly, X., Bourlat, S.J., Jondelius, U., Littlewood, D.T., Podsiadlowski, L. **2010.** The phylogenetic position of Acoela as revealed by the complete mitochondrial genome of *Symsagittifera roscoffensis*. *BMC Evolutionary Bioogy.* 10: 309.

Nachtwey, R. 1925. Untersuchungen über die Keimbahn, Organogenese und Anatomie von *Asplanchna priodonta* Grosse. *Zeitschrift für Wissenschaftliche Zoologie*. 126: 139-492.

Nair, S.G. 1956. On the embryology of the isopod *Irona*. *Journal of Developmental and Experimental Morphology.* 4(1): 1-33.

Nederbragt, A.J., Lespinet, O., van Wageningen, S., van Loon, A.E., Adoutte, A., Dictus, W.J. **2002**. A lophotrochozoan twist gene is expressed in the ectomesoderm of the gastropod mollusk *Patella vulgata*. *Evolution and Development*. 4(5): 334-343.

Nelson, J.A. 1904. The early development of *Dinophilus*: a study in cell-lineage. *Proceedings of the Academy of Natural Sciences of Philadelphia*. 56: 687–737.

Nielsen, C. 1995. *Animal Evolution: Interrelationships of the Living Phyla*. Oxford: Oxford University Press.

Nielsen, C. 2004. Trochophora larvae: cell-lineages, ciliary bands, and body regions. 1. Annelida and Mollusca. *Journal of Experimental Zoology*. 302: 35-68.

Nielsen, C. 2005. Trochophora larvae and adult body regions in annelids: some conclusions. *Hydrobiologia*. 535/536: 23-24.

Nielsen, C. 2010. Some aspects of spiralian development. *Acta Zoologica*. 91: 20-28.

Nishida, H. 1987. Cell lineages analysis in ascidian embryos by intracellular injections of a tracer enzyme III. Up to the tissue restricted stage. *Developmental Biology*. 121: 526-541.

Nishida, H. 2005. Specification of embryonic axis and mosaic development in ascidians. *Developmental Dynamics.* 233(4): 1177-1193.

Nishida, H., Satoh, N. **1983**. Cell lineages analysis in ascidian embryos by intracellular injections of a tracer enzyme I. up to the eight-cell stage. *Developmental Biology*. 99: 382-394.

Nishida, H., Satoh, N. **1985**. Cell Lineage Analysis in Ascidian Embryos by Intracellular Injection of a Tracer Enzyme II. The 16- and 32-Cell Stages. *Developmental Biology*. 110: 440-454.

Nußbaum, M., 1890. *Anatomische Studien an Californischen Cirripedien*. Bonn.

Oakley, T.H., Wolfe, J.M., Lindgren, A.R., Zaharoff, A.K. **2013**. Phylotranscriptomics to bring the understudied into the fold: monophyletic ostracoda, fossil placement, and pancrustacean phylogeny. *Molecular Biology and Evolution.* 30(1): 215-233.

Papillon, D., Perez, Y., Caubit, X., Le Parco, Y. **2006**. Systematics of Chaetognatha under the light of molecular data, using duplicated ribosomal 18S DNA sequences. *Molecular Phylogenetics and Evolution.* 38(3): 621-634.

Pawlak, J.B., Sellars, M.J., Wood, A., Hertzler, P.L. **2010.** Cleavage and gastrulation in the Kuruma shrimp *Penaeus (Marsupenaeus) japonicus* (Bate): a revised cell lineage and identification of a presumptive germ cell marker. *Development, Growth and Differentiation.* 52(8): 677-692.

Pennerstorfer, M., Scholtz, G. **2012**. Early cleavage in *Phoronis muelleri* (Phoronida) displays spiral features. *Evolution and Development.* 14(6): 484-500.

Peterson, K.J., Eernisse, D.J. **2001**. Animal phylogeny and the ancestry of bilaterians: inferences from morphology and 18S rDNA gene sequences. *Evolution and Development*. 3(3): 170-205.

Philippe, H., Telford, M.J. **2006**. Large-scale sequencing and the new animal phylogeny. *Trends in Ecology and Evolution.* 21(11): 614-620.

Philippe, H., Brinkmann, H., Martinez, P., Riutort, M., Baguñá, J. **2007**. Acoel flatworms are not platyhelminthes: evidence from phylogenomics. *PLoS ONE.* 2(8): e717.

Philippe, H., Derelle, R., Lopez, P., Pick, K., Borchiellini, C., Boury-Esnault, N., Vacelet, J., Renard, E., Houliston, E., Queinnec, E., Da Silva, C., Wincker, P., Le Guyader, H., Leys, S., Jackson, D.J., Schreiber, F., Erpenbeck, D., Morgenstern, B., Worheide, G., Manuel, M. **2009.** Phylogenomics revives traditional views on deep animal relationships. *Current Biology*. 19: 1-7.

Philippe, H., Brinkmann, H., Copley, R.R., Moroz, L.L., Nakano, H., Poustka, A.J., Wallberg, A., Peterson, K.J., Telford, M.J. **2011.** Acoelomorph flatworms are deuterostomes related to *Xenoturbella*. *Nature*. 470: 255-260.

Pick, K.S., Philippe, H., Schreiber, F., Erpenbeck, D., Jackson, D.J., Wrede, P., Wiens, M., Alie, A., Morgenstern, B., Manuel, M., Worheide, G. **2010.** Improved phylogenomic taxon sampling noticeably affects nonbilaterian relationships. *Molecular Biology and Evolution.* 27(9): 1983-1987.

Price, A.L., Modrell, M.S., Hannibal, R.L., Patel, N.H. **2010.** Mesoderm and ectoderm lineages in the crustacean *Parhyale hawaiensis* display intra-germ layer compensation. *Developmental Biology.* 341:256-266.

Priess, J.R. 2005. Notch signaling in the *C. elegans* embryo. *WormBook*. (ed. The *C. elegans* Research Community), doi/10.1895/wormbook.1.4.1

Priess, J.R., Thomson, J.N. 1987. Cellular interactions in early *C. elegans* embryos. *Cell.* 48(2): 241-250.

Regier, J.C., Shultz, J.W., Kambic, R.E. **2005**. Pancrustacean phylogeny: hexapods are terrestrial crustaceans and maxillopods are not monophyletic. *Proceedings of the Royal Society of London, series B: Biological Sciences* 272: 395-401.

Regier, J.C., Shultz, J.W., Ganley, A.R.D., Hussey, A., Shi, D., Ball, B., Zwick, A., Stajich, J.E., Cummings, M.P., Martin, J.W., Cunningham, C.W. **2008**. Resolving Arthropod Phylogeny: Exploring Phylogenetic Signal within 41 kb of Protein-Coding Nuclear Gene Sequence. *Systematic Biology.* 57(6): 920-938.

Regier, J.C., Shultz, J.W., Zwick, A., Hussey, A., Ball, B., Wetzer, R., Martin, J.W., Cunningham, C.W. **2010.** Arthropod relationships revealed by phylogenomic analysis of nuclear protein-coding sequences. *Nature.* 463(7284): 1079-1083.

Reichenbach, H. 1886. Studien zur Entwicklungsgeschichte des Flusskrebses. *Abhandlungen der Senckenbergischen Naturforschenden Gesellschaft.* 124: Plates.

Render, J. 1997. Cell fate maps in the *Ilyanassa obsoleta* embryo beyond the third division. *Developmental Biology*. 189: 301-310.

Richter, S. 2002. The Tetraconata concept: hexapod-crustacean relationships and the phylogeny of Crustacea. *Organisms Diversity and Evolution.* 2: 217-237.

Richter, S., Scholtz, G. **2001**. Phylogenetic analysis of the Malacostraca (Crustacea). *Journal of Zoological Systematics and Evolutionary Research*. 39(3): 113-136.

Rodaway, A., Patient, R. **2001**. Mesendoderm: An Ancient Germ Layer? *Cell.* 105(2): 169-172.

Rodaway, A., Takeda, H., Koshida, S., Broadbent, J., Price, B., Smith, J.C., Patient, R., Holder, N. **1999**. Induction of the mesendoderm in the zebrafish germ ring by yolk cell-derived TGF-beta family signals and discrimination of mesoderm and endoderm by FGF. *Development.* 126(14): 3067-3078.

Rota-Stabelli, O., Campbell, L., Brinkmann, H., Edgecombe, G.D., Longhorn, S.J., Peterson, K.J., Pisani, D., Philippe, H., Telford, M.J. **2011**. A congruent solution to arthropod phylogeny: phylogenomics, microRNAs and morphology support monophyletic Mandibulata. *Proceedings of the Royal Society, series B: Biological Sciences.* 278(1703): 298-306.

Röttinger, E., Dahlin, P., Martindale, M.Q. **2012**. A framework for the establishment of a cnidarian gene regulatory network for "endomesoderm" specification: the inputs of ss-catenin/TCF signaling. *PLoS Genetics.* 8(12): e1003164.

Ruiz-Trillo, I., Riutort, M., Littlewood, D.T., Herniou, E.A., Baguñá, J. **1999**. Acoel flatworms: earliest extant bilaterian Metazoans, not members of Platyhelminthes. *Science.* 283(5409): 1919-1923.

Sagawa, K., Yamagata, H., Shiga, Y. **2005**. Exploring embryonic germ line development in the water flea, *Daphnia magna*, by zinc-finger-containing VASA as a marker. *Gene Expression Patterns*. 5(5): 669-678.

Sandig, M., Dohle, W. **1988**. The cleavage pattern in the leech *Theromyzon tessulatum* (Hirudinea, Glossiphoniidae). *Journal of Morphology.* 196: 217-252.

Schiemann, S., Hejnol, A. **2011**. A 4D-microscopic analysis of the cell lineage of the bdelloid rotifer *Adineta vaga*. *Abstracts of the 2nd International Congress on Invertebrate Morphology.* 134.

Schierenberg, E. 2005. Unusual cleavage and gastrulation in a freshwater nematode: developmental and phylogenetic implications. *Development Genes and Evolution*. 215: 103-108.

Schnabel, R. 1991. Cellular interactions involved in the determination of the early *C. elegans* embryo. *Mechanisms of Development*. 34: 85-100

Schnabel, R., Hutter, H., Moerman, D., Schnabel, H. **1997**. Assessing normal embryogenesis in *Caenorhabditis elegans* using a 4D Microscope: variability of development and regional specification. *Developmental Biology*. 184(2): 234-265.

Scholtz, G. 1990. The formation, differentiation and segmentation of the post-naupliar germ band of the amphipod *Gammarus pulex* L. (Crustacea, Malacostraca, Peracarida). *Proceedings of the Royal Society, series B: Biological Sciences.* 239:163-211.

Scholtz, G. 1997. Cleavage, germband formation and head segmentation: the ground pattern of the Euarthropoda. in *Arthropod Relationships* (ed. Fortey, R.A., Thomas, R.H.). Chapman and Hall. 317-332.

Scholtz, G. 2000. Evolution of the nauplius stage in malacostracan crustaceans. *Journal of Zoological Systematics and Evolutionary Research.* 38(3): 175-187.

Scholtz, G. 2004. Colelenterata versus Acrosomata-zur Position der Rippenquallen (Ctenophora) im phylogenetischen System der Metazoa. *Sitzungsberichte der Gesellschaft Naturforschender Freunde zu Berlin.* 43: 15-33.

Scholtz, G. 2005. Homology and ontogeny: Pattern and process in comparative developmental biology. *Theory in Biosciences.* 124: 121-143.

Scholtz, G., Wolff, C. **2002**. Cleavage, gastrulation, and germ disc formation of the amphipod crustacean *Orchestia cavimana* (Crustacea, Malacostraca, Peracarida). *Contributions to Zoology*. 71(1/3): 9-28.

Scholtz, G., Wolff, C. **2013**. Arthropod Embryology: Cleavage and Germ Band Development. in: *Arthropod Biology and Evolution,* (ed. Minelli, A., Fusco, G., Boxshall, G.). Springer-Verlag Berlin Heidelberg.

Scholtz, G., Ponomarenko, P., Wolff, C. **2009**. Cirripede cleavage patterns and the origin of the rhizocephala (crustacea: thecostraca). *Arthropod Systematics and Phylogeny.* 67(2): 219-228.

Schulze, J., Schierenberg, E. **2011**. Evolution of embryonic development in nematodes. *EvoDevo*. 2(18): 1-16.

Seipel, K., Schmid, V. **2005**. Evolution of striated muscle: jellyfish and the origin of triploblasty. *Developmental Biology.* 282(1): 14-26.

Selenka, E. 1881. Zur Entwicklungsgeschichte der Seeplanarien. *Zoologische Studien*. 11: 1-32.

Semmler, H., Wanninger, A., Høeg, J.T., Scholtz, G. **2008**. Immunocytochemical studies on the naupliar nervous system of *Balanus improvisus* (Crustacea, Cirripedia, Thecostraca). *Arthropod Structure and Development.* 37: 383-395.

Semmler, H., Høeg, J.T., Scholtz, G., Wanninger, A. **2009**. Three-dimensional reconstruction of the naupliar musculature and a scanning electron microscopy atlas of nauplius development of *Balanus improvisus* (Crustacea: Cirripedia: Thoracica). *Arthropod Structure and Development.* 38: 135-145.

Shimotori, T., Goto, T. **2001**. Developmental fates of the first four blastomeres of the chaetognath *Paraspadella gotoi*: Relationship to protostomes. *Development Growth and Differentiation*. 43: 371-382.

Shirase, S., Yanagimachi, R. **1957**. The early development of *Peltogastrella socialis* Krüger (a Rhizocephalan). *Zoological Magazine (Tokyo)*. 66: 253-257.

Siewing, R. 1969. *Lehrbuch der vergleichenden Entwicklungsgeschichte der Tiere*. Verlag Parey Paul, Berlin.

Siewing, R. 1977. Mesoderm bei Ctenophoren. *Zeitung für zoologische Systematik und Evolutionsforschung*. 15: 1-8.

Siewing, R. 1979. Homology of cleavage types? *Fortschritte in der zoologischen Systematik und Evolutionsforschung.* 1: 7-18.

Stach, T., Winter, J., Bouquet, J.-M., Chourrout, D., Schnabel, R. **2008**. Embryology of a planktonic tunicate reveals traces of sessility. *Proceedings of the National Academy of Sciences of the United States of America*. 105(20): 7229-7234.

Steinmetz, P., Kraus, J., Larroux, C., Hammel, J., Amon-Hassenzahl, A., Houliston, E., Wörheide, G., Nickel, M., Degnan, B., Technau, U. **2012**. Independent evolution of striated muscles in cnidarians and bilaterians. *Nature.* 487(231-236.

Sulston, J.E., Schierenberg, E., White, J.G., Thomson, J.N. **1983**. The embryonic cell lineage of the nematode *Caenorhabditis elegans*. *Development Biology*. 100: 64-119.

Surface, F.M. 1907. The early development of a polyclad, *Planocera inquilina* Wh. *Proceedings of the Academy of Natural Sciences of Philadelphia*. 59: 514-559.

Tannreuther, G.W. 1915. The embryology of *Bdellodrilus philadelphicus*. *Journal of Morphology*. 26(2): 143-216.

Tannreuther, G.W. 1920. The development of *Asplanchna ebbesbornii* (Rotifer). *Journal of Morphology*. 33(2): 388-437.

Taube, E. 1909. Beiträge zur Entwicklungsgeschichte der Euphausiden. I. Die Furchung des Eies bis zur Gastrulation. *Zeitschrift für Wissenschaftliche Zoologie.* 92: 427-464.

Technau, U. 2001. *Brachyury*, the blastopore and the evolution of the mesoderm. *BioEssays.* 23: 788-794.

Technau, U., Scholz, C.B. **2003**. Origin and evolution of endoderm and mesoderm. *International Journal of Developmental Biology*. 47: 531-539.

Temereva, E.N., Malakhov, V.V. **2007.** Embryogenesis and larval development of phoronid *Phoronopsis harmeri* Pixell, 1912: dual origin of the coelomic mesoderm. *Invertebrate Reproduction and Development*. 50(2): 57-66

Tessin, G. 1886. Über Eibildung und Entwicklung der Rotatoria. *Zeitschrift für Wissenschaftliche Zoologie*. 44: 273-302.

Torrey, J.C. 1903. The early embryology of *Thalassema mellita* (Conn). *Annals of the New York Academy of Sciences*. 14: 165-246.

Treadwell, A.L. 1901. Cytogeny of *Podarke obscura* Verrill. *Journal of Morphology.* 17: 399-486.

Turquier, Y. 1967. L´embryogenèse de *Trypetesa nassarioides* Turquier (Cirripède. Acrothoracique) ses rapports avec celle des autres cirripèdes. *Archives de Zoologie Experimentale et Generale*. 108: 111-137.

Ungerer, P., Scholtz, G. **2009**. Cleavage and gastrulation in *Pycnogonum litorale* (Arthropoda, Pycnogonida): morphological support for the Ecdysozoa? *Zoomorphology*. 128: 263-274.

Uzman, J.A., Jeffery, W.R. **1986**. Cytoplasmic determinants for cell lineage specification in ascidian embryos. *Cell Differentiation.* 18(4): 215-224.

Vagin, V.L. **1949**. On development in Ascothoracida Vagin (Crustacea, Entomostraca) and original types of cleavage in Arthropoda. *Ucenye Zapiski Leningradskogo Ordena Lenina Gosudarstvennogo Universiteta Imeni A.A. Zdanova, Serija Biologiceskich Nauk*, 113: 143-180.

Valentine, J.W. 1997. Cleavage patterns and the topology of the metazoan tree of life. *Proceedings of the National Acadamy of Sciences of the United States of America*. 94: 8001-8005.

van den Biggelaar, J.A.M. 1976. Development of dorsoventral polarity preceding the formation of the mesendoblast in *Lymnaea stagnalis*. *Proceedings of the Koninklijke Nederlandse Akademie van Wetenschappen: Series C: Biological and Medical Sciences.* 79: 412-426.

van den Biggelaar, J.A.M. 1977. Development of dorsoventral polarity and mesendoblast determination in *Patella vulgata*. *Journal of Morphology*. 154: 157-186.

van den Biggelaar, J.A.M. 1996. Cleavage pattern and mesendoblast formation in *Acanthochiton crinitus* (Polyplacophora, Mollusca). *Developmental Biology*. 174: 423-430.

van den Biggelaar, J.A.M., Faber, J. **1994**. Spiral cleavage and cell position contribute to the specification of the dorsoventral axis in the embryo of the archaeogastropod *Haliotis tuberculata*. *Journal of Morphology.* 219(1): 21-33.

van den Biggelaar, J.A.M., Wim, J.A.G., Dictus, W.J.A.G., van Loon, A.E. **1997**. Cleavage patterns, cell-lineages and cell specification are clues to phyletic lineages in Spiralia. *Seminars in Cell and Developmental Biology*. 8: 367-378.

von Reumont, B.M., Meusemann, K., Szucsich, N.U., Dell'Ampio, E., Gowri-Shankar, V., Bartel, D., Simon, S., Letsch, H.O., Stocsits, R.R., Luan, Y.X., Wagele, J.W., Pass, G., Hadrys, H., Misof, B. **2009**. Can comprehensive background knowledge be incorporated into substitution models to improve phylogenetic analyses? A case study on major arthropod relationships. *BMC Evolutionary Biology.* 9: 119.

von Reumont, B.M., Jenner, R.A., Wills, M.A., Dell'ampio, E., Pass, G., Ebersberger, I., Meyer, B., Koenemann, S., Iliffe, T.M., Stamatakis, A., Niehuis, O., Meusemann, K., Misof, B. **2012**. Pancrustacean phylogeny in the light of new phylogenomic data: support for Remipedia as the possible sister group of Hexapoda. *Molecular Biology and Evolution.* 29(3): 1031-1045.

Voronov, D.A., Panchin, Y.V. **1998**. Cell lineage in marine nematode *Enoplus brevis*. *Development*. 125: 143-150.

Walker, G. 1992. Cirripedia. in: (ed. Harrison, F.W., Humes, A.G.) *Microscopic Anatomy of Invertebrates. 9: Crustacea.* Wiley-Liss Inc, New York. 249-311

Walley, L.J., Rees, E.I.S. **1969**. Studies on the larval structure and metamorphosis of *Balanus balanoides* (L.). *Philosophical Transactions of the Royal Society of London, series B: Biological Sciences.* 256: 237-280.

Wang, S.W., Hertzler, P.L., Clark, W.H.J. **2008**. Mesendoderm cells induce oriented cell division and invagination in the marine shrimp *Sicyonia ingentis*. *Developmental Biology*. 320: 175-184.

Weisblat, D.A., Huang, F.Z. **2001**. An overveiw of glossiphoniid leech development. *Canadian Journal of Zoology.* 79: 218-232.

Weisblat, D.A., Kim, S.Y., Stent, G.S. **1984**. Embryonic origins of cells in the leech *Helobdella triserialis*. *Developmental Biolog*y. 104: 65-85.

Wennberg, S.A., Janssen, R., Budd, G.E. **2008**. Early embryonic development of the priapulid worm *Priapulus caudatus*. *Evolution and Development*. 10(3): 326-338.

Weygoldt, P. 1958. Die Embryonalentwicklung des Amphipoden *Gammarus pulex pulex* (L). *Zoologische Jahrbücher der Anatomie. Abteilung für Anatomie und Ontogenie der Tiere*. 77(1): 51-110.

Weygoldt, P. 1960a. Embryologische Untersuchungen an Ostracoden: Die Entwicklung von *Cyprideis litoralis* (G.S.Brady) (Ostracoda, Podocopa, Cytheridae). *Zoologische Jahrbücher. Abteilung für Anatomie und Ontogenie der Tiere*. 78(3): 369-426.

Weygoldt, P. 1960b. Mehrphasige Gastrulationen bei Arthropoden. *Zoologischer Anzeiger*. 164(7/10): 381-385.

Whitman, C.O. 1886. The Germ-Layers of *Clepsine*. *Zoologischer Anzeiger*. 218: 171-176.

Whitman, C.O. 1887. A contribution to the history of the germ-layers in *Clepsine*. *Journal of Morphology.* 1(1): 105-182.

Wiegner, O., Schierenberg, E. **1998**. Specification of Gut Cell Fate Differs Significantly between the Nematodes *Acrobeloides nanus* and *Caenorhabditis elegans*. *Developmental Biology*. 204: 3-14.

Willems, M., Egger, B., Wolff, C., Mouton, S., Houthoofd, W., Fonderie, P., Couvreur, M., Artois, T., Borgonie, G. **2009.** Embryonic origins of hull cells in the flatworm *Macrostomum lignano* through cell lineage analysis: developmental and phylogenetic implications. *Development Genes and Evolution*. 219: 409-417.

Williams, T.A., Müller, G.B. **1996**. Limb development in a primitive crustacean, *Triops langicaudatus*: subdivision of the early limb bud gives rise to multibranched limbs. *Development Genes and Evolution*. 206: 161-168.

Wilson, E.B. 1889. The embryology of the earthworm. *Journal of Morphology.* 3(3): 387-462.

Wilson, E.B. 1892. The cell-lineage of *Nereis*. *Journal of Morphology*. 6(3): 363-463.

Wilson, E.B. 1898. Considerations of cell-lineage and ancestral reminiscence. *Annals of the New York Academy of Sciences.* 11: 1-27.

Witschi, E. 1934. On determinative cleavage and yolk formation in the harpactid copepod *Tisbe furcata* (Baird). *The Biological Bulletin*. 67(3): 335-340.

Wolff, C., Scholtz, G. **2002**. Cell lineage, axis formation, and the origin of germ layers in the amphipod crustacean *Orchestia cavimana*. *Developmental Biology*. 250: 44-58.

Wolff, C. 2004. Zur Beinentwicklung des amphipoden Krebses *Orchestia cavimana* (Peracarida, Malacostraca)- ein zellgenealogische Studie. *Dissertation*. Humboldt-Universität zu Berlin, Berlin.

Woods, F.H. **1931.** History of the germ cells in *Sphaerium striatinum* (Lam.) *Journal of Morphology*. 51(2): 545-595.

Wray, G.A., Raff, R.A. **1990.** Novel origins of lineage founder cells in the direct-developing sea urchin *Heliocidaris erythrogramma*. *Developmental Biology.* 141(1): 41-54.

Wray, G.A. 1994. The evolution of cell lineage in echinoderms. *American Zoologist* 34: 353-363.

Xiao, S., Zhang, Y., Knoll, A.H. **1998**. Three-dimensional preservation of algae and animal embryos in a Neoproterozoic phosphorite. *Nature.* 391(6667): 553-558.

Zalokar, M., Sardet, C. **1984**. Tracing of cell lineage in embryonic development of *Phallusia mammillata* (Ascidia) by vital staining of mitochondria. *Developmental Biology.* 102(1): 195-205.

Zelinka, C. 1891. Studien über Rädertiere. III. Zur Entwicklungsgeschichte der Räderthiere nebst Bemerkungen über ihre Anatomie und Biologie. *Zeitschrift für Wissenschaftliche Zoologie*. 53: 1-159.

Zilch, R. 1978. Embryologische Untersuchungen an der holoblastischen Ontogenese von *Penaeus trisulcatus* Leach (Crustacea, Decapoda). *Zoomorphologie*. 90: 67-100.

Zilch, R. 1979. Cell lineage in arthropods? *Fortschritte in der zoologischen Systematik und Evolutionsforschung.* 1: 19-41.

Zrzavý, J. 2003. Gastrotricha and metazoan phylogeny. *Zoologica Scripta*. 32(1): 61-81.

Zrzavý, J., Štys, P. **1997**. The basic body plan of arthropods: insights from evolutionary morphology and developmental biology. *Journal of Evolutionary Biology.* 10 (3): 353-367

Zrzavý, J., Mihulka, S., Kepka, P., Bezdek, A., Tietz, D. 1998. Phylogeny of the Metazoa based on morphological and 18S ribosomal DNA evidence. *Cladistics*. 14: 249-285.

LIST OF PUBLICATIONS

PAPERS

- Scholtz G., Ponomarenko E. A., Wolff C., Cirripede cleavage patterns and the origin of the Rhizocephala (Crustacea: Thecostraca) // Arthropod Systematics & Phylogeny. 2009, Vol. 67 (2), 219-228 pp.
- Ponomarenko E.A., Korn O.M. First record of Facetotectan larvae in Peter the Great Bay // Russian Journal of Marine Biology. 2006, Vol. 32 (5), 299-301 pp.
- Ponomarenko E.A. Infraclass Facetotecta Grygier, 1985 (book chapter) in “Biota of the Russian Waters of the Sea of Japan”, Ed.-in-Chief A.V. Adrianov, 2006, Vol. 5.
- Ponomarenko E.A. Facetotecta - Unsolved riddle of marine biology (review) // Russian Journal of Marine Biology. 2006, Vol. 32 (Suppl. 1), 1-10 pp.
- Rybakov A.V., Korn O.M., Ponomarenko E.A. The Coastal Crab *Hemigrapsus longitarsis* (Decapoda: Grapsidae)–Coastal crab *Hemigrapsus longitarsis* (Decapoda: Varunidae)—A new host for the rhizocephalan barnacle *Polyascus polygenea* (Cirripedia: Sacculinidae) // Russian Journal of Marine Biology. 2006, Vol. 32 (2), 127-128 pp.
- Ponomarenko E.A., Korn O.M., Rybakov A.V. Larval development of the parasitic barnacle *Heterosaccus papillosus* (Cirripedia: Rhizophala: Sacculinidae) studied under laboratory conditions // Journal of the Marine Biology Association of the United Kingdom. 2005, Vol. 85, 921–928 pp.

CONFERENCE ABSTRACTS

Oral presentations:

- Ponomarenko E.A., Wolff C., Scholtz G., From cells to fibers: Developmental aspects on naupliar mesoderm in Cirripedia // Crustaceologentagung, April 7-10, 2011, Regensburg, Deutschland
- Ponomarenko E.A., Wolff C., Scholtz G., Cell lineage studies on a cirriped crustacean // Crustaceologentagung: Crusttag '09, April 2-5, 2009, Rostock, Deutschland.
- Ponomarenko E.A., Wolff C., Scholtz G., Spiral cleavage in Crustacea? // Tagung „Celebrating Darwin–From The Origin of Species to Deep Metazoan Phylogeny", 4-6 March 2009, Berlin, Deutschland.
- Ponomarenko E.A., Wolff C., Scholtz G., Developmental evidence for the origin of Rhizocephala // International Symposium "Advances in Crustacean Phylogenetics" October 7-11, 2008, Rostock, Deutschland.
- Ponomarenko E.A., Wolff C., Scholtz G., Spiral cleavage in Cirriped Crustacea // First international congress on invertebrate morphology. August 17-21, 2008, Copenhagen, Denmark, P. 1470.
- Ponomarenko E.A. Larval development of *Lernaeodiscus* sp. Reared under laboratory conditions // Conference on the Problems of Biodiversity Conservation. October 7-11, 2005, IMB FEB RAS, Vladivostok (Russia) (in Russian).
- Ponomarenko E.A. Comparative Morphological Analysis of Three Rhizocephalan Species: *Sacculina pinnotherae, S. confragosa* and *Heterosaccus papillosus* // VI Regional Conference of Students, Postgraduates and Young Scientists on Modern Problems of Ecology, Marine Biology and Biotechnology. November of 2003. Vladivostok. FENU Press. 2003. P. 76-77 (in Russian);

Poster presentations:

- Ponomarenko E.A., Scholtz G., Wolff C., Larval musculature of barnacles: Origin, development, anatomy // Second international congress on invertebrate morphology. June 17-21, 2011, Harvard University, Cambridge, United States.
- Ponomarenko E.A., Wolff C., Scholtz G., Developmental evidence for the origin of Rhizocephala // Second Euro Evo Devo conference. 29th July-1st August 2008, Ghent, Belgium, 267-268 pp.

ACKNOWLEDGEMENTS

First of all, I would like to thank Prof. Dr. Gerhard Scholtz and Dr. Carsten Wolff not only for proposing me this fascinating subject for PhD project, but also for supervising and guiding me through these long years of the research work. I am also very grateful for their valuable corrections and comments on the manuscript draft.

Of course, my huge gratitude goes to Markus Pennerstorfer, who had outstanding scrupulousness and enormous patience while reading through my thesis, not mentioning his generous addition of 754 articles into the text. Thank you!!! For additional corrections on some parts of the thesis I want to thank Kai Lindemann and Georg Brenneis. Your input won't be forgotten!

The crew of Wilhelmshaven Aquarium under the lead of Arno Otten and Piratenhostel with Arend Roland Rath as a main pirate are deeply thanked for warm welcoming and providing all the necessary conditions during the animal collection tours.

I also would like to thank all the members of Vergleichende Zoologie AG for the assistance, fun, and just being there! Specifically I want to mention the former members of our working group, who created gorgeous atmosphere and without whom my last seven years would not have been the same: Frederike Alwes, Anke Braband, Franziska Caspari, Maria Geppert, Vera Hunnekuhl, Marleen Klann, Kai Lindemann, Tino Pabst, Andre Reimann, and Petra Ungerer.

My deepest gratitude extends also to the people who initiated my interest in cirripeds as well as helped to establish a profound basis of knowledge on invertebrate zoology Olga M. Korn, Alexey V. Rybakov, and Olga I. Dashchenko.

Most certainly I want to acknowledge the entire Voland's crew, who helped me in various ways (not to forget nutrition supply over the last month) and some of whom entered a circle of real friends!

For the constant and intense support as well as a brave bearing of all my mood and motivation shifts during the last months I am forever indebted to Caterina Biffis, Carles Gonzales, Tatiana Kovalenko, Markus Pennerstorfer, and Tuuli Turunen!

I would also love to thank my family for the moral support and long term patience!

Last, but definitely not least: my endless gratitude is extended to Alexey V. Rybakov, Vladimir L. Kasyanov, and to my grandpa Gennady V. Chichvarov for their being in my normal and scientific life. The time, which I had spent with you, was and will remain priceless!

The research was funded by Marie Curie Foundation, Early research training program (project MOLMORPH, from 01 Aug 2006 to 31 Jul 2009), DAAD (Abschlussstipendium from Sep 2009 to Feb 2010), Frauenförderung (Abschlussstipendium from Apr to Oct 2010).

Obviously, I couldn't miss the opportunity to express the millions of thanks to facebook.com for globally expanding my knowledge by providing amazing hints to many essential areas of life (e.g. conditions of poppy and pumpkin planting or caring for unicorns, the shapes and flags of Lesotho, Mozambique and other countries, tricks of drug and weapon smuggling, etc...). I am also extraordinarily thankful to Travian, which supported and led me through most of my emotional blows over the last couple of years. Devs, you did a great job!

SELBSTSTÄNDIGKEITSERKLÄRUNG

Hiermit versichere ich, dass ich die vorliegende Dissertation selbstständig und nur unter Verwendung der angegebenen Quellen und Hilfsmittel erarbeitet und verfasst habe. Diese Arbeit wurde keiner anderen Prüfungsbehörde vorgelegt.

Berlin, den

APPENDIX:

I. List of abbreviations used in the work

a – anterior
ag – anterior ganglion
aI – antenna I (antennula)
aII – antenna II (antenna)
aIn – nerve of *aI*
aIIn – nerve of *aII*
amg – anterior midgut
an – animal pole
ao – anal opening
aon – innervation of anal opening, anal plexus
apc – anterior part of protocerebral commissure
bd – blastoderm
bs - basipodite
c – cytoplasm
cc – central cluster
cs – caudal spine
cx – coxopodite
d – dorsal
dcg – deuto-cerebral ganglion
dg – developing ectodermal parts of the gut
dlc – dorso-median component of lateral cup of nauplius eye
dm – distal muscles of labrum
dmg – dorsal nerves of midgu
dv – dorso-ventral muscles
eb – endoblast
em – external muscles of labrum
emb – embryo
en – endopodite
end – endoderm
ex – exopodite
fc – furca
ff – frontal filament
ffn – frontal filament nerve
fft – frontal filament tract
fh – fronto-lateral horns
fhn – nerve of fronto-lateral horn
fm – fertilisation membrane
gpc – globular dorsal ganglia of protocerebrum (related to both somatic and neurite parts)
gr – granules
hb – hind body
hg – hindgut
ien – inferior oesophageal nerve
im – internal muscles of labrum
isc – inferior sensory cell
isn – inter-segmental nerve
ivn – inferior ventricular nerve
l – left
lb – labrum
lbc – labral commissure
lbn – labral nerves
lc – lateral clusters
lln – lateral nerve of the lateral cup of nauplius eye
lm – lateral muscles of labrum
lmn – median nerve of the lateral cup of nauplius eye
lne – lateral cup of nauplius eye
mb – mandibula
mbc – mandibular commissure
mbg – mandibular ganglion
mbl – mesoblast
mbn – nerve of mandible
mc – median cup of nauplius eye
mcn – nerve of the median cup
md – mesoderm
mg – midgut
mn – median nerve
mo – mouth opening
n – nucleus
ne – nauplius eye
oe – oesophagus
p – posterior
pb – polar body
pcc – proto-cerebral commissure
pcg – proto-cerebral ganglia
pg – pigmental cell
pgc – primordial germ cells
pln – posterior-lateral nerves
pm – proximal muscles of labrum
pmg – posterior mandibular ganglia
pmn – posterior median nerve
ppc – posterior part of protocerebral commissure
r – right
sen – superior oesophageal nerve
sgn – stomatogastric nerve
sns – stomatogastric nervous system
ssc – superior sensory cell
tcc – trito-cerebral commissure
tcg – trito-cerebral ganglion
uc1 – unidentified cells 1
uc2 – unidentified cells 2
v – ventral
vg – vegetal pole
vlc – ventro-lateral component of lateral cup of nauplius eye
vmg – ventral nerves of midgut
y – yolk
yc – yolk-containing cells

APPENDIX:

II. Explanation to the Fig. 4.2.4.

The embryo shown in Fig. 4.2.4. belongs to the rhizocephalan *Peltogasterella gracilis*, a parasite of *Pagurus brachiomastus*. The view of the externae containing the embryos is shown on the left image below. The image on the right shows the zoomed in externae, one can see small embryos inside. The specimen was collected in the marine biostation “Vostok” of the Sea of Japan (Nakhodka, Russian Federation). The embryos were obtained in the laboratory conditions and fixed in the 4% solution of PFA in PBS. The staining demonstrated in Fig. 4.2.4. is Sytox Green.